TTI: 0-6932

Texas A&M Transportation Institute

Pavement Safety-Based Guidelines for Horizontal Curve Safety

Technical Report 0-6932-R1

Cooperative Research Program

TEXAS A&M TRANSPORTATION INSTITUTE
COLLEGE STATION, TEXAS

in cooperation with the
Federal Highway Administration and the
Texas Department of Transportation
http://tti.tamu.edu/documents/0-6932-R1.pdf

Technical Report Documentation Page

1. Report No.	2. Government Accession No.	3. Recipient's Catalog No.
FHWA/TX-18/0-6932-R1		

4. Title and Subtitle	5. Report Date
PAVEMENT SAFETY-BASED GUIDELINES FOR HORIZONTAL CURVE SAFETY	Published: November 2018
	6. Performing Organization Code

7. Author(s)	8. Performing Organization Report No.
Michael P. Pratt, Srinivas R. Geedipally, Bryan Wilson, Subasish Das, Marcus Brewer, and Dominique Lord	Report 0-6932-R1

9. Performing Organization Name and Address	10. Work Unit No. (TRAIS)
Texas A&M Transportation Institute College Station, Texas 77843-3135	11. Contract or Grant No. Project 0-6932

12. Sponsoring Agency Name and Address	13. Type of Report and Period Covered
Texas Department of Transportation Research and Technology Implementation Office 125 E. 11th Street Austin, Texas 78701-2483	Technical Report: September 2016–August 2018
	14. Sponsoring Agency Code

15. Supplementary Notes

Project performed in cooperation with the Texas Department of Transportation and the Federal Highway Administration.

Project Title: Developing Pavement Safety-Based Guidelines for Improving Horizontal Curve Safety

URL: http://tti.tamu.edu/documents/0-6932-R1.pdf

16. Abstract

The Texas Department of Transportation is increasing its efforts to improve rural highway curve safety by including high-friction surface treatments in the Highway Safety Improvement Program (HSIP). A handful of efforts are underway in the state to install these treatments or others that are intended to improve safety by increasing pavement skid resistance. However, HSIP funds are very limited. Hence, it is necessary to prioritize projects carefully to spend the limited funds where they would yield the greatest benefit in terms of crashes reduced and injuries and fatalities prevented.

Documents like the *Roadway Safety Design Workbook* and the *Highway Safety Manual* contain much useful information about the safety effects of design characteristics like curve radius and cross-sectional widths, but pavement characteristics are not yet included in these documents. In this research project, researchers calibrated detailed safety prediction models to account for the effects of key curve characteristics, including geometry, pavement variables (particularly skid resistance), and weather patterns. Additionally, researchers developed estimates of the service life for various surface treatments that may be used to increase skid resistance. By combining safety prediction models, weather data, and service life data, researchers created guidelines and a life-cycle benefit-cost evaluation framework to assist practitioners in choosing effective safety treatments for curves.

17. Key Words	18. Distribution Statement
Highway Design, Highway Safety, Rural Highways, Highway Curves, Pavement, Skid Resistance, Crash, Crash Risk	No restrictions. This document is available to the public through NTIS: National Technical Information Service Alexandria, Virginia 22312 http://www.ntis.gov

19. Security Classif. (of this report)	20. Security Classif. (of this page)	21. No. of Pages	22. Price
Unclassified	Unclassified	174	

PAVEMENT SAFETY-BASED GUIDELINES FOR HORIZONTAL CURVE SAFETY

by

Michael P. Pratt, P.E.
Assistant Research Engineer

Srinivas R. Geedipally, Ph.D., P.E.
Associate Research Engineer

Bryan Wilson, P.E.
Associate Research Scientist

Subasish Das, Ph.D.
Associate Transportation Researcher

Marcus Brewer, P.E.
Associate Research Engineer

Texas A&M Transportation Institute

and

Dominique Lord, Ph.D.
Professor

Texas A&M University

Report 0-6932-R1
Project 0-6932
Project Title: Developing Pavement Safety-Based Guidelines for Improving Horizontal Curve Safety

Performed in cooperation with the
Texas Department of Transportation
and the
Federal Highway Administration

Published: November 2018

TEXAS A&M TRANSPORTATION INSTITUTE
College Station, Texas 77843-3135

DISCLAIMER

The contents of this report reflect the views of the authors, who are responsible for the facts and the accuracy of the data published herein. The contents do not necessarily reflect the official view or policies of the Federal Highway Administration (FHWA) and/or the Texas Department of Transportation (TxDOT). This report does not constitute a standard, specification, or regulation. It is not intended for construction, bidding, or permitting purposes. The engineer in charge of the project was Michael P. Pratt, P.E. #102332.

NOTICE

The United States Government and the State of Texas do not endorse products or manufacturers. Trade or manufacturers' names appear herein solely because they are considered essential to the object of this report.

ACKNOWLEDGMENTS

TxDOT and FHWA sponsored this research project. Mr. Michael Pratt, Dr. Srinivas Geedipally, Mr. Bryan Wilson, Dr. Subasish Das, and Mr. Marcus Brewer with the Texas A&M Transportation Institute, and Dr. Dominique Lord with Texas A&M University prepared this report.

The researchers acknowledge the support and guidance that the project monitoring committee provided:

- Mr. Darrin Jensen, Project Manager (TxDOT, Research and Technology Implementation Office).
- Mr. Tommy Abrego (TxDOT, Policy and Standards).
- Mr. Epigmenio Gonzalez (TxDOT, Pharr District).
- Mr. John Bassett (TxDOT, Construction Division).
- Mr. Soojun Ha (TxDOT, Houston District).
- Ms. Patti Dathe, Contract Specialist (TxDOT, Research and Technology Implementation Office).

In addition, the researchers acknowledge the valuable contributions of Mr. Tom Freeman, Mr. Yash Menaria, Mr. Soheil Sohrabi, Ms. Ruth Iroanya, Mr. Pawan Dixit, and Ms. Katherine Lufkin, who assisted with various tasks during the conduct of the project.

TABLE OF CONTENTS

LIST OF FIGURES

LIST OF TABLES

Page

CHAPTER 1: OVERVIEW

INTRODUCTION

Horizontal curves are a necessary part of the highway system, but statistics have consistently shown that curves represent significant safety concerns. These concerns arise from the increased driver workload associated with traversing a curve, driver errors like failing to detect a curve or judge its sharpness correctly, and the possibility of obtaining inadequate side friction supply from the tire-pavement interface in inclement weather conditions.

Statistics have consistently shown that the crash rate on horizontal curves is significantly greater than that on tangent roadway segments of similar character. This trend may be caused by drivers failing to detect the presence of a curve or attempting to negotiate the curve at unsafe speeds. In Texas Department of Transportation (TxDOT) research project 0-6031, Lord et al. examined the effects of roadway geometry, curve presence and density, weather, and other factors on roadway departure crashes in Texas (*1*). Their findings confirmed the general trends that crash rates on rural highways are influenced by both presence and sharpness of horizontal curvature, and that curve-related crashes are more frequent on higher-speed roadways. They found that the fatal-and-injury roadway departure crash rate in Texas is 1.9 per million vehicle miles for tangent highway segments and 4.2 per million vehicle miles for curved highway segments.

The application of pavement-related treatments at appropriate horizontal curve locations throughout the state has the potential to improve driver performance and reduce the number of crashes, particularly wet-surface crashes, experienced at horizontal curves. These treatments must be implemented judiciously due to their cost and based on consideration of wet-weather exposure, but they have the potential to improve safety at lower cost than geometric improvements like curve straightening, and with greater effectiveness than control-device treatments like installing delineators or Chevrons. Research is needed to prioritize projects carefully to spend the limited funds where they would yield the greatest benefit in terms of crashes reduced and injuries and fatalities prevented and to develop an evaluation framework that allows the practitioner to estimate the life-cycle benefits of a curve safety treatment.

RESEARCH APPROACH

Researchers augmented a previously developed analysis framework to assess the need for surface treatments at curves based on the concept of margin of safety analysis (*2*). Margin of safety is defined as side friction demand subtracted from side friction supply (*3*). Vehicle speed, curve geometric characteristics (such as radius and superelevation rate), and curve travel path characteristics all affect friction demand. Meanwhile, pavement characteristics (particularly skid number) and weather conditions affect friction supply.

Researchers developed updated safety prediction models to quantify the relationship between curve crash frequency and characteristics like radius, lane width, shoulder width, skid number, and annual precipitation rate. These models allow the analyst to assess the safety performance of a curve of interest by accounting for curve geometry, pavement skid resistance,

and exposure to the wet-weather conditions that are most relevant for considerations of skid resistance.

Researchers assembled the preceding information to develop guidelines for assessing the benefit of installing a high-friction surface treatment on a rural highway horizontal curve. The guidelines are formulated as an Excel®-based spreadsheet program called Texas Curve Margin of Safety (TCMS). The TCMS program accepts curve geometry, traffic control characteristics, annual precipitation rate, and proposed treatment type and cost as inputs, and provides information about margin of safety, expected crash frequency, and life-cycle benefit as outputs. The spreadsheet tool is envisioned to be incorporated into TxDOT's pavement design guidance in a similar manner as the existing Form 2088, which is used to select surface aggregates for repaving projects based on a qualitative analysis of friction supply and demand (*4*).

CHAPTER 2: STATE OF THE PRACTICE: CURVE CRASH TRENDS AND PAVEMENT MANAGEMENT PRACTICES

INTRODUCTION

Pavement-related treatments are one option to reduce the number of crashes experienced at horizontal curves. These treatments must be implemented judiciously due to their cost but have the potential to improve safety at lower cost than geometric improvements like curve straightening, and with greater effectiveness than control-device treatments like installing delineators or Chevrons. Implementation of these treatments must be prioritized carefully to spend limited funds where they would yield the greatest benefit in terms of crashes reduced and injuries and fatalities prevented.

This chapter consists of four parts. The first part summarizes curve safety performance trends documented in the literature. The second part describes the effectiveness and service life of various surface treatments that are available for improving curve safety. The third part summarizes state agency practices for pavement performance monitoring, with a focus on skid resistance. The fourth part discusses other issues relevant to curve safety and pavement management.

CURVE SAFETY PERFORMANCE AND CRASH TRENDS

The research literature indicates that curve safety performance is most affected by curve geometry, curve traffic control devices, weather conditions, and pavement characteristics. The first three of these subjects are discussed in this part of the chapter. The final subject is discussed in the next part.

Safety performance can be described in terms of expected crash frequency or rate, crash severity distribution, or expected changes in the foregoing quantities as a result of a safety treatment. Crash frequency is typically estimated using a safety prediction model, which consists of a safety performance function (SPF) that computes the crash frequency for a base, or typical, roadway segment, and one or more crash modification factors (CMFs), which are multiplicative adjustment factors that adjust the base crash frequency to account for the presence of conditions that deviate from base conditions. Safety prediction models for roadway segments are often described as follows (*5*):

$$\begin{aligned}\mu &= L \times \alpha \times AADT^{\beta_0} \times CMF_1 \times CMF_2 \times \ldots \times CMF_n \\ &= L \times \alpha \times AADT^{\beta_0} \times e^{x_1\beta_1} \times e^{x_2\beta_2} \times \ldots \times e^{x_n\beta_n}\end{aligned} \quad (1)$$

where:

- μ = average annual predicted crash frequency, crashes/yr.
- L = segment length, mi.
- α = calibration constant.
- β_i = calibration coefficients.
- x_i = site characteristic *i* (lane width, shoulder width, etc.).
- CMF_i = CMF for site characteristic *i*.

Curve Geometry

The American Association of State Highway and Transportation Official's *A Policy on Geometric Design of Highways and Streets* (*Green Book*) states that the design of horizontal curves should be based on a proper relationship between speed, curvature, superelevation rate, and side friction demand (*6*). The *Green Book* offers the following equation to describe the relationship between these variables:

$$f_D = \frac{v^2}{gR} - \frac{e}{100} \quad (2)$$

where:

f_D = side friction demand (lateral acceleration divided by g).
v = vehicle speed, ft/s.
g = gravitational constant (= 32.2 ft/s^2).
R = curve radius, ft.
e = superelevation rate, percent.

This equation is referred to as the point-mass model or the simplified curve formula. It shows that the side friction demand of a vehicle traveling at a given speed increases as curve radius or superelevation rate decrease. For design purposes, the *Green Book* recommends side friction factors that represent driver comfort limits. These factors are used to determine an appropriate curve radius and superelevation rate for the roadway's design speed.

A quantity called margin of safety has been described by various authors, including Pratt et at. (*2*), for analyzing safety at various points along a curve's length. Margin of safety is defined as side friction demand f_D subtracted from side friction supply f_s. Side friction demand is a function of curve geometry and vehicle speed, as shown in Equation 2, while side friction supply is a function of pavement surface and tire characteristics.

The simplified curve formula shows that side friction demand increases with decreasing curve radius and is mitigated by increasing superelevation. The effects of these variables on curve safety performance are summarized in the following paragraphs.

Radius

Previous studies indicate that curve radius has been considered as one of the most significant factor affecting crash risk at horizontal curves. In general, sharper curves are associated with higher crash frequency (*7*). The probability of experiencing a crash on a curve with a radius of 500 ft is about twice that of experiencing a crash on a tangent segment (*8*). Numerous CMFs have been developed to quantify the effect of curve on horizontal curve safety.

Harwood et al. (*9*) developed a CMF for horizontal curves on rural two-lane highways based on the previous study conducted by Zegeer et al. (*7*). This CMF is included in the *Highway Safety Manual* (HSM) (*5*) and is described as follows:

$$CMF_R = \frac{1.55L_c + \frac{80.2}{R} - 0.012I_s}{1.55L_c} \quad (3)$$

where:

L_c = curve length, ft.

I_s = indicator variable for spiral transitions (= 1.0 if spiral transitions are present on both approaches to the curve, 0.5 if present on one approach, 0.0 if not present).

Wu et al. noted that Equation 3 regards a curve as a hazard with two point locations (*10*). When comparing a horizontal curve with an adjacent tangent of the same length, the increase in crashes at the curve is only related to its radius, not the curve length. In other words, the risk of crashing in a curve is related to how the driver enters and leaves the curve. Once the driver has entered the curve and is driving on the curve proper, the predicted crash frequency is similar to what would be observed on the adjacent tangent. The margin of safety is often lower near the beginning and ending points of a curve (PC and PT, respectively) than the curve midpoint (MC) due to the combination of several factors, such as the lack of fully-developed superelevation, speeds in excess of the curve speed, and possible braking or acceleration on the part of the driver (*6, 11*).

Bonneson and Pratt described a procedure for developing CMFs by using a cross-sectional study and further calibrated a CMF for curve radius (*12*). This CMF is described as follows:

$$CMF_R = 1.0 + 0.106\left(\frac{5730}{R}\right)^2 \quad (4)$$

The base condition for this CMF is no curvature present (i.e., $R = \infty$). For the base condition, the CMF logically bounds to a value of 1.0. CMFs with a similar functional form have been calibrated by others (*6, 13*) and are compared in Figure 1.

Gooch et al. quantified the safety performance of horizontal curves on two-lane rural highways using the propensity scores-potential outcome framework (*14*). Data on about 10,000 miles of highways in Pennsylvania with eight years of crash records were analyzed. The results indicate that the presence of a horizontal curve and its degree of curvature are the most significant variables associated with crash frequency. A CMF for horizontal curves as a function of curve radius was developed as follows:

$$CMF_R = e^{\left(0.053I_c + \frac{309.4}{R}\right)} \quad (5)$$

where:

I_c = indicator variable for curve presence (= 1.0 if a curve is present, 0.0 otherwise).

As was the case with Equation 4, the base condition for this CMF is no curvature present, in which case the CMF logically bounds to a value of 1.0. Fitzpatrick et al. calibrated a CMF with a similar functional form but omitting the indicator variable (*15*). These CMFs are shown in Figure 2 along with the CMF for two-lane highways from reference *6* for comparison.

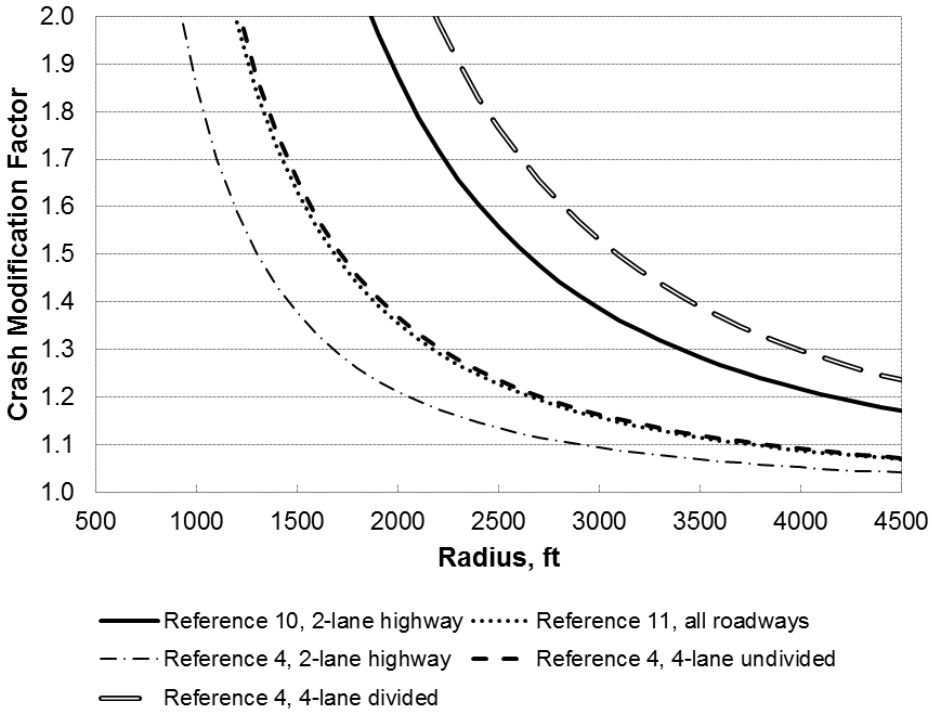

Figure 1. Curve Radius CMFs.

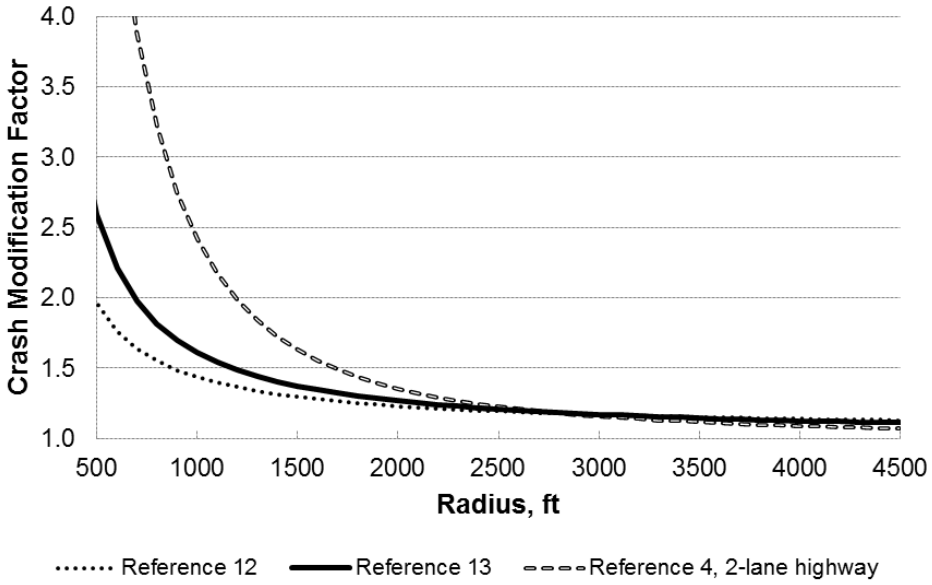

Figure 2. Curve Radius CMFs.

Banihashemi investigated the influence of horizontal curves on crash risk on rural multilane highways (*16*) and urban arterials (*17*). The research included five years (2007 through 2011) of crash data on more than 200 miles of multilane highways in Washington State. A cross-sectional modeling method was used to calibrate the curve radius CMFs for rural multilane highways and urban arterials that are presented in Equations 6 and 7, respectively.

$$CMF_R = \begin{cases} 1.0, \text{tangent} \\ \max\left(1.0, \frac{197.6}{R^{0.633}}\right), \text{curve} \end{cases} \quad (6)$$

$$CMF_R = \begin{cases} 1.0, \text{tangent or curve with } R > 1320 \text{ ft} \\ \frac{537.77}{R^{0.875}}, \text{curve with } R \leq 1320 \text{ ft} \end{cases} \quad (7)$$

Wu et al. (*10*) improved the methodology used by Banihashemi and developed the following CMF for horizontal curves on rural two-lane undivided highways using five years of Texas crash data:

$$CMF_R = \frac{196.4}{R^{0.65}} \quad (8)$$

The preceding three CMFs are shown in Figure 3 along with the CMF for two-lane highways from reference *6* for comparison.

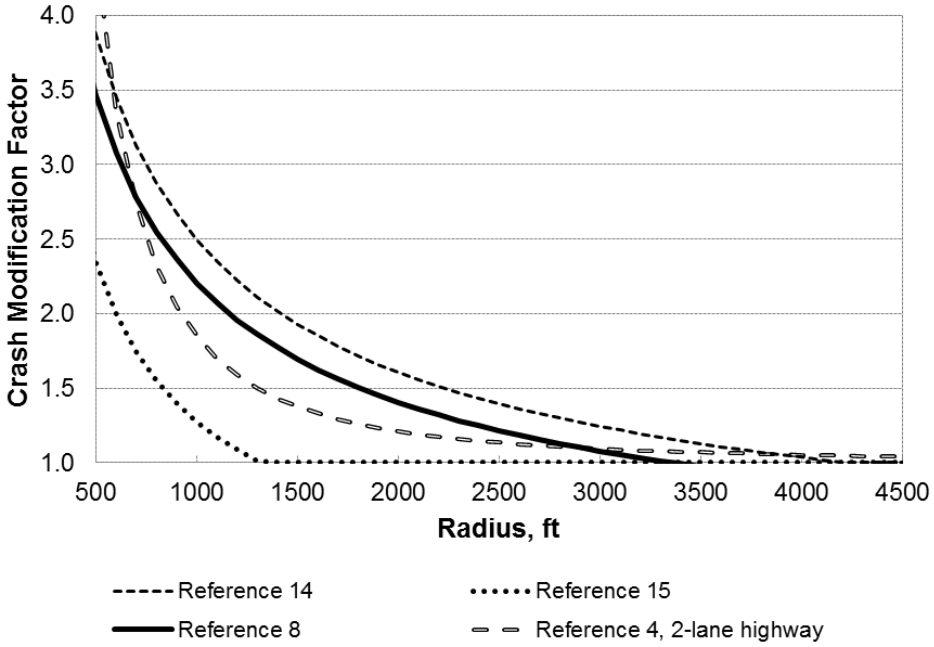

Figure 3. Curve Radius CMFs.

Superelevation Rate

Harwood et al. (*9*) developed a CMF for superelevation deficiency, as follows:

$$CMF_{SD} = \frac{1.22 + \frac{1604}{R} + \frac{9.52}{SD}}{1.22 + \frac{1604}{R}} \quad (9)$$

where:

CMF_{SD} = superelevation deficiency CMF.
SD = superelevation deficiency (superelevation rate subtracted from design superelevation rate), percent.

They considered the fact that superelevation deficiency is more important on sharper curves (i.e., smaller radius), and revised the CMF as follows (*5*):

$$CMF_{SD} = \begin{cases} 1.0, SD < 0.01 \\ 1.0 + 6(SD - 0.01), 0.01 \leq SD < 0.02 \\ 1.06 + 3(SD - 0.02), SD \geq 0.02 \end{cases} \quad (10)$$

Figure 4 illustrates this CMF.

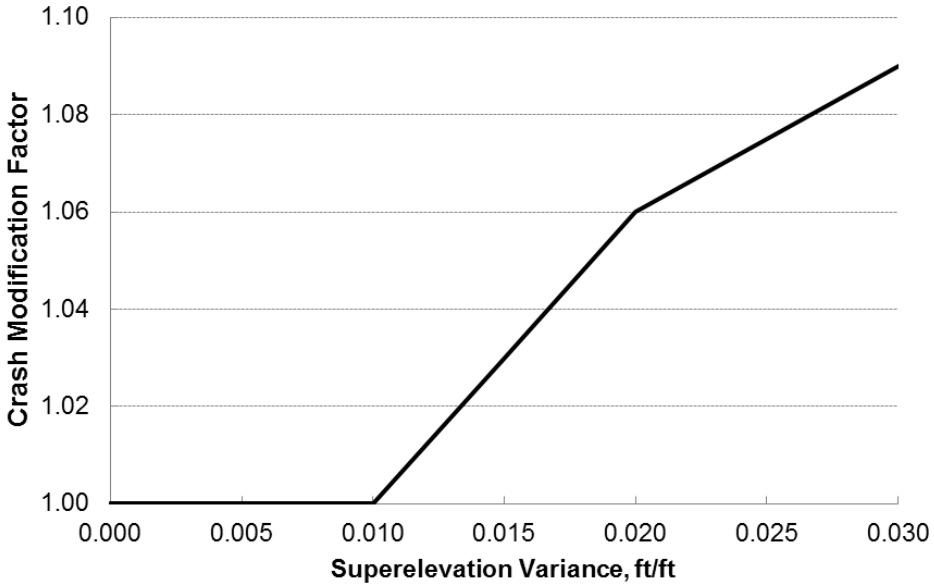

Figure 4. Superelevation Deficiency CMF (*5*).

Curve Traffic Control Devices

In order to reduce the number and severity of crashes on horizontal curves, safety practitioners have proposed various types of traffic control device treatments, such as curve warning signs, chevrons, and delineators. Some studies have evaluated the effects of these traffic control devices on reducing horizontal curve-related crashes.

Lalani (*18*) collected crash records one year before and after the installation of Chevrons at three sites in California. A naïve before-after comparison showed the crashes reduced by 64 percent in the after period (i.e., CMF = 0.36).

Srinivasan et al. (*19*) obtained geometric, traffic, and crash data at 89 treated curves in Connecticut and 139 treated curves in Washington to determine the safety effectiveness of improved curve delineation. The researchers conducted an empirical Bayes (EB) before-after

analysis to account for potential selection bias and regression-to-the-mean bias. Results revealed an 18.0 percent reduction in injury and fatal crashes, a 27.5 percent reduction in crashes during dark conditions, and a 25.0 percent reduction in lane departure crashes during dark conditions. The combined CMF, using meta-analysis, is 0.86. This is a little higher than that provided by TxDOT's Work Code Table (i.e., 0.75). Srinivasan et al. conducted a further economic analysis. Results revealed that improving curve delineation with signing improvements is a very cost-effective treatment with the benefit-cost ratio exceeding 8:1. More recently, Choi et al. (*20*) analyzed the safety effect of Chevrons on three freeways in Korea using an EB before-after study. Their estimated CMF for installing Chevron signs is 0.72, which is fairly close to the result found by Srinivasan et al. (*19*).

Montella (*21*) comprehensively evaluated the safety effectiveness of improving horizontal curve delineation. The researcher collected crash data at 15 curves in Italy and performed an EB before-after study. Total, nighttime, daytime, rainy, non-rainy, run-off-road (ROR), and property-damage-only crashes reduced significantly after improving curve delineation. Specifically, total crash reduced by about 39.4 percent. The most effective treatment was the installation of curve warning signs, Chevron signs, and sequential flashing beacons along the curve. Table 1 lists the CMFs for these treatments.

Table 1. Curve Delineation CMFs.

Crash Type	Chevrons	Curve Warning Sign and Chevrons	Curve Warning Sign, Chevrons, and Beacon
Total	0.97	0.59	0.52
Nighttime	1.92	0.66	0.23
Daytime	0.63	0.56	0.63
Rainy	0.41	0.49	0.56
Non-Rainy	1.27	0.69	0.48
ROR	0.90	0.56	0.52
Non-ROR	1.29	0.76	0.53
Injury	1.46	1.18	0.62
Property-damage-only	0.83	0.46	0.44

Tsyganov et al. (*22*) studied the safety effects of edgelines on rural two-lane highways. Their research found that edgelines on rural two-lane roadways may reduce crash frequency up to 26 percent and the highest safety impacts occur on curved segments of roadways with lane widths of 9 to 10 ft. As such, researchers estimated CMFs for installing edgeline markings on rural two-lane curves as 0.67 (for 9-ft-wide lanes) and 0.74 (for 9- to 11-ft lanes).

Elvik and Vaa (*23*) reviewed previous studies and provided the CMF for the Combination Horizontal Alignment and Advisory Speed sign as 0.87.

Weather

Weather-related crashes are those that occur in the presence of rain, sleet, snow, fog, wet pavement, snowy/slushy pavement, and/or icy pavement. Weather acts through visibility impairments, precipitation, high winds, and temperature extremes to affect driver capabilities, vehicle performance (i.e., traction, stability, and maneuverability), pavement friction, and

roadway infrastructure. These impacts can increase crash risk and severity. Several studies have been conducted on driver behavior and crashes during rainfall or snowfall. Examination of free-flow speeds on curved highway sections in rural New York State illustrated that drivers did not reduce speeds sufficiently on curves during wet-pavement conditions (*24*). The investigators concluded that drivers did not recognize that pavement friction is lower on wet pavement as compared with dry pavement.

In a study of crashes during and after rain events in Calgary and Edmonton, Canada (*25*), investigators concluded that crash risk during rainfall was 70 percent higher than crash risk under clear, dry conditions. In an assessment of weather and seasonal effects on highway crashes in California (*26*), weather was found to be a major factor. On very wet days, crash frequency was twice the rate on dry days. Using data from the United States and Israel, researchers analyzed crash risk during rainy weather (*27*). They learned that injury crash risk was two to three times higher than in dry conditions. Researchers also reported that crash risk was greater when rain followed a period of dry weather.

Jackson and Sharif (*28*) used fatal crash data and geospatial analysis to examine the temporal and spatial distribution of rain-related fatal crashes in Texas from 1982 to 2011. The data obtained from the Fatality Analysis and Reporting System was used to identify spatial clustering patterns of rain-related fatal crashes and their correlation with rainfall and to compare them to spatial patterns of other crashes. Study results suggest that rain is a contributor to crashes in few counties but at less than 95 percent confidence in some of the wetter counties. The authors recommended that these counties should be the focus of further research and detailed analysis to identify underlying crash contributing factors.

EFFECTIVENESS AND SERVICE LIFE OF SURFACE TREATMENTS

The performance of a pavement treatment is defined as either the immediate or long-term improvement of a given performance indicator. These indicators may quantify the treatment's physical condition (e.g., surface distress), functional performance (e.g., skid resistance), or relate to user satisfaction (e.g., ride roughness). This research will focus on two functional performance indicators: skid resistance and crash reduction effectiveness. The distress condition of pavement treatments will also be considered.

For skid resistance and distress condition, immediate improvements, long-term improvements, and treatment service life will be evaluated. Figure 5 illustrates how each of these terms is defined in relation to a pavement performance curve. The blue line represents the condition of the pavement over time. At year 14, a treatment is applied, resulting in an immediate performance improvement. Since the benefit of the treatment will degrade over time, the long-term improvement is defined as the area under the curve (but still above the predicted performance curve of no action and the failure criteria) until the benefit has returned to the performance level before the treatment. The time until the performance returns is the treatment service life.

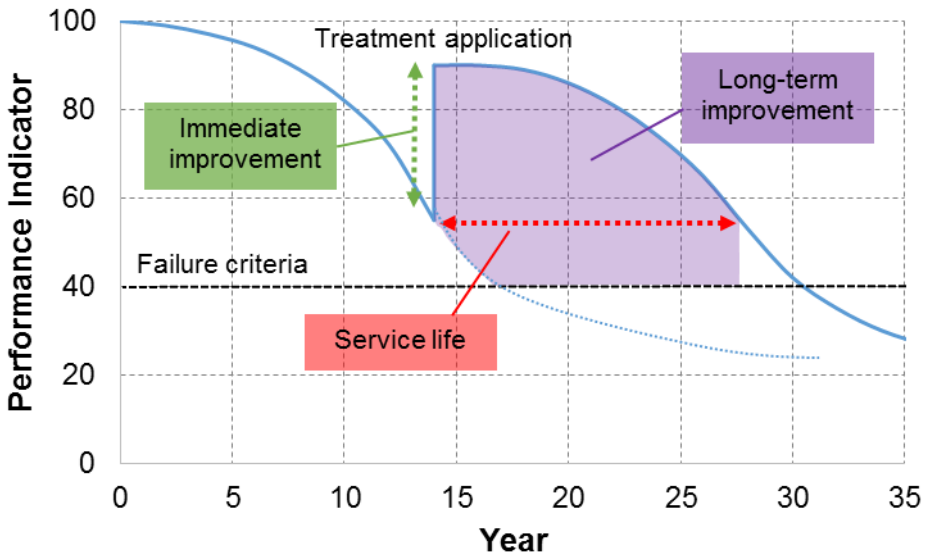

Figure 5. Performance Improvement of a Pavement Treatment.

When measuring crash reduction effectiveness, the analysis is performed by comparing the average annual crash rates for several years before and several years after installation. This analysis does not acutely consider the diminishing performance of a treatment with time as would an analysis on skid resistance or distress.

Treatment Descriptions

The following pavement treatments will be evaluated in this project:

- High friction surface treatment (HFST).
- Seal coat (chip seal).
- Thin asphalt overlay.
- Permeable friction course.
- Friction abrading or pavement texturing.
- Water blasting (for flushed seal coats).

This section defines each treatment and summarizes performance data from the literature. Appendix A contains details results from the literature review. One thorough research report on these treatments was performed by Merritt et al. (*29*), sponsored by the Federal Highway Administration (FHWA). Results from this report are cited several times throughout this review, especially as concerns crash reduction performance.

High Friction Surface Treatment

HFST is a safety-first pavement treatment intended to restore and maintain pavement friction to reduce crashes, especially around horizontal curves during wet weather (*30*). It is a thin layer of high-quality polish-resistant aggregate bonded to the pavement surface with polymer resin binder (see Figure 6). The most common aggregate used is calcined bauxite and the binder is often an epoxy resin or polyester resin.

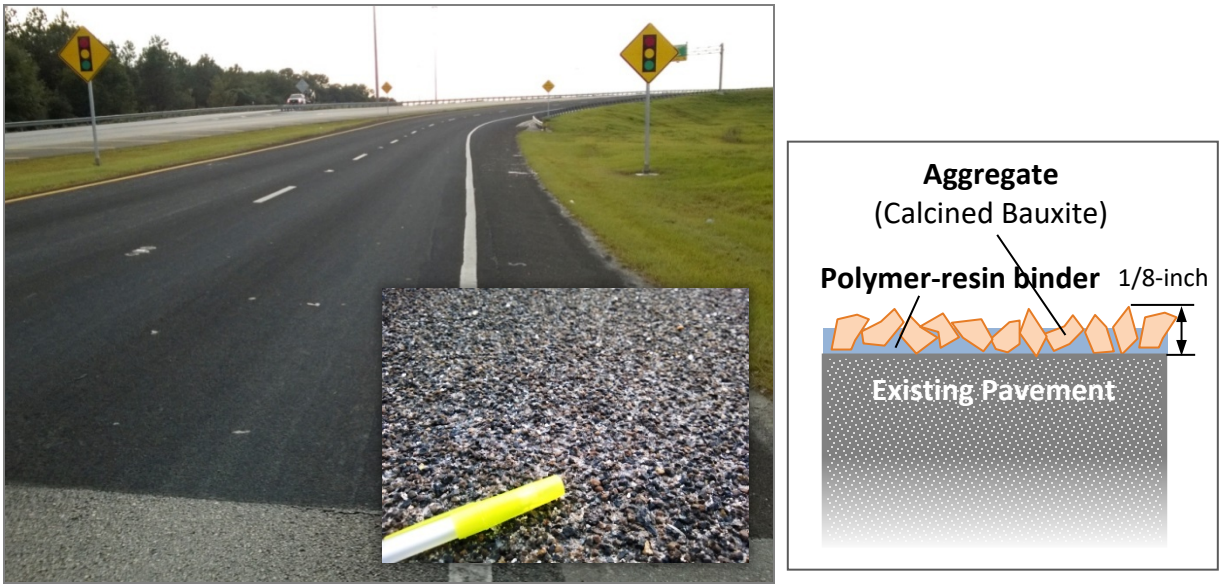

Figure 6. HFST.

Seal Coat

Seal coats, also known as chip seals and surface treatments, are a common inexpensive maintenance surface treatment in which a layer of asphalt emulsion or binder is overlaid by aggregate to seal the surface against oxidation and moisture (see Figure 7). Seal coats also provide a new aggregate wearing surface that improves skid resistance (*31*). Loss of skid resistance will occur over time, not just with polishing, but as the aggregates are shifted into more flat positions and especially as bleeding occurs (asphalt migrating to the surface).

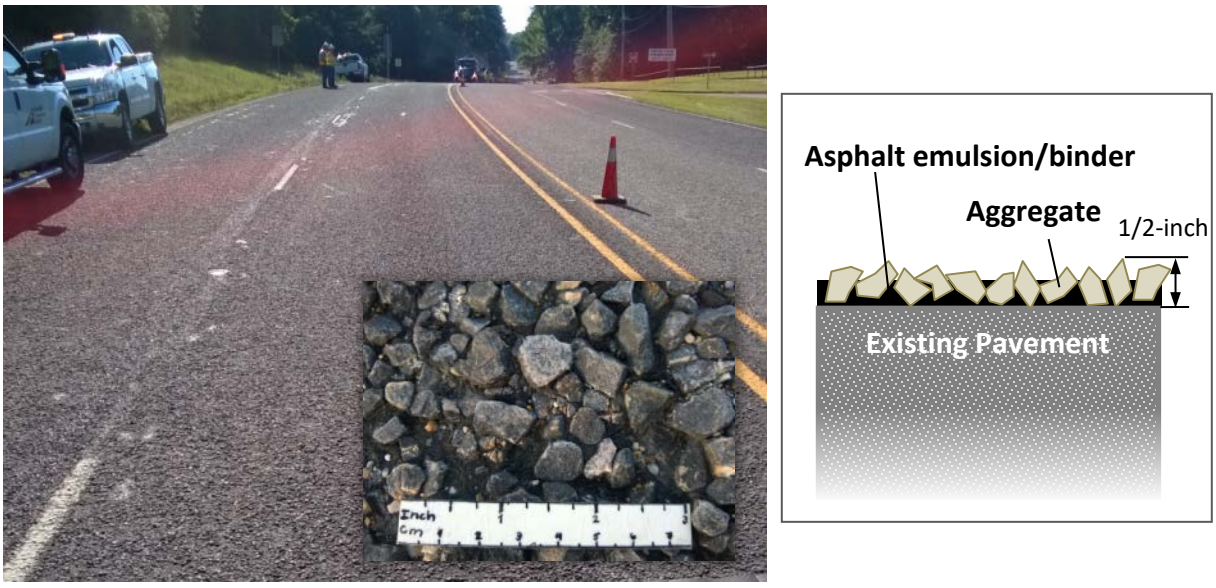

Figure 7. Seal Coat.

Thin Asphalt Overlay

A thin asphalt overlay is a thin lift of dense- or gap-graded asphalt concrete (AC), less than 1.5 in. thick (see Figure 8). They are used primarily for maintenance purposes and provide little in the way of structural capacity. Thin overlays are more expensive than seal coats but have the added benefit of resisting severe traffic movements (start-stop and turning), improving ride quality, and reducing noise. For these reasons, they are more often used for urban areas.

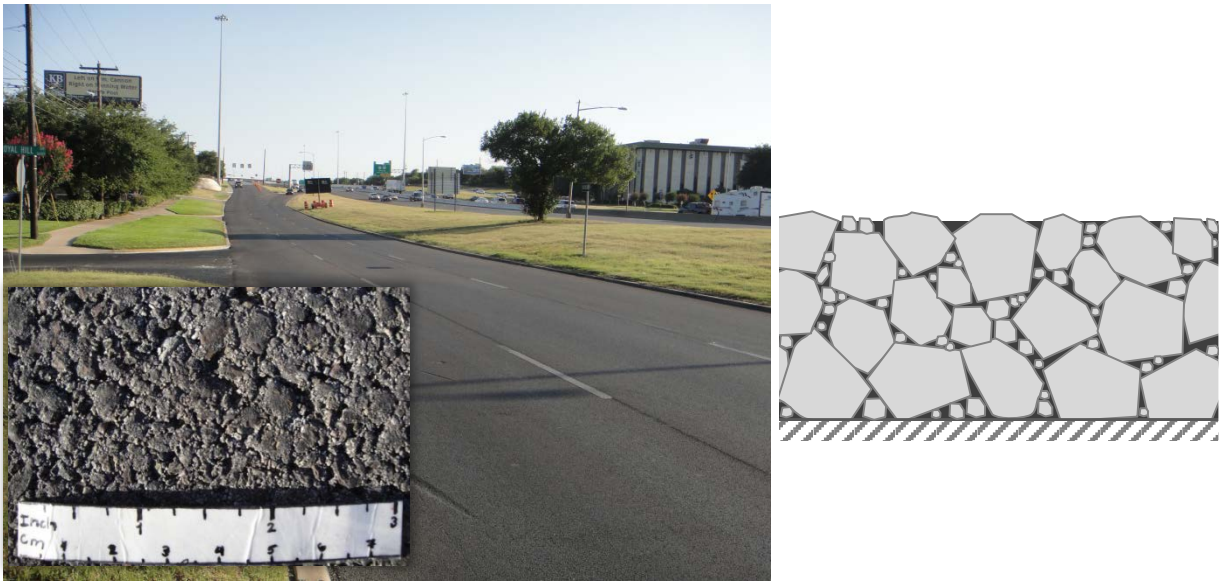

Figure 8. Thin Asphalt Overlay.

Permeable Friction Course

A permeable friction course (PFC) (or open graded friction course [OGFC]) is an open-graded hot mix asphalt (HMA) concrete laid at 1 to 2 in. thick (see Figure 9). It provides functional improvement to the existing pavement in terms water removal, reduced splash and spray, and skid. It is used in the areas of heavy rainfall but often not in colder climates due to inefficiency in freeze-thaw cycles and problems with black ice. PFC often uses higher quality materials than typical dense-graded HMA since the durability is compromised by the open-graded design.

Friction Abrading and Pavement Texturing

Diamond grinding is the process of remove a thin layer of concrete (typically less than 0.25 in.) with closely spaced saw blades. The process removes surface irregularities and improves skid resistance. Diamond grooving is a treatment in which the pavement surface is saw-cut (usually longitudinally) forming narrow grooves about 0.75 in. apart (see Figure 10).

Micro-milling, unlike diamond grinding, uses impact technique in which milling teeth would shave the surface to improve surface friction. Shot blasting or abrading removes the very top-most surface of concrete by projecting thousands of steel pellets or shots against the pavement, wearing off the aged surface. The loose shot is continuously picked off the pavement in the process.

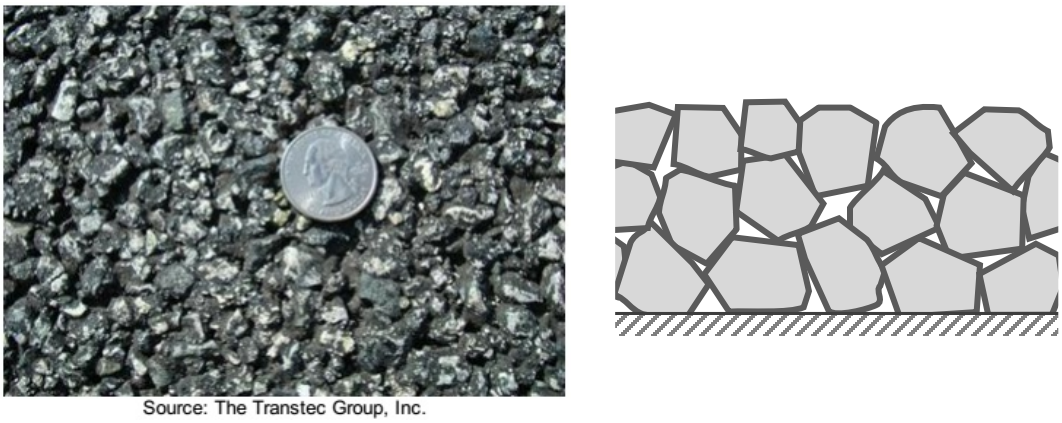

Source: The Transtec Group, Inc.

Figure 9. Surface Texture of PFC.

Source: The Transtec Group, Inc.

Figure 10. Grooved Surface (Left) and Diamond Ground Concrete Pavement Surface (Right).

Water Blasting

Water blasting is an emerging technology that used ultra-high pressure water to remove excess binder and impurities from a flushed seal coat pavement surface. The macrotexture of the road is restored, thus improving skid resistance (see Figure 11). The process does not improve the surface texture of the aggregate. Fine jets of ultra-high pressure water (36,000 psi) are directed onto the road surface at an ultrasonic velocity (Mach 1.5) (*32*).

Figure 11. Effects of Water Blasting Test (*32*).

Treatment Performance and Cost

Skid Resistance and Texture

Skid resistance is a measurement of the surface friction characteristics as measured with a tire. In the United States, this is most often performed with a locked wheel skid trailer at between 40 and 60 mph. Texas and a handful of other states use a smooth wheel for testing, while other states use a ribbed wheel. The values in Table 2 are average results only. The variation of each value within a treatment is considerably large, considering different aggregate types and seasonal variability. Most of these values also represent the skid resistance along simple tangent sections. In actuality, the skid number around horizontal curves is often much lower that before or after the curve.

Mean texture depth is a measurement of macrotexture (large scale texture variability). Macrotexture is an important component of skid resistance, especially for vehicles traveling at higher speeds and under wet conditions. Again, the values in Table 3 are typical values only.

Table 2. Skid Resistance for Various Pavement Treatments.

Treatment Type	Test Method *	Approximate Skid Number		Comments
		Initial	Terminal	
HFST	SK40R	< 70	< 60	Calcined bauxite
			55	Flint
Seal coats	SK60	60	55	
Thin asphalt overlays	SK (Smooth)	50	30	
PFC	SK40R	35–65	20–55	6-yr term
Shot blasting	N/A	53	48 (11 mo.)	
Abrading	N/A	48	38 (11 mo.)	
Water blasting	N/A	N/A	N/A	

* SK = skid number
N/A = not available

Table 3. Mean Texture Depth for Various Pavement Treatments.

Treatment Type	Approximate Mean Texture Depth, mm
HFST	> 1.5
Seal Coats	> 1.0
Thin Asphalt Overlays	0.4–0.6 (dense-graded), > 1.0 (stone-matrix asphalt)
PFC	1.5–3.0
Abrading and texturing	0.7–1.2 (grinding), 0.9–1.4 (grooving)
Water blasting	Varies (depends on aggregate)

Service Life

Service life is largely dependent on the existing pavement condition, traffic severity, and climate severity. Table 4 gives the typical service life of pavement treatments. A longer service life, in particular with high skid performance, increases the long-term benefit of a given safety treatment.

Table 4. Service Life for Various Pavement Treatments.

Treatment Type	Approximate Service Life, yr
HFST	7–12
Seal Coats	3–15
Thin Asphalt Overlays	8–15
PFC	10–15
Diamond grinding	8
Abrading and shot blasting	2
Water blasting	Data not available

Cost

Table 5 gives approximate unit costs of different treatment types. The most expensive treatment is HFST, and the cheapest are seal coats and water blasting. Some of these costs would change depending on the treatment thickness.

Table 5. Unit Cost for Various Pavement Treatments.

Treatment Type	Approximate Unit Cost
HFST	$\$21/yd^2$
Seal Coats	$\$1–\$2.50/yd^2$
Thin Asphalt Overlays	$\$3–\$6/yd^2$
PFC	$\$7/yd^2$
Diamond grinding	$\$1.70–\$6.70/yd^2$
Shot blasting (48-in. width)	$\$3/yd^2$
Abrading (72-in. width)	$\$2/yd^2$
Water blasting	$\$1/yd^2$ less expensive than the average strip/spot sealing

Summary of Treatment Safety Effectiveness

Table 6 summarizes CMFs for various pavement treatments. Most of these values are derived from statistically powerful studies, considering hundreds or thousands of miles of pavement, and comparing against appropriate reference sections. The CMFs for HFST, however, were obtained from far fewer study locations, and it was difficult to identify good reference sections. The data for abrading and texturing also did not have a significantly large sample size.

Table 6. Crash Reduction Performance for Various Pavement Treatments.

Treatment Type	Section Type	Crash Type	Approximate CMF Value 1	
			Average	Range
HFST	Curves and ramps, generally high-accident locations	Wet	0.34	0.14–0.48
		Total	0.72	0.65–0.75
Seal coats	Two-way and multi-lane roads (not high-accident specific)	Wet	0.76	0.42–1.60
		Total	1.15	0.83–1.52
Thin asphalt overlays	Multi lane roads and freeways	Wet	0.87	0.53–1.27
		Total	0.99	0.93–1.20
PFC	Freeways (California and North Carolina)	Wet	0.68	0.51–1.04
		Total	0.94	0.74–1.10
Abrading and texturing	California freeways	Wet	2.03	N/A
		Total	0.77	N/A
Water blasting	N/A	N/A	N/A	N/A

Notes:
1: CMF = 1 – crash reduction factor (CRF)/100
N/A = not available

The CMF values and ranges in Table 6 summarize various studies that were documented in the literature. Appendix A lists the studies individually.

Influence of Pavement Variables on Crash Frequency

The 1998 FHWA strategic plan defined a qualitative pavement condition term: pavement serviceability rating (PSR) or pavement serviceability index (PSI). International roughness index (IRI) is considered as the closest corresponding term. As an alternate to PSR/PSI, the American Society for Testing and Materials (ASTM) defined Pavement Condition Rating (PCR). It has a numerical index in between 0 to 100 where 0 indicates extremely poor pavement condition and 100 indicates excellent pavement condition. Rutting depth (RD), another measure of pavement condition, is defined as a depression into the pavement by vehicle wheels or by erosion. Finally, there is another indicator of pavement condition that is known as pavement surface deflection from the falling-weight deflectometer (FWD). It measures the magnitude and the shape of the deflection and is a function of pavement structure, traffic, temperature, and other associated factors. Among the several pavement performance indicators, IRI, PCR, RD, and FWD are mostly used in many studies. Pavement condition related safety studies can be divided into three broader groups:

- Studies that considered curve information as an explanatory variable.
- Studies that only considered safety analysis on curved roadways.
- Studies that did not account curve information as an explanatory variable.

The following paragraphs summarize the results of these three groups of studies.

Curve as an Explanatory Variable

There has been an abundance of past research investigating the association between pavement condition and crash frequencies or injury types. Many studies used horizontal curve related information as an explanatory variable while performing safety analysis. Short reviews on these studies are described here.

McCullough and Hankins (*33*) calculated a minimum desirable friction coefficient of 0.40 measured at 30 mph from a study of 571 sites in Texas. The study examined the relationship between skid resistance and crash frequencies. The findings showed that a large proportion of crashes occurred with low skid resistance and relatively few occurred with high skid resistance. The recommended value was obtained as an applicable value close to the point where the slope of the resultant curves decreased.

Larson (*34*) attempted to determine association between pavement surface properties and risk of crashes in France. The results showed that every reduction in surface friction of 0.05 increases the severity of crashes and increases the cost to society by nearly 50 percent. Moreover, severe injuries were found to be higher for shorter curve radius.

Xiao et al. (*35*) developed two fuzzy-logic models and evaluated using crash data and the corresponding traffic data collected from 123 sections of highway in Pennsylvania during 1984–1986. This study reported that an increase in skid resistance reduces the likelihood of crash occurrence on wet pavements. This study suggests that pavement skid resistance is one of the most important parameters that influence crash rate.

Tighe et al. (*36*) developed a systematic approach for the coordination of pavement maintenance programs with road safety improvement in Canada. This study developed a regression analysis technique to relate the crash rate with pavement condition indicators (IRI or PSR) and road geometric variables. Two multiplicative regression equations were established to best fit the data. Both models and their regression parameters were statistically significant at the 95 percent confidence level.

$$SVCR = 0.32IRI^{-0.73}(1 + HC)^{3.90}RHR^{0.64} \quad (11)$$

$$SVCR = 0.022PSR^{-1.49}(1 + HC)^{4.78}RHR^{0.55} \quad (12)$$

where:

SVCR = single-vehicle crash rate, crashes per million vehicle kilometers.
IRI = international roughness index, m/km.
HC = number of horizontal curves with degree of curve 5 or greater per kilometer of road segment.
PSR = pavement serviceability rating.
RHR = average roadside hazard rating.

Mayora and Pina (*37*) analyzed 10 years of crash data from two-lane rural roads on the Spanish National Road System and estimated a skid threshold. This study collected crash data from over 1085 miles of rural two-lane roadways with skid resistance values. The results showed that pavement friction improvement yielded significant reductions in wet-pavement crash rates averaging around 68 percent. The results confirmed the importance of maintaining adequate levels of pavement friction to safeguard traffic safety. Figure 12 shows crash rate for different alignments. It is seen that roadways with curves have higher crash rates than roadways with tangent in wet condition.

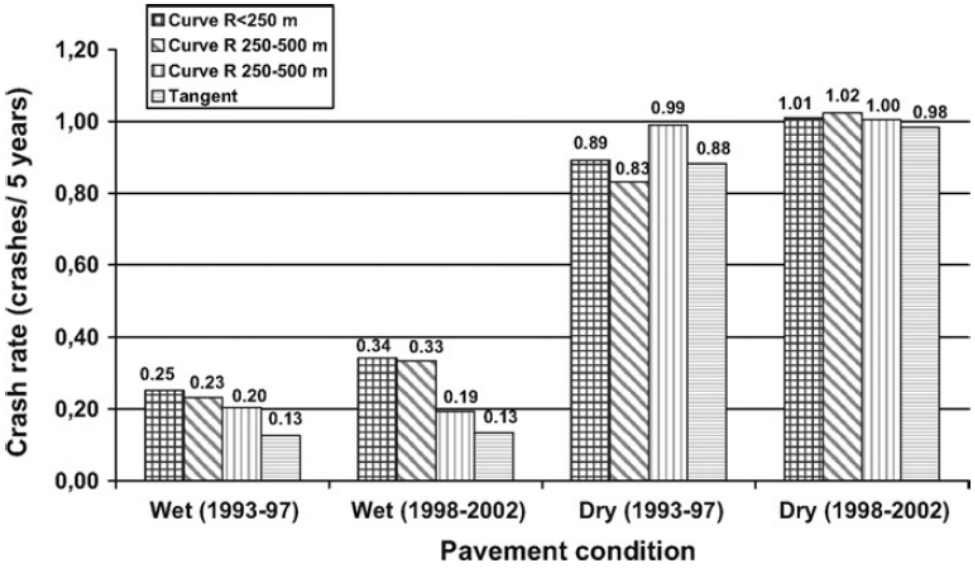

Figure 12. Crash Rates for Different Alignments (*37*).

Milton et al. (*38*) stated that the likelihood of a crash becoming fatal could be reduced by increasing pavement surface friction. This study allowed the possibility that estimated model parameters can vary randomly across roadway segments. This would help in accounting unobserved effects potentially relating to roadway characteristics, environmental factors, and driver behavior. Using traffic crash data from Washington State, a mixed logit model was estimated in this study. In this analysis, factors such as average daily traffic per lane, average daily truck traffic, truck percentage, interchanges per mile and weather effects are modeled as random-parameters; while other factors such as the number of horizontal curves, number of grade breaks per mile and pavement friction were considered as fixed parameters. The number of horizontal curves per mile in the roadway segment was found to be a fixed parameter that significantly reduced the likelihood of injury crashes for all roadway segments. This finding is consistent with the findings of Shankar et al. (*39*).

In the U.K., a policy establishes acceptable friction levels for different road and traffic situation. Table 7 summarizes the values taken with the Side force Coefficient Road Inventory Machine (SCRIM) device. Noyce et al. (*40*) determined the association between pavement surface friction and driver behavior. The results suggested that low skid resistance results in increased numbers of wet pavement crashes.

In the study of McCarthy et al. (*41*), skid resistance was measured with a continuous friction measurement, fixed-slip device called a GripTester. The GripTester constantly measures friction and the system reports an average measurement of friction, called a grip number (which is analogous to skid number), at 3-ft intervals. Negative binomial regression was used to relate the crash data to the average annual daily traffic (AADT), skid resistance, and horizontal radius of curvature. This study developed the following equation for primary routes:

$$\mu = e^{-0.25+0.37\ln(AADT)-GN+\frac{0.04}{R}} \quad (13)$$

where:

GN = grip number.

Table 7. U.K.'s Investigative Skid Resistance Values for Curves (*40*).

Skid Resistance Measure	Site Category	Skid Resistance Value
SCRIM at 30 mph	Curve with radius < 250 m not subject to 65 km/h speed limit or lower	0.45
SCRIM at 12 mph	Curve with radius < 100 m not subject to 65 km/h speed limit or lower	0.55

Considering Curved Roadway Crash Data

There has been limited research that focused on a curve-only safety analysis by using pavement condition data. Buddhavarapu et al. (*42*) attempted to establish a relationship between crash severities on horizontal curves and pavement surface condition indices. This study used two TxDOT maintained databases: (a) Crash Record Information System (CRIS) data, and (b) Pavement Management Information System (PMIS) data. These two data sets are linked using data fields such as crash location and crash year to create an assimilated database. The combined data set contains information pertaining to 22,199 crashes that occurred on a total of two-lane horizontal curves during 2006–2009. Five different pavement condition indices were used for analysis: (a) Skid Index, (b) Distress Index, (c) Ride Index, (d) IRI, and (e) Condition Index. This study used an ordered probit response model structure for severity modeling. The findings are:

- Skid number was poorly correlated with crash injury severity on two-lane horizontal curves.
- The Distress Index and IRI were found to have a statistically significant effect on crash injury severity.

Pratt et al. calibrated skid number CMFs for rural highways using the TxDOT crash, curve, and pavement management databases (*2*). Their analysis included only curved highway segments, and was repeated for all crashes, ROR crashes, wet-weather crashes, and wet-weather ROR crashes, for an assumed base-condition skid number of 40. Their results showed that higher skid resistance reduces the frequency of all crash categories but has a greater effect on wet-weather crashes. This result is intuitive because even relatively low skid resistance is typically adequate for dry-weather conditions. The skid number CMFs are described as follows:

$$CMF_{SK} = e^{\beta_5(SK-40)} \quad (14)$$

where:

SK = skid number.
β_s = calibration coefficient.

Table 8 provides the calibration coefficients for the models calibrated by Pratt et al.

Table 8. Skid Number CMF Calibration Coefficients.

Roadway Type	Skid Number CMF Calibration Coefficient by Crash Type	
	Total Crashes	Wet-Weather Crashes
Two-Lane Undivided	−0.0032	−0.0189
Four-Lane Undivided	−0.0077	−0.0331
Four-Lane Divided	−0.0071	−0.0319

Curvature Not Used as an Explanatory Variable

There has been an abundance of past research investigating the association between pavement condition and crash frequencies. Many researchers did not use horizontal curve related information in their studies. That is, the safety analyses focused on roadways in general, not specifically on curves, and did not necessarily take curvature into account.

Chan et al. (*43*) used the Tennessee Pavement Management System and crash data to investigate the relationship between crash frequency and pavement distress variables. Focusing on four urban interstates with asphalt pavements, divided median types, and 55 mph speed limits, 21 negative binomial regression models were developed to predict crash frequencies based on different pavement condition variables, including RD, IRI, and PSI. This study suggested that the PSI crash prediction models should be considered as a comprehensive approach to integrate the highway safety factors into the pavement management system.

Li et al. (*44*) linked TxDOT CRIS data and PMIS data to examine the impact of pavement conditions on traffic crashes in depth. The results in general suggested that poor pavement condition scores and ratings were associated with proportionally more severe crashes, but very poor pavement conditions were actually associated with less severe crashes. This implies that drivers usually drive slowly on poorly maintained roadways. Due to the behavioral adaptation, very good pavement conditions might induce speeding behaviors and therefore could have caused more severe crashes, especially on non-freeway arterials. In addition, the results showed that the effects of pavement conditions on crash severity were more evident for passenger vehicles than for commercial vehicles.

Using two years (2008–2009) of crash data on Texas non-freeway flexible pavements, Li and Huang (*45*) analyzed the association between four key pavement condition scores and crash rates. The results overwhelmingly suggest that very good pavement conditions coincide with much lower crash rates compared with very poor conditions.

Zeng et al. (*46*) quantitatively evaluated the safety effectiveness of good pavement conditions versus deficient pavement conditions on rural two-lane undivided roadways in Virginia. The results of the EB method shows that good pavements could reduce fatal and injury crashes by 26 percent compared with deficient pavements, but good pavements did not have a statistically significant impact on overall crash frequency. Further analysis indicated that there was no statistically significant change in the safety benefit of improvements in pavement condition for fatal and injury crashes as the lane or shoulder width increased.

Najafi et al. (*47*) used New Jersey crash data and pavement condition data to develop regression models to examine the effect of friction on the rate of wet- and dry-condition vehicle crashes for various types of urban roads. The findings showed that friction is not only associated with the rate of wet-condition vehicle crashes, but it also influences the rate of dry condition vehicle crashes.

A before-after examination of wet-weather crashes and pavement friction on several rural highway types was conducted by Blackburn et al. (*48*). They derived the relationship between skid number and wet-pavement crash rate that is illustrated in Figure 13. As expected, wet-weather crash rates are highly influenced by pavement friction.

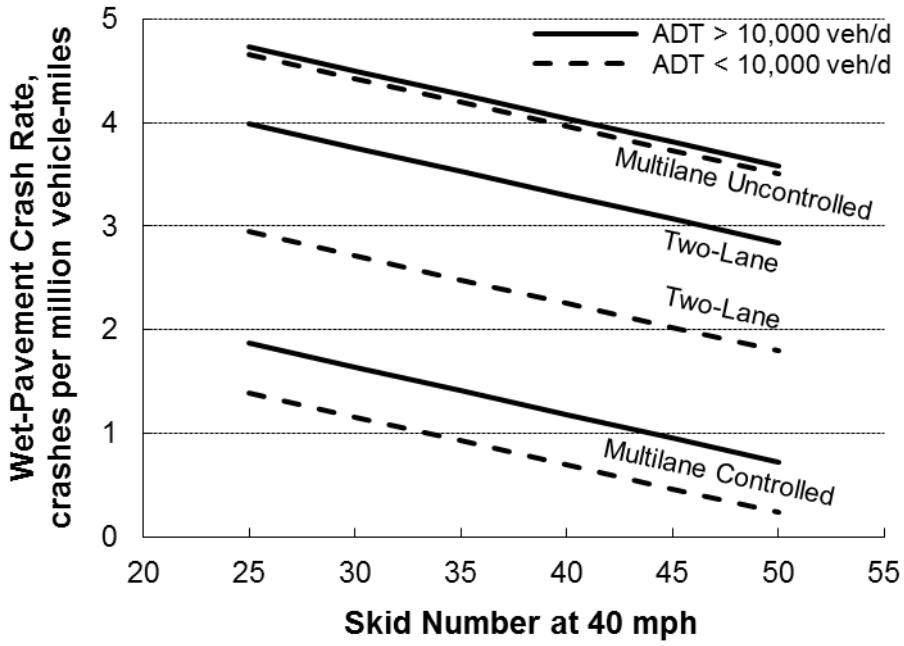

Figure 13. Relationship between Pavement Friction and Wet-Weather Crash Rate (*48*).

If the trends in Figure 13 for multilane uncontrolled-access and controlled-access highways are averaged, the following observations can be derived:

- On two-lane highways, the crash rate for a skid number of 25 is about 1.30 times the crash rate for a skid number of 40, while the crash rate for a skid number of 50 is about 0.80 times the crash rate for a skid number of 40.

- On multilane highways, the crash rate for a skid number of 25 is about 1.56 times the crash rate for a skid number of 40, while the crash rate for a skid number of 50 is about 0.63 times the crash rate for a skid number of 40.

The proportions stated in the preceding observations can be interpreted as CMF values for a base skid number of 40.

Wu et al. analyzed TxDOT's databases and developed guidance for incorporating skid resistance in pavement management decision-making (*49*). Their analysis included several crash rate ratio models, which included components that can be interpreted as skid number CMFs. Their CMFs for total crashes and wet-weather crashes are described by Equations 15 and 16, respectively:

$$CMF_{SK} = 3.894e^{-0.04605\,SK} \quad (15)$$

$$CMF_{SK} = 5.023e^{-0.05292\,SK} \quad (16)$$

De Leon Izeppi et al. used continuous friction measuring equipment to collect a continuous profile of grip number measurements and merged these data with crash and roadway data for analysis (*50*). They developed CMFs for grip number, a measurement that they described as "similar to a locked wheel with a smooth tire." Their CMFs for interstate highways, primary highways, and secondary highways are described by Equations 17, 18, and 19, respectively:

$$CMF_{GN} = e^{-1.19GN} \quad (17)$$

$$CMF_{GN} = e^{-1.00GN} \quad (18)$$

$$CMF_{GN} = e^{-0.56GN} \quad (19)$$

Grip number is reported in decimal quantities (0.0–1.0), while skid number is reported as a percentage (0–100).

Comparison of Skid Number CMFs

A comparison of the skid number CMFs described by Equations 14–19 is provided in Figure 14 (for total crashes) and Figure 15 (for wet-weather crashes). All CMFs were adjusted as needed to achieve a common base condition of *SK* = 40 for comparison.

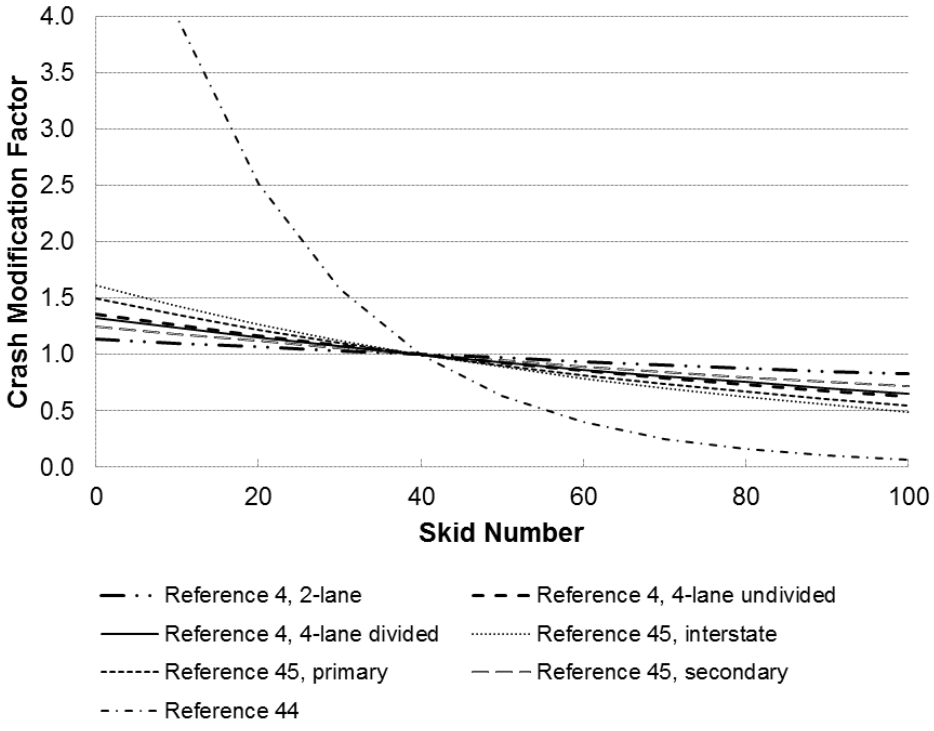

Figure 14. Skid Number CMFs for Total Crashes.

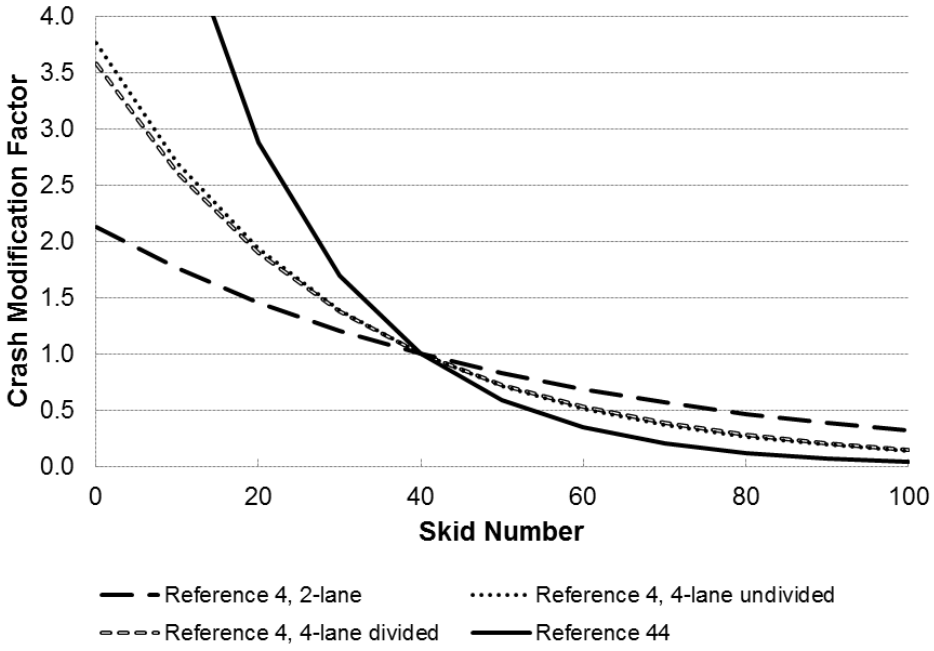

Figure 15. Skid Number CMFs for Wet-Weather Crashes.

The CMFs show similar trends for wet-weather crashes and, with one exception, for total crashes. The slopes of the lines are higher for wet-weather crashes, showing that skid resistance has a greater effect on wet-weather crashes than on dry-weather crashes (which will represent

most crashes overall). The exception is the total-crash skid number CMF from Wu et al. (*49*). Compared to the other total-crash skid number CMFs, theirs shows high sensitivity.

STATE AGENCY PRACTICES

TxDOT's procedures for selecting paving materials are described in the *Pavement Design Guide* (*4*). This *Guide* provides a general description for the state's Wet-Surface Crash Reduction Program (WSCRP). Key highlights of the WSCRP include the following:

- Crash analysis: TxDOT is charged to develop and implement methods to detect and improve pavement in areas with notable numbers of wet-surface crashes though a query of crash records.
- Aggregate selection: TxDOT maintains a list of pavement aggregates that are categorized based on frictional and durability characteristics. This list is available to practitioners who are seeking to choose aggregates for paving.
- Skid testing: TxDOT collects skid resistance data on state-maintained roadways and archives these data in the PMIS database.

As an appendix to the *Guide*, TxDOT provides Form 2088, which is titled "Surface Aggregate Selection Form." This form provides a qualitative framework for conducting a margin of safety analysis while selecting pavement aggregates. The analysis includes consideration of rainfall rate, wet-surface crash percentage, degree of curve, pavement cross slope, and aggregate type, among other variables. Based on the principles of this form, Pratt et al. (*2*) developed a more detailed margin-of-safety analysis tool that can be implemented using a spreadsheet.

A review of other state DOT websites revealed that most states have documents describing material specifications for pavement friction treatments, but relatively few guidance documents exist that provide explicit guidance on identifying problems and selecting treatments. At the national level, HFST received increased attention when they were recognized as a proven countermeasure in FHWA's Every Day Counts 2 initiative (*51*).

To gain further insight into the practices of TxDOT and other state DOT practitioners, researchers conducted an online survey. The purpose of this survey was twofold: 1) obtain more insights into best agency practices (which may be insightful if not thoroughly documented), and 2) identify materials that should be included in the field and laboratory testing task later in this research project. The following sections provide the questions for this survey and summarize the responses.

Survey Questions

Introduction

Q1. Are you willing to take this survey?
Q2. If you can recommend someone else who can take this survey and would be a good contact? We would appreciate it if you could please give us the person's contact information.

Q3. Please provide your contact information. Remember, all responses will be kept confidential and will be reported only in anonymous or aggregated format. You may leave the fields blank if you wish to remain anonymous.

Item	Fill-in box
Name	
Agency	
District / division	
Title	
Phone number	
E-mail address	

Q4. What is your role in monitoring safety or pavement maintenance trends? Check all that apply.

Item	Check box
Safety and crash data analysis	
Pavement monitoring and maintenance	
Project planning or programming	
Traffic operations	
Roadway design	
District- or division-level engineering or decision-making	
Other (please describe)	

Best Practices

We want to ask you about:

- How your agency monitors pavement friction on highway curves.
- How you choose which curves deserve pavement friction treatments.
- What types of treatments you would consider.

A pavement friction treatment includes any type of treatment intended to improve skid resistance and friction, including the following:

- A conventional material like chip seal (seal coat) or hot-mix asphalt (HMA), if installed more frequently or ahead of schedule due to concerns about pavement friction.
- A higher-quality material like ultra-thin bonded wearing course (UTBWC, formerly known as NovaChip) or PFC.
- A premium material like a high-friction surface treatment (HFST) using calcined bauxite.
- Methods to modify the existing pavement texture, such as abrading, micro-milling, and ultra-high-pressure water cutting.

For the following questions, please consider only treatments that were implemented (or accelerated) specifically because of concerns about skid resistance and friction, not treatments that are installed as part of normal maintenance operations.

Q5. What percentage of your roadway network is covered by skid testing efforts in a given year?

Q6. Which criteria or thresholds does your agency use to identify and rank curves for pavement friction treatments? Check all that apply.

Item	Check box
Stay with routine maintenance schedule.	
Consider presence of visual distress (e.g., bleeding, flushing, polishing, raveling).	
Analyze crash history.	
Choose sites based solely on skid number (please specify threshold if applicable).	
Rank based on skid number and roadway functional class (please specify thresholds if applicable).	
Conduct a margin-of-safety analysis accounting for pavement characteristics and curve geometry.	
Conduct a benefit-cost analysis.	
Other (please describe)	
None/not applicable	

Q7. Do you have copies of written policies or practices about site identification and ranking that you are willing to share?

Q8. What types of curve pavement friction treatments has your agency implemented in the past 10 years? Please consider treatments intended to address skid resistance on specific curves, not routine maintenance activities.

Treatment	Frequency (allow one choice per row)			
	Never	Once or twice	Less than annually (3–9 times)	At least annually (10 or more times)
HFST				
UTBWC or PFC				
Thin HMA overlay				
Chip seal (seal coat)				
Abrading or micro-milling (texturing)				
Ultra-high-pressure water cutting (for bleeding or flushed seal coats)				
Other (please describe)				

Q9. Which aggregate types have you used in your friction treatments? (Select all that apply.)

Aggregate Type in Treatment	Check box
Calcined bauxite	
Flint	
Granite	

Trap rock (basalt)	
Expanded shale (lightweight aggregate)	
Sandstone	
Gravel	
Limestone	
Other (please describe)	

Study Sites

We want to identify sites within the state where friction treatments have been implemented on curves within the past 10 years. Our goal is to query crash records and conduct a before-after study to assess the effectiveness of the treatment. Ideally, the following data would be available to share:

- Approximate construction date (month and year).
- Treatment design (type and layout).
- Construction plans.
- Historic skid data before and after installation.
- Historic crash data before and after installation.

Q10. Do you have this information available for one or more curve sites in your jurisdiction? (Allow them to indicate yes for conventional treatments and/or yes for special treatments.)

(If the answer to Q10 is yes) Thank you, we may follow up with you later about your site(s).

Survey Responses

A total of 12 people completed the survey. All 12 respondents were TxDOT district personnel, representing districts from both eastern and western parts of Texas. The respondents' descriptions of their roles in safety and pavement maintenance monitoring are provided in Table 9. Most respondents indicated that they are involved with monitoring safety and pavement maintenance, district-level decision-making, project planning, and traffic operations.

Table 9. Survey Respondents' Roles.

Response	Count
Safety and crash data analysis	10
Pavement monitoring and maintenance	11
Project planning or programming	8
Traffic operations	8
Roadway design	2
District- or division-level engineering or decision-making	11
Other (please describe)	0

When asked how much of their district's roadway network is covered by skid testing each year, most of the respondents stated that their networks are covered every 2–4 years. Three respondents stated that 25 percent of their network is tested every year (which corresponds to a four-year rotation), four respondents stated 30–35 percent (which corresponds to a three-year rotation), two respondents stated 50 percent (which corresponds to a two-year rotation), and one respondent stated 75 percent. Two respondents did not provide a response to this question.

When asked about criteria or thresholds used to prioritize curves for pavement friction treatments, all the respondents stated that they consider visual pavement distress and crash history (see Table 10). Half of the respondents stated that they typically stay with their routine maintenance schedule. A few respondents acknowledged choosing sites for treatment based on measured skid numbers, benefit-cost analysis, or roadway geometry.

Table 10. Criteria and Thresholds for Applying Pavement Friction Treatments.

Criterion or Threshold	Count
Stay with routine maintenance schedule.	6
Consider presence of visual distress (e.g., bleeding, flushing, polishing, raveling).	12
Analyze crash history.	12
Choose sites based solely on skid number (please specify threshold if applicable).	3
Rank based on skid number and roadway functional class (please specify thresholds if applicable).	1
Conduct a margin-of-safety analysis accounting for pavement characteristics and curve geometry.	1
Conduct a benefit-cost analysis.	2
Other: Consider roadway geometry	1
None/not applicable	0

The respondents stated that their most commonly used pavement friction treatments include chip seal and thin HMA overlays, followed by abrading and micro-milling, UTBWC, and PFC. Half of the respondents have seen HFSTs used once or twice in their district. Table 11 shows the full summary of the respondents' answers to the question about treatment implementation frequency. The respondents indicated that limestone is the most commonly used aggregate in pavement friction treatments (8 responses), followed by calcined bauxite and granite (5 responses each) and expanded shale and gravel (4 responses each). These responses are shown in Table 12.

Table 11. Pavement Friction Treatment Implementation Frequency by Type.

Treatment	Frequency (Number of Responses)			
	Never	Once or twice	Less than annually (3–9 times)	At least annually (10 or more times)
HFST	6	6	0	0
UTBWC or PFC	7	1	3	1
Thin HMA overlay	2	3	4	3
Chip seal (seal coat)	1	1	1	9
Abrading or micro-milling (texturing)	3	3	4	2
Ultra-high-pressure water cutting (for bleeding or flushed seal coats)	12	0	0	0
Other: Mill and inlay	0	0	1	0
Other: Polymer surface treatment	0	0	1	0
Other: Unspecified	0	0	0	1

Table 12. Pavement Friction Treatment Aggregate Types.

Aggregate Type in Treatment	Number of Responses
Calcined bauxite	5
Flint	0
Granite	5
Trap rock (basalt)	2
Expanded shale (lightweight aggregate)	4
Sandstone	3
Gravel	4
Limestone	8
Other: Rhyolite	1

OTHER ISSUES

Design Considerations

The TxDOT *Roadway Design Manual* (RDM) (*52*) contains basic guidance on horizontal alignment of highways in Chapter 2, Section 4. Under "General Considerations for Horizontal Alignment," the RDM states that there are a number of general considerations that are important in achieving safe, smooth-flowing, and aesthetically pleasing facilities. The practices described below are particularly applicable to high-speed facilities:

- Flatter than minimum curvature for a certain design speed should be used where possible, retaining the minimum guidelines for the most critical conditions.
- Compound curves should be used with caution and should be avoided on main lanes where conditions permit the use of flat simple curves. Where compound curves are used, the radius of the flatter curve should not be more than 50 percent greater than the radius of the sharper curve for rural and urban open highway conditions. For intersections or

other turning roadways (such as loops, connections, and ramps), this percentage may be increased to 100 percent.

- Alignment consistency should be sought. Sharp curves should not follow tangents or a series of flat curves. Sharp curves should be avoided on high, long fill areas.
- Reverse curves on high-speed facilities should include an intervening tangent section of sufficient length to provide adequate superelevation transition between the curves.
- Broken-back curves (two curves in the same direction connected with a short tangent) should normally not be used. This type of curve is unexpected by drivers and is not pleasing in appearance.
- Horizontal alignment and its associated design speed should be consistent with other design features and topography. Coordination with vertical alignment is discussed in "Combination of Vertical and Horizontal Alignment" in Chapter 2, Section 5.

Chapter 2, Section 4 also provides guidance for minimum curve radii, superelevation rate, and transition areas, and recommended sight distance on horizontal curves.

Chapter 4 of the RDM describes additional guidance for non-freeway rehabilitation (3R) design criteria. In Section 2, on Design Characteristics, it states that 3R projects will typically involve minor or no changes in either vertical or horizontal alignment. However, straightening of curves or other improvements may be considered where suggested by crash history, or where existing curvature is inconsistent with prevailing conditions within the project or on similar roadways in the area. Where appropriate, improvements in superelevation may also be a consideration. Substantial changes in existing horizontal and/or vertical alignment are considered reconstruction, and these projects should be developed to reconstruction standards. For roadways not meeting the suggested 3R design speeds, an evaluation should be done to examine locations with a high frequency of crashes and potential crash sites to determine whether cost-effective alignment revisions can be accomplished with the resources available.

Section 3 of Chapter 4 focuses on safety enhancements for 3R projects. In discussing considerations for safety design on horizontal curves, the RDM recommends that at horizontal curves where reconstruction cannot be accomplished, designers should evaluate less costly safety measures such as widening narrow pavements, flattening steep side slopes, removing or relocating roadside obstacles, or installing traffic control devices and pavement markings.

Older Drivers

FHWA's *Handbook for Designing Roadways for the Aging Population* (*53*) contains several suggested treatments for horizontal curves to improve the roadway and driving environment for older drivers. Some of these treatments are also mentioned in other guidelines and policies, but they are listed here in the context of locations that are likely to have a substantial proportion of older drivers among the user population.

The *Handbook* has a unique section within its chapter on roadway segments that focuses on horizontal curves, citing a body of research dating to 1956 that describes the challenges to older drivers that are presented by horizontal curves and the proportionally higher involvement of older drivers in crashes on horizontal curves. To that end, the *Handbook* lists four specific proven practices to improve the driving environment for older drivers: edgelines, retroreflective

pavement markers, post-mounted delineators, and pavement width, examples of which are shown in Figure 16.

Figure 16. White Edgelines, Centerline RRPMs, and Chevrons on a Horizontal Curve (*53*).

The *Handbook* emphasizes edgelines because not all rural highways have them, but they are a useful treatment for identifying the edge of the travel lane, particularly for older drivers and for any drivers in nighttime and/or wet conditions. Edgelines can help reduce the frequency of ROR crashes on horizontal curves.

The *Handbook* recommends the use of retroreflective raised pavement markers (RRPMs) to improve the visibility of surface delineation treatments on horizontal curves in the following situations where demands on motorists for path maintenance and vehicle guidance are increased:

- For curves with radii greater than 1640 ft and less than 3280 ft, it is recommended that standard centerline markings be supplemented with RRPMs installed at standard spacing (i.e., 40 ft apart), and that they be applied for a distance of 5 s of driving time (at 85th percentile speed) on the approach to the curve and continued throughout the length of the curve. The HSM cites a negative effect on roadway crashes for some drivers when RRPMs are installed on curves with radii less than 1640 ft.
- Where engineering judgment indicates that nighttime wet pavement visibility for surface delineation treatments is a priority for safe operations, regardless of curve radius, the use of RRPMs is recommended.

In addition to the installation of Chevron signs (W1-8), the *Handbook* states that roadside post-mounted delineators should be installed on horizontal curves with approximate uniform spacing as shown in Table 13.

Table 13. Recommended Spacing for Post-Mounted Delineators (*53*).

Curve Radius (*R*), ft	Approximate Spacing (*S*), ft
< 600	40
700	75
800	80
900	85
> 1000	90
Note: Spacing based on the following formula from the *Manual of Uniform Traffic Control Devices* (MUTCD) (Table 3F-1): $S = 3\sqrt{R - 50}$	

On two-lane rural roads, the *Handbook* recommends that the combined (lane plus shoulder) paved width in one direction should be at least 18 ft throughout the length of the curve for a horizontal curve with a radius less than 1900 ft.

Besides treatments specifically prescribed for horizontal curves, the *Handbook* contains recommendations for other treatments that could also be used on horizontal curves, particularly at intersections. Some of those treatments include:

- Intersecting angle: preferred 90°, not less than 75°. That is, preferred 0° skew angle, not more than 15°.
- Intersection sight distance: use 8.0 s, plus 0.5 s for each additional lane crossed, as the gap value in intersection sight distance calculations to accommodate the slower decision-making and maneuver times of older drivers for maneuvers not controlled by a protected signal phase.
- Lighting: where crash experience or engineering judgment indicates potential for wrong-way movement; where shifting lane alignment or pavement-width transition forces a path-following adjustment; where at-grade highway-rail grade crossings are present.
- Construction/work zone traffic control devices: signs and markings at, and in advance of, work zones as described in the MUTCD and related manuals and guidelines.

A promising practice listed in the *Handbook* for horizontal curves is HFST. Promising practices are treatments being used by transportation agencies that should benefit aging road users as determined by a subjective assessment by staff participating on the development of the *Handbook*. Current trends indicate these practices have a positive impact on aging road user safety. Other guidelines and references also recommend the use of HFST on horizontal curves, but there are particular benefits that could be realized for older drivers. The *Handbook* recommends HFST for use on horizontal and vertical curves (such as the example shown in Figure 17), at intersections, at on- and off-ramps, on bridge decks, locations prone to frequent rain, snow, or ice, or where additional side friction is beneficial.

Figure 17. High-Friction Surface Treatment on a Horizontal Curve (*53*).

Motorcyclists

The National Cooperative Highway Research Program (NCHRP) recently supported a domestic scan tour to document best practices in successful strategies for motorcyclist safety. The report from that scan tour (*54*) provides information on infrastructure improvements, event and travel planning, data collection and analysis, coordination and outreach, advocacy, and implementation plans. One of the topic areas discussed under infrastructure improvements is pavement conditions; a selection of their findings is summarized below:

- **Milling.** Many conditions that are challenging or threatening to motorcyclists may not normally be so intimidating to motorists. The milling of pavement as part of resurfacing operations is one such example. The irregular and grooved surface, coupled with roadway scaling and loose material, are particularly hazardous to motorcyclists. This is further exacerbated in cases where only one lane is milled and the adjacent lane is in the original condition. This differential pavement height is most critical when a motorcyclist must go from the milled lane (low side) to the original roadway (high side). Maryland established a mill-and-pave standard that specifies that a milled lane must be repaved within 24 hours of milling. Additionally, it states that if the height differential is 2.5 in. or less, the lane must be signed. In cases where the differential is greater than 2.5 in., Maryland closes the lane. Florida requires that milling and repaving occur during the same day to minimize the impact on motorcyclists. Colorado also has milling specifications that are provided in more detail in the Scan Team Report.

- **Steel Plates.** Steel plates that cover open excavations or similar roadway irregularities provide little traction to motorcycles, and their thickness presents a hump on the roadway. Maryland has recognized this potential hazard and, when employing steel plates, it recesses them to match the roadway surface, minimizing the speed bump characteristic for non-recessed use.
- **Sealants.** A common practice is to apply hot tar to seal roadway cracks and preclude moisture from further undermining the integrity of the pavement. Excess tar can create humps, bumps, and slick surfaces that are hazardous to riders. Without proper control, these tar snakes (see Figure 18) present opportunities for motorcycle tires to lose traction with the road surface and can result in unintended consequences, including loss of control. Maryland has adopted a specification that crack sealants cannot exceed 1/16 in. above the surface of the roadway, thereby reducing these hazards. Florida generally does not use joint sealant or fill cracks since its climate does not include periods of severe freezing. Idaho uses the specifications defined by Colorado for filling roadway cracks.

Figure 18. Excess Sealant (Tar Snakes) Reduces Surface Friction (*54*).

- **Loose Material.** Gravel, sand, and other loose material on the roadway surface also present hazards to motorcycle riders by interrupting the traction between the motorcycle tires and the roadway. While often annoying to motorists, this loss of traction can be catastrophic to the rider. As a maintenance practice, sweeping to remove loose sand and gravel is important, particularly as winter transitions to spring. The residual sand used during the winter months to enhance traction during snow and ice events becomes a hazard to motorcyclists in the spring and the beginning of a new riding season. The scan team did not find a statewide plan for removing materials applied during winter weather events, instead leaving it to the discretion of local highway officials, who often rely on rain to clean the roadways after winter operations.
- **Curves.** An approach used in Wisconsin is to sign curves with advisory signs even if the curve can be navigated at the posted speed limit. The thought is that advance warning to motorcyclists (and motorists) alerts them to the challenge ahead. Similarly, Wisconsin is

installing Chevron signing in curves in areas popular with motorcycle riders. The state is also using specific signage in construction zones to warn of uneven pavement.

- **Safety Edge.** Wisconsin is also piloting the use of safety edge treatments on state roads as a countermeasure to ROR crashes that could benefit motorcyclists.

A recent TxDOT-sponsored research project (*1*) investigating causes of and countermeasures to roadway departure crashes found that nearly a quarter (23.3 percent) of the crashes observed at the study sites in four TxDOT districts involved a motorcycle. In many cases, the motorcycle was approaching or traveling through a curve at the time of the crash. Specifically, a full two-thirds of the single-vehicle run-off-road (SVROR) crashes identified at study sites in the San Angelo District involved a motorcycle, and nearly 95 percent of the crashes there took place on a curve, which is also a function of the alignment of the roadways on the study sites there. The two findings were related, because the study sites near Leakey were noted as being popular among the motorcyclist community because of the varying horizontal and vertical alignment. The changes in alignment that make the roadway a popular location to drive, however, also increase the likelihood of an ROR crash. The research report for this project contains a chapter on engineering countermeasures, of which a separate category of treatments for horizontal curves is discussed. Those treatments include:

- Edgeline markings.
- Advisory speed signs.
- Chevrons.
- Post-mounted delineators.
- Flashing beacon.
- Reflective barrier delineation.
- Profile thermoplastic markings.
- Dynamic curve warning system.
- Speed limit advisory marking lane.
- Paved shoulders.
- Install/improve lighting.
- Skid resistive pavement surface treatment.

These treatments were proposed with the intent of benefiting all motorists, but motorcyclists on horizontal curves could see benefits from these treatments, given their disproportionate involvement in crashes on curves.

CHAPTER 3: PAVEMENT TREATMENT AND AGGREGATE DATA COLLECTION

INTRODUCTION

Researchers built a database of pavement treatment safety performance and friction-related properties of aggregates. Treatment performance focused on skid resistance as measured by the locked-wheel skid trailer, surface texture and friction as per the circular track meter (CTM), and the dynamic friction tester (DFT). Aggregate properties of interest were angularity and texture as measured by the aggregate image measurement system (AIMS). These data provide insight into pavement performance from the perspective of both treatment type and aggregate type used in the treatment. The information was obtained from the following sources:

- Inventory of data collected in previous research projects.
- TxDOT's PMIS database.
- New field data collection using the skid trailer.
- New laboratory testing of treatment properties.
- New laboratory testing of aggregate properties.

This chapter discusses the general methods of data collection and provides aggregated summaries of the data. These data were used to modify the skid prediction models as discussed in Chapter 4.

METHODS

Four pavement treatments were considered in this data collection effort:

- AC overlays (dense- and gap-graded).
- PFC.
- Seal coat.
- HFST.

Aggregate data were collected for many of the approved aggregate sources listed in the TxDOT's bituminous rated source quality catalog, with an emphasis on the specific aggregates used in test sites. These include:

- Limestone and dolomite.
- Sandstone.
- Igneous (various types).
- Gravel (limestone parent rock)
- Gravel (siliceous parent rock).
- Lightweight aggregate (expanded shale and clay).
- Flint.
- Calcined bauxite.

Historic Data from Literature

Significant skid resistance and aggregate has been previously collected in several past research studies as listed in Table 14. These data comprised 137 test sections and 171 aggregate sources. The specific types of data that were extracted are listed in Table 15.

Table 14. Data Sources from the Literature.

Source	Data Description
TxDOT 0-5836 – Performance and cost effectiveness of permeable friction course (*55*)	PFC test sites. AC overlay test sites.
TxDOT 0-6746 – Validation of asphalt mixture pavement skid prediction model and development of skid prediction model for surface treatments (*56*)	Seal coat test sites. AC overlay test sites. Aggregate properties.
TxDOT AIMS database for bituminous rated source quality catalog	Aggregate properties.
TxDOT 0-6714 – Evaluating the Need for Surface Treatments to Reduce Crash Frequency on Horizontal Curves (*2*)	HFST test sites.
TxDOT 0-6615 – Design and construction recommendations for thin overlays in Texas (*57*)	PFC laboratory friction. AC overlay laboratory friction.
TxDOT 0-6742 – Evaluation of design and construction issues of thin HMA overlays (*58*)	AC overlay laboratory friction. Aggregate properties.
FDOT BDR74-977-05 – Alternative aggregates and materials for high friction surface treatment (*59*)	HFST test sites. Aggregate properties.

Table 15. Type of Data Collected.

Project Data	Treatment Data
• Site location. • Treatment type. • Skid number (SK_{50S}). • Construction date. • AADT. • Roadway type and lane configuration. • Curve radius.	• Gradation. • Aggregate type. • Aggregate angularity and texture with polishing. • Macro texture (mean-profile depth). • Wet-coefficient of friction.

Skid data from the Florida DOT project was collected with a skid trailer equipped with a ribbed test tire, as opposed to the smooth test tire used in Texas. Furthermore, the data were often collected at different speeds from the 50 mph Texas standard. These data were converted to the Texas standard (SK_{50S}) using Equations 20, 21, 22, and 23. (*60*, *61*) The data were first adjusted to 40 mph, then converted from ribbed tire to smooth tire, and then adjusted back to 50 mph.

$$SK_2 = SK_1 * e^{\left(\frac{V_1 - V_2}{S_p}\right)} \quad (20)$$

$$S_p = 14.2 + 89.7MPD \quad (21)$$

$$SK_{40S} = 0.84 * SK_{40R} + 11.18 * MTD - 11.18 \quad (22)$$

$$MTD = 0.947 * MPD + 0.069 \quad (23)$$

where:

SK_2 = corrected skid number;
SK_1 = skid number at measurement speed;
S_p = speed gradient;
V_2 = desired speed (= 50 mph), mph; and
V_1 = speed during skid number measurement, mph.
MPD = mean profile depth calculated from a laser profile, mm;
SK_{40S} = predicted skid number measured at 40 mph with a smooth tire;
SK_{40R} = skid number measured at 40 mph with a ribbed tire;
MTD = mean texture depth as measured with the sandpatch test, mm;

PMIS Queries

Historic skid data were queried from the sites identified in the literature sources from Table 14. PMIS data were available for the years 2003 through 2016. A total of 81 site locations were queried. For this effort, a site location typically consisted of a continuous roadway section with skid number measurements every half mile. The availability of data varied among the different projects ranging from one year of data to several years.

The PMIS database query process was conducted as follows:

1. Select by:
    a. Roadbed ID (route and lane).
    b. Between beginning and ending Texas reference markers.
    c. From the first year of construction until last known year to exist.
2. Average each project by year.

Only the year of testing, not the month, was available in the PMIS, making it difficult to decide if the measured skid number came before or after treatment construction. First, if the construction date was after September (end of annual testing cycle) the skid data were omitted. Similarly, if construction was before April, the data were included. For everything in between, if skid data were available within three years before construction, and there was a 20+ jump in skid number at the year of construction, the data were included. For all other cases, the data were omitted.

Field Testing of Skid Number

A subset of the sites from the literature sources and some new HFST sites were selected for skid testing to obtain the latest skid data at the time of the study. Figure 19 shows the locations of these 40 sites through central, east, and near-west Texas. The treatments at these sites included 8 HMAs, 9 PFCs, 13 seal coats, and 8 HFSTs. The sites were chosen not only for the various treatment types but also for the variety of aggregate types, traffic conditions, and treatment ages.

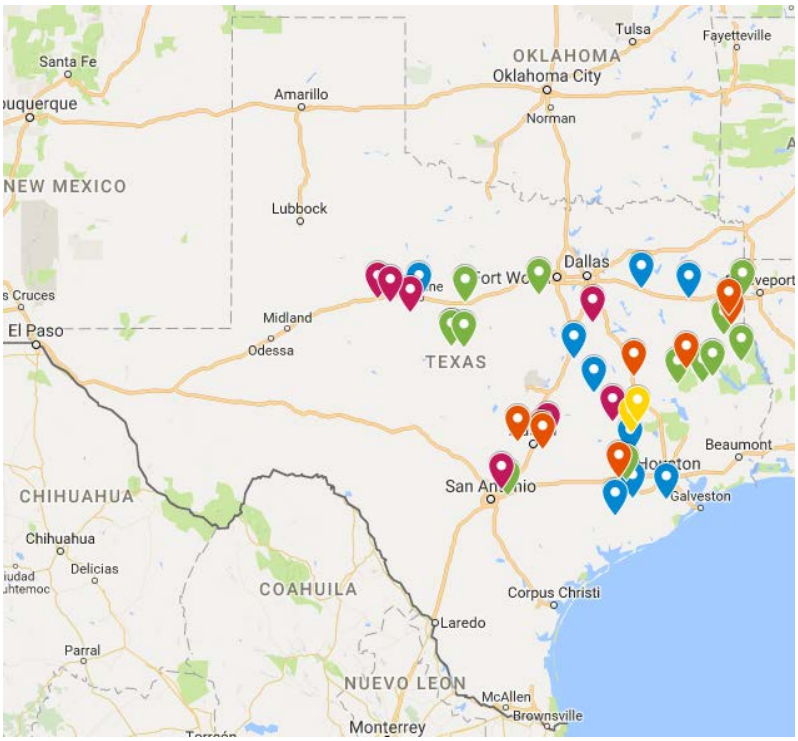

Figure 19. Skid Trailer Test Sites.

Skid testing was done according to the ASTM E274 procedure (Standard Test Method for Skid Resistance of Paved Surfaces Using a Full-Scale Tire), with a smooth tire at a speed of 50 mph. Generally, six measurements were made over a 1-mile interval. Non-uniform pavement conditions, cross streets, and access points such as driveways were avoided during testing.

At some sites, a slower test speed was warranted for safety reasons. In these cases, the data were corrected for speed using Equations 20 and 21. Mean profile depth measurements were not available in field testing; therefore, researchers estimated mean profile depth values based on visual observations and experience.

The new skid data were added to the historic skid data and the PMIS-queried data to be analyzed as a single data set.

Laboratory Testing of Treatment Properties

Field skid data that are collected several years apart is often highly variable. This is due to differences in pavement temperature, tire wear, spatial variation of skid properties, and difficultly of repeating measurements over the same location. To offset this variability, additional measurements were made in a laboratory environment where these factors can be controlled. The laboratory measurements were then transformed into predicted skid number.

Some data from the literature included laboratory measurements of AC overlays and PFCs. In this project, additional testing was done on HFST treatments and non-traditional treatments using larger aggregates bound in epoxy. The treatments were tested for friction

properties to compute the international friction index (IFI), which was then converted to skid number (SK_{50S}).

AC slabs, 40 cm × 50 cm × 3.8 cm, were molded with a laboratory asphalt roller compactor. The slabs served as substrates for the HFST treatments. Two-part epoxy was thoroughly mixed and spread over the slab with a rubber v-notched squeegee and aggregate was spread uniformly to cover the epoxy. Table 16 shows the aggregates tested. For traditionally sized aggregate (passing the No. 6 and retained on the No. 16 sieves), the applied epoxy was 50 mils thick. For larger gradations, the target embedment depth was approximately half the aggregate diameter.

Table 16. Aggregates Used in Laboratory Testing.

Aggregate Type	Size	Producer/ Distributor	Source	Test Type	
				Treatment Friction	Agg. Angularity and Texture
Calcined bauxite	6×16	Great Lakes Minerals	China	X	X
Calcined bauxite	6×16	Ashapura	India	X	X
Flint	6×16	Flintrock Products	Oklahoma	X	X
Lightweight agg.	Grade 4	TXI	Riverlite	X	X
Lightweight agg.	Grade 4	TXI	Streetman	X	X
Gravel	Grade 4	Pharr	Pharr	X	X
Limestone	Grade 4	TCS	Feld	X	X
Limestone rock asphalt	Grade 4	Vulcan	Uvalde		X

Friction testing was done with a CTM and a DFT. The CTM is a laser-based device used to measure mean profile depth (Figure 20). A laser sensor, attached to a rotating arm, collects 1024 height measurements along a circular profile. The mean profile depth is then calculated according to ASTM E2157. The DFT measures the wet-coefficient of friction along the same path as the CTM. Three rubber pads are attached to a motorized spinning disk (Figure 21). The disk, held above the surface, rotates up to speeds near 80 km/hr. The disc then contacts the surface to measure the coefficient of friction. Measurements are made continuously as the disk slows down.

Figure 20. Circular-Track Meter.

Figure 21. Dynamic Friction Tester.

Friction testing was done on the new treatment and subsequently at different levels of simulated traffic. The National Center for Asphalt Technology (NCAT) three-wheel polisher (Figure 22) applies a vertical 105-lb load and rotates along the same circular path at 60 rpms. Water is sprayed onto the surface to remove debris and manage generated heat. The samples were tested at 0, 1k, 5k, 30k, and 80k cycles. Terminal friction is generally achieved between 50k and 100k cycles.

The IFI can be computed directly from the CTM and DFT data. The IFI was defined during the Harmonization Experiment for Skid Resistance in 1993, overseen by the Permanent International Association of Road Congress (*60*). It is composed of a harmonized friction measurement at 60 km/h (*F60*) and the speed gradient (S_p), which is a measurement of macrotexture. The calculation is shown in Equations 24 and 25. To improve variability in the data, the average friction coefficient between 20 through 60 km/hr was used rather than the coefficient just at 20 km/hr.

$$F60 = 0.081 + 0.732(\mu_{DFT})e^{\frac{-40}{S_p}} \quad (24)$$

$$S_p = 14.2 + 89.7MPD \quad (25)$$

where:

μ_{DFT} = Wet-coefficient of friction as measured by the DFT.
MPD = Mean profile depth, mm

Figure 22. NCAT Three-Wheel Polisher with Water Bath.

The IFI was then converted to skid number (SK_{50S}) (i.e., the skid number measured at 50 mph with a locked wheel skid trailer equipped with a smooth tire using Equations 26 and 27).

$$SK_{50S} = 4.81 + 140.32(IFI - 0.045)e^{\frac{-20}{S_p}} \quad (26)$$

$$S_p = 14.2 + 89.7MPD \quad (27)$$

Laboratory Testing of Aggregate Properties

A critical component of the skid prediction model is the influence of aggregate type in the treatment to predict overall pavement friction. Aggregate angularity and aggregate texture properties, as measured by the AIMS, were available for many aggregate sources in the literature. Researchers needed to test these properties for some aggregates missing from the data set. Table 16 lists these aggregates.

The AIMS uses high resolution imaging and image processing technique to quantify the angularity and texture of aggregates (Figure 23). Testing was done before and after polishing in the micro-deval. The standard program settings were used to measure aggregates larger than the No. 4 sieve. For the small 6×16 aggregate, the camera settings were manually adjusted to capture data for aggregates retained on the No. 8 sieve. (Smaller aggregate particles were not tested.) Testing was done on new aggregate and after polishing in the micro-deval.

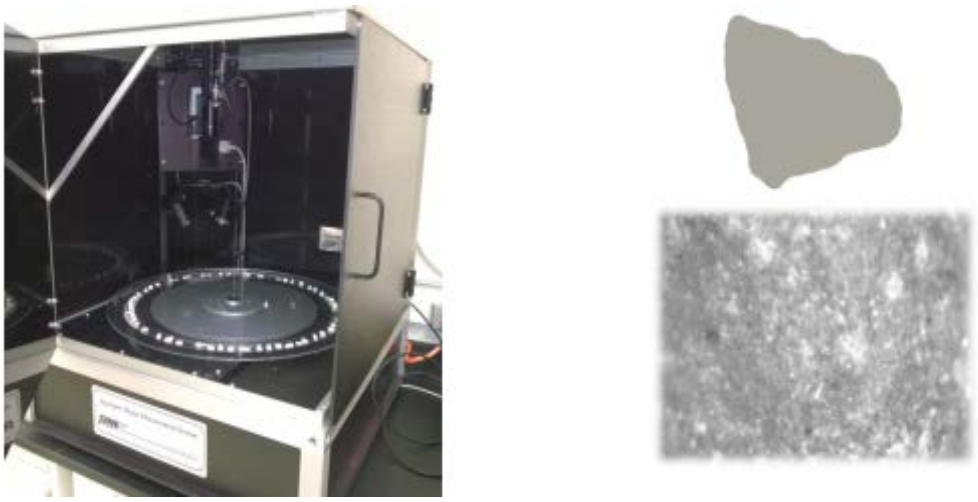

Figure 23. AIMS Device (Left), Angularity (Top-Right), and Texture (Bottom-Right).

The micro-deval is typically used to evaluate aggregate resistance to abrasion. A cylinder is filled with a 1500-g aggregate sample, steel balls, and water (Figure 24). The container is rapidly rotated a predetermined amount in accordance with Tex-461: Test Procedure for Micro-Deval Abrasion of Aggregate. In this effort, samples were polished first to 105 minutes, tested with the AIMS, and then polished to 180 minutes and tested again. Select aggregates were also tested at smaller intervals.

Figure 24. Micro-Deval (Left) and Interaction between Aggregates and Steel Balls (Right).

RESULTS

Test Sites, Treatment Designs, and Aggregates

Table 17 summarizes the types of test sites used in this analysis. A total of 134 sites were analyzed with over 30 sites for each treatment type. AC overlays, PFCs, and seal coats employed a wide range of aggregate types while HFST was confined to calcined bauxite and flint. Flint is actually not allowed in HFST, but it is common in similar bridge deck overlay treatments. The earliest sites were constructed between 2003 and 2008. Appendix A provides specific site details.

Table 17. Summary of Test Sites.

Treatment Type	Site Count	Aggregate Type (site count)	Earliest Construction Date
AC Overlay	33	Limestone (3) Dolomite (1) Sandstone (9) Igneous (15) Gravel (3) Unknown (2)	2003
PFC	35	Limestone (8) Sandstone (9) Igneous (10) Gravel (3) Unknown (4)	2003
Seal Coat	34	Limestone (16) Sandstone (4) Igneous (3) Gravel (2) Limestone rock asphalt (2) Lightweight (8)	2008
HFST	32	Bauxite (26) Flint (6)	2006

Skid Number

Table 18 summarizes the collected skid data, broken down by data source. Nearly 4,000 skid measurements were made. When averaging these by test site and test date, there are 525 skid data points for analysis. These data do not include laboratory measurements converted to skid number. Figure 25 shows the results based on treatment type. The highest skid numbers, with averages around 70, were measured on HFST projects. AC overlay and PFC treatments averaged around 30 with highs in the 40s and lows around 20. The skid numbers of seal coats ranged from 5 to 90, with an average of 40. The lowest skid number values were bleeding seal coats, with values less than 15. Differentiating between non-bleeding and bleeding seal coats was only possible for the new TTI site testing. Some site measurements in the literature and PMIS data were likely also bleeding surfaces.

Figure 26 shows skid number by aggregate type. The highest skid numbers were for calcined bauxite and flint, around 70. These aggregates were only used in HFST treatments. Lightweight aggregate had the next highest skid number range of between 30 and 70, with an average of 55. Surface Aggregate Classification (SAC) A aggregates (sandstone, igneous, and gravel, etc.) roughly averaged between 35 and 45. Limestone and dolomite were lower at 28 and 23, respectively. The very lowest skid number was for limestone rock asphalt (LRA) with an average below 20.

Table 18. Summary of Skid Resistance Data.

Data Source	Treatment Types	Data Count	Comments
TxDOT 0-6746	AC Overlay Seal Coat	126	
FDOT BDR74-977-05	HFST	47	Data converted from ribbed tire.
PMIS (sites from TxDOT 0-5836 and 0-6746)	PFC AC Overlay Seal Coat	312	
New Data Collection	AC Overlay PFC Seal Coat HFST	40	

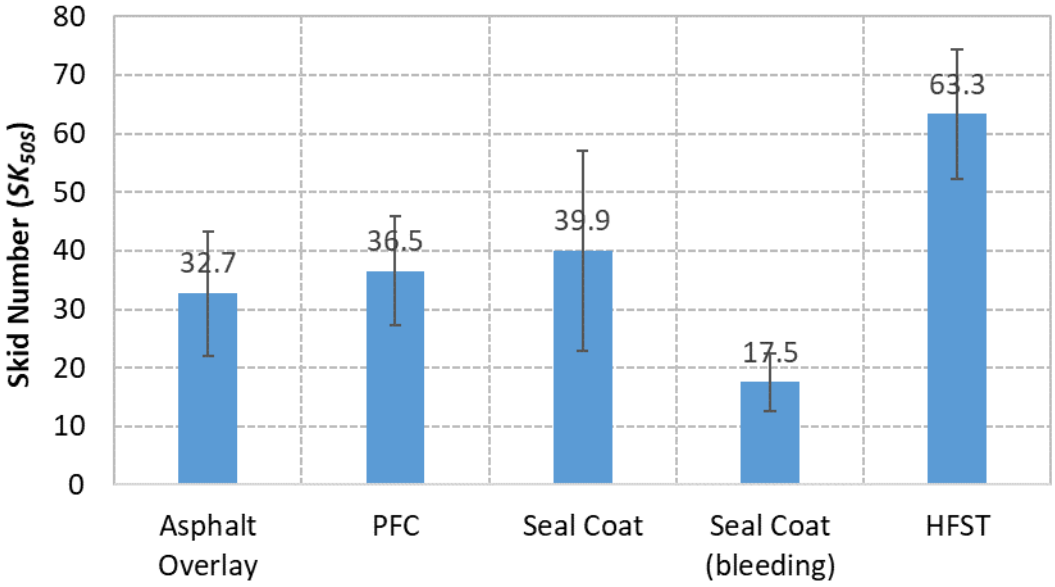

Figure 25. Skid Number by Treatment Type as Measured by Researchers.

Figure 27 and Figure 28 show the trend of skid number versus time by treatment type and aggregate type, respectively. Skid number starts high but immediately decreases and gradually approaches a terminal value. The plotted regression lines are a simple power equation fit. Modeling in the next chapter uses a more accurate fit. Without the initial skid measurement, skid number can be approximated linearly. To improve the prediction, therefore, measurements from the shoulders or between the wheel paths acted as surrogate initial skid measurements.

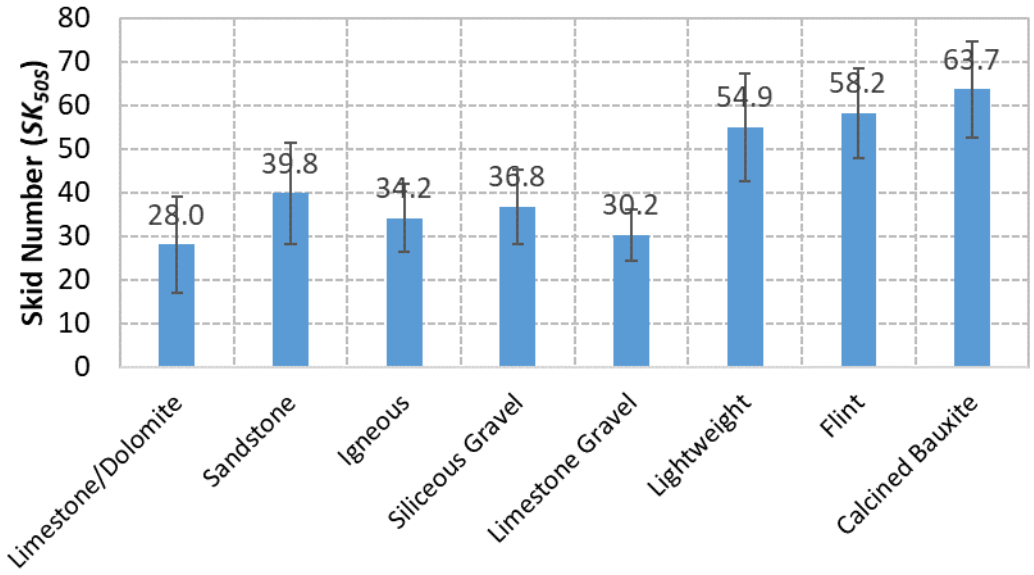

Figure 26. Skid Number by Aggregate Type as Measured by Researchers.

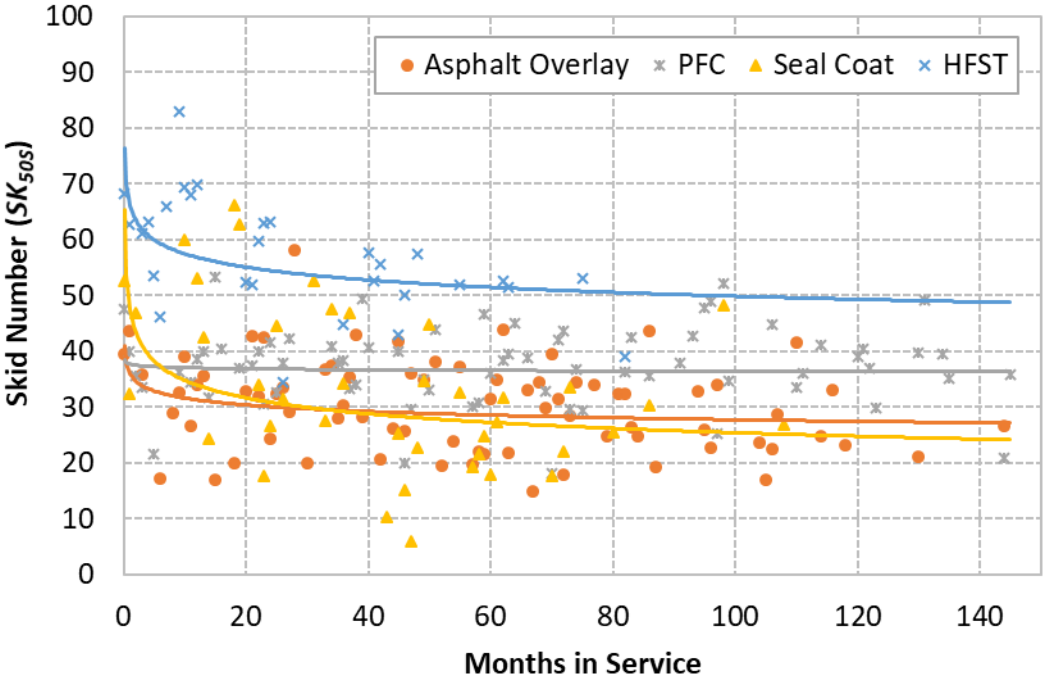

Figure 27. Skid Number with Time by Treatment Type.

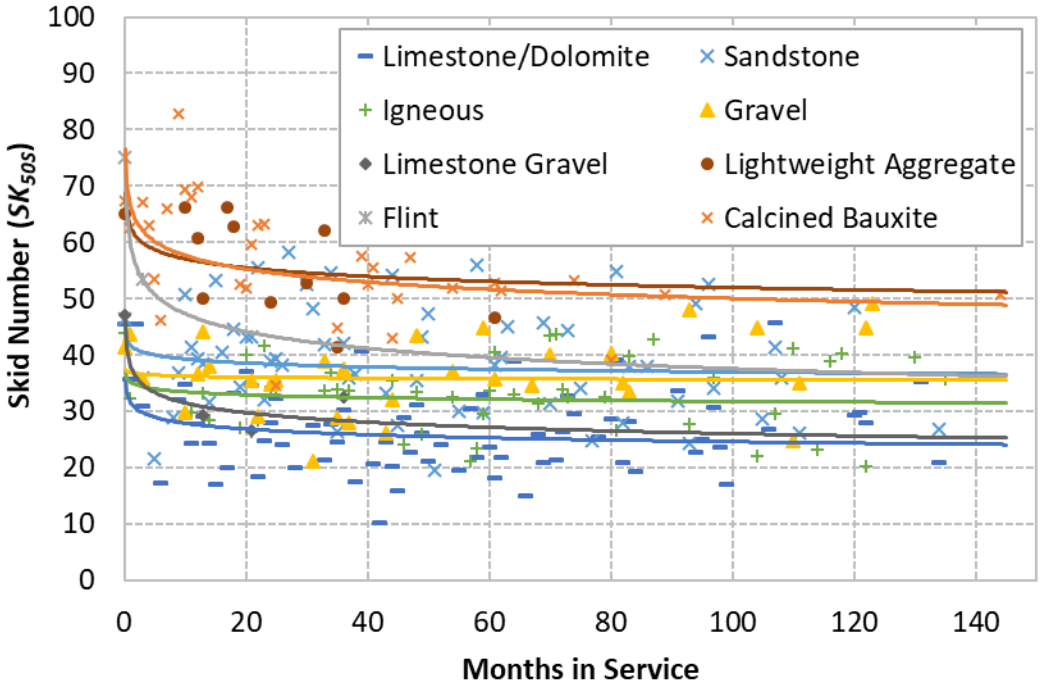

Figure 28. Skid Number with Time by Aggregate Type.

Treatment Friction and Texture

Figure 29 and Figure 30 show the trend of friction and texture versus laboratory polishing. The first graph shows friction by aggregate type. Calcined bauxite and lightweight aggregate have the highest coefficient of friction (0.8) while limestone and dolomite have the lowest friction (0.3–0.5). The texture trends for different treatments show that the experimental coarse HFST, using Grade 4 aggregate, had the highest texture depth (3.5–5 mm). This is very coarse and at the feasibility limits for rideability. HFST also had high texture (1.75–2.0 mm), followed by PFC (1.3 mm), then dense and gap-graded mixtures (0.5–0.9 mm). Seal coat was not considered in these laboratory tests.

Aggregate Texture and Angularity

Figure 31 and Figure 32 show aggregate texture and angularity indices, respectively. A higher value means the aggregate is more aggressive in that property. In angularity, an index greater than 3975 is high and below 2100 is low. Limestone rock asphalt had the lowest angularity and igneous rock and bauxite had the highest. Gravel had the smallest change from before to after polishing. In texture, the high and low indices are above 500 and below 200, respectively. LRA had a highest texture index, which is surprising given that the field performance of LRA is suboptimal. In other friction tests, calcined bauxite and lightweight aggregate have the highest friction performance. In this study, one bauxite source had high texture but the other had very low texture, averaging to moderate texture. The lowest texture was for limestone aggregate. Researchers have found the AIMS procedure for measuring texture is prone to mischaracterization of for multicolored aggregates, which may be the case in the data for LRA (*62*).

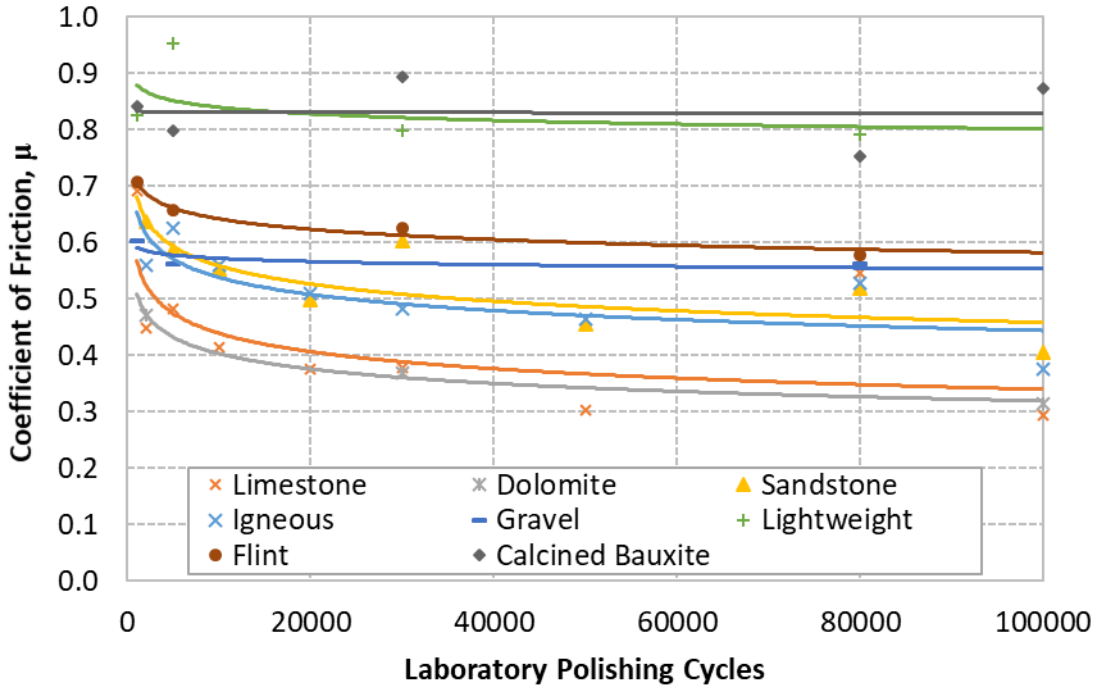

Figure 29. Coefficient of Friction with Lab Polishing by Aggregate Type.

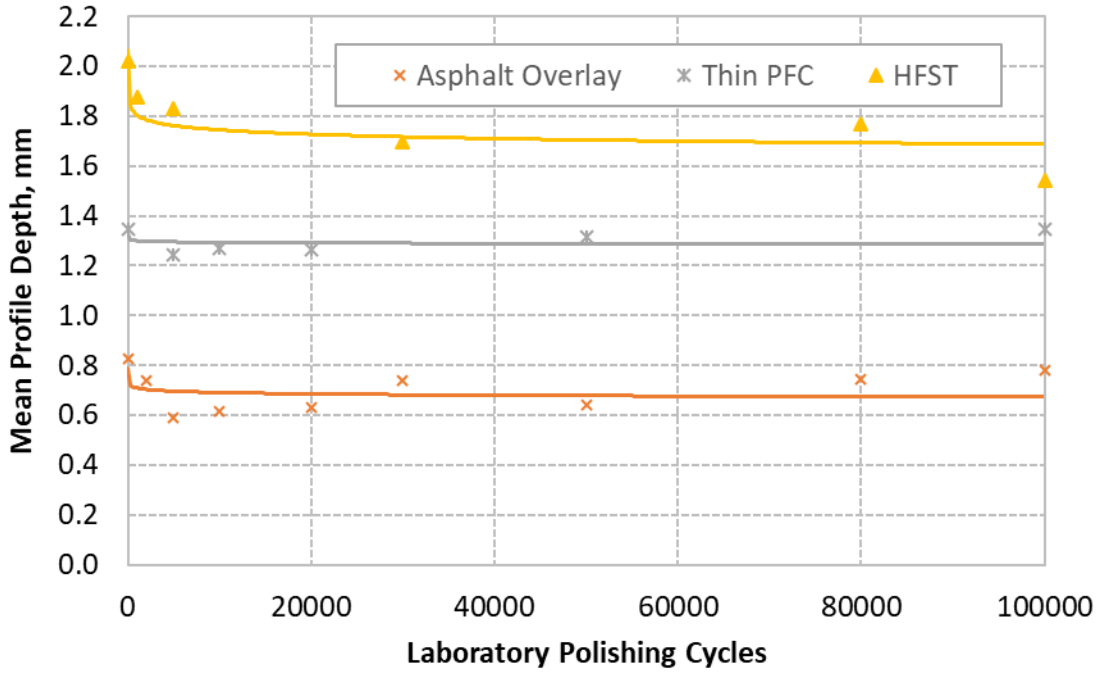

Figure 30. Mean Texture Depth for Treatment Types.

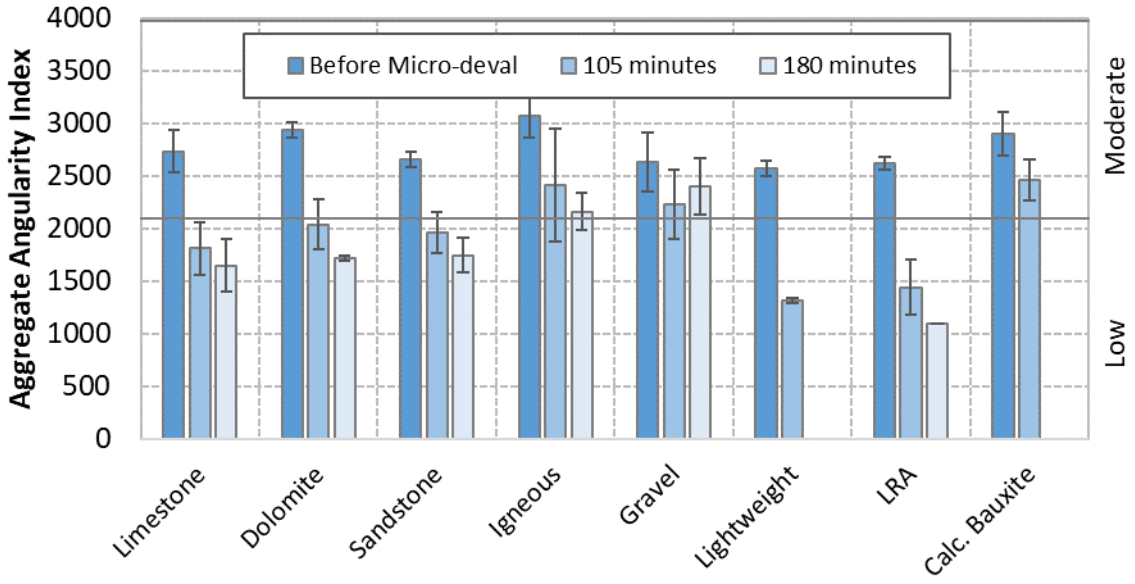

Figure 31. Angularity Index by Aggregate Type.

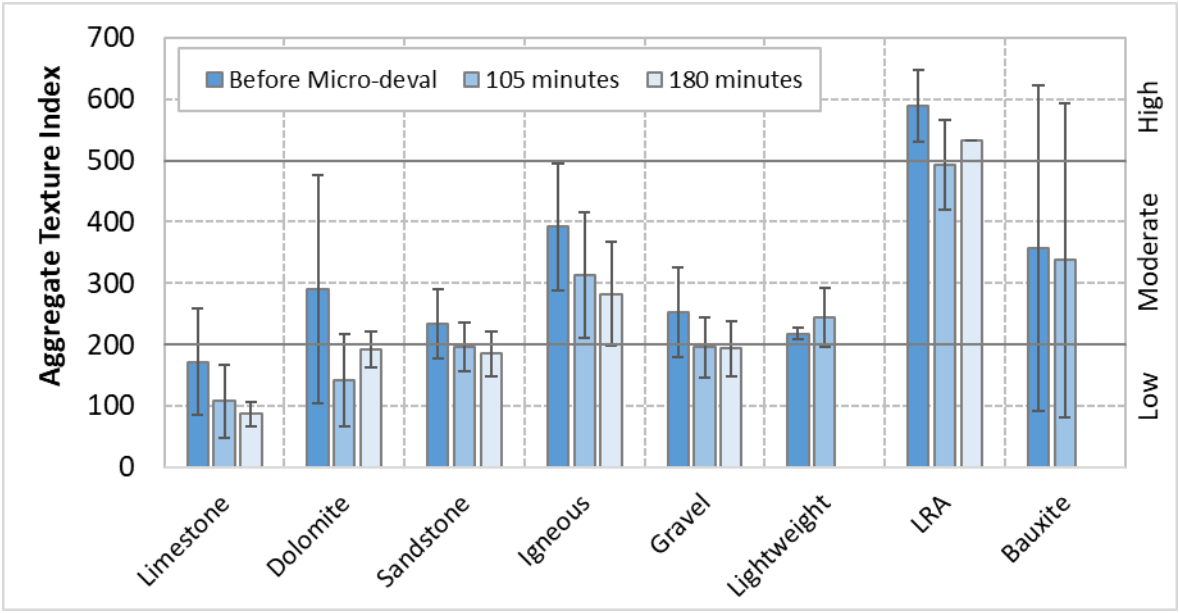

Figure 32. Texture Index by Aggregate Type.

CHAPTER 4: PAVEMENT SKID RESISTANCE MODELING

INTRODUCTION

TTI researchers have developed prediction models of asphalt pavement (*56*, *60*, *63*, *64*, *65*). These models describe the skid resistance of asphalt pavements as a function of aggregate characteristics, mixture gradation, and traffic levels. Each model iteratively built on the preceding one. The first prediction model by Masad et al. in 2010 (*63*) tested the friction of laboratory slabs in terms of IFI and correlated the results with texture parameters of the coarse aggregate and mixture gradation. The IFI was then correlated with field skid results. The study by Kassem et al. in 2013 (*65*) validated Masad's model and expanded on the prediction by incorporating aggregate angularity. The work by Chowdhury et al. in 2017 (*56*) further validated the models with extensive field data and extended to the prediction of seal coats. For the seal coat prediction, a separate model was needed, of the same form, but with different parameter coefficients. The objective of the modeling in this project is to extend the prediction to include HFST and to simplify unnecessarily complex portions of the model.

Figure 33 gives an overview of the steps in the Chowdhury et al. model. The trend of skid number versus time is dependent on the treatment type, aggregate texture, aggregate angularity, and mixture gradation. Traffic condition is considered in terms of AADT, percent truck traffic, and distribution of traffic within the lane.

A recurring assumption within the model is that friction-related properties decrease along an exponential path and stabilize at a terminal value, according to the equation illustrated in Figure 34. The three parameters (*a*, *b*, and *c*) define the initial value (*a*+*b*), terminal value (*a*), and rate of decay (*c*) for the curve. This equation is applied to the decrease in aggregate texture and aggregate angularity. The same trend is used to model IFI, though the model is more complex with the *a*, *b*, and *c* parameters being derived from other variables.

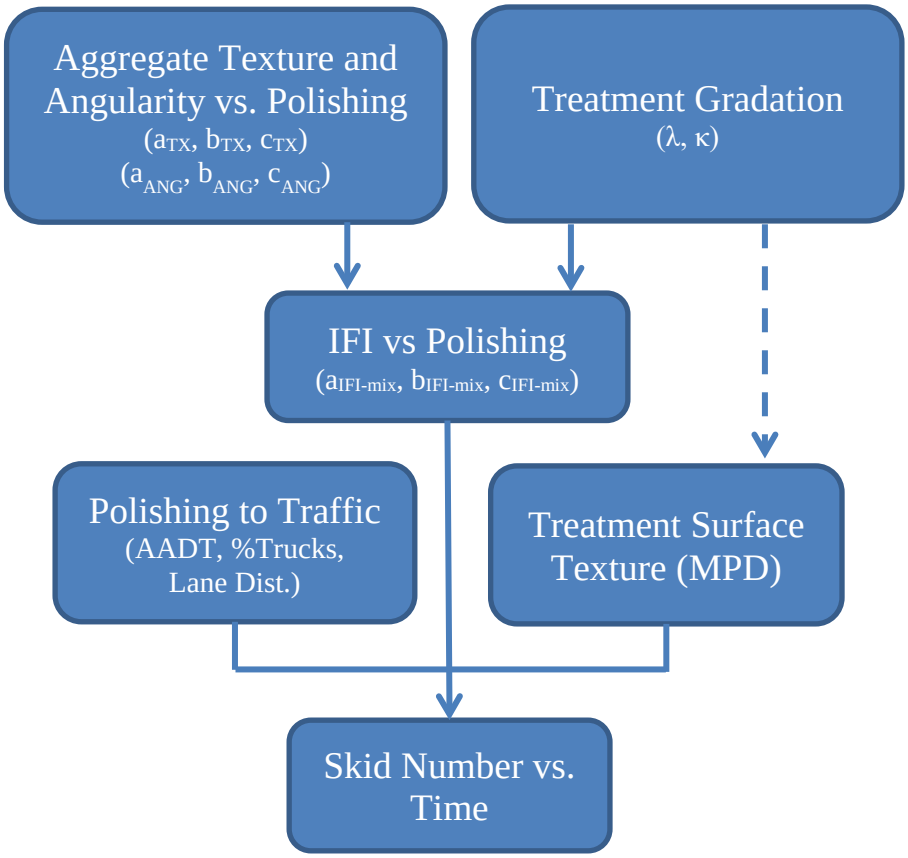

Figure 33. Overview of Skid Prediction Model from Chowdhury et al. Model.

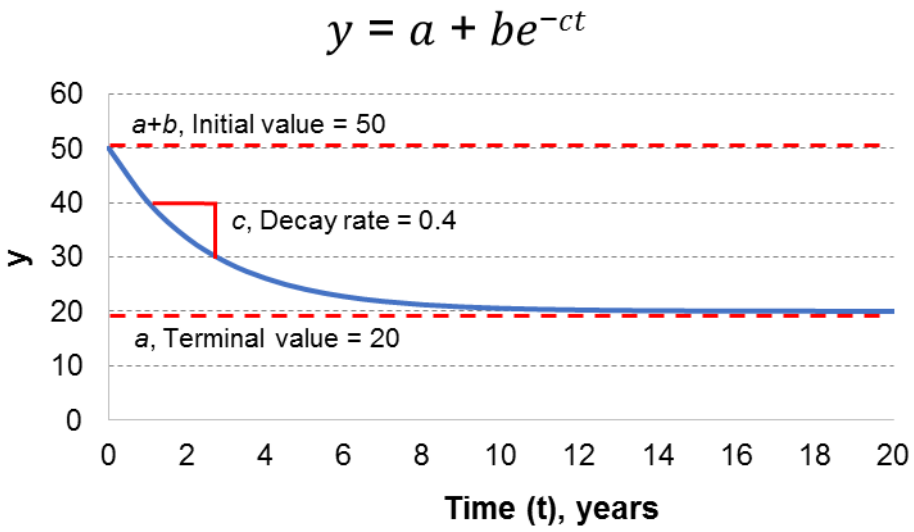

Figure 34. Exponential Decay Model.

METHODS

As discussed in the previous chapter, researchers reassembled the data from Chowdhury et al., added data from other research projects, and collected new data with an emphasis on

HFST. With this larger data set, a new model could be generated that fits a wider range of skid performance scenarios.

The following list describes the specific areas of the model that were improved. The steps and equations listed here refer to those in Chowdhury et al. (*56*), Appendices C and D: SAAP Flow Chart for Asphalt Mixture and for Surface Treatment.

List of changes:

- **Step 1b: Determine the gradation parameters λ and κ.**
  Option 2: Select a standard mix gradation.
  - The number of standard mix gradations was consolidated from 14 to 10.
- **Step 3a: Input aggregate texture data for each aggregate source.**
  - Removed the option of predicting the texture and angularity decay curves with only two points. Instead, default curve parameters were generated for each aggregate type.
  - Default curves were built using all available data, both with two point and three points, by aggregate type, and finding the best-fit line of form $y=a+be^{-ct}$.
- **Step 5: Use the parameters obtained from the previous step to calculate a_{mix}, b_{mix}, and c_{mix} using Equations 6, 7, and 8.**
  - Rather than predict the model parameters of IFI vs cycles (a_{mix}, b_{mix}, and c_{mix}), the new model directly predicts similar parameters for skid number vs cycles.
  - The original calculations of a_{mix}, b_{mix}, and c_{mix} parameters have been simplified and based on a_{tx}, b_{tx}, c_{ang}, and λ. A unique set of calculations are still needed for each major treatment type (asphalt overlay, seal coat, and HFST).
- **Step 6: Obtain the mixture MPD.**
  - Step removed. By calibrating directly to *SK*, this estimation of MPD over time was not needed.
- **Step 9: Calculate equivalent number of polishing cycles *N*.**
  - Use a constant value of 0.07 in place of c_{mix}.
  - The original equation assumed that the equivalent laboratory polishing effort for a given traffic situation would change based on the depending on surface characteristics. This assumption had no supporting evidence, so the surface variable was replaced by the average value of all c_{mix} values.
- **Step 10: Calculate IFI as a function of equivalent number of polishing cycles.**
  - Changed to a prediction of *SK* as a function of polishing cycles.
- **Step 11. Calculate *SK* as a function of vehicles.**
  - Step removed because the model is already predicting *SK*.
- **Step 12. Plot *SK* as a function of *N*.**
  - Changed to plot *SK* as a function of years.
- **Steps 13 – 15.**
  - Steps for ranking and analyzing data removed.

Two adjustments were necessary to make to the texture data before generating the final model. The issue was that limestone rock asphalt, the aggregate with the lowest skid performance in the field, actually had the highest aggregate texture index in laboratory testing. Recent studies have identified a critical shortcoming of the AIMS device when measuring

aggregate texture (*66, 67*). Because the system uses variability in the digital image as a surrogate for aggregate texture, any type of dark and light contrast will yield a higher texture index.

Additionally, darker-colored aggregates produce a higher texture index than lighter aggregates. This surrogate prediction usually works well since smoother aggregates, like limestone, are lighter and more uniformly colored than gravels, sandstones, and igneous aggregate. Limestone rock asphalt, however, is a white and black speckled aggregate (limestone with pores filled with asphalt). The speckled pattern produced an abnormally high index. Consequently, the four seal coat projects with limestone rock asphalt were designated as average limestone seal coats for modeling. The other issue was with lightweight aggregate. Sections in the field perform very well; however, the texture index was ranked lower than all other aggregates except limestone. In this case, the aggregate samples were lighter-colored and did not have developed mineral crystals to increase the image variability. Consequently, the average texture index was artificially raised by 200 to provide a reasonable match with observed field data.

PROPOSED MODEL

Figure 35 gives an overview of the proposed model.

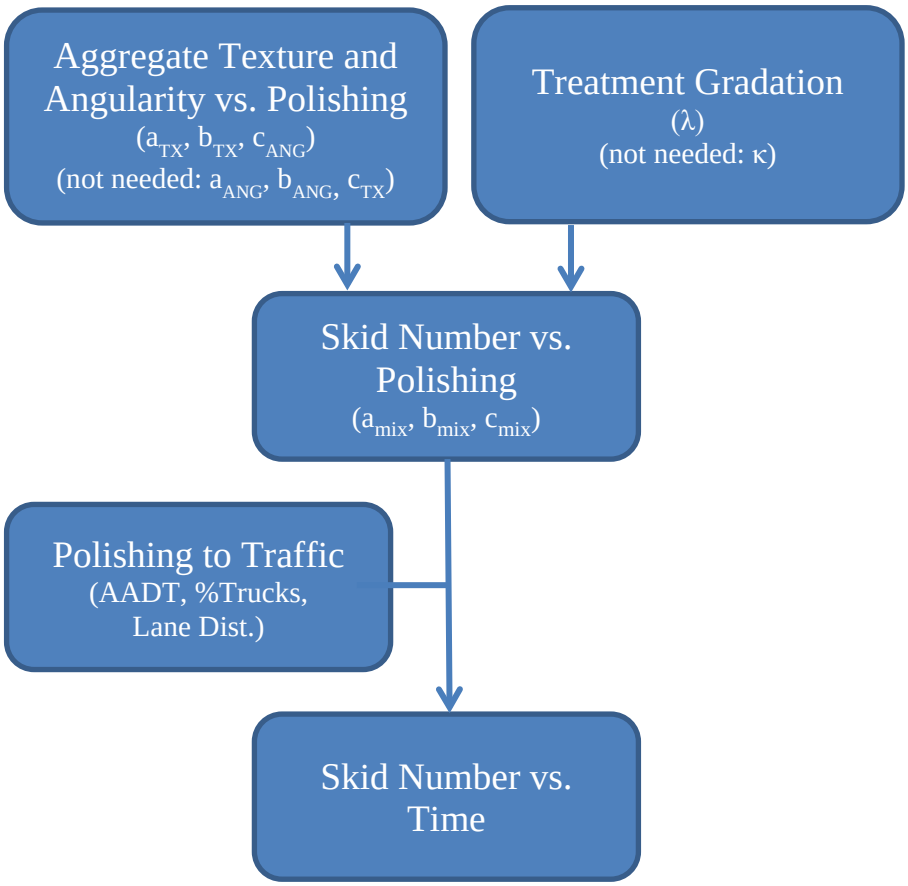

Figure 35. Overview of Proposed Skid Prediction Model.

The change in aggregate texture and angularity with time is modeled with the exponential decay functions in Equations 28 and 29. The parameters *a*, *b*, and *c* for each aggregate can be determined by laboratory tests and non-linear regression. Alternatively, the analyst can use default parameters for a given aggregate type based on averages from the data collected in this research project (Table 19). For mixtures with multiple aggregate types, the parameters are weighted based on the aggregate percentage by weight and the amount of aggregate retained on the No. 4 (4.75 mm) sieve.

Table 19. Average Texture and Angularity Regression Constants.

Aggregate Type	Angularity			Texture		
	a_{ang}*	b_{ang}*	c_{ang}	a_{tx}	b_{tx}	c_{tx}*
Limestone/Dolomite	1514	1470	0.011	108	68	0.021
Sandstone	1716	1024	0.010	206	62	0.063
Siliceous Gravel	1929	986	0.005	329	84	0.022
Limestone Gravel	2048	544	0.013	196	79	0.050
Igneous (Granite, Rhyolite, Quartzite, Trap rock)	1966	535	0.019	150	50	0.018
Lightweight Aggregate	1746	1359	0.017	455	24	0.006
Flint	1921	916	0.018	622	150	0.047
Calcined Bauxite	2895	559	0.008	176	102	0.020

*Not needed for the model

$$TX\ (t) = \ a_{tx} + b_{tx} * e^{(-c_{tx} * t)} \quad (28)$$

$$ANG\ (t) = \ a_{ang} + b_{ang} * e^{(-c_{ang} * t)} \quad (29)$$

where:

$TX(t)$ = change in texture vs. polishing time.
a_{tx}, b_{tx}, c_{tx} = regression constants for aggregate texture.
t = time taken to polish aggregates in micro-deval, minutes.
$ANG(t)$ = change in angularity vs. polishing time.
$a_{ang}, b_{ang}, c_{ang}$ = regression constants for aggregate angularity.

Mixture gradations, in percent passing vs. aggregate size, are modeled using a Weibull distribution (Equation 30). Typical shape and scale parameters for various treatments are given in Table 20 and illustrated in Figure 36.

$$F(x, \lambda, \kappa) = 1 - e^{-\left(\frac{x}{\lambda}\right)^{\kappa}} \quad (30)$$

where:

x = aggregate size, mm.
κ, λ = shape and scale parameters, respectively.

Table 20. Average Gradation Parameters.

Treatment Type		Weibull Parameters	
		λ (scale)	κ (shape)*
Asphalt Overlay	Type C (DG, SP)	5.14	0.919
	Type D (DG, SP)	4.76	0.937
	Type F (DG, SP), CAM	1.74	0.865
	SMA (Type D, Type C)	7.71	1.33
	TOM, CMHB-F	4.25	1.11
	Thin PFC	5.95	3.06
	PFC	9.77	2.24
Seal Coat	Grade 3	12.2	8.80
	Grade 4	9.17	5.14
	Grade 5	5.55	5.37
HFST		2.41	3.29

*Not needed for the model

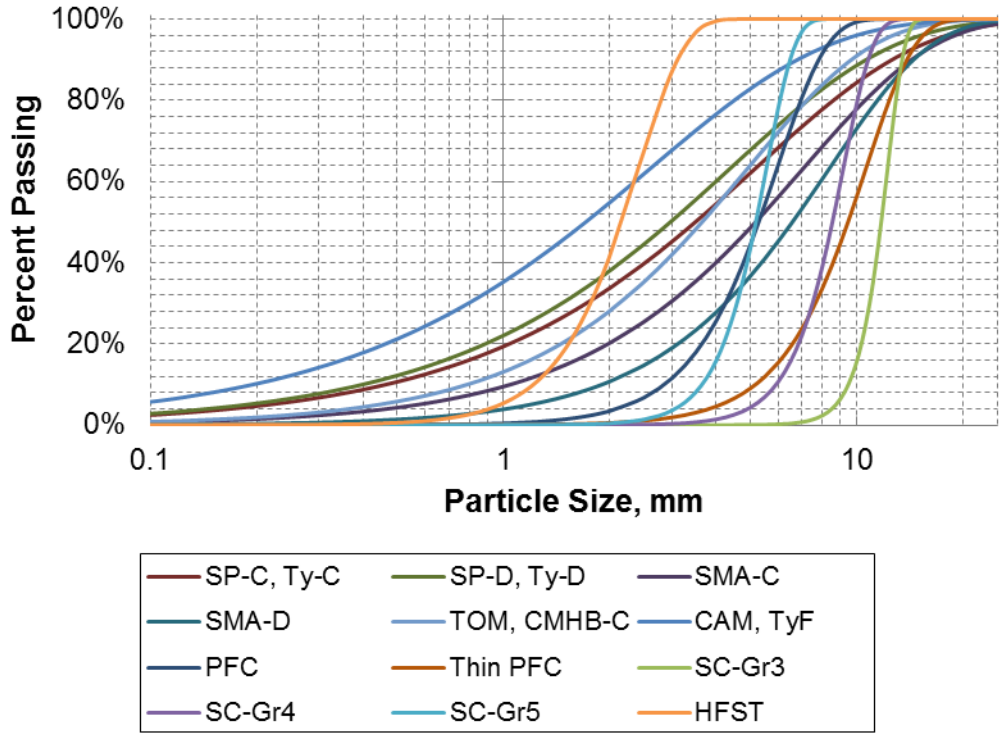

Figure 36. Example Mixture Gradations.

The aggregate and gradation parameters are used to predict the change in *SK* (50 mph, smooth tire) with respect to the number of polishing cycles (Equation 31). Separate regressions are used for asphalt overlays (Equations 32–34), seal coat (Equations 35–37), and HFST (Equations 38–40).

$$SK_{50S}(N) = a_{mix} + b_{mix}e^{-c_{mix}N} \quad (31)$$

where:

N = Number of laboratory polishing cycles.
a_{mix}, b_{mix}, c_{mix} = regression parameters as defined below.

For asphalt overlays:

$$a_{mix} = 21.8 + 0.026a_{tx} + 0.87\lambda \quad (32)$$

$$b_{mix} = 5.6 \quad (33)$$

$$c_{mix} = 0.010c_{ang} \quad (34)$$

For seal coats:

$$a_{mix} = 11.9 + 0.09a_{tx} \quad (35)$$

$$b_{mix} = 25.3 \quad (36)$$

$$c_{mix} = 0.008c_{ang} \quad (37)$$

For high friction surface treatments:

$$a_{mix} = 54.2 + 0.006a_{tx} \quad (38)$$

$$b_{mix} = 0.10b_{tx} \quad (39)$$

$$c_{mix} = 0.095c_{ang} \quad (40)$$

Substituting the regression parameters into Equation 31 yields the following:

Asphalt overlays $$SK_{50S}(N) = 21.8 + 0.026a_{tx} + 0.87\lambda + 5.6e^{-0.010c_{ang}N} \quad (41)$$

Seal coats $$SK_{50S}(N) = 11.98 + 0.09a_{tx} + 25.3e^{-0.008c_{ang}N} \quad (42)$$

HFST $$SK_{50S}(N) = 54.2 + 0.006a_{tx} + 0.101b_{tx}e^{-0.095c_{ang}N} \quad (43)$$

Next, the lab cycles can be converted to field traffic conditions as follows:

$$N = TMF \times 10^{\left(1/\left[A+0.07B+\frac{C}{0.07}\right]\right)} \quad (44)$$

$$TMF = \frac{Days\ between\ construction\ and field\ testing \times adjusted\ traffic}{1000} \quad (45)$$

$$Adjusted\ traffic = \frac{AADT \times (100 - PTT) \times DL_{AADT}}{100} + \frac{AADT \times PTT \times DL_{truck} \times 20}{100} \quad (46)$$

where:

TMF = traffic multiplication factor.
AADT = average annual daily traffic in both directions, veh/d.
DL_{AADT} = design lane factor of AADT (see Table 21).
DL_{truck} = design lane factor of trucks (see Table 21).
PTT = percent truck traffic.
A, B, C = coefficients (-0.452, -58.95, 5.83×10^{-6}, respectively).

Table 21. Design Lane Factors of AADT and Truck.

Rural Highway				
Number of lanes in one direction	**Undivided**		**Divided**	
	DL_{AADT}	DL_{truck}	DL_{AADT}	DL_{truck}
1	0.50	0.50	0.50	0.50
2	0.40	0.45	0.40	0.45
3	0.30	0.40	0.20	0.25
Urban Highway				
Number of lanes in one direction	**Undivided**		**Divided**	
	DL_{AADT}	DL_{truck}	DL_{AADT}	DL_{truck}
1	0.50	0.50	0.50	0.50
2	0.30	0.45	0.35	0.45
3	0.25	0.40	0.20	0.25
4	Not available	Not available	0.15	0.20

To illustrate the model results, Figure 37 shows the predicted skid number over time for different treatments and aggregate types. These predictions assumed traffic on a two-lane rural road, AADT of 5,000 veh/d, and 20 percent truck traffic. The first figure shows different treatment types with igneous aggregate type held constant. The only exception is for HFST, which is only placed using calcined bauxite. The second figure shows the effect of aggregate type for seal coat. Again, HFST using calcined bauxite is also shown for comparison. All else held constant, skid numbers are higher for coarser treatments and for more aggressively textured aggregates.

Table 22 shows estimated skid numbers for typical treatments with different aggregates. This shows the initial and terminal skid numbers, and the expected year to reach within a *SK* of 1 within the terminal value for both urban and rural applications. The urban scenario was a divided 4-lane road with 20,000 veh/day and 10 percent trucks. The rural scenario was the same as described above.

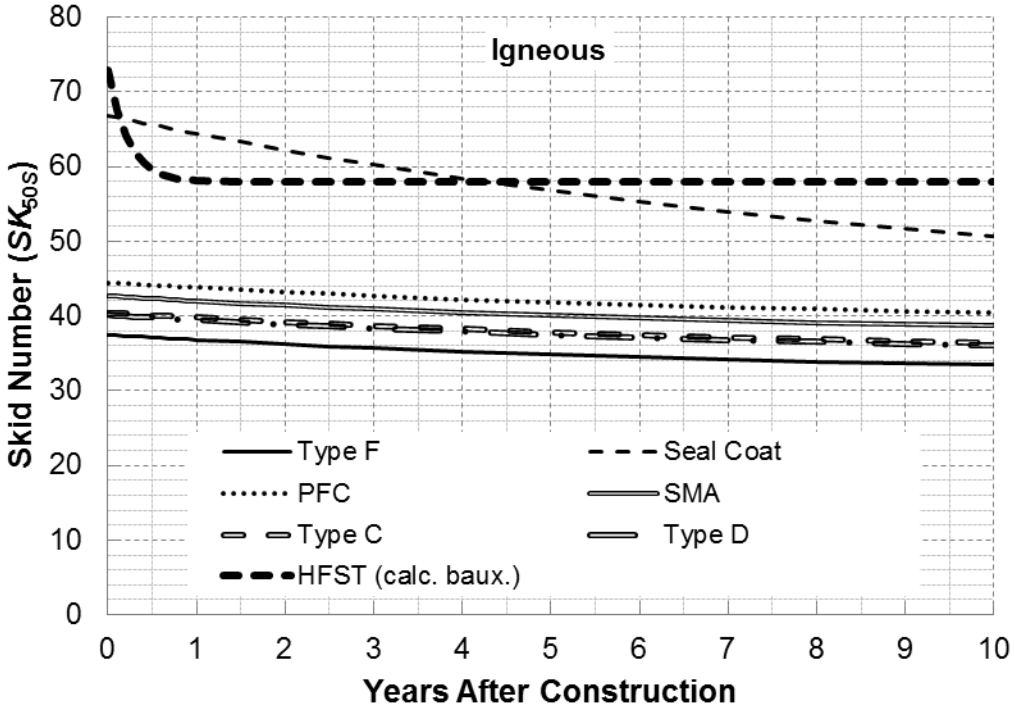

a. Different Treatments

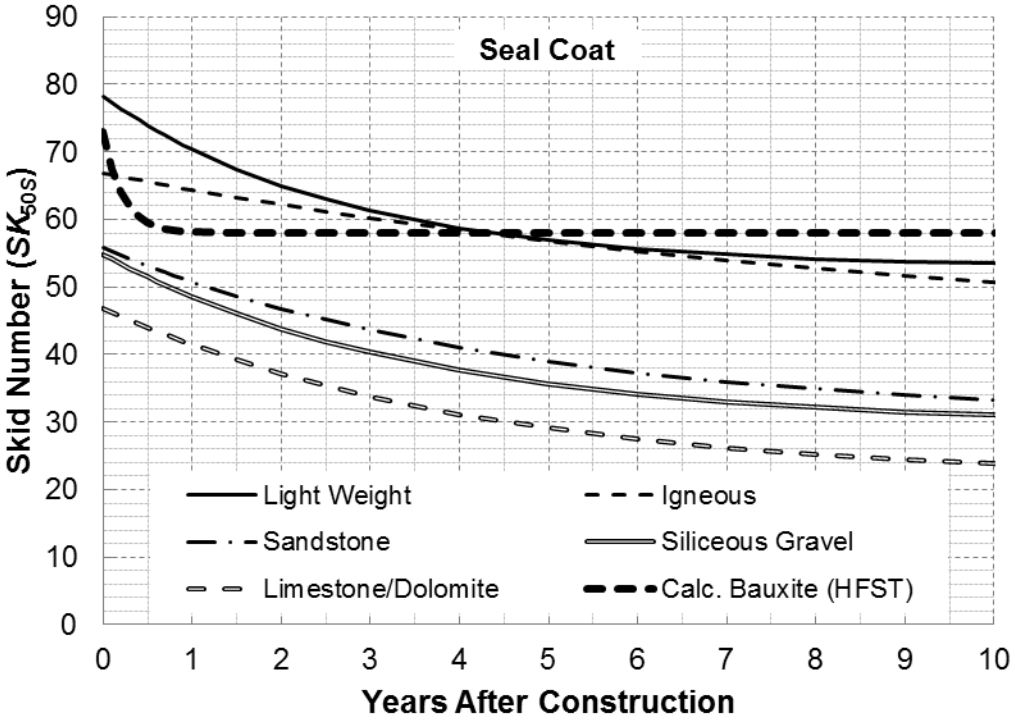

b. Different Aggregates

Figure 37. Skid Number versus Time for Treatments and Aggregates.

Table 22. Predicted Skid Numbers for Typical Treatments.

Treatment Type		Aggregate Type	Skid Number (SK_{50S})		Exponential Decay Rate (SK/yr)	Years to Terminal	
			Initial	Terminal		Urban	Rural
AC Overlay	Type C (DG, SP)	Limestone	35	35	0.11	3	6
		Sandstone	40	35	0.10	3	6
		Gravel (Siliceous)	37	32	0.13	2	5
		Igneous	43	37	0.05	7	14
	SMA (Type D, Type C)	Limestone	40	34	0.11	3	6
		Sandstone	41	36	0.10	3	6
		Gravel (Siliceous)	44	39	0.13	2	5
		Igneous	43	37	0.05	7	14
	TOM, CMHB-F	Limestone	40	34	0.11	3	6
		Sandstone	40	34	0.10	3	6
		Gravel (Siliceous)	36	31	0.13	2	5
		Igneous	34	28	0.05	7	14
	PFC	Limestone	44	39	0.11	3	6
		Sandstone	41	36	0.10	3	6
		Gravel (Siliceous)	41	35	0.13	2	5
		Igneous	39	33	0.05	7	14
Seal Coat	Gr. 3, Gr. 4, Gr. 5	Lightweight	78	53	0.09	7	13
		Limestone	67	42	0.08	7	15
		Sandstone	56	30	0.11	6	11
		Gravel (Siliceous)	55	30	0.04	16	32
		Igneous	47	22	0.14	4	9
HFST		Calcined Bauxite	73	58	1.67	0.3	0.6
		Flint	65	55	0.76	0.6	1.2

A comparison between the original model from TxDOT research project 0-6746 and the proposed model is given in Table 23. The mean absolute error between the predicted *SK* and the actual *SK* was about 14 for the original model and was between 7 and 13 for the proposed model. Perhaps more importantly, the proposed model simpler, requiring 9 input variables and 7 regression coefficients. In contrast, the original model required 12 variables and 28 regression coefficients. The R^2 values were weak, ranging from 0.12 to 0.43. This is due, in part, to the highly variable nature of field skid data. Though the models demonstrate general trends in *SK* versus traffic and time, they are not recommended for detailed long-term predictions.

Table 23. Model Performance Comparison.

Model	Mean Absolute Error (*SK*)		Percent Improvement (%)	R^2 Value for Predicted vs. Observed SK
	Original Model (0-6746)*	Proposed Model		
Asphalt Overlay	13.6	7.0	49	0.12
Seal Coat	14.1	12.3	13	0.43
HFST	NA	7.0	NA	0.37

* Small modification to calculation of mean profile depth to reduce outliers

CHAPTER 5: SAFETY AND WEATHER DATA ANALYSIS

INTRODUCTION

Statistics have consistently shown that the crash rate on horizontal curves is significantly greater than that on tangent roadway segments of similar character. This trend may be caused by drivers failing to detect the presence of a curve or attempting to negotiate the curve at unsafe speeds. Motorists may adopt unsafe speeds if they misjudge the sharpness of the curve, or if they neglect to adjust to adverse weather conditions. Speeds that may be safe during dry-surface conditions may not be safe during wet-surface conditions, depending on speed and curve geometry. The frequency of wet-surface crashes on curves is affected by site characteristics, traffic volume, curve length, and exposure to precipitation, particularly rain.

The application of pavement friction treatments at appropriate horizontal curve locations has the potential to improve driver performance and reduce the number of crashes, especially wet-surface crashes, experienced at horizontal curves. These treatments must be implemented judiciously due to their cost but have the potential to improve safety at lower cost than geometric improvements like curve straightening, and with greater effectiveness than control-device treatments like installing delineators or Chevrons. Candidate sites for pavement friction treatments should be prioritized based on a margin-of-safety analysis that accounts for the curve's geometry, vehicle speed (*2*), and exposure to wet-surface conditions.

This chapter consists of two parts. The first part presents an analysis of weather patterns and trends in the state of Texas for a 30-year period, focusing on rainfall totals. The second and third parts describe crash data analyses consisting of regression modeling and before-after evaluation.

WEATHER PATTERNS AND TRENDS

Adverse weather is a concern for safe vehicle operation. The risk posed by rain, snow, and sleet is attributed to a combination of poor pavement friction (due to the moisture on the surface) and low visibility. Friction is reduced even more if the temperature is near or below freezing (*68*). Theofilatos and Yannis summarized studies presented at conferences or published in international journals that focus on the effects of traffic, weather, and the combined effect of traffic and weather on road safety (*69*). They showed that precipitation has been widely investigated, and that the occurrence of precipitation consistently results in an increase in crashes.

Traffic Crashes during Adverse Weather Conditions

Researchers gathered Texas adverse-weather crash data from TxDOT's CRIS database. Adverse weather conditions include rain, sleet/hail, snow, fog, blowing sand/snow, and severe crosswinds. In the years 2009–2016, around 416,000 crashes (approximately 52,000 crashes/year) occurred in Texas due to adverse weather conditions. These crashes comprise approximately 10 percent of total crashes on Texas roadways. According to the frequency analysis in Table 24, the large majority of weather-related crashes (around 95 percent) occurred in conditions of rain, sleet/hail, and snow.

Table 24. Total Crashes during Adverse Weather Conditions.

Weather Event	2009	2010	2011	2012	2013	2014	2015	2016	Annual Mean
Rain	53,254	43,317	26,373	36,815	44,924	44,357	63,582	54,100	45,840
Sleet/Hail	1,291	483	1,537	387	2,182	3,222	2,283	193	1,447
Snow	1,947	2,626	2,811	1,106	1,141	2,190	2,722	245	1,849
Fog	2,928	1,655	1,757	2,486	2,100	2,620	2,766	2,557	2,359
Blowing Sand/Snow	340	194	373	271	200	281	181	144	248
Severe Crosswinds	345	288	324	270	290	282	186	242	278
Total	**60,105**	**48,563**	**33,175**	**41,335**	**50,837**	**52,952**	**71,720**	**57,481**	**52,021**

Climate Normal Data

The term “climate normal” is used in a broad sense to refer to a full suite of products issued by the National Oceanic and Atmospheric Administration (NOAA) that describes climatological conditions with 30-year averages and other statistics (*70*). For example, the precipitation normal in January for a station would be computed by taking the average of the 30 January values of monthly average precipitations from 1981 to 2010. Each of the 30 monthly values was in turn derived from averaging the daily observations of precipitation for the station. These data provide users with many tools to understand typical climate conditions for thousands of locations across the United States. Meteorologists and climatologists regularly use NOAA climate normal data for placing recent climate conditions into a historical context. This standardized data set is suitable for showing the precipitation trends over specific regions like counties or districts.

Researchers used two 30-year climate normal data sets (1971–2000 and 1981–2010) and tabulated annual precipitation rates by county. Appendix C provides these totals. Figure 38a shows the locations of the weather stations that are included in the analysis. Figure 38b illustrates annual average precipitation rate (in.) by county using the NOAA 1981–2010 climate normal data set. The trend shows that the west regions experience less amount of precipitation than the east regions. Appendix C shows monthly precipitation trends (using the 1981–2010 NOAA climate normal dataset).

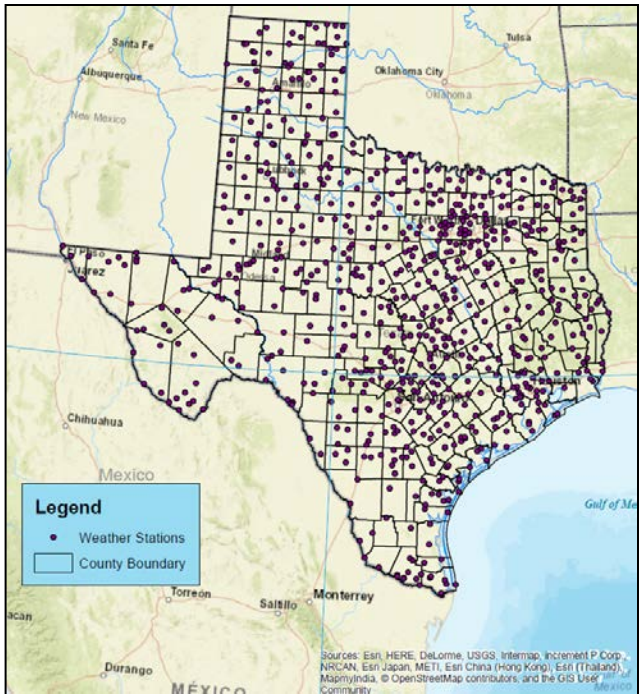

a. Weather Stations in Texas

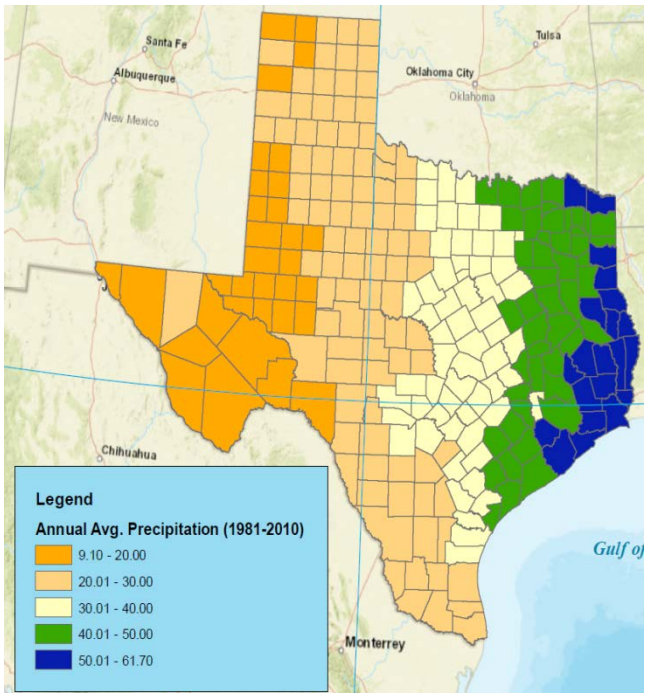

b. Annual Precipitation (in.) by County

Figure 38. Weather Stations and Annual Precipitation Rate (in.) by County (1981–2010 NOAA Normal).

Table 25 lists annual precipitation (in.) by TxDOT districts. The same trends are shown in Figure 39. The precipitation trends in Figure 38b and Figure 39 are similar to those shown in Figure 1 of TxDOT's *Wet Surface Crash Reduction Program Guidelines* (*71*). The latter map is repeated as Figure 40 below. These trends are useful in efforts to prioritize pavement friction treatments both across districts and between counties within districts. Specifically, the site selection guidelines provided in the *Wet Surface Crash Reduction Program Guidelines* and also in TxDOT's Form 2088 (*4*) define the rainfall rate r as:

- Low: $r \leq 20$ in.
- Medium: 20 in. $< r \leq 40$ in.
- High: $r > 40$ in.

On Form 2088, low, medium, and high rainfall rates are given values of 1, 2, and 3, respectively, on a qualitative pointing scale. This pointing scale accounts for rainfall exposure, traffic volume, regulatory speed limit, truck percentage, vertical grade, horizontal curvature, driveway presence, intersecting roadway traffic volume, and wet-surface crash percentage. The guidance on Form 2088 applies to continuous roadway sections, not to individual curves.

Table 25. Annual Average Precipitation (in.) by TxDOT District.

District (Number)	Annual Avg. Precipitation (in.) 1971–2000 NOAA Normal	Annual Avg. Precipitation (in.) 1981–2010 NOAA Normal
Paris (1)	45.53	45.91
Fort Worth (2)	33.32	35.61
Wichita Falls (3)	30.58	31.95
Amarillo (4)	20.31	20.76
Lubbock (5)	19.51	20.19
Odessa (6)	13.93	14.67
San Angelo (7)	21.99	23.15
Abilene (8)	24.12	23.97
Waco (9)	35.35	34.99
Tyler (10)	46.14	46.65
Lufkin (11)	50.08	52.07
Houston (12)	48.65	49.04
Yoakum (13)	41.19	41.42
Austin (14)	33.87	33.68
San Antonio (15)	30.39	30.88
Corpus Christi (16)	32.29	32.84
Bryan (17)	40.93	42.45
Dallas (18)	38.92	39.44
Atlanta (19)	48.99	49.01
Beaumont (20)	57.53	58.33
Pharr (21)	24.16	24.91
Laredo (22)	21.68	22.7
Brownwood (23)	28.34	29.8
El Paso (24)	13.7	15.18
Childress (25)	23.5	24.49
All Districts	33.00	33.76

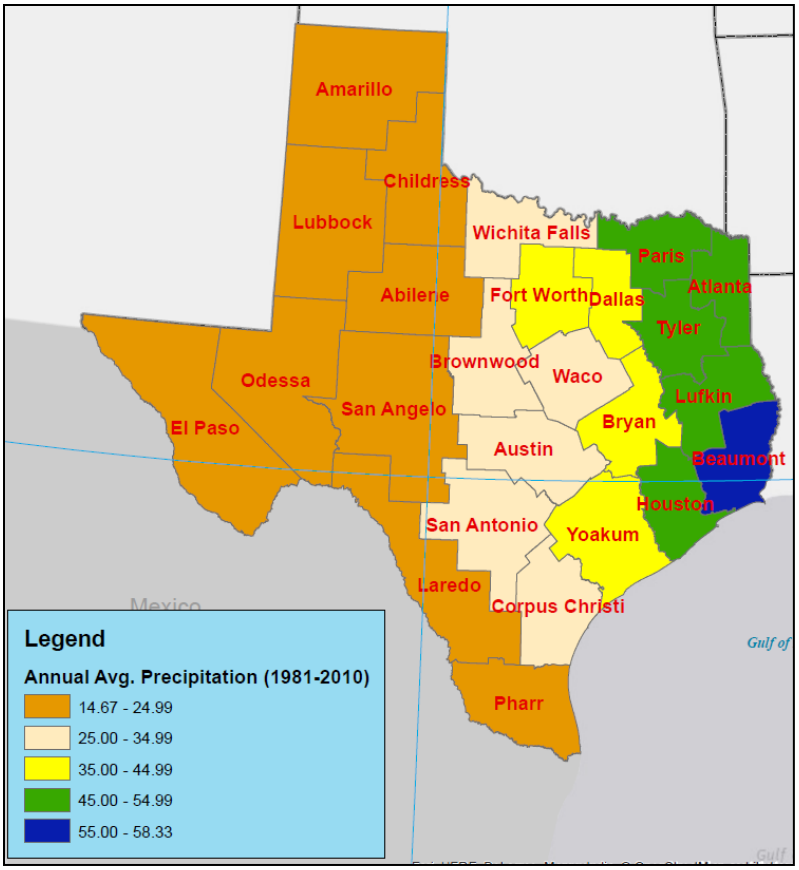

Figure 39. Annual Precipitation (in.) by TxDOT District (1981–2010 NOAA Normal).

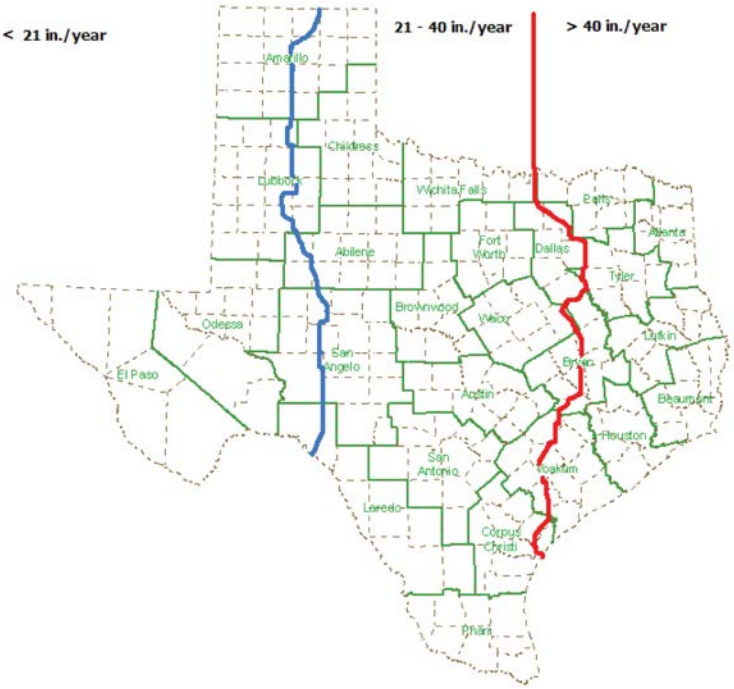

Figure 40. Boundaries of Low, Moderate, and High Rainfall Areas (*71*).

In summary, analysis of the 1981–2010 NOAA climate normal data set yielded trends similar to those shown in TxDOT's *Wet Surface Crash Reduction Program Guidelines* document, but with finer resolution. These trends allow the analyst to consider wet-surface exposure in the ranking of candidate pavement friction treatments across a set of curve sites.

REGRESSION MODELING

Researchers examined the relationship between curve geometry, pavement characteristics, traffic volume, and crash frequency using cross-sectional modeling and panel modeling.

Database Development

The database assembled for developing the regression models consisted of a set of similar horizontal curves. The horizontal curve information was extracted from the Texas Reference Marker System (TRM) Geometrics (Geo-Hini) database for the year 2012. The Geo-Hini database contains geometrics for all curves on all highways in the state. Each curve is given a unique curve identifier number, and the beginning and ending milepoints of each curve are located through a given reference marker and curve length from that marker. Only normal curves (i.e., curves that deflect at a constant rate and do not have spiral transitions) that are ≥ 0.1 miles in length were considered in this analysis.

The horizontal curve database was combined with the TxDOT's Road-Highway Inventory Network (RHiNo) database using the control section numbers and milepoints. Variables extracted from the RHiNo database included average daily traffic (ADT), truck percentage, shoulder widths, lane width, median width, and number of lanes. Only those sites that have at least 400 vehicles per day were considered in this study.

Pavement data were obtained from the PMIS database for the years 2012 to 2016. Specifically, the following quantities were extracted:

- Skid score (or skid number).
- Condition score.
- Distress score.
- Ride score.
- IRI.

These quantities provide insight into friction supply and general pavement condition. The curves of interest were located in the PMIS database using reference markers and displacements.

Researchers retrieved crash data for the years 2012–2016 from the CRIS database. These data consisted of information describing date and location of the crash, severity, and weather conditions. Since it is widely recognized that property damage only (PDO) crash counts vary widely on a regional basis due to significant variation in reporting threshold, only those crashes that are associated with injury or fatality were considered in this analysis. The following four crash severity levels were used: fatal (K), incapacitating injury (A), non-incapacitating injury (B), and possible injury (C).

Once the crash and road-related data were collected for each horizontal curve, the data were combined using control section number and milepoints. Separate databases were built for curves on two-lane highways, four-lane undivided highways, and four-lane divided highways.

Table 26 presents the summary statistics of the variables used for SPF development with cross-sectional data. The database assembled for calibration included crash frequency over a five-year period as the dependent variable. The crash data were separated into four categories:

- All crashes.
- All wet-weather-related crashes.
- ROR crashes.
- ROR wet-weather-related crashes.

Table 26. Summary Statistics for Horizontal Curve SPF Development.

Variable	Two-Lane			Four-Lane Undivided			Four-Lane Divided		
	Range	Mean (SD)*	Total	Range	Mean (SD)*	Total	Range	Mean (SD)*	Total
Curve Length (Miles)	0.05–0.99	0.14 (0.09)	5961	0.1–0.92	0.21 (0.1)	151	0.1–0.99	0.27 (0.16)	416.7
ADT (Vehicles/day)	10–14765	1038 (1332)	--	475–26587	7133 (4731)	--	727–63935	14400 (10370)	--
Average Lane Width (ft)	5.5–16	10.97 (1.0)	--	10.5–15	11.9 (0.8)	--	11–15.5	12.0 (0.34)	--
Average Inside Shoulder Width (ft)	--	--	--	--	--	--	0–13	4.57 (1.68)	--
Average Outside Shoulder Width (ft)	0–17	3.3 (5.7)	--	0–13	3.9 (3.5)	--	0–16	9.68 (1.92)	--
Radius (ft)	106–28633	2869 (2954)	--	169–24548	4326 (3303)	--	127–29982	6977 (5168)	--
Maximum Speed (Miles/hour)	30–75	60.1 (8.0)	--	30–75	65.0 (10.6)	--	35–85	72.8 (6.3)	--
Skid Number	3-99	46.0 (14.1)	--	9-73	38.4 (12.4)	--	7-64	35.0 (10.6)	--
Annual Precipitation (inches)	9.1–63.1	38.5 (11.3)	--						
All Crashes	0–11	0.13 (0.5)	5546	0–5	0.51 (0.86)	486	0–21	1.27 (1.93)	1950
All Wet-Weather Crashes	0–9	0.02 (0.15)	733	0–4	0.10 (0.36)	65	0–15	0.30 (0.86)	458
ROR Crashes	0–10	0.11 (0.41)	4735	0–4	0.34 (0.65)	270	0–14	0.84 (1.36)	1292
ROR Wet-Weather Crashes	0–8	0.02 (0.14)	665	0–4	0.08 (0.32)	46	0–12	0.22 (0.67)	342

*SD: standard deviation

Geometric design features, traffic control features, and traffic characteristics were included as independent variables.

Methodology

The primary objective of this task was to develop SPFs to describe the relationship between crash frequency and traffic and geometric variables for horizontal curves in Texas. The probabilistic structure used for developing the models or SPFs was the following: the number of crashes at the i^{th} segment, Y_i, when conditional on its mean μ_i, is assumed to be Poisson distributed and independent over all segments as (*72*):

$$Y_i|\mu_i \sim Po(\mu_i) \tag{47}$$

where:

i = 1, 2, …, I.

The mean of the Poisson distribution is structured as:

$$\mu_i = f(X;\beta)e^{e_i} \tag{48}$$

where:

$f(.)$ = function of the covariates (X).
β = vector of unknown coefficients.
e_i = model error independent of the covariates.

It is usually assumed that e^{e_i} is independent and Gamma-distributed with a mean equal to 1 and a variance equal to $1/\phi$ for all i (with $\phi > 0$). With this characteristic, it can be shown that Y_i, conditional on $f(.)$ and ϕ, is distributed as a negative binomial (or Poisson-gamma) random variable with a mean $f(.)$ and a variance $f(.)(1+f(.)/\phi)$, respectively. The term ϕ is usually defined as the "inverse dispersion parameter" for the negative binomial distribution.

Although the dispersion parameter ($\alpha = 1/\phi$) or its inverse (ϕ) is now often modeled as a function of the covariates in the data (*72*, *73*, *74*, *75*), the models were estimated using a fixed dispersion parameter to simplify the model development.

An important characteristic associated with the development of statistical relationships is the choice of the functional form linking crashes to the covariates. For this work, the functional form is as follows:

$$\mu_i = L \times y \times e^{\beta_0} \times F^{\beta_1} \times CMF_1 \times \ldots \times CMF_k \tag{49}$$

where:

μ_i = estimated annual number of crashes per mile.
L = segment length, mi.
y = number of years of crash data, years.
F = traffic volume, vehicles per day.

The coefficients of the regression models for both cross-sectional and panel models were estimated using the Statistical Analysis Software program (*76*). The log-likelihood and Akaike

Information Criterion (AIC) statistics were used to assess the model goodness-of-fit. Only variables that had a large influence on the predicted values were included in the models.

Cross-Sectional Modeling

This section presents the results of the cross-sectional statistical analysis. The development of cross-sectional safety prediction models offers the advantage of quantifying the effects of a range of variables even if some of the variables are correlated, yielding insight that is more applicable to a range of sites. In general, a robust safety prediction methodology would require the use of a cross-sectional study approach.

Cross-sectional data each have an independent variable value averaged for each site over a particular period of time. The cross-sectional data approach has the following advantages:

- It provides a more robust predictive model than panel data when the year-to-year variability in the independent variables is largely random.
- Fewer or no observations with missing values, since some operational features may not be collected every year.
- Using cross-sectional data for model calibration will minimize the problems associated with over-representation of segments or intersections with zero crash.

This section consists of three parts. The first part describes the development of a horizontal curve safety database. The second part documents the regression analysis. The third part summarizes the analysis findings.

Modeling Results - Two-Lane Horizontal Curves

Table 27 summarizes the parameter estimates associated with the calibrated SPFs for horizontal curves on two-lane highways. The predictive models were developed separately for the four categories described above. The variables that are significant for all type of crashes were also significant for ROR crashes. In general, the sign and magnitude of the regression coefficients in Table 27 are logical and consistent with previous research findings (*2*). The list of variables presented in Table 27 reflects the findings from several preliminary regression analyses where different combinations of variables were examined. The list that is presented represents the variables that are significant in the model, while also having coefficient values that are logical and constructs that are theoretically defensible and properly bounded.

Figure 41 shows the fit of the all crash model for two-lane horizontal curves. This figure compares the predicted and observed crash frequency in the calibration database. The data points shown represent the total crash frequency for two-lane horizontal curves used to calibrate the corresponding model. The data were sorted by ADT and combined into 42 groups. Each group has equal number of observations and contain at least three predicted crashes. Each data point shown in Figure 41 represents the total predicted and total observed crash frequency in a particular group. The purpose of this grouping was to reduce the number of data points shown in the figure and, thereby, to facilitate an examination of trends in the data. A linear trendline is fitted and the corresponding equation and R^2 fit statistic are reported. In general, the data shown in the figure indicate that the model provides an unbiased estimate of expected crash frequency.

Table 27. Cross-Sectional Parameter Estimation for Two-Lane Highway Curves.

Variable	All Crashes		Wet-Weather Crashes		ROR Crashes		Wet-Weather ROR Crashes	
	Estimate	Std. err.	Estimate	Std. err.	Estimate	Std. err.	Estimate	Std. err.
Intercept	−7.733	0.156	−10.686	0.472	−8.000	0.174	−10.844	0.488
LN (ADT)	0.790	0.019	0.881	0.049	0.791	0.020	0.878	0.051
Curve Radius	0.461	0.038	0.579	0.118	0.577	0.049	0.703	0.142
Lane Width	−0.040	0.017	--	--	−0.063	0.018	--	--
Shoulder Width	−0.041	0.006	-0.029	0.014	−0.046	0.006	−0.030	0.015
Skid Number	−0.005	0.001	−0.034	0.003	−0.006	0.001	−0.035	0.003
Annual Prec.	0.015	0.002	0.035	0.004	0.016	0.002	0.037	0.004
Inverse Dispersion	0.855	0.049	0.317	0.051	0.929	0.071	0.299	0.050
AIC	29731		6286		26789		5834	

Note: -- = calibration coefficient is highly insignificant

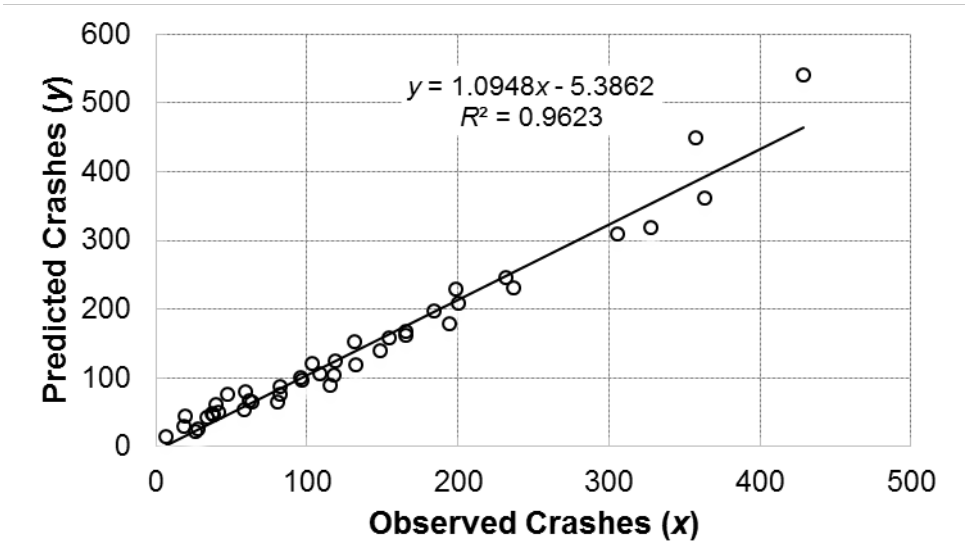

Figure 41. Observed versus Predicted Crashes, 2U Cross-Sectional Model.

The annual crash frequency for horizontal curves on two-lane highways is obtained by combining Equation 49 with the coefficients in Table 27 as follows:

$$\mu_{2U} = L \times y \times e^{-7.733} \times F^{0.790} \times CMF_R \times CMF_{LW} \times CMF_{SW} \times CMF_{SK} \times CMF_{AP} \quad (50)$$

with:

$$CMF_R = 1 + 0.461(0.147V)^4 \frac{(1.47V)^2}{32.2R^2} \quad (51)$$

$$CMF_{LW} = e^{-0.040(LW-12)} \quad (52)$$

$$CMF_{SW} = e^{-0.041(SW-8)} \quad (53)$$

$$CMF_{SK} = e^{-0.005(SK-40)} \quad (54)$$

$$CMF_{AP} = e^{0.015(AP-30)} \quad (55)$$

where:

μ_{2U} = estimated number of crashes per year per mile for curves on two-lane highways.
CMF_R = horizontal curve radius crash modification factor.
CMF_{LW} = lane width crash modification factor.
CMF_{SW} = shoulder width crash modification factor.
CMF_{SK} = skid number crash modification factor.
CMF_{AP} = annual precipitation crash modification factor.
R = curve radius, ft.
V = regulatory speed limit, mph.
LW = lane width, ft.
SW = shoulder width, ft.
SK = skid number.
AP = annual precipitation rate, in.

The annual wet-weather crash frequency for horizontal curves on two-lane highways can be estimated by the following equation:

$$\mu_{2U} = L \times y \times e^{-10.686} \times F^{0.881} \times CMF_R \times CMF_{SW} \times CMF_{SK} \times CMF_{AP} \quad (56)$$

with:

$$CMF_R = 1 + 0.579(0.147V)^4 \frac{(1.47V)^2}{32.2R^2} \quad (57)$$

$$CMF_{SW} = e^{-0.029(SW-8)} \quad (58)$$

$$CMF_{SK} = e^{-0.034(SK-40)} \quad (59)$$

$$CMF_{AP} = e^{0.035(AP-30)} \quad (60)$$

The annual ROR crash frequency for horizontal curves on two-lane highways can be estimated by the following equation:

$$\mu_{2U} = L \times y \times e^{-8.000} \times F^{0.791} \times CMF_R \times CMF_{LW} \times CMF_{SW} \times CMF_{SK} \times CMF_{AP} \quad (61)$$

with:

$$CMF_R = 1 + 0.577(0.147V)^4 \frac{(1.47V)^2}{32.2R^2} \quad (62)$$

$$CMF_{LW} = e^{-0.063(LW-12)} \quad (63)$$

$$CMF_{SW} = e^{-0.046(SW-8)} \quad (64)$$

$$CMF_{SK} = e^{-0.006(SK-40)} \quad (65)$$

$$CMF_{AP} = e^{0.016(AP-30)} \quad (66)$$

The annual wet-weather ROR crash frequency for horizontal curves on two-lane highways can be estimated by the following equation:

$$\mu_{2U} = L \times y \times e^{-10.844} \times F^{0.878} \times CMF_R \times CMF_{SW} \times CMF_{SK} \times CMF_{AP} \quad (67)$$

with:

$$CMF_R = 1 + 0.703(0.147V)^4 \frac{(1.47V)^2}{32.2R^2} \quad (68)$$

$$CMF_{SW} = e^{-0.030(SW-8)} \quad (69)$$

$$CMF_{SK} = e^{-0.035(SK-40)} \quad (70)$$

$$CMF_{AP} = e^{0.037(AP-30)} \quad (71)$$

Modeling Results - Four-Lane Horizontal Curves

Table 28 summarizes the parameter estimates associated with the calibrated SPFs for horizontal curves on four-lane undivided highways. In general, the sign and magnitude of the regression coefficients in this table are logical and consistent with previous research findings (*2*). The list of variables reflects the findings from several preliminary regression analyses where different combinations of variables were examined. The list represents the variables that provided the best fit to the data, while also having coefficient values that are logical and constructs that are theoretically defensible and properly bounded.

Table 28. Cross-Sectional Parameter Estimation for Four-Lane Undivided Highway Curves.

Variable	All Crashes		Wet Weather Crashes		ROR Crashes		Wet Weather ROR Crashes	
	Estimate	Std. err	Estimate	Std. err	Estimate	Std. err	Estimate	Std. err
Intercept	−5.330	0.778	−6.172	1.710	−5.169	0.893	−5.954	1.788
LN(ADT)	0.510	0.086	0.397	0.191	0.432	0.098	0.339	0.199
Curve Radius	0.3991	0.155	0.592	0.367	0.723	0.256	0.834	0.497
Skid Number	--	--	−0.0188	0.011	--	--	−0.018	0.012
Inverse Dispersion	2.174	0.679	0.951	0.722	3.040	1.682	2.358	4.170
AIC	1352		452		1068		386	

Note: -- = calibration coefficient is highly insignificant

Figure 42 shows the fit of the all crash model for four-lane undivided horizontal curves. This figure compares the predicted and observed crash frequency in the calibration database. The data were sorted by ADT and combined into 49 groups. Each data point shown in Figure 42 represents the total predicted and total observed crash frequency in a particular group. The data shown in the figure indicate that the model may provide a biased estimate of expected crash frequency.

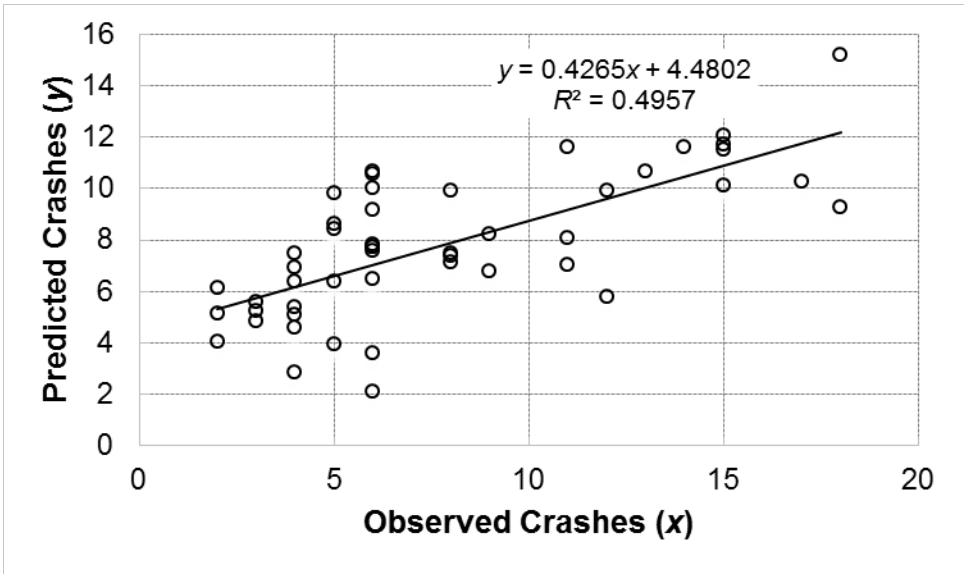

Figure 42. Observed versus Predicted Crashes, 4U Cross-Sectional Model.

The annual crash fatal-and-injury frequency for horizontal curves on four-lane undivided highways is obtained by combining the Equation 49 with the coefficients in Table 28 as follows:

$$\mu_{4U} = L \times y \times e^{-5.330} \times F^{0.510} \times CMF_R \tag{72}$$

with:

$$CMF_R = 1 + 0.3991(0.147V)^4 \frac{(1.47V)^2}{32.2R^2} \tag{73}$$

where:

μ_{4U} = estimated number of crashes per year per mile for curves on four-lane undivided highways.

The annual wet-weather crash frequency for horizontal curves on four-lane undivided highways can be estimated by the following equation:

$$\mu_{4U} = L \times y \times e^{-6.172} \times F^{0.397} \times CMF_R \times CMF_{SK} \tag{74}$$

with:

$$CMF_R = 1 + 0.592(0.147V)^4 \frac{(1.47V)^2}{32.2R^2} \tag{75}$$

$$CMF_{SK} = e^{-0.0188(SK-40)} \tag{76}$$

The annual ROR crash frequency for horizontal curves on four-lane undivided highways can be estimated by the following equation:

$$\mu_{4U} = L \times y \times e^{-5.169} \times F^{0.432} \times CMF_R \tag{77}$$

with:

$$CMF_R = 1 + 0.723(0.147V)^4 \frac{(1.47V)^2}{32.2R^2} \tag{78}$$

The annual wet-weather ROR crash frequency for horizontal curves on four-lane undivided highways can be estimated by the following equation:

$$\mu_{4U} = L \times y \times e^{-5.954} \times F^{0.339} \times CMF_R \times CMF_{SK} \quad (79)$$

with:

$$CMF_R = 1 + 0.834(0.147V)^4 \frac{(1.47V)^2}{32.2R^2} \quad (80)$$

$$CMF_{SK} = e^{-0.018(SK-40)} \quad (81)$$

Table 29 summarizes the parameter estimates associated with the calibrated SPFs for horizontal curves on four-lane divided highways. In general, the sign and magnitude of the regression coefficients in Table 29 are logical and consistent with previous research findings. The list of variables presented in this table reflects the findings from several preliminary regression analyses where different combinations of variables were examined. Similar to the results for undivided curved segments, the list represents the variables that provided the best fit to the data, while also having coefficient values that are logical and constructs that are theoretically defensible and properly bounded.

Table 29. Cross-Sectional Parameter Estimation for Four-Lane Divided Highway Curves.

Variable	All Crashes		Wet Weather Crashes		ROR Crashes		Wet Weather ROR Crashes	
	Estimate	Std. err	Estimate	Std. err	Estimate	Std. err	Estimate	Std. err
Intercept	−8.095	0.423	−10.041	0.853	−7.253	0.486	−8.986	0.916
LN(ADT)	0.845	0.044	0.879	0.089	0.713	0.051	0.740	0.096
Inside Shoulder Width	−0.073	0.019	–0.0548	0.039	−0.079	0.022	−0.031	0.042
Outside Shoulder Width	−0.012	0.017	--	--	--	--	--	--
Skid Number	−0.0038	0.003	−0.0236	0.006	−0.0072	0.003	−0.026	0.006
Dispersion	2.638	0.315	0.861	0.155	2.344	0.339	0.846	0.183
AIC	4407		1961		3664		1684	

Note: -- = calibration coefficient is highly insignificant

Figure 43 shows the fit of the all crash model for four-lane divided horizontal curves. This figure compares the predicted and observed crash frequency in the calibration database. The data were sorted by ADT and combined into 54 groups. Each data point shown in Figure 43 represents the total predicted and total observed crash frequency in a particular group. In general, the data shown in the figure indicate that the model provides an unbiased estimate of expected crash frequency.

The annual crash frequency for horizontal curves on four-lane divided highways is obtained by combining Equation 49 with the coefficients in Table 29.

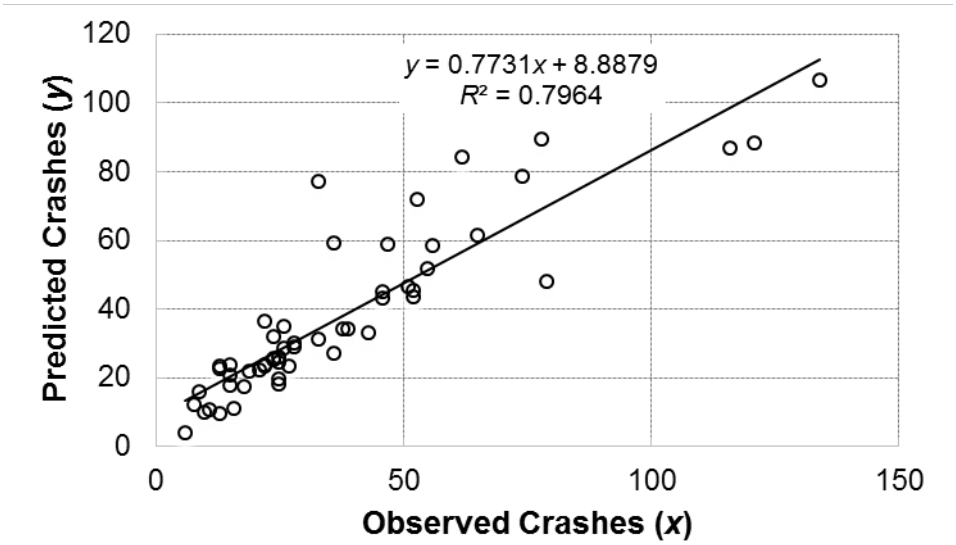

Figure 43. Observed versus Predicted Crashes, 4D Cross-Sectional Model.

The annual fatal-and-injury crash frequency for horizontal curves on four-lane divided highways can be estimated by the following equation:

$$\mu_{4D} = L \times y \times e^{-8.095} \times F^{0.845} \times CMF_{ISW} \times CMF_{OSW} \times CMF_{SK} \quad (82)$$

with:

$$CMF_{ISW} = e^{-0.073(ISW-4)} \quad (83)$$

$$CMF_{OSW} = e^{-0.012(OSW-8)} \quad (84)$$

$$CMF_{SK} = e^{-0.0038(SK-40)} \quad (85)$$

where:

μ_{4D} = estimated number of crashes per year per mile for curves on four-lane divided highways.
CMF_{ISW} = inside shoulder width crash modification factor.
CMF_{OSW} = outside shoulder width crash modification factor.
ISW = inside shoulder width, ft.
OSW = outside shoulder width, ft.

The annual wet-weather crash frequency for horizontal curves on four-lane divided highways can be estimated by the following equation:

$$\mu_{4D} = L \times y \times e^{-10.041} \times F^{0.879} \times CMF_{ISW} \times CMF_{SK} \quad (86)$$

with:

$$CMF_{ISW} = e^{-0.0548(ISW-4)} \quad (87)$$

$$CMF_{SK} = e^{-0.0236(SK-40)} \quad (88)$$

The annual ROR crash frequency for horizontal curves on four-lane divided highways can be estimated by the following equation:

$$\mu_{4D} = L \times y \times e^{-7.253} \times F^{0.713} \times CMF_{ISW} \times CMF_{SK} \quad (89)$$

with:

$$CMF_{ISW} = e^{-0.079(ISW-4)} \quad (90)$$

$$CMF_{SK} = e^{-0.0072(SK-40)} \quad (91)$$

The annual wet-weather ROR crash frequency for horizontal curves on four-lane divided highways can be estimated by the following equation:

$$\mu_{4D} = L \times y \times e^{-8.986} \times F^{0.740} \times CMF_{ISW} \times CMF_{SK} \quad (92)$$

with:

$$CMF_{ISW} = e^{-0.031(ISW-4)} \quad (93)$$

$$CMF_{SK} = e^{-0.026(SK-40)} \quad (94)$$

Panel Data Modeling

The data set used in this study contains some variables that vary by year. In such situations, cross-sectional modeling framework may not identify realistic patterns in the data variables. Panel data modeling is a different modeling approach that is recommended when the variables are observed over time. The panel data models allow the safety effects of changing variables to be quantified more precisely when independent variable value is measured for each site for each year. In this particular data set, in addition to ADT, skid number and precipitation rate are known to change notably between years, as skid number degrades over time and precipitation varies naturally. In this study, researchers repeated the site for each year and the variables ADT, skid number, and precipitation are unique for each year. Panel data modeling has the following advantages (*77*):

- From the statistical perspective, the increase in number of observations leads to higher degree of freedom and less collinearity, which in turn improves the parameter estimation accuracy.
- It will allow researchers to test whether more simplistic specifications are appropriate.
- The panel models can be used to analyze some specific questions, such as change in the variable effect over time, that cannot be answered with cross-sectional modeling.

As discussed by Lord and Persaud (*78*), analyzing time-series or panel data in this manner can create temporal or serial correlation. Random effects models and those estimated using the generalized estimating equations can be used for handling serial correlation (*78*). However, after further investigation, it was determined that the serial correlation had a minimal impact on the modeling results. Hence, to simplify the modeling effort, the models were estimated using the generalized linear models.

Modeling Results—Two-Lane Horizontal Curves

Table 30 summarizes the parameter estimates associated with the calibrated SPFs for horizontal curves on two-lane highways. The predictive models were developed separately for the four categories described above. The variables that are significant for all type of crashes were

also significant for ROR crashes. In general, the sign and magnitude of the regression coefficients in Table 30 are logical and consistent with previous research findings. The list of variables presented in Table 30 reflects the findings from several preliminary regression analyses where different combinations of variables were examined. The list that is presented represents the variables that are significant in the model, while also having coefficient values that are logical and constructs that are theoretically defensible and properly bounded.

Table 30. Panel-Data Parameter Estimation for Two-Lane Highway Curves.

Variable	All Crashes		Wet Weather Crashes		ROR Crashes		Wet Weather ROR Crashes	
	Estimate	**Std. err.**	**Estimate**	**Std. err.**	**Estimate**	**Std. err.**	**Estimate**	**Std. err.**
Intercept	−7.439	0.246	−10.108	0.782	−7.648	0.275	−10.157	0.795
LN (ADT)	0.760	0.027	0.841	0.072	0.752	0.029	0.834	0.076
Curve Radius	0.356	0.050	--	--	0.474	0.065	--	--
Lane Width	−0.064	0.025	--	--	−0.088	0.027	--	--
Shoulder Width	−0.040	0.009	−0.058	0.021	−0.044	0.009	−0.057	0.022
Skid Number	−0.009	0.002	−0.038	0.005	−0.010	0.002	−0.038	0.005
Annual Prec.	0.014	0.002	0.031	0.007	0.014	0.003	0.032	0.007
Dispersion	0.585	0.073	0.277	0.121	0.504	0.067	0.224	0.098
AIC	16326		3023		14414		2805	

Note: -- = calibration coefficient is highly insignificant

Figure 44 shows the fit of the all crash model for two-lane horizontal curves. This figure compares the predicted and observed crash frequency in the calibration database. The data were sorted by ADT and combined into 45 groups. Each data point shown in Figure 44 represents the total predicted and total observed crash frequency in a particular group. In general, the data shown in the figure indicate that the model provides an unbiased estimate of expected crash frequency. Although the fit statistic is the same as the cross-sectional models, the slope is almost equal to 1, which means panel model provides slightly better fit.

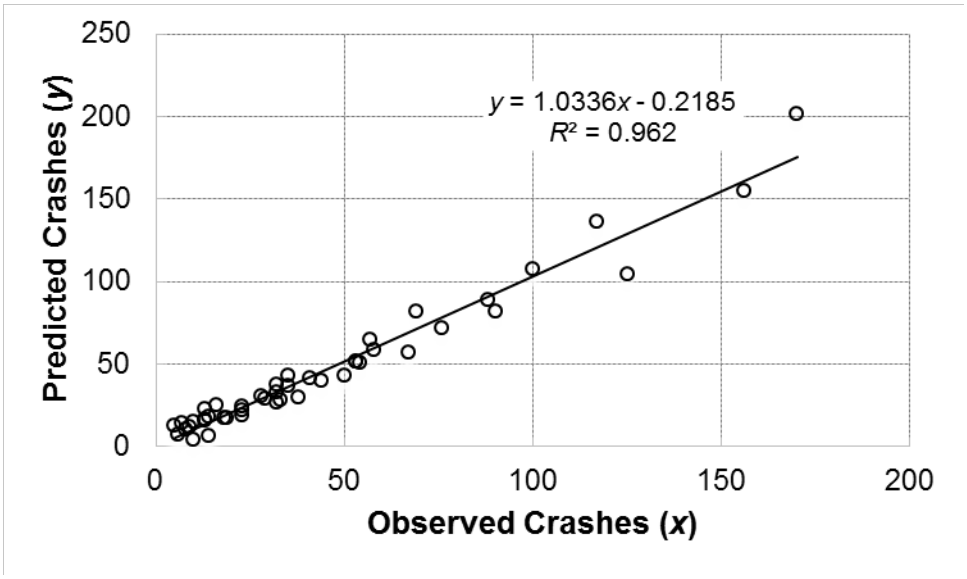

Figure 44. Observed versus Predicted Crashes, 2U Panel Model.

The annual crash frequency for horizontal curves on two-lane highways is obtained by combining Equation 49 with the coefficients in Table 30 as follows:

$$\mu_{2U} = L \times y \times e^{-7.439} \times F^{0.760} \times CMF_R \times CMF_{LW} \times CMF_{SW} \times CMF_{SK} \times CMF_{AP} \quad (95)$$

with:

$$CMF_R = 1 + 0.356(0.147V)^4 \frac{(1.47V)^2}{32.2R^2} \quad (96)$$

$$CMF_{LW} = e^{-0.064(LW-12)} \quad (97)$$

$$CMF_{SW} = e^{-0.040(SW-8)} \quad (98)$$

$$CMF_{SK} = e^{-0.009(SK-40)} \quad (99)$$

$$CMF_{AP} = e^{0.014(AP-30)} \quad (100)$$

The annual wet-weather crash frequency for horizontal curves on two-lane highways can be estimated by the following equation:

$$\mu_{2U} = L \times y \times e^{-10.108} \times F^{0.841} \times CMF_{SW} \times CMF_{SK} \times CMF_{AP} \quad (101)$$

with:

$$CMF_{SW} = e^{-0.058(SW-8)} \quad (102)$$

$$CMF_{SK} = e^{-0.038(SK-40)} \quad (103)$$

$$CMF_{AP} = e^{0.031(AP-30)} \quad (104)$$

The annual ROR crash frequency for horizontal curves on two-lane highways can be estimated by the following equation:

$$\mu_{2U} = L \times y \times e^{-7.648} \times F^{0.752} \times CMF_R \times CMF_{LW} \times CMF_{SW} \times CMF_{SK} \times CMF_{AP} \quad (105)$$

with:

$$CMF_R = 1 + 0.474(0.147V)^4 \frac{(1.47V)^2}{32.2R^2} \quad (106)$$

$$CMF_{LW} = e^{-0.088(LW-12)} \quad (107)$$

$$CMF_{SW} = e^{-0.044(SW-8)} \quad (108)$$

$$CMF_{SK} = e^{-0.010(SK-40)} \quad (109)$$

$$CMF_{AP} = e^{0.014(AP-30)} \quad (110)$$

The annual wet-weather ROR crash frequency for horizontal curves on two-lane highways can be estimated by the following equation:

$$\mu_{2U} = L \times y \times e^{-10.157} \times F^{0.834} \times CMF_{SW} \times CMF_{SN} \times CMF_{AP} \quad (111)$$

with:

$$CMF_{SW} = e^{-0.057(SW-8)} \quad (112)$$

$$CMF_{SK} = e^{-0.038(SK-40)} \quad (113)$$

$$CMF_{AP} = e^{0.032(AP-30)} \quad (114)$$

Modeling Results—Four-Lane Horizontal Curves

Table 31 summarizes the parameter estimates associated with the calibrated SPFs for horizontal curves on four-lane undivided highways. In general, the sign and magnitude of the regression coefficients in this table are logical and consistent with previous research findings. The list of variables reflects the findings from several preliminary regression analyses where different combinations of variables were examined. The list represents the variables that provided the best fit to the data, while also having coefficient values that are logical and constructs that are theoretically defensible and properly bounded.

Table 31. Panel-Data Parameter Estimation for Four-Lane Undivided Highway Curves.

Variable	All Crashes		Wet Weather Crashes		ROR Crashes		Wet Weather ROR Crashes	
	Estimate	Std. err	Estimate	Std. err	Estimate	Std. err	Estimate	Std. err
Intercept	−5.158	1.052	−7.097	2.445	−4.179	1.252	−6.551	2.659
LN(ADT)	0.484	0.115	0.491	0.267	0.308	0.137	0.387	0.289
Curve Radius	0.505	0.194	0.689	0.502	0.939	0.363	1.112	0.788
Skid Number	−0.007	0.005	−0.034	0.013	-0.011	0.006	−0.047	0.015
Dispersion	4.192	5.089	1.186	2.636	9.877	40.692	0.816	1.517
AIC	1381		387		1027		335	

The annual crash fatal-and-injury frequency for horizontal curves on four-lane undivided highways is obtained by combining Equation 49 with the coefficients in Table 31 as follows:

$$\mu_{4U} = L \times y \times e^{-5.158} \times F^{0.484} \times CMF_R \times CMF_{SK} \quad (115)$$

with:

$$CMF_R = 1 + 0.505(0.147V)^4 \frac{(1.47V)^2}{32.2R^2} \quad (116)$$

$$CMF_{SK} = e^{-0.007(SK-40)} \quad (117)$$

Figure 45 shows the fit of the all crash model for four-lane undivided horizontal curves. This figure compares the predicted and observed crash frequency in the calibration database. The data were sorted by ADT and combined into 50 groups. Each data point shown in Figure 45 represents the total predicted and total observed crash frequency in a particular group. The data shown in the figure indicate that the model may provide a biased estimate of expected crash frequency.

The annual wet-weather crash frequency for horizontal curves on four-lane undivided highways can be estimated by the following equation:

$$\mu_{4U} = L \times y \times e^{-7.097} \times F^{0.491} \times CMF_R \times CMF_{SK} \quad (118)$$

with:

$$CMF_R = 1 + 0.689(0.147V)^4 \frac{(1.47V)^2}{32.2R^2} \quad (119)$$

$$CMF_{SK} = e^{-0.034(SK-40)} \quad (120)$$

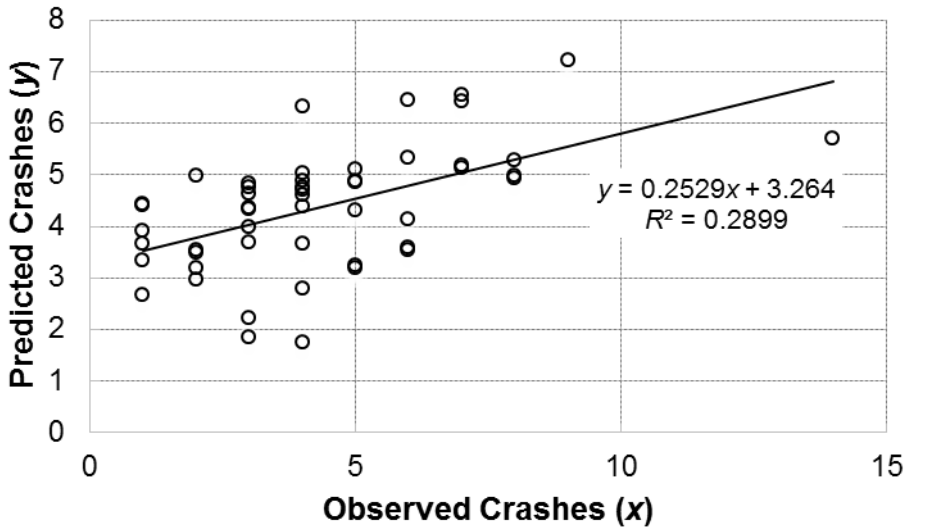

Figure 45. Observed versus Predicted Crashes, 4U Panel Model.

The annual ROR crash frequency for horizontal curves on four-lane undivided highways can be estimated by the following equation:

$$\mu_{4U} = L \times y \times e^{-4.179} \times F^{0.308} \times CMF_R \times CMF_{SK} \quad (121)$$

with:

$$CMF_R = 1 + 0.939(0.147V)^4 \frac{(1.47V)^2}{32.2R^2} \quad (122)$$

$$CMF_{SK} = e^{-0.011(SK-40)} \quad (123)$$

The annual wet-weather ROR crash frequency for horizontal curves on four-lane undivided highways can be estimated by the following equation:

$$\mu_{4U} = L \times y \times e^{-6.551} \times F^{0.387} \times CMF_R \times CMF_{SK} \quad (124)$$

with:

$$CMF_R = 1 + 1.112(0.147V)^4 \frac{(1.47V)^2}{32.2R^2} \quad (125)$$

$$CMF_{SK} = e^{-0.047(SK-40)} \quad (126)$$

Table 32 summarizes the parameter estimates associated with the calibrated SPFs for horizontal curves on four-lane divided highways. In general, the sign and magnitude of the regression coefficients in Table 32 are logical and consistent with previous research findings. The list of variables presented in this table reflects the findings from several preliminary regression analyses where different combinations of variables were examined. Similar to the results for undivided curved segments, the list represents the variables that provided the best fit

to the data, while also having coefficient values that are logical and constructs that are theoretically defensible and properly bounded.

Table 32. Panel-Data Parameter Estimation for Four-Lane Divided Highway Curves.

Variable	All Crashes		Wet Weather Crashes		ROR Crashes		Wet Weather ROR Crashes	
	Estimate	Std. err	Estimate	Std. err	Estimate	Std. err	Estimate	Std. err
Intercept	−8.088	0.536	−9.843	1.161	−7.741	0.621	−8.156	1.302
LN(ADT)	0.843	0.055	0.838	0.119	0.766	0.064	0.633	0.135
Inside Shoulder Width	−0.063	0.024	--	--	−0.080	0.030	--	--
Skid Number	−0.004	0.003	−0.0274	0.007	−0.0060	0.0037	−0.033	0.008
Annual Prec.	0.003	0.003	0.0140	0.007	--	--	0.014	0.008
Dispersion	2.388	0.511	0.676	0.215	1.730	0.421	0.378	0.118
AIC	4767		1637		3664		1336	

Note: -- = calibration coefficient is highly insignificant

Figure 46 shows the fit of the all crash model for four-lane divided horizontal curves. This figure compares the predicted and observed crash frequency in the calibration database. The data were sorted by ADT and aggregated into 64 groups. Each data point shown in Figure 46 represents the total predicted and total observed crash frequency in a particular group. In general, the data shown in the figure indicate that the model provides an unbiased estimate of expected crash frequency. The fit statistic shows that the panel model provides slightly better fit than the cross-sectional models.

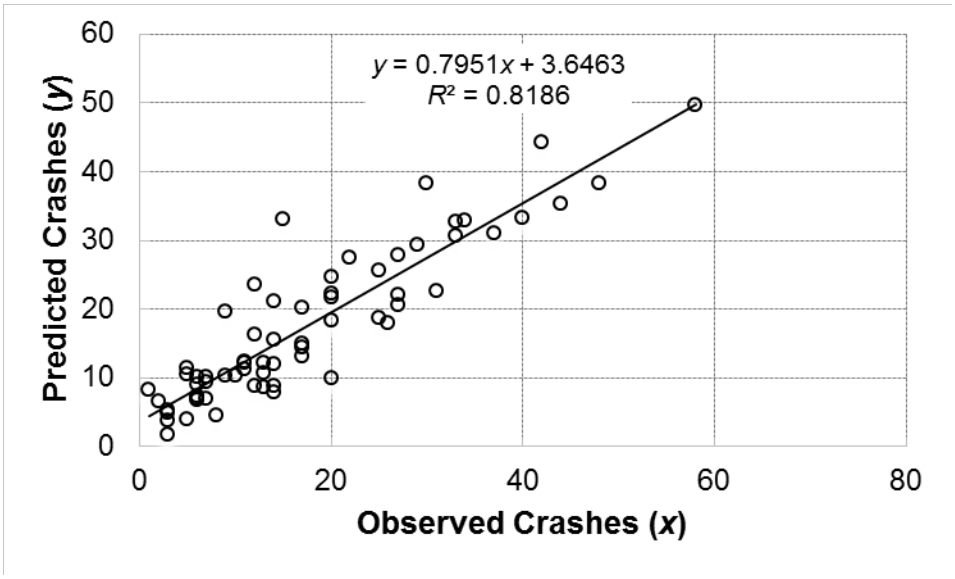

Figure 46. Observed versus Predicted Crashes, 4D Panel Model.

The annual crash frequency for horizontal curves on four-lane divided highways is obtained by combining Equation 49 with the coefficients in Table 32 as follows:

$$\mu_{4D} = L \times y \times e^{-8.088} \times F^{0.843} \times CMF_{ISW} \times CMF_{SK} \times CMF_{AP} \quad (127)$$

with:

$$CMF_{ISW} = e^{-0.063(ISW-4)} \quad (128)$$

$$CMF_{SK} = e^{-0.004(SK-40)} \quad (129)$$

$$CMF_{AP} = e^{0.003(AP-30)} \quad (130)$$

The annual wet-weather crash frequency for horizontal curves on four-lane divided highways can be estimated by the following equation:

$$\mu_{4D} = L \times y \times e^{-9.843} \times F^{0.838} \times CMF_{SK} \times CMF_{AP} \quad (131)$$

with:

$$CMF_{SK} = e^{-0.0274(SK-40)} \quad (132)$$

$$CMF_{AP} = e^{0.014(AP-30)} \quad (133)$$

The annual ROR crash frequency for horizontal curves on four-lane divided highways can be estimated by the following equation:

$$\mu_{4D} = L \times y \times e^{-7.741} \times F^{0.766} \times CMF_{ISW} \times CMF_{SK} \quad (134)$$

with:

$$CMF_{ISW} = e^{-0.080(ISW-4)} \quad (135)$$

$$CMF_{SK} = e^{-0.006(SK-40)} \quad (136)$$

The annual wet-weather ROR crash frequency for horizontal curves on four-lane divided highways can be estimated by the following equation:

$$\mu_{4D} = L \times y \times e^{-8.156} \times F^{0.633} \times CMF_{SK} \times CMF_{AP} \quad (137)$$

with:

$$CMF_{SK} = e^{-0.033(SK-40)} \quad (138)$$

$$CMF_{AP} = e^{0.014(AP-30)} \quad (139)$$

Crash Modification Factors

This section presents the results related to CMFs for curve radius, skid number, and annual precipitation. The CMFs for lane and shoulder widths are similar to those presented in Pratt et al. (*2*) and thus not described here.

Curve Radius

Figure 47 plots the curve radius CMFs for the all-crash models (Equations 51, 73, 96, and 116). For all four cases (two-lane highways versus four-lane undivided highways, cross-sectional analysis versus panel-data analysis), the knee of the curve is at about 1500 ft, suggesting that crash frequency increases significantly when curve radius decreases below that value. For both

analyses, the curve radius CMF was statistically insignificant for four-lane divided highways, likely because relatively few sharp curves exist on these types of highways, making it difficult to quantify their safety effect.

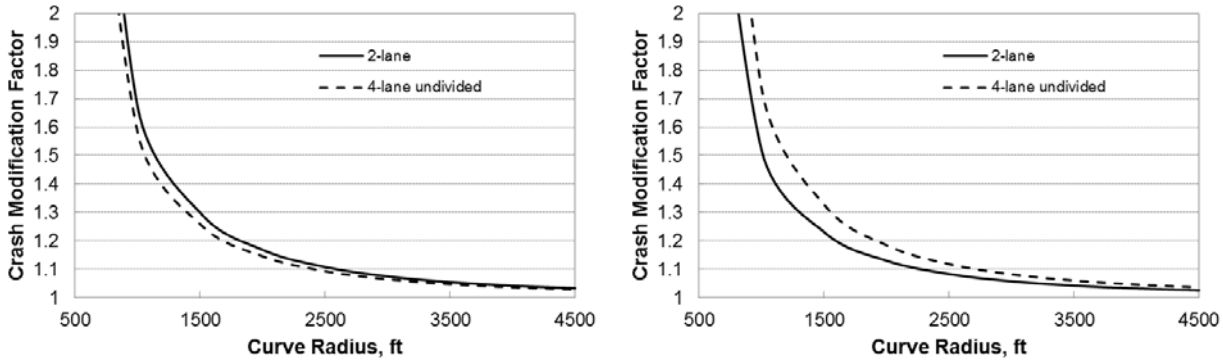

a. Cross-Sectional Analysis **b. Panel-Data Analysis**

Figure 47. Curve Radius CMFs.

Skid Number

Figure 48 plots the skid number CMFs for the all-crash models (Equations 54, 85, 99, 117, and 129). In all cases, the influence of skid number was subtle because the all-crash model includes dry-weather crashes in addition to wet-weather crashes, and dry-weather crashes are seldom attributable to inadequate skid resistance. For the case of four-lane undivided highways, the skid number CMF was found to be statistically significant in the panel-data analysis but not the cross-sectional analysis. The insignificance of the variable may be attributed to low or no variability among the sites for that particular variable. A CMF value of 1.0 is shown as a placeholder for four-lane undivided highways in Figure 48a.

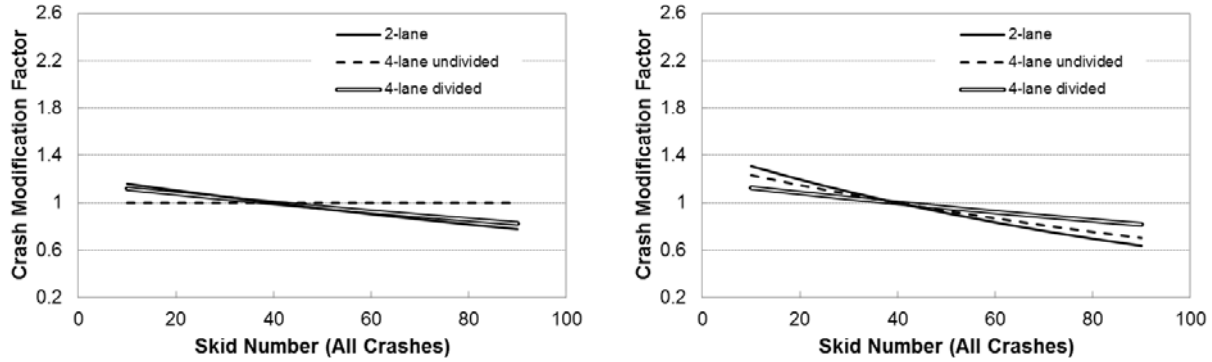

a. Cross-Sectional Analysis **b. Panel-Data Analysis**

Figure 48. Skid Number CMFs – All Crashes.

Figure 49 plots the skid number CMFs for the wet-weather crash models (Equations 59, 76, 88, 103, 120, and 132). In all cases, the CMF was found to be statistically significant, as the influence of skid resistance is much more notable for wet-weather crashes than dry-weather crashes. The skid number CMF trends were similar across the different highway types and analysis methods.

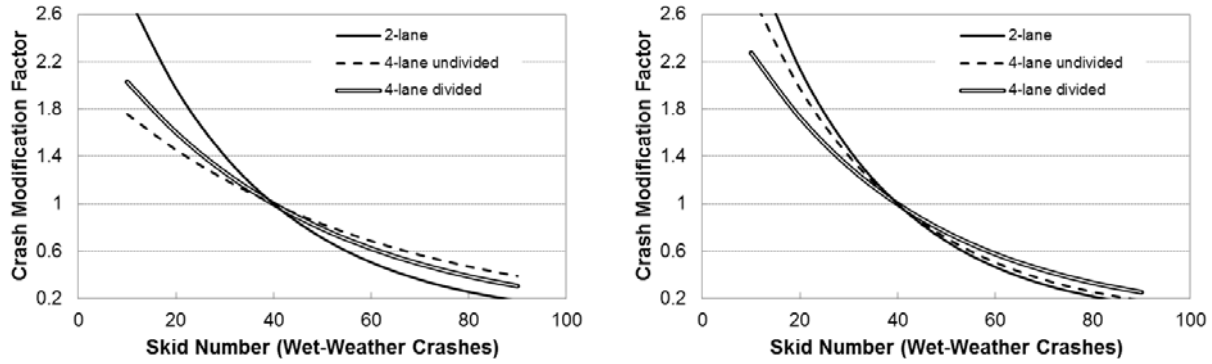

a. Cross-Sectional Analysis **b. Panel-Data Analysis**

Figure 49. Skid Number CMFs – Wet-Weather Crashes.

For both analysis methods, the skid number CMFs for ROR crashes were very similar to those for all crashes, and the skid number CMFs for wet-weather ROR crashes were very similar to those for wet-weather crashes.

Annual Precipitation

Figure 50 plots the annual precipitation rate CMFs (Equations 55, 60, 66, 71, 100, 104, 110, and 114) for two-lane highways. As was the case with the skid number CMFs, the annual precipitation rate CMFs are much more notable for wet-weather crashes than for all crashes. Note that the annual precipitation rate CMFs from the panel-data analysis for all crashes and ROR crashes are superimposed because they have the same calibration coefficient (0.014).

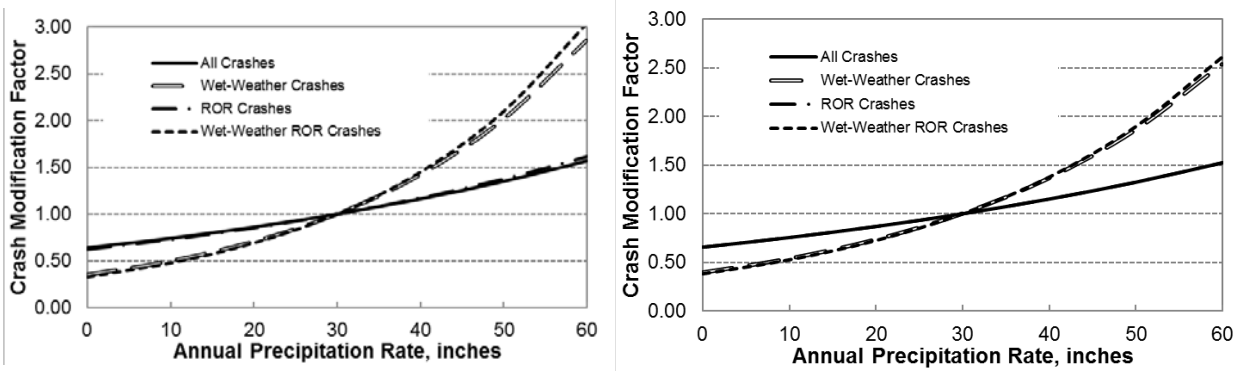

a. Cross-Sectional Analysis **b. Panel-Data Analysis**

Figure 50. Annual Precipitation Rate CMFs for Two-Lane Highways.

None of the annual precipitation CMFs for four-lane undivided highways were found to be statistically significant, and only three of the annual precipitation CMFs for four-lane divided highways were found to be statistically significant. These were the CMFs for all crashes, wet-weather crashes, and wet-weather ROR crashes.

Figure 51 compares annual precipitation CMFs (Equations 104 and 133) for wet-weather crashes from the panel-data analysis. For both highway types shown, higher annual precipitation results in an increase in wet-weather crashes, with a much more notable increase on two-lane highways compared to four-lane divided highways.

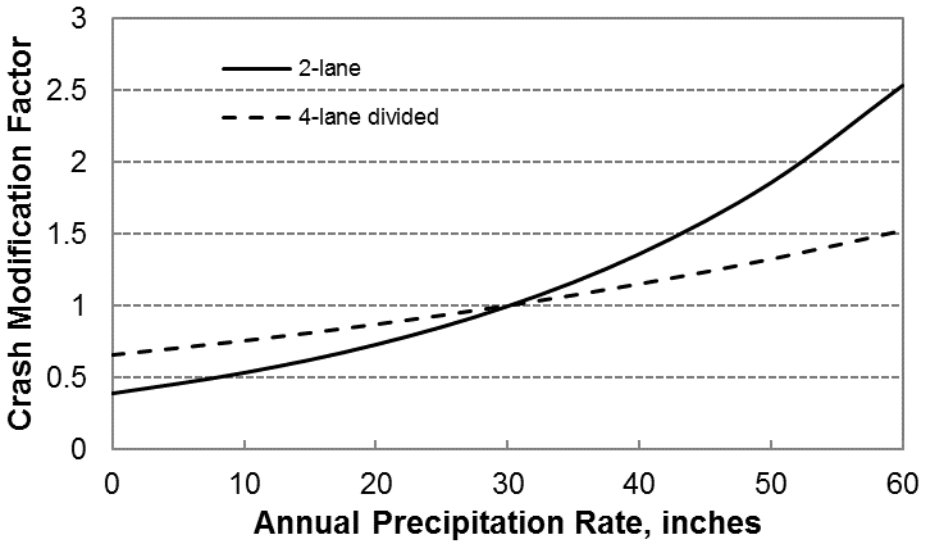

Figure 51. Annual Precipitation Rate CMFs for Wet-Weather Crashes, Panel-Data Analysis.

BEFORE-AFTER EVALUATION

This section evaluates the safety effectiveness of providing pavement treatments at horizontal curves on rural two-lane and four-lane highways in Texas. The EB before-after method is used in this study to evaluate the safety effectiveness. The EB method uses statistical models and combines the information from both observed count of crashes at the site and the predicted crash frequency based on the safety performance of similar sites. This successfully accounts for the regression-to-the-mean bias. Regression to the mean is the statistical tendency for locations chosen because of high crash histories to have lower crash frequencies in subsequent years even without treatment. SPFs for horizontal curves documented in the above section were used to predict the crash frequency at each site.

Methodology

The EB approach has been recognized as a robust method for developing CMFs. The EB method is able to account for the regression-to-the-mean bias, other changes over time not due to the treatment, and to reduce the level of uncertainty in the estimates of safety effect. This analysis mainly followed the procedures of EB analyses that have been extensively documented in the HSM (*5*) and in other literature (*79, 80, 81*). The steps are summarized below.

Step 1: Estimate the Expected Number of Crashes in the Before Period

Using the SPF and a set of CMFs provided in the above section, calculate the expected number of crashes for a segment, as shown in Equation 140:

$$E\left[\hat{k}_i\right] = t \times f(ADT, length) \times CMF_1 \times \cdots \times CMF_k \quad (140)$$

where:

$E[\hat{k}_i]$ = predicted number of target crashes (e.g., SVROR+OD) for site *i*.
t = duration of the study period (usually in years).

$f(ADT, length)$ = SPF for a set of base conditions, which only includes the traffic volume (represented as ADT) and curve length (mi).

$CMF_1, \ldots, CMF_k$ = a set of CMFs for variables (e.g., lane width, shoulder width, skid number).

The EB method estimates the expected number of crashes ($E[\hat{k}_i|K_i]$) before the installation of pavement treatments at each segment and the variance of $E[\hat{k}_i|K_i]$. The estimate $E[\hat{k}_i|K_i]$ is calculated by combining the predicted crashes ($E[k]_i$) with the observed count of crashes (K_i) in the before period, and is given as follows:

$$E[\hat{k}_i|K_i] = \hat{w}_i \cdot E[\hat{k}_i] + (1 - \hat{w}_i) \cdot \tau_i \tag{141}$$

where:

$E[\hat{k}_i|K_i]$ = EB estimate of the expected number of crashes for site *i*.

$\hat{w}_i$ = weight factor.

τ_i = observed number of crashes.

The weight $\hat{w}_i$ is given as:

$$\hat{w}_i = \frac{1}{1 + \alpha E[\hat{k}_i]} \tag{142}$$

where:

α = over-dispersion parameter.

The variance of the estimate is given as:

$$Var\left[E[\hat{k}_i|K_i]\right] = (1 - \hat{w}_i) \cdot E\left[\hat{k}_i\middle|K_i\right] \tag{143}$$

Step 2: Calculate the Ratio of the After Period Crash Estimate to the Before Period Estimate

With the SPFs used in Step 1, estimate the expected number of crashes ($E[z_i]$) in the after period at each treatment site, not accounting for pavement treatment. The ratio of the after-period crash estimate to the before-period estimate (P_i) is calculated as:

$$P_i = \frac{E\left[\hat{Z}_\iota\right]}{E\left[\hat{k}_\iota\right]} \tag{144}$$

Step 3: Obtain the Estimated Crashes ($\hat{\pi}_i$) and its Variance

Calculate the estimated crashes during the after period that would have occurred without treatment. The estimated number of crashes ($\hat{\pi}_i$) is given by:

$$\hat{\pi}_i = P_i \times E[\hat{k}_i|K_i] \tag{145}$$

The estimated variance of $\hat{\pi}_i$ is given by:

$$Var[\hat{\pi}_i] = P_i{}^2 Var\left[E[\hat{k}_i|K_i]\right] = P_i{}^2(1-\hat{w}_i)\cdot E\left[\hat{k}_i\middle|K_i\right] \quad (146)$$

Step 4: Compute the Sum of the Estimated and Observed Crashes over all Sites in the Treatment Group

The number of after-period crashes for a group of sites had the treatment not been implemented at the treated sites is given as:

$$\hat{\pi} = \sum_{i=1}^{J} \hat{\pi}_i \quad (147)$$

where:

J = total number of sites in the treatment group.
$\hat{\pi}$ = estimated after-period crashes for all treated sites had there been no treatment.

Step 5: Compute the Sum of the Actual Crashes over All Treated Sites

For a treated site, crashes in the after period are influenced by the implementation of the treatment. The safety effectiveness of a treatment is assessed by comparing the actual crashes with the treatment to the estimated crashes without the treatment. The actual number of after-period crashes for a group of treated sites is given as:

$$\hat{\lambda} = \sum_{i=1}^{J} \rho_i \quad (148)$$

where:

ρ_i = crash frequency during the after period at site *i*.

The estimate of $\hat{\lambda}$ is equal to the sum of the observed number of crashes at all treated sites during the after study period.

Step 6: Estimate $\boldsymbol{Var}\left[\hat{\boldsymbol{\lambda}}\right]$ *and* $\boldsymbol{Var}[\hat{\boldsymbol{\pi}}]$

Based on the assumption of a Poisson distribution, the estimate of variance of $\hat{\lambda}$ is assumed to be equal to ρ. The estimate of variance of $\hat{\pi}$ can be calculated as follows:

$$Var\left[\hat{\lambda}_i\right] = \rho_i \quad (149)$$

$$Var[\hat{\lambda}] = \sum_{i=1}^{J} Var[\hat{\lambda}_i] \quad (150)$$

$$Var[\hat{\pi}_i] = P_i{}^2(1-\hat{w}_i)\cdot E\left[\hat{k}_i\middle|K_i\right] \quad (151)$$

$$Var[\hat{\pi}] = \sum_{i=1}^{j} Var[\hat{\pi}_i] \tag{152}$$

Step 7. Compute the Safety-Effectiveness of the Treatment

The CMF is estimated as the ratio of what the safety performance was with the treatment to what it would have been without the treatment, as follows:

$$\widehat{CMF} = \frac{\frac{\hat{\lambda}}{\hat{\pi}}}{1 + \frac{Var[\hat{\pi}]}{\hat{\pi}^2}} \tag{153}$$

The percent change (known as CRF) in the number of target crashes due to the treatment is calculated by 100(1-$\widehat{CMF}$) percent. If $\widehat{CMF}$ is less than 1, then the treatment has a positive safety effect. The estimated variance and standard error of the estimated safety effectiveness are given by:

$$Var(\widehat{CMF}) = \widehat{CMF}^2 \times \frac{\left(\frac{1}{\hat{\lambda}} + \frac{Var[\hat{\pi}]}{\hat{\pi}^2}\right)}{\left(1 + \frac{Var[\hat{\pi}]}{\hat{\pi}^2}\right)} \tag{154}$$

$$s.e.(\widehat{CMF}) = \sqrt{Var(\widehat{CMF})} \tag{155}$$

The approximate 95-percent confidence interval for $\widehat{CMF}$ is given by adding and subtracting $1.96 \times s.e.(\widehat{CMF})$ from $\widehat{CMF}$. If the confidence interval contains the value 1, then no significant effect has been observed.

Sample Size Requirements

In order to reliably estimate the safety effects of treatments, researchers need to collect enough crashes in the before and after periods. Collecting enough data allows the effects to be statistically significant. The sample size requirement is calculated as follows (*82*):

$$\sum \kappa = \frac{\left(\theta / r_d + \theta^2\right)}{Var(\theta)} \tag{156}$$

where:

$\sum \kappa$ = the total number of crashes collected in the before period;

θ = the safety index or the estimated reduction in the number of crashes in percent (i.e., $\theta = 0.90$ or a 10% reduction in crashes) (this has also been defined as a CMF);

r_d = the ratio of the time period after over the time period before; and,

$Var(\theta)$ = variance of the safety index.

The sample size is a function of the magnitude of the reduction, its variance, and the ratio between the time periods. More specifically, the smaller the reduction, more data are needed in the before period (e.g., $\theta = 0.95$ vs $\theta = 0.70$). A smaller variance also leads to a greater sample size requirement, as well as a smaller ratio r_d. For the latter, collecting more data in the after period reduces the sample requirement. For example, collecting three years for the before and after periods leads to an $r_d = 1$, whereas collecting only one year during the after period leads to an $r_d = 0.33$.

Researchers calculated the sample size requirement for a change in skid number, as applicable to different treatments, for all crashes. Researchers used the skid number CMFs for the all-crash models (Equations 99, 117, and 129) for two scenarios: a change in skid numbers from 20, 30 and 40 to 50 (Scenario A) and a change in skid numbers from 20, 30, 40, 50 and 60 to 70 (Scenario B). Table 33, Table 34, and Table 35 provide the sample size for two-lane, four-lane undivided and four-lane divided highways, respectively. The sample size was calculated for three r_d values: 1, 0.67 and 0.33.

Table 33. Sample Size Requirement for Two-Lane Highways

Scenario	Change in *SK*	θ	Sample Size, crashes, by r_d value		
			1.00	**0.67**	**0.33**
A	20-50	0.76	538	689	1158
	30-50	0.84	613	778	1292
	40-50	0.91	700	880	1442
B	20-70	0.64	418	543	936
	30-70	0.70	474	611	1040
	40-70	0.76	538	689	1158
	50-70	0.84	613	778	1292
	60-70	0.91	700	880	1442

Table 34. Sample Size Requirement for Four-Lane Undivided Highways

Scenario	Change in *SK*	θ	Sample Size, crashes, by r_d value		
			1.00	**0.67**	**0.33**
A	20-50	0.81	587	747	1245
	30-50	0.87	650	821	1356
	40-50	0.93	721	904	1478
B	20-70	0.70	481	619	1053
	30-70	0.76	531	680	1145
	40-70	0.81	587	747	1245
	50-70	0.87	650	821	1356
	60-70	0.93	721	904	1478

Table 35. Sample Size Requirement for Four-Lane Divided Highways

Scenario	Change in *SK*	θ	Sample Size, crashes, by r_d value		
			1.00	**0.67**	**0.33**
A	20-50	0.89	669	844	1390
	30-50	0.92	710	892	1460
	40-50	0.96	754	943	1534
B	20-70	0.82	596	757	1261
	30-70	0.85	631	799	1323
	40-70	0.89	669	844	1390
	50-70	0.92	710	892	1460
	60-70	0.96	754	943	1534

Data Collection

TxDOT provided a list of the highway projects where pavement treatments were installed during 2003 to 2013. Researchers used control section numbers and Texas references markers to identify the horizontal curves on the treatment sections from the Geo-Hini database from the year 2012. The horizontal curve database was combined with the RHiNo database using control section numbers and reference markers. Variables extracted from the RHiNo database included ADT, truck percentage, shoulder widths, lane width, median width, and number of lanes. Skid number was obtained from the PMIS database for the three-year period before the installation. The CRIS database was used to obtain the crash frequency in the before and after periods at each horizontal curve. Only fatal-and-injury (FI) were extracted because the SPFs were developed using these crash severities only. In addition, ROR and wet weather crashes were extracted.

Researchers used 5-minute precipitation data from the Automated Surface Observing Systems (ASOS) to evaluate annual precipitation as an exploratory variable in the safety analysis efforts. The ASOS project is a joint effort of the National Weather Service, the Federal Aviation Administration, and the Department of Defense. It serves as the nation's principal surface weather observing network. ASOS weather stations provide non-stop, updating observations every minute, 24 hours a day, every day of the year (*83*). For this effort, researchers used 2001–2016 ASOS data to evaluate annual precipitation per weather stations. As the before-after periods range between 2000 and 2015, researchers used 2000–2016 ASOS data in place of 1981–2010 NOAA climate normal for this evaluation. Figure 52 shows a 5-mile buffer considered surrounding the weather stations. The black dots (·) indicate the locations of curves. If a curve is located inside the weather-station buffer, the average precipitation of the weather station is considered as the average precipitation of the curve. If the curve is located outside the buffer, the nearest buffer is considered for the annual precipitation value. For few locations, an average of two buffers was calculated due to the similar distances from both buffers.

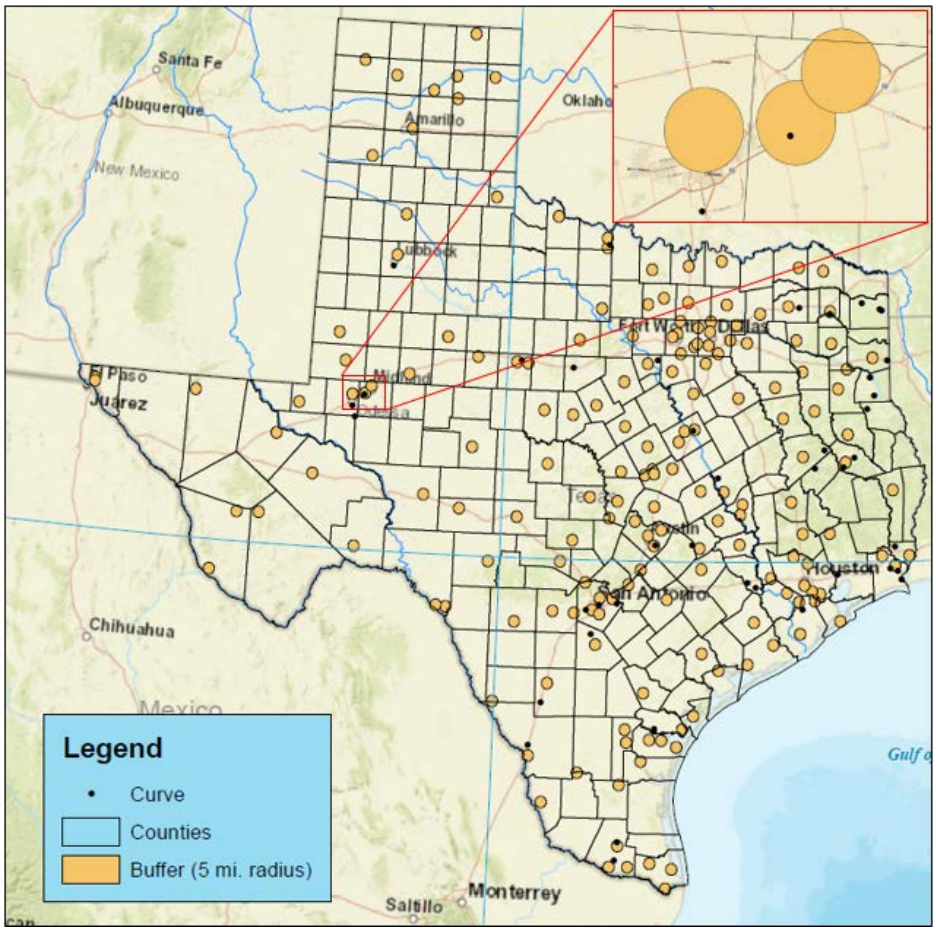

Figure 52. ASOS Weather Stations and Curve Locations.

Table 36 provides the number of sites by the highway type and surface treatment type used for the before-after analysis.

Table 36. Number of Sites Used for Before-After Analysis.

Roadway Type	Surface Treatment Type			Total
	HMA	PFC	Seal Coat	
Two-Lane Undivided	6	0	56	62
Four-Lane Undivided	6	2	11	19
Four-Lane Divided	8	10	25	43
Total	20	12	92	124

Results

This section presents the crash rate comparisons followed by the EB before-after analysis.

Crash Rate Comparisons

Table 37 shows the crash rates in the before and after periods and the difference by various criteria. According to the crash rate comparisons, when all the treatments were considered together, the effect is more on FI crashes and in particular on ROR crashes. When annual precipitation is considered, the effectiveness is greater at sites with high precipitation. The seal coat treatments were more effective than other treatment types. The crash rate comparison also shows that the effectiveness is greater on two-lane highways than on four-lane highways.

Table 38 shows the FI crash rate comparisons for after periods of different lengths. In almost all cases, the safety effectiveness is higher in the first year. By the third year, the comparisons show that there is almost no effect. This trend is consistent with the expected wearing of pavement material over time and the resulting loss of skid resistance. However, the crash rate analysis results have several limitations. First, the crash rate method completely depends on observed crash data, in this case from law enforcement reports submitted to the state. The issues of data quality and accuracy arise due to limitations in recording, reporting, and measuring crash data with accuracy and consistency in different time periods. Second, crash rates presume a linear relationship between crash frequency and the measure of exposure, which is typically not true. Third, when the number of crashes in the data sample is meager (as is the case in this analysis), the results are highly biased.

EB Before-After Analysis

Further analysis was conducted using the FI and FI ROR crashes without separating wet-weather and dry-weather crashes. Table 39 shows the results of this analysis for rural two-lane horizontal curves. The top half of the table provides results for all treatments together. The bottom half provides the estimation results for seat coat treatment only. Results related to all treatments show that crashes slightly increased after the installation of treatments but none of them is statistically significant, even at 60 percent confidence level. When just the seal coat is considered, crashes slightly decreased but the results are not statistically significant either. This means, it is highly likely the increase or decrease in crashes is by chance and not due to the treatment itself. As shown in Table 33, the minimum number of crashes required for two-lane highways for obtaining significant results is at least 400. The total number of crashes in Table 39 is much lower than the required sample size and for this reason, the results are statistically insignificant.

Table 37. Crash Rate in the Before and After Periods.

Criteria		Crash Type	Crash Rate, crashes per million vehicle-miles		
			Before	After	Difference
Combined		All	0.701	0.551	21.4%
		FI	0.325	0.245	24.5%
		FI ROR	0.257	0.136	47.2%
Annual Precipitation	High (>45.7 in.)	All	0.900	0.472	47.6%
		FI	0.386	0.184	52.4%
		FI ROR	0.325	0.138	57.4%
	Low (≤45.7 in.)	All	0.503	0.630	−25.4%
		FI	0.263	0.306	−16.4%
		FI ROR	0.190	0.134	29.6%
Surface Type	HMA	All	0.577	0.512	11.3%
		FI	0.104	0.113	−8.8%
		FI ROR	0.046	0.055	−21.0%
	PFC	All	0.359	1.068	−197.8%
		FI	0.252	0.476	−89.3%
		FI ROR	0.252	0.038	85.0%
	Seal coat	All	0.773	0.492	36.3%
		FI	0.382	0.243	36.3%
		FI ROR	0.304	0.166	45.3%
Road Type	2U	All	0.854	0.394	53.9%
		FI	0.467	0.254	45.6%
		FI ROR	0.415	0.203	51.2%
	4U	All	0.835	0.937	−12.2%
		FI	0.119	0.254	−112.8%
		FI ROR	0.020	0.016	19.7%
	4D	All	0.421	0.607	−44.2%
		FI	0.210	0.228	−8.5%
		FI ROR	0.135	0.093	31.0%

Table 38. FI Crash Rate with Different Length of After Periods.

Criteria		Crash Rate						
		Before Period	After Period			Difference		
			1 year	2 years	3 years	1 year	2 years	3 years
Combined		0.325	0.177	0.272	0.245	45.6%	16.2%	24.5%
Annual Precip.	High (>45.7 in.)	0.386	0.132	0.230	0.184	65.7%	40.5%	52.4%
	Low (≤45.7 in.)	0.263	0.221	0.314	0.306	16.0%	−19.4%	−16.4%
Surface Type	HMA	0.104	0.131	0.135	0.113	−26.3%	−30.0%	−8.8%
	PFC	0.252	0.128	0.162	0.476	49.1%	35.7%	−89.3%
	Seal Coat	0.382	0.193	0.316	0.243	49.5%	17.3%	36.3%
Road Type	2U	0.467	0.251	0.350	0.254	46.4%	25.0%	45.6%
	4U	0.119	0.058	0.328	0.254	51.0%	−175.1%	−112.8%
	4D	0.210	0.122	0.135	0.228	41.7%	35.9%	−8.5%

Table 39. Treatments on Two-Lane Horizontal Curves.

Treatment Type	Variable	FI Crashes *	FI ROR Crashes *
All Treatments (62 sites)	Predicted Crashes	11.5 (1.9)	8.8 (1.4)
	Observed Crashes	15.0 (3.9)	11.0 (3.3)
	CMF	1.27 (0.38)	1.22 (0.41)
	CRF (%)	−26.6 (37.9)	−22.0 (40.6)
	Confidence Level	52%	41%
Seal Coat (56 sites)	Predicted Crashes	10.2 (3.5)	7.7 (1.3)
	Observed Crashes	12.0 (2.0)	9.0 (3.0)
	CMF	1.14 (0.37)	1.13 (0.41)
	CRF (%)	−13.8 (37.4)	−13.1 (41.1)
	Confidence Level	29%	25%

*: Values in the parentheses are standard errors of the estimated variable.

Table 40 shows the before-after estimation results for installing pavement treatments on rural four-lane undivided horizontal curves. The top half of the table provides results for all treatments together. The bottom half provides the estimation results for seat coat and HMA treatments combined. Because there were no reported crashes in the after period, an analysis could not be conducted to determine the effectiveness of seal coat and HMA treatments on FI ROR crashes. The estimation results show that FI crashes increased for all treatments but decreased after the installation of seal coat and HMA treatments, although both results are highly insignificant. At the same time, the results show that the FI ROR crashes decreased and the results are statistically significant. Given the meager crash frequency, these results should be used with caution. Also, the sample size in Table 40 is much smaller than the required, shown in Table 34, for obtaining reliable results.

Table 40. Treatments on Four-Lane Undivided Horizontal Curves.

Treatment Type	Variable	FI Crashes *	FI ROR Crashes *
All Treatments (19 Sites)	Predicted Crashes	6.9 (1.8)	4.6 (1.2)
	Observed Crashes	11.0 (3.3)	2.0 (1.4)
	CMF	1.48 (0.55)	0.41 (0.29)
	CRF (%)	−48.8 (55.1)	59.1 (28.8)
	Confidence Level	62%	96%
Seal Coat and HMA (17 sites)	Predicted Crashes	5.4 (1.6)	Not Available
	Observed Crashes	4.0 (2.0)	
	CMF	0.68 (0.36)	
	CRF (%)	31.9 (36.2)	
	Confidence Level	62%	

*: Values in the parentheses are standard errors of the estimated variable.

Table 41 shows the before-after estimation results for installing pavement treatments on rural four-lane divided horizontal curves. The top half of the table provides results for all treatments together. The bottom half provides the estimation results for seat coat and HMA treatments combined. All the results show that crashes decreased after the installation of treatments and the results are marginally significant for seal coat and HMA treatments on the FI crashes. Given the meager crash frequency, these results should be used with caution. Also, the sample size in Table 41 is much smaller than the required, shown in Table 35, for obtaining reliable results.

Table 41. Treatments on Four-Lane Divided Horizontal Curves.

Treatment Type	Variable	FI Crashes	FI ROR Crashes
All Treatments (43 Sites)	Predicted Crashes	21.1 (3.5)	13.2 (2.5)
	Observed Crashes	17.0 (4.1)	10.0 (3.2)
	CMF	0.78 (0.22)	0.73 (0.26)
	CRF (%)	21.6 (22.4)	26.6 (26.1)
	Confidence Level	66%	69%
Seal Coat and HMA (33 sites)	Predicted Crashes	18.8 (3.4)	11.5 (2.4)
	Observed Crashes	13.0 (3.6)	9.0 (3.0)
	CMF	0.67 (0.21)	0.75 (0.28)
	CRF (%)	33.0 (21.4)	24.9 (28.3)
	Confidence Level	88%	62%

*: Values in the parentheses are standard errors of the estimated variable.

Summary

This section provided the results of the before-after evaluation. First, the crash rates in the before and after periods were compared. The crash rate comparisons show that the treatments had a positive effect on safety. The positive effect is more prevalent at sites that experienced more precipitation, when the seal coat was used, or on two-lane highway curves. The treatments were more effective in the first year after the installation of treatments. The EB before-after analysis results show a mixed effect on safety and almost all results are statistically insignificant. The number of reported crashes was too low to draw any meaningful conclusions.

CHAPTER 6: GUIDELINE AND EVALUATION FRAMEWORK DEVELOPMENT

INTRODUCTION

This research project developed guidelines and an evaluation framework to assist practitioners in diagnosing safety concerns on horizontal curves, identifying effective treatments, and computing expected benefits of alternative treatments. Diagnosis is defined as identifying curves, or specific parts of a curve of interest, where crash frequency is expected to be elevated compared to similar sites. Treatments are identified by examining curve characteristics to determine if geometric, traffic control, or pavement deficiencies exist, and then determining which treatment options can address any identified deficiencies. Benefits are estimated by comparing the costs of the treatment options with the crash reduction benefits that are expected as a result of implementing the treatment.

Based on the results described in the preceding chapters, researchers developed the following resources:

- Guidelines for conducting a planning-level analysis to identify curves where pavement-based safety treatments would likely be cost-effective.
- A spreadsheet-based evaluation framework for conducting a detailed analysis to determine the effectiveness of a treatment at a specific curve of interest.

This chapter describes the development of these resources. The final version of these resources and a User Guide for applying the evaluation framework are documented in a stand-alone product that accompanies this report.

GUIDELINES

Researchers developed guidelines based on the findings of the safety and weather data analyses that were described in Chapter 4. These guidelines can be incorporated into TxDOT's WSCRP (*71*), *Pavement Design Guide* (*4*), or other documents as needed. Note that the WSCRP was formerly known as Wet-Weather Accident Reduction Program (WWARP).

Background

The *Pavement Design Guide* provides the following description of TxDOT's approach to addressing wet-surface safety issues:

> The WWARP allows the department to take advantage of the increased knowledge gained through our research efforts and to more effectively and efficiently address the various regional demands of Texas pavements. WWARP addresses three separate but interrelated phases of pavement friction safety. The three phases are accident analysis, aggregate selection, and skid testing.

TxDOT's *Wet-Surface Crash Reduction Program Guidelines* (*71*) contains guidance for identifying roadway sections that are susceptible to increased wet-surface crash frequency based

on examining the proportion of wet-surface crashes. This document contains a map (see Figure 40) that splits the state of Texas into three regions defined as having low, moderate, or high rainfall. Hence, the analyst is directed to consider both crash trends (in terms of wet-surface crash proportion) and geographic exposure to wet weather. The WSCRP document also describes a process of sorting and ranking state-maintained highway sections (i.e., continuous stretches of both curves and tangents) by wet-surface crash proportion to identify candidate locations for safety countermeasures.

Guideline Development

To augment this process and adapt it to a specific evaluation of curves, the safety trends shown by the previously-discussed CMFs for skid number and annual precipitation rate can be combined and applied to jurisdictions of interest. The panel-data wet-weather CMFs for skid number and annual precipitation rate for rural two-lane highways (Equations 103 and 104, respectively) are combined as follows:

$$CMF_{sk|ap} = CMF_{sk}CMF_{ap} = e^{-0.038(SK-40)}e^{0.031(p-30)} \quad (157)$$

$$SK = 0.816p - 26.316ln\left(CMF_{sk|ap}\right) + 15.526 \quad (158)$$

The $CMF_{sk|ap}$ quantity represents the proportional change in crash frequency that occurs in wet-weather conditions given the specified skid number. This quantity also represents the potential reduction in wet-weather crashes that can be achieved through the provision of increased skid resistance. For a given annual precipitation rate, the provision of higher skid resistance would mitigate the increase in crashes that can be attributed to wet weather.

Researchers examined the distribution of the $CMF_{sk|ap}$ quantity across two-lane highway curves statewide using a methodology similar to that described by Long et al. (*84*). This methodology is summarized as follows:

1. Generate a list of the state's roadway sections, sorted in ascending order of skid number.
2. Determine the cumulative distribution of crash counts across the roadway sections.
3. Determine the cumulative distribution of lane-mileage across the roadway sections.
4. For each skid number value from 0 to 100, compute a crash rate ratio (CRR) as the total crashes for the skid number (from step 2) divided by the total lane-mileage for the skid number (from step 3).
5. Define threshold CRR values to indicate whether a roadway section of interest should be considered for a pavement friction treatment.

Long et al. defined the CRR thresholds in the second column of Table 42 based on the input of an Expert Working Group consisting of pavement expert practitioners within TxDOT. The CRR values are interpreted as follows:

- CRR $\geq$ 3: Consider short-term treatment action to improve skid resistance.
- 2 $\leq$ CRR < 3: Conduct detailed project-level testing to determine if a treatment to improve skid resistance is needed.

- $1 \leq CRR < 2$: Vigilance is recommended to identify possible issues with skid resistance and crash frequency.
- $CRR < 1$: Improving skid resistance may have little effect on reducing crash frequency.

Table 42. CRR and Skid Resistance Thresholds (*84*).

Skid Resistance Level	Corresponding CRR Value	Suggested Threshold *SK* value	
		All Crashes	Wet-Weather Crashes
SK_1	3	14	17
SK_2	2	28	29
SK_3	1	74	74

Long et al. acknowledged that their guidance can be augmented by incorporating weather data into the methodology, since pavement friction treatments have the greatest effect on wet-weather crashes. Based on these findings and recommendations, researchers examined the distribution of the $CMF_{sk|ap}$ quantity across Texas' rural highway curves. Figure 53 shows crash rate (in terms of crashes per 1000 vehicle-miles) as a function of the $CMF_{sk|ap}$ quantity. This trend was developed using the same set of curves that comprised the safety model calibration data set described in Chapter 5. Crash rate is used as the *y*-axis variable to account for both crashes and exposure (i.e., volume and length) and plotted after sorting the curves in ascending order of $CMF_{sk|ap}$. The $CMF_{sk|ap}$ quantity accounts for both skid resistance and wet weather exposure.

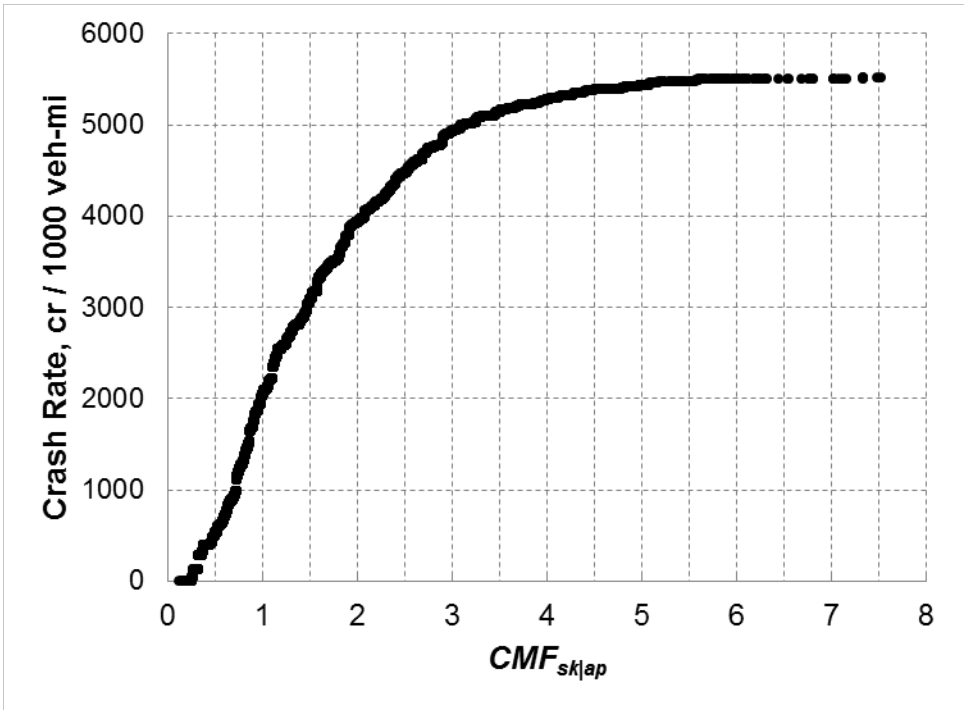

Figure 53. Distribution of Combined CMF Values and Crash-to-Length Ratios for Two-Lane Highways.

Similar distributions are shown in Figure 54 for four-lane undivided highways and Figure 55 for four-lane divided highways. Due to the smaller sample size of curves for these highway

types, the trends are not as clearly defined as that for two-lane highways in Figure 53. However, all three figures show a general trend of increasing $CMF_{sk|ap}$ values as crash rate increases. This trend is intuitive because wet-weather crashes are expected to increase as exposure to wet weather increases or skid resistance decreases.

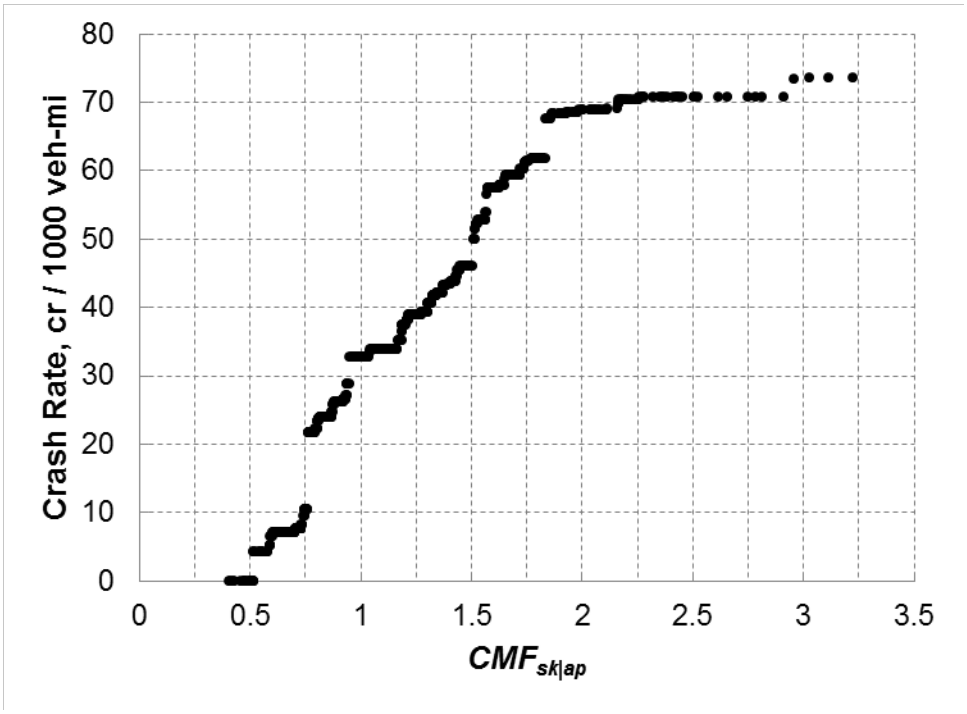

Figure 54. Distribution of Combined CMF Values and Crash-to-Length Ratios for Four-Lane Undivided Highways.

Hence, for the purpose of conducting a planning-level analysis to identify candidate sites for pavement friction treatments, researchers recommend the thresholds in Table 43. These thresholds are identified based on the key breaking points on the preceding distributions (Figure 53, Figure 54, and Figure 55) and extension of the judgment of the Expert Working Group that advised Long et al. (*84*). For all three roadway types, the first threshold is $CMF_{sk|ap} = 1$. The second threshold is $CMF_{sk|ap} = 2.5$ for two-lane highways and 1.5 for four-lane highways, based on the knees of the distribution plots. The third threshold is $CMF_{sk|ap} = 4$ for two-lane highways and $CMF_{sk|ap} = 2$ for four-lane highways. The thresholds are described as follows:

- If a curve has a $CMF_{sk|ap}$ value below the first threshold (1 or less), its skid resistance is likely high enough to mitigate crash risk in wet-weather conditions.
- If a curve has a $CMF_{sk|ap}$ value between the first and second thresholds, it may represent an elevated risk for wet-weather crashes, so it should be monitored. If actual crash data reveal an elevated number of wet-weather crashes at the curve, or if the curve is located on a roadway section that is on the WSCRP location report for the district, it should be analyzed further to determine the potential benefit of a pavement friction treatment.

- If a curve has a $CMF_{sk|ap}$ value between the second and third thresholds, it should be analyzed further to determine the potential benefit of a pavement friction treatment.
- If a curve has a $CMF_{sk|ap}$ value above the third threshold, it should be considered a high priority for implementation of a pavement friction treatment.

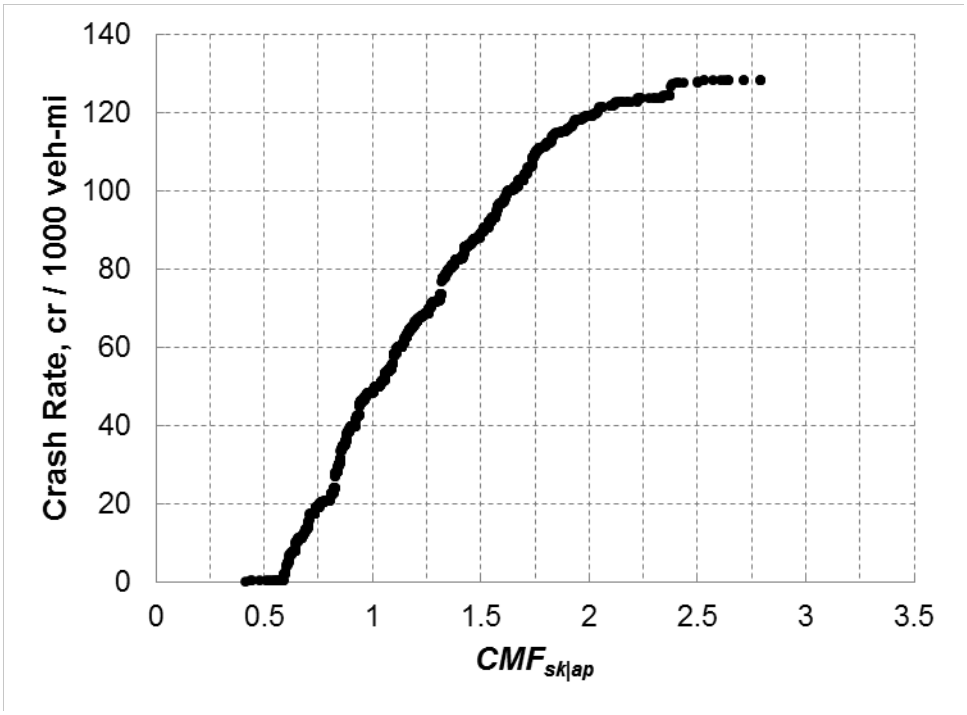

Figure 55. Distribution of Combined CMF Values and Crash-to-Length Ratios for Four-Lane Divided Highways.

Table 43. Recommended Combined CMF Thresholds.

Description	Combined CMF Range by Roadway Type		
	2-Lane	4-Lane Undivided	4-Lane Divided
Friction treatments will not likely yield cost-effective wet-weather crash reduction	$CMF_{sk\|ap} \leq 1$	$CMF_{sk\|ap} \leq 1$	$CMF_{sk\|ap} \leq 1$
Monitor the curve for elevated wet-weather crash frequency	$1 < CMF_{sk\|ap} \leq 2.5$	$1 < CMF_{sk\|ap} \leq 1.5$	$1 < CMF_{sk\|ap} \leq 1.5$
Conduct a detailed analysis to determine potential benefit of a friction treatment	$2.5 < CMF_{sk\|ap} \leq 4$	$1.5 < CMF_{sk\|ap} \leq 2$	$1.5 < CMF_{sk\|ap} \leq 2$
The curve is a high-priority location for a friction treatment	$CMF_{sk\|ap} > 4$	$CMF_{sk\|ap} > 2$	$CMF_{sk\|ap} > 2$

Figure 56 shows a nomograph that represents Equation 158 plotted with $CMF_{sk|ap}$ values of 1, 2.5, and 4. The four regions on the nomograph represent the four thresholds and their

descriptions in Table 43. The nomograph provides a visual tool that allows the analyst to consider both variables (skid number and annual precipitation rate) that are needed to determine the $CMF_{sk|ap}$ value and evaluate the curve. As shown, a curve is more likely to be identified as a priority for pavement friction treatment if its skid number is low and/or if its annual precipitation rate is high.

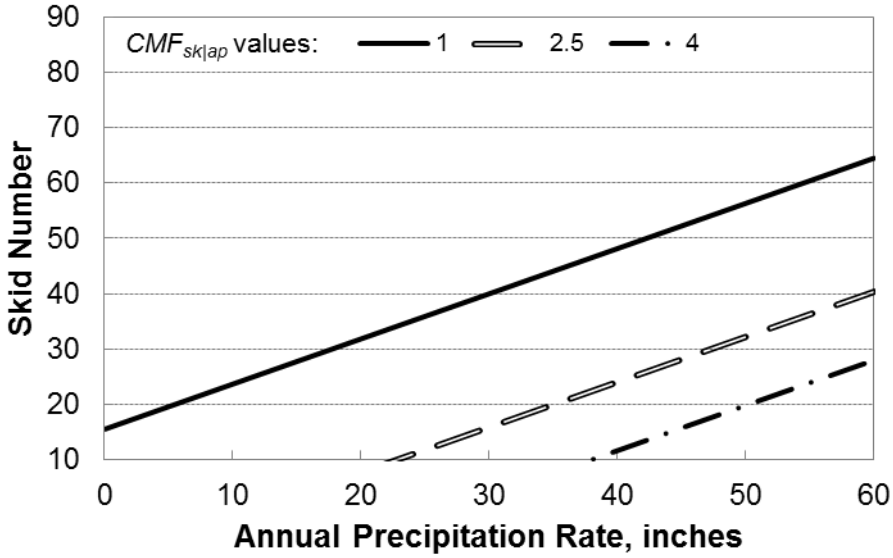

Figure 56. Combined Skid Number and Annual Precipitation Rate Nomograph for Two-Lane Highways.

Figure 57 shows a similar nomograph for four-lane undivided highways. Since an annual precipitation CMF could not be developed for four-lane undivided highways, the nomograph represents a combination of the skid number CMF for four-lane *undivided* highways and the annual precipitation CMF for four-lane *divided* highways (Equations 120 and 133, respectively). Figure 58 shows a nomograph for four-lane divided highways (based on Equations 132 and 133). The contour lines on Figure 57 and Figure 58 have smaller slopes than the lines on Figure 56, suggesting that skid resistance has less of an influence on wet-weather crash frequency on four-lane highways compared to two-lane highways. Much of this difference is attributable to the differences in the annual precipitation CMFs for these two roadway types (see Figure 51).

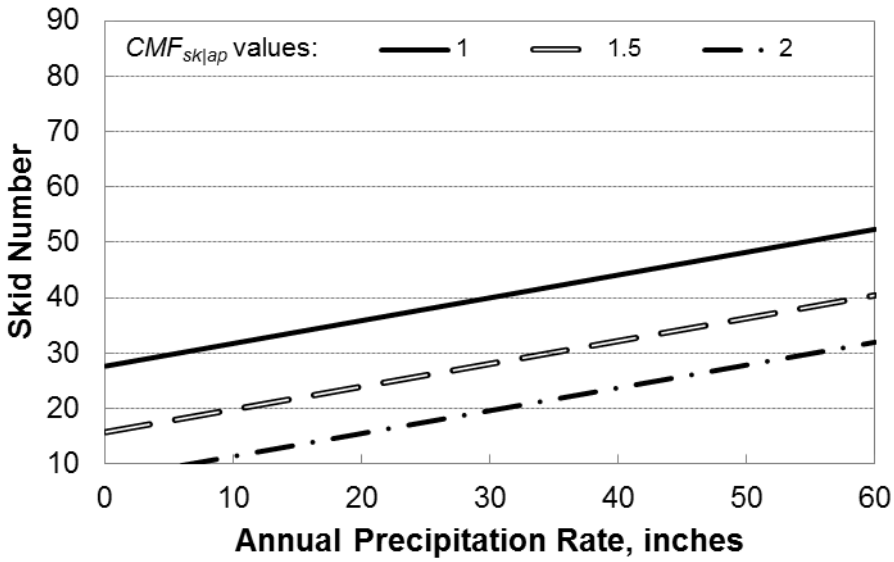

Figure 57. Combined Skid Number and Annual Precipitation Rate Nomograph for Four-Lane Undivided Highways.

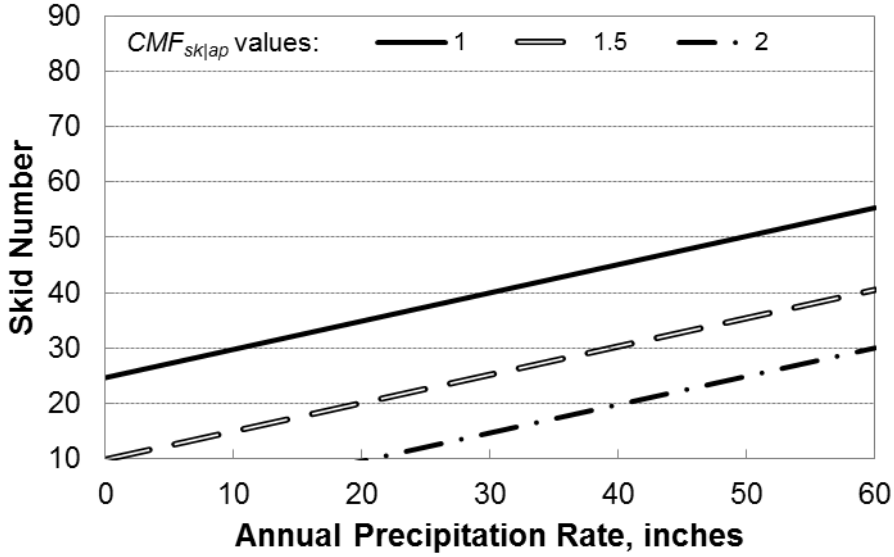

Figure 58. Combined Skid Number and Annual Precipitation Rate Nomograph for Four-Lane Divided Highways.

Discussion

In addition to the combined CMF values shown in the nomographs, it is important to consider the total number of wet-weather crashes predicted at curves of interest. Wet-weather crash frequency is estimated using the SPFs described by Equations 101, 118, and 131. Table 44 shows example crash count calculations for the following four scenarios:

1. A TxDOT district is analyzing 25 two-lane highway curves within its jurisdiction to determine the cost-effectiveness of pavement friction treatments.
2. At the statewide level, TxDOT is conducting a similar analysis on a set of 100 curves statewide, focusing on higher-volume curves than those in scenario 1.
3. A TxDOT district is conducting a similar analysis of 25 four-lane undivided highway curves within its jurisdiction.
4. A TxDOT district is conducting a similar analysis of 25 four-lane divided highway curves within its jurisdiction.

Table 44. Crash Count Analysis Scenarios.

Analysis Scenario	**1**	**2**	**3**	**4**
Number of Curves	25	100	25	25
Number of Analysis Years	10	10	10	10
Average Curve Length, ft	0.15	0.15	0.2	0.25
Average Curve Volume, veh/d	1000	3700	7000	15,000
Base Wet-Weather Crash Count	0.20	2.42	3.20	6.89
Count with $CMF_{sk\|ap}$ value of 2.0	0.40	4.83	6.39	13.78
Count with $CMF_{sk\|ap}$ value of 3.0	0.60	7.26	9.59	20.67
Count with $CMF_{sk\|ap}$ value of 4.0	0.80	9.68	12.79	27.56
Count with $CMF_{sk\|ap}$ value of 5.0	1.00	12.10	15.98	34.45

The following observations are apparent from the results in Table 44:

- For typical two-lane highway curves, such as those on FM roads, traffic volumes are sufficiently low that the total predicted number of wet-weather crashes is small. Even a $CMF_{sk|ap}$ value of 4.0 would suggest an increase in crash count from 0.20 crashes to 0.80 crashes on a set of 25 curves over a 10-year period (e.g., scenario 1).
- Higher-volume curves, such as those on state or U.S. highways, will experience a larger number of wet-weather crashes, such that pavement friction treatments are more likely to be beneficial on these curves. As these curves represent a small percentage of rural two-lane highway curves, they are more likely to be identified in a statewide analysis than a district-level analysis.
- Curves on four-lane highways (both divided and undivided) are also more likely to experience notable numbers of wet-weather crashes, so these curves are more likely to benefit from pavement friction treatments.

Table 45 shows skid number values that correspond with the high-priority threshold $CMF_{sk|ap}$ values and the annual precipitation rates for two example districts. Curves with skid numbers below those in Table 45 would be considered high priority in these districts. The skid number thresholds suggest that District A, which experiences low precipitation, pavement friction treatments are likely to be cost-beneficial only curves with very low skid numbers. Conversely, in District B, which experiences high precipitation, pavement friction treatments are likely to be cost-beneficial on many curves.

Table 45. Skid Number Thresholds for High-Priority Sites in Selected Districts.

Roadway Category	Skid Number Threshold for District (Annual Precipitation Rate)	
	A (15 in./yr)	B (60 in./yr)
Two-lane highways	Negligible	28
Four-lane undivided highways	13	32
Four-lane divided highways	7	30

Summary

Wet-weather crashes are a safety concern on all state-maintained highways, but they are more prevalent in areas experiencing higher annual precipitation rates. TxDOT currently examines wet-surface crash trends annually and generates a list of locations where treatments (particularly pavement resurfacing) should be considered to reduce wet-surface crash frequency. The WSCRP procedure is implemented on roadway sections that consist of both curves and tangents. To supplement these procedures, researchers developed curve safety prediction models, analyzed overall wet-weather crash trends, and formulated guidelines including nomographs to assist practitioners in identifying individual curves where pavement friction treatments are likely to be justified.

The guidelines should be considered as the first step in a process to rank and prioritize curves that may be good candidates for pavement friction treatments. The second step is to apply a more detailed evaluation framework, which is described in the next section. Practitioners *may* apply the evaluation framework for any curve of interest, but *should* apply the evaluation framework if one or more of the conditions are met:

1. The skid number and annual precipitation rate for the curve plot into either of the bottom regions of the nomographs (curves in the bottommost region are considered highest priority).
2. The curve is located on a roadway section that is on the district's WSCRP location report and its skid number and annual precipitation rate plot into the second nomograph region from the top. That is, the curve's $CMF_{sk|ap}$ value exceeds 1.
3. The curve has a radius less than or equal to 1146 ft, or a degree of curve of 5 or greater. As shown in Figure 47, crash frequency increases notably when curve radius decreases below this value.
4. The curve has been identified as having elevated crash frequency based on another type of analysis, crash data query, or citizen complaints.

EVALUATION FRAMEWORK

Overview

Researchers developed an evaluation framework that allows for a more thorough, detailed analysis of a candidate pavement treatment, which may include resurfacing to increase skid resistance and/or increasing superelevation rate. The evaluation framework accounts for crash costs and treatment costs to yield a benefit-cost ratio, and also includes a margin-of-safety

analysis. The evaluation framework is built into an updated version of the TCMS spreadsheet program, which was originally developed in TxDOT research project 0-6714 (*2*).

Benefit-Cost Analysis

The benefit-cost analysis compares the expected cost to implement one of the pavement treatment products to the benefit of reducing crashes over the life of the treatment. Table 46 gives costs for various treatments. The HFST and seal coat costs come from the literature. The asphalt overlay costs come from asphalt production data in TxDOT from 2015.

Table 46. Unit Cost for Various Pavement Treatments.

Treatment Type	Thickness (in.)	Approximate Unit Cost	
		$/ton	$/yd^2
HFST	Not applicable	NA	19–25
Seal Coat	Not applicable	NA	2.50
Asphalt Overlay			
Dense Graded	1.5–2.0	79	6.50–8.75
Super Pave	1.5–2.0	86	7.25–9.75
Stone Matrix Asphalt	1.5–2.0	105	7.25–8.75
Thin Overlay Mix	1.0–1.25	116	6.50–8
PFC (SAC A)	1.5	110	9

To compute a benefit-cost ratio for a proposed curve pavement treatment, the following steps are required:

1. Estimate the fatal-and-injury crash frequency of the curve for a time period before the treatment is implemented. This estimated crash frequency is based on the curve's characteristics, particularly its skid number, in the before period.
2. Identify a proposed pavement treatment and determine the increase in skid number that can be obtained from the treatment.
3. Estimate the fatal-and-injury crash frequency of the curve for a time period after the treatment is implemented. The crash frequency will change between the before and after periods due to the change in skid number, but no other variables (and hence no other CMF values) will change. This crash frequency can be improved using the EB adjustment (*85*) if actual crash data are available for the before period.
4. Compute the reduction in fatal-and-injury crashes between the before and after periods.
5. Using default crash severity distribution proportions, compute the number of PDO crashes in both time periods and the reduction in these crashes between the time periods.
6. Using crash cost values for all severity levels (K, A, B, C, and PDO), compute the treatment benefit in terms of crash costs reduced following installation of the treatment.
7. Compute the proposed treatment cost.
8. Compute the benefit-cost ratio by dividing the benefit obtained in step 6 by the cost obtained in step 7.

Table 47 provides the default crash costs and severity distribution used in TCMS. Researchers derived the severity distributions from a query of the TRM and CRIS databases, the

fatal-and-injury crash costs from U.S. Department of Transportation guidance (*86*), and the PDO crash costs from the guidance provided by Council et al. (*87*).

Table 47. Crash Costs and Severity Distribution.

Crash Severity	Crash Cost	Severity Distribution (proportion)
K	$9,100,000	0.0335
A	$3,908,450	0.0626
B	$691,600	0.1567
C	$27,300	0.1449
PDO	$10,350	0.6023

Spreadsheet Updates

To develop the evaluation framework, researchers made the following key changes to the TCMS spreadsheet:

- Incorporating the new safety prediction models that were described in Chapter 5.
- Adding data input cells to allow the analyst to describe the annual precipitation rate and the treatment cost.
- Adding calibration cells and model calculations to compute the life span of pavement materials, based on considerations of initial and final skid number and rate of change of skid number as described in Chapter 4.
- Updating the margin of safety analysis calculations and graphs to show margins of safety for three time periods:
    - Before – before the treatment is implemented.
    - After – immediately after the treatment is implemented (i.e., the initial period).
    - Terminal – after the treatment has existed long enough that its skid number has degraded to the terminal value.
- Removing calculations that are relevant to operational analysis but not safety evaluation. These calculations include:
    - Curve severity category and recommended advisory speed (*88*).
    - Curve travel path distributions (Chapter 4 of Reference *2*).

Figure 59 and Figure 60 show screenshots of the first and second pages of the updated TCMS program's analysis worksheet. The analysis worksheet is still organized such that it can be printed on six pages, with the analysis inputs and findings presented on the first two pages. The rest of the pages contain calibration coefficients and intermediate calculations.

The TCMS program can be used to compute the benefit-cost ratio and net benefit of a proposed pavement treatment, which can consist of a new surface to improve pavement friction and/or an increasing of the superelevation rate. The program also provides the margin of safety, which is computed as the difference between side friction supply and side friction demand (*2*). Margin of safety is provided for the beginning, middle, and ending points of the curve (PC, MC, and PT, respectively) so the analyst can determine which points of the curve could most benefit from a safety treatment.

Texas Curve Margin of Safety Worksheet

General Information					
District		Control section		Date	November 6, 2018
Highway		Beginning milepoint		Analyst	
Curve ID number		Ending milepoint		Curve deflection	Right

Site Characteristics Input Data		
Average daily traffic volume (ADT, veh/d)		18000
Truck percentage		10
ADT growth rate (%)		2
Roadway configuration		2U
Curve radius (ft)		500
Deflection angle (degrees)		40
85th % tangent speed (mph)		
Regulatory speed limit (mph)		70
Advisory speed (mph)		45
Average lane width (ft)		11
Average shoulder width (ft)		2
Grade (%) (Deflection to Right)	PC	2
	MC	0
	PT	-2
Annual precipitation rate (inches)		35

Superelevation rate (%)		Before	After
Deflection to Left	PC	4.5	6.5
	MC	6	8
	PT	4.5	6.5
Deflection to Right	PC	6.5	8.5
	MC	8	10
	PT	6.5	8.5

Pavement Treatment Input Data	
Skid number for existing surface	30
Proposed treatment type	PFC
Aggregate type 1	Siliceous Gravel
% contribution to coarse aggregate	50
Aggregate type 2 (optional)	Dolomite
% contribution to coarse aggregate	50
Economic discount rate	3.0%
Treatment cost	$50,000

Crash Analysis Input Data		
Analysis period (yr)		7
Crash data period (yr)		7
Reported crash count by type	All	10
	Wet-weather	3
	Run-off-road (ROR)	9
	Wet-weather ROR	2

Skid Number Calculations			
Skid number	Before	After	Terminal
at advisory speed	31.8	44.0	39.6
at skid test speed	30.0	41.6	37.4

Crash Prediction Model Calculations		
Predicted Crash Counts in Analysis Period		
	Before	After
All	6.974	6.406
Wet-weather	0.438	0.294
Run-off-road (ROR)	7.085	6.414
Wet-weather ROR	0.401	0.267
Predicted Change in Crash Count		
All		-9.9%
Wet-weather		-35.6%
Run-off-road (ROR)		-10.9%
Wet-weather ROR		-35.6%
Overall Crash Modification Factors (CMFs)		
Curve radius	6.179	
Annual precip.	1.632	
Skid number	1.094	0.986
Skid x Precip.	1.786	1.609
Wet-Weather CMFs		
Curve radius	1.000	
Annual precip.	2.959	
Skid number	1.462	0.942
Skid x Precip.	4.328	2.787
Run-off-Road CMFs		
Curve radius	7.895	
Annual precip.	1.632	
Skid number	1.105	0.984
Skid x Precip.	1.804	1.607
Wet-Weather Run-off-Road CMFs		
Curve radius	1.000	
Annual precip.	3.065	
Skid number	1.462	0.942
Skid x Precip.	4.482	2.886

Benefit-Cost Analysis Calculations	
Average crash cost	$668,082
Analysis period (yr)	7
SK at end of analysis period	36.3
Benefit-cost ratio	4.48
Net benefit	$174,146
Period of improved *SK* (yr)	21
SK at end of improved period	36.0
Benefit-cost ratio	8.79
Net benefit	$389,285

Page 1

Figure 59. TCMS Analysis Worksheet, Page One.

Texas Curve Margin of Safety Worksheet

Margin of Safety Analysis — Tabular Results

Correcting		Before	After	Terminal	Change before-after	Change before-terminal
Deflection to Left	PC	0.000	0.094	0.050	+ 0.094	+ 0.05
	MC	0.172	0.306	0.258	+ 0.133	+ 0.086
	PT	0.126	0.252	0.206	+ 0.125	+ 0.08
Deflection to Right	PC	0.000	0.115	0.071	+ 0.115	+ 0.071
	MC	0.164	0.296	0.249	+ 0.132	+ 0.085
	PT	0.086	0.209	0.164	+ 0.123	+ 0.078

Margin of Safety Analysis — Graphical Results

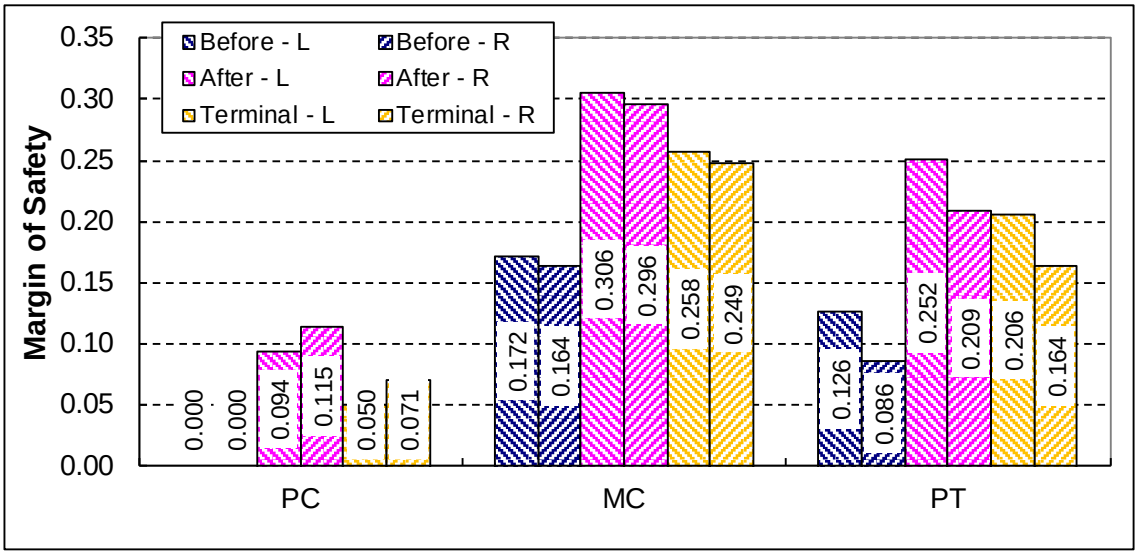

Pavement Treatment Skid Number

Years to effective terminal *SK*: 4 Effective terminal *SK*: 37.4 *Page 2*

Figure 60. TCMS Analysis Worksheet, Page Two.

APPENDIX A: PAVEMENT DATA FROM LITERATURE SOURCES

Table 48. Literature on CMFs of Pavement Treatments.

Year	Study Scope	Section Type	Crash Type	Crash Mod. Factor	Reference
High Friction Surface Treatments					
2015	8 states, 57 sections, sufficient before-after data, and reference sites	Ramps	Wet	0.139	(*29*)
			Total	0.653	
		Curves	Wet	0.481	
			Total	0.759	
2013	Kentucky, 43 sections (Overlaps with Merritt ’15)	Curves	Wet	0.14	(*29*)
			Total	0.27	
		Ramps	Wet	0.15	
			Total	0.34	
2016	Florida, 40 sections	Tight curves and ramps	Wet	0.25	(*59*)
			Total	0.68	
		Wide curves and tangents	Wet and Total	Not significant	
NCHRP		High wet-weather accident locations	Wet	0.76	(*89*)
			Total	0.43	
2012	Literature review		Wet	0.50	(*90*)
			Total	0.80–0.70	
2008	Wisconsin			0.07	(*91*)
	Michigan, 4 sites, 1-yr. (Overlaps with Merritt ’15)			0.40	(*92*)
Seal Coats					
1995	NYDOT (Thin Overlays)	36 Sites, Long Island	Wet	0.50	(*29*)
1997			Total	0.80	
2015	4 States, 2557 miles	Multilane	Wet	0.775	(*29*)
			Total	1.147	
		Two-Lane	Wet	0.950 (0.830 initial) (0.952 3-yr)	
			Total	0.939	
1990	Utah DOT, 34 one-mile long sections	Non-Interstate, low volume roadways	Wet	0.61	(*93*)
			Dry	0.55	
Thin Asphalt Overlays					
2015	California and North Carolina	Freeway	Wet	0.91	(*29*)
			Total	1.0	
		Multilane	Wet	0.91	
			Total	1.05	
		Two-Lane	Wet	1.15	
			Total	1.19	
Permeable Friction Course					
2009	Louisiana Police Report, US 71	I-20	Wet	0.24	(*94*)
			Total	0.43	

		(study of one application)			
				Decreasing over 4 years	(*29*)
Abrading and Texturing					
1990	3 years before and 1-yr after, California	Grooving	Wet	0.28	(*95*)
1975	Freeways, Los Angeles	Grooving	Wet	0.31	(*96*)
-	NYDOT (41 sites)	Grooving	Wet Total	0.45 0.77	(*29*)

Table 49. Literature Review on Skid Resistance of Pavement Treatments.

Study Year	Study Scope	Measurement Type	Initial Value	Years Later	Later Value	Reference
High Friction Surface Treatment						
2008	Wisconsin	SK	73	5	59	(*91*)
2016	Florida	SK40R	>70	6	63–78	(*59*)
2001	Iowa bridge deck	SK	67.5	4	64.5	(*97*)
2015	Kansas, flint aggregate	SK	88	4	54	(*98*)
Seal Coat						
2004	Utah	SK_R	Avg. 60	6	Avg. 57	(*99*)
Thin Overlay						
2004	VDOT	SK	46.7	1		(*100*)
	Penn DOT	μ from DFT	0.60–0.62	-	-	(*101*)
2016	Penn DOT	SK40	50	-		(*101*)
		MPD (CTM test)	0.69	-	-	
Permeable Friction Course						
2012	WSDOT	FN40R OGFC-HMA	54	3	51	(*102*)
1997	GDOT, 6 sections	FN40R	49	-	51	(*103*)
Texturing						
	Shotblasting	SK	53	1	44	
	Abrading	SK	48	1	38	
	Milling	SK	44			

Table 50. Literature Review on Service Life of Pavement Treatments.

Study Year	Study Scope	Years	Comment	Reference
High Friction Surface Treatment				
2014	International	7–12		(*104*)
	Bridge decks (some)	>15		
	Vendor report	5–8	15,000 veh/day	
	Vendor report	Up to 5	50,000 veh/day	
	Michigan bridge decks	12–15	Includes site with 48,000–62,000 ADT	
2016, 2011	New Zealand, Florida	<1	Poor construction practices	(*59*, *105*)
Seal Coat				
2012	Survey of 22 State DOTs	6.5 (3–15)		(*106*)
	New York	3–4		
	Washington	5–7		
	Texas	4–7	5,000 veh/day	
2013		3–15	In general	(*107*)
		4–6	Single	
		5–7	Double	
	Survey of 31 U.S. State Highway agencies and 6 Canadian agencies from Ministry of Transportation	5.6–7.8	New construction	(*108*)
		6–7.5	Over chip seal	
		6.5–7.4	Over existing asphalt	
		8.2–10.2	Grade 4	(*109*)
		5.4–8.1	Grade 3	
		5.9–7.7	Grade 2	
2004	Utah	27	Skid function only	(*99*)
Thin Overlay				
2000	National Study	4–6		(*110*)
2008	Texas	8–15		(*111*)
2004	NCDOT and VDOT	3+		(*100*)
		8+	Replacement	
2009		10+	Over flexible	(*112*)
		6–10	Over rigid	
Permeable Friction Course				
	Ultra-thin PFC	7+		(*113*, *114*)
Texturing				
	SHRP 2	8	Diamond grinding	(*29*)
2005	California	16–17	Diamond grinding	(*115*)
	Oklahoma DOT	2	Abrading and shot blasting	(*116*)
2015		1	Milling on seal coats	(*117*)
		1.5	Milling on HMA	

Table 51. Literature Review on Unit Cost of Pavement Treatments.

Study Year	Study Scope	$/sq-yd	Comments	Reference
High Friction Surface Treatment				
2014	NA	$25–$35	Historic	(*104*)
	NA	$19–$21	Rolling several projects together	
2016	Florida, 40 sections	$34 ($26–$40)	Unit cost	(*59*)
		$59 ($36–$113)	Comprehensive unit cost	
Seal Coat				
2008	Cost Index Number Analysis	$0.82	Emulsion-SC	(*118*)
		$0.92	Asphalt-SC	
2011		$1–$2		(*119*)
2005		$0.70–$1.25	Single	(*120*)
		$1.25–$2.50	Double	
Thin Overlay				
2014		$2.07	$14,600 per lane mile	(*121*)
2000		$1.75		(*110*)
2000?		$1.75	$25/ton, 1.25-inch thick	(*110*)
		$3–$6		(*122*)
Permeable Friction Course				
2001	47 responses	$2.75	Novachip	(*114*)
2004	47 responses	$6.35	Novachip	(*120*)
		$7.34	NovaChip	(*123*)
		$12.43	Includes 2″ SMA	(*94*)

APPENDIX B: SITE, TREATMENT, AND AGGREGATE DATA FOR SKID NUMBER MODELING

Table 52. Site Data.

Section ID	Treatment Type-Route-County-District	Treatment Detail	Const Date	Proj Beginning	Proj End	Direction	Latitude	Longitude	Aggregate Type	New Skid Testing	PMIS Query	Data Source
1	HMA-US 77-Kennedy-Pharr	Type D	Feb-13	758+0.0	750+0.0	NB	26.637417	-97.767150	Gravel		X	0-6746
2	HMA-US 281-Hidalgo-Pharr	Type D	Aug-11	772+0.5	768+0.5	NB	26.349544	-98.148075	Gravel		X	0-6746
3	HMA-US 259-Rusk-Tyler	Type C	Feb-07	338+0.0	334+0.0	NB	31.865894	-94.680128	Sandstone + Limestone		X	0-6746
4	HMA-FM 973-Travis-Austin	Type C	Jan-12	448+1.0	452+0.0		30.221703	-97.634250	Limestone	X	X	0-6746
5	HMA-SH 71-Travis-Austin-A	TOM	Jul-13	584+0.0	588+0.0	WB	30.188325	-97.593578	Sandstone + Limestone	X	X	0-6746
6	HMA-FM 3238-Travis-Austin	TOM	Jul-13	514+0.5	522+0.0	WB	30.287778	-98.051458	Sandstone + Limestone	X	X	0-6746
7	HMA-IH 45-Leon-Bryan	Type C	Aug-08	164+0.0	167+0.7	NB	31.284031	-95.992708	Sandstone + Gravel + Limestone	X	X	0-6746
8	HMA-IH 10-Austin-Yoakum	Type D	Jul-11	710+1.5	726+1.5	EB	29.754089	-96.255375	Dolomite-Limestone	X	X	0-6746
9	HMA-SH 36-Austin-Yoakum	Type D	Jul-06	612+1.0	618+1.0	SB	29.686158	-96.129456	Limestone		X	0-6746
10	HMA-SH 7-Houston-Lufkin	Type D	May-13	694	702	WB	31.391175	-95.073669	Granite + Limestone		X	0-6746

11	HMA-IH 35-Webb-Laredo	SMA	Jun-08	7+0.868	12+0.9	SB	27.675356	-99.468097	Traprock + Gravel		X	0-6746
12	HMA-IH 35-La Salle-Laredo-A	SMA	Jun-04	TRM 65	TRM 69+0.5	NB			Basalt + Traprock			0-6746
13	HMA-IH 35-La Salle-Laredo-B	SMA	Jun-04	49+0.431	53+0.42	SB	28.220956	-99.302306	Traprock + Limestone		X	0-6746
14	HMA-US 385-Ector-Odessa	CMHB-F	Oct-05	356+0.76	370+0.0	NB	31.650977°	-102.329029°	Rhyollite and LS Scrn		X	0-6746
15	HMA-IH 20-Midland-Odessa-A	SP-D	Jun-12	149+0.7	144-0.281	any	32.083019	-101.905331	Rhyollite and Dolomite		X	0-6746
16	HMA-IH 20-Martin-Odessa	SP-C	Apr-12	163+0.228	158+0.981	any	32.156964	-101.714761	Rhyollite and Dolomite		X	0-6746
17	HMA-IH 20-Midland-Odessa-B	SP-D	Jun-13	136+0.141	121+0.467	any	31.919564	-102.200139	Rhyollite and Dolomite		X	0-6746
18	HMA-IH 10-Jefferson-Beaumont	SMA-D	Jul-09	839+0.405	848+0.772	WBOL	29.988564	-94.207322	Granite		X	0-6746
19	HMA-US 90-Jefferson-Beaumont	SMA	May-13	900+1.061 FM 1009	902+0.260 FM 365	EBOL	30.037194	-94.411994	Sandstone + Limestone		X	0-6746
20	HMA-SH 82-Jefferson-Beaumont	SMA	Apr-13	454-0.513	456+0.496	SBOL	29.879622	-93.981919	Granite		X	0-6746
21	HMA-Loop 207-Chambers-Beaumont	Type D	May-13	462-0.068	462+0.602	NB	29.851764	-94.892603	Sandstone + Limestone		X	0-6746
22	HMA-US 59-Panola-AtlantaS Carthage	Type D	Apr-12	324+3.02	316+1.0	SB	32.047683	-94.291450	Quartzite	X	X	0-6746
23	HMA-US 59-Panola-AtlantaN Carthage	Type D	Jun-11	TRM 310+0.2	304+.4	SB	32.188106	-94.338764	Quartzite	X	X	0-6746

24	HMA-US 59-Panola-Atlanta	CMHB-F	Aug-05	304+.4	300 +.0	NB and SB	32.285569	-94.350125	Quartzite		X	0-6746
25	HMA-IH 30-Bowie-Atlanta	SMA-F	Feb-10	208+1.0	TRM 206	EB and WB	33.475136	-94.285958	Sandstone + Gravel		X	0-6746
26	HMA-IH 20-Harrison-Atlanta	SMA-C	NA	632+0.19	636+0.11		32.479767	-94.091219	Quartzite		X	0-6746
27	HMA-US 271-Camp-Atlanta	CMHB-F	Jun-08	TRM 262	TRM 266+0.3	NB and SB	33.065194	-94.964239	Siliceous Gravel		X	0-6746
28	HMA-US 59-Wharton-Yoakum (Hillje)	NA	NA	~591	~593	SB	29.128103	-96.377950	Unknown	X	X	0-5836
29	HMA-SH 71-Travis-Austin-B	NA	Apr-08	0.6 MI W OF RIVERSIDE DR	PRESIDENTIAL DRIVE	WB	30.209954	-97.652454	Limestone + Field Sand		X	0-5836
30	HMA-US 59-Wharton-Yoakum (Kendelton)	NA	Sep-04	560-0.090	566+0.261	NB	29.428783	-96.030583	Unknown		X	0-5836
31	HMA-SH 154-Hopkins-Paris	NA	May-03	672+1.703	672-0.246	NB	33.077067	-95.598650	Sandstone		X	0-5836
32	PFC-US 59-Wharton-Yoakum (Kendelton)		Jun-07	0.20 miles past Ora Lee Rd		SB	29.432483	-96.025067	Limestone	X	X	0-5836
33	PFC-US 59-Wharton-Yoakum (Hillje)		NA	588+1.720	594+1.773	NB	29.128103	-96.377950	Unknown	X	X	0-5836
34	PFC-SH 288-Brazoria-Houston		Oct-06	484+0.730	498+1.955	SB	29.408617	-95.427433	Granite + Limestone		X	0-5836
35	PFC-SH 288-Brazoria-Houston-A		Jul-17	484+0.385	496+1.664	SB	29.408617	-95.427433	Unknown	X	X	0-6932
36	PFC-SH 288-Brazoria-Houston-B		Jun-11	496+1.966	506+1.331	SB			Unknown	X	X	0-6932

37	PFC-US 290-Bastrop-Austin		Apr-07	626+0.083	632+0.000	EB	30.207600	-97.092483	Sandstone		X	0-5836
38	PFC-IH 30-Hopkins-Paris	TBPFC	May-06	127+0.133	134+0.605	WB	33.147867	-95.451150	Sandstone		X	0-5836
39	PFC-SH 6-Robertson-Bryan		May-09	544+0.922	554+0.445	NB	31.032750	-96.709233	Sandstone + Limestone	X	X	0-5836
40	PFC-IH 20-Taylor-Abilene		Jun-05	279-0.44	283+0.463	WB	32.480700	-99.777867	Limestone			0-5836
41	PFC-US 83-Taylor-Abilene		Sep-05	322+0.75	328+0.065	NB	32.444267	-99.786633	Limestone	X	X	0-5836
42	PFC-SH 240-Wichita-Wichita Falls	UTBHMWC	May-08	468+0.489	470+1.436	NB	33.905500	-98.460800	Siliceous + Limestone		X	0-5836
43	PFC-SH 6-McLennan-Waco		Aug-05	570+0.454	508-0.716	WB	31.541017	-97.048083	Limestone	X	X	0-5836
44	PFC-US 281-Bexar-San Antonio-A		May-05	534+0.361	530+1.996	SB	29.483883	-98.481940	Traprock		X	0-5836
45	PFC-SH 6-Waller-Houston		Jul-05	626+1.074	632+3.108	NB	30.122867	-96.074383	Igneous Rock	X	X	0-5836
46	PFC-IH 37-San Patricio-Corpus Christi		May-04	0.5 MI S OF MEDINA RIVER	MEDINA RIVER	NB	27.909300	-97.633817	Limestone + Gravel		X	0-5836
47	PFC-IH 37-Nueces-Corpus Christi		Apr-04	0+0.000	16+0.644	NB	27.882483	-97.624367	Limestone		X	0-5836
48	PFC-US 77-San Patricio-Corpus Christi		Jul-09	656+1.96	654+0.572	NB	27.913383	-97.621367	Limestone + Gravel		X	0-5836
49	PFC-IH 35-McLennan-Waco		May-03	340+0.052	343+0.622	NB	31.632385	-97.095510	Rhyolite		X	0-5836
50	PFC-IH 20-Van Zandt-Tyler		Jun-08	524+0.577	527+0.476	EB	32.584567	-95.870650	Unknown	X	X	0-5836

51	PFC-IH 20-Smith-Tyler		Aug-09	534+0.787/ 571	597+0.000/ 580	EB	32.437433	-95.022317	Sandstone	X	X	0-5836
52	PFC-US 281-Bexar-San Antonio-B		Sep-06	534+0.361	536+0.515	SB	29.458035	-98.481533	Sandstone + Limestone		X	0-5836
53	PFC-SH 6-Fort Bend-Houston	TBPFC	Apr-05	678+2.323	684+1.127	SB	29.646883	-95.651517	Quartzite		X	0-5836
54	PFC-US 287-Clay-Wichita Falls	UTBHMWC	Aug-05	362+0.916	366+0.622	NB	33.793100	-98.177200	Granite + Dolomite		X	0-5836
55	PFC-US 82-Clay-Wichita Fals	UTBHMWC	Aug-05	530+0.678	542+0.895	NB	33.875367	-98.383183	Granite + Dolomite		X	0-5836
56	PFC-SL 473-Wichita-Wichita Falls	UTBHMWC	May-08	192+0.854	194+1.673	SB	33.896933	-98.483683	Granite + Dolomite		X	0-5836
57	PFC-US 281-Hidalgo-Pharr		May-04	778+0.3	782+0.4	SB	26.256383	-98.168550	Gravel		X	0-5836
58	PFC-US 90-Waller-Houston		Mar-04	794-0.723	794+1.327	WB	29.784000	-95.983450	Sandstone		X	0-5836
59	PFC-SL 289-Lubbock-Lubbock		Oct-10	312+0.364	308+0.128	WB	33.529274	-101.877332	Gravel + Limestone		X	0-5836
60	PFC-I 37-Bexar-San Antonio	TBPFC	Feb-13	125+0.0	133+0.5	SB			Sandstone			0-6746
61	PFC-I 45-NA-Bryan	TBPFC	Jul-09	167+0.9	178+0.0	NB			Limestone			0-6746
62	PFC-SH 6-0-6932-Bryan	TBPFC	Nov-09	598+1.14	602+0.0	SB			Sandstone + Limestone			0-6746
63	PFC-SH 6-Old-Bryan	TBPFC	Jun-07	596+0.60	598+1.14	SB			Sandstone + Limestone			0-6746
64	PFC-US 69-Jefferson-Beaumont	TBPFC	Sep-11	522+4.227	532+0.151	SB			Granite + Limestone			0-6746
65	PFC-I 20-Martin-Odessa		Jun-04						Rhyolite Gravel		X	0-6746

66	Seal Coat-US 77-Cameron-Pharr	Grade 3	May-13	786+0.0	778+0.0	NB	26.286450	-97.758349	Limestone		X	0-6746
67	Seal Coat-US 281-Hidalgo-Pharr	Grade 3	May-13	766+0.5	766+0.0	NB	26.496741	-98.133478	Limestone		X	0-6746
68	Seal Coat-US 281-Brooks-Pharr-A	Grade 3, Precoated	May-11	752+0.0	735+0.0	NB	26.781980	-98.103380	Limestone		X	0-6746
69	Seal Coat-US 281-Brooks-Pharr-B	Grade 3	Sep-11	722+0.0	716+0.0	NB	27.099125	-98.146266	Limestone		X	0-6746
70	Seal Coat-US 377-Hood-Dallas-FW	Grade 3	Jul-10	328+1.5	322+0.00	SB	32.494509	-97.663436	Limestone	X	X	0-6746
71	Seal Coat-SH 199-Parker-Dallas-FW	Grade 3	Jul-11	534+0.00	544+0.00	NB	32.997915	-97.829536	Limestone		X	0-6746
72	Seal Coat-US 377-Tarrant-Dallas-FW	Grade 3	Jul-10	312+0.00	306+0.00	NB	32.639709	-97.512254	Limestone		X	0-6746
73	Seal Coat-US 67-Coleman-Brownwood	Grade 4	Jul-10	586+0.000	592+1.917	WB	31.727124	-99.205986	Limestone	X	X	0-6746
74	Seal Coat-US 67-Brown-Brownwood	Grade 4	Jul-10	580+1.223	586+0.000	WB	31.726689	-99.201810	Limestone	X	X	0-6746
75	Seal Coat-US 183-Eastland-Brownwood	Grade 4	Jul-12	330+0.461	338+0.570	SB	32.372362	-98.970318	Limestone	X	X	0-6746
76	Seal Coat-US 377-Brown-Brownwood	Grade 4	Jul-12	427-0.088	432+0.108	SB	31.711410	-98.990709	Limestone	X	X	0-6746
77	Seal Coat-US 90/IH 10-Bexar-San Antonio	Grade 4	Jun-13	563+0.5	560+0.5	WB	29.386688	-98.679846	Limestone		X	0-6746
78	Seal Coat-FM 1518-Bexar-San Antonio	Grade 3	Jun-13	490+2.0	502+0.0	SB	29.471056	-98.217401	Sandstone	X	X	0-6746

79	Seal Coat-SH 16-Atascosa-San Antonio-A	Grade 4	Jun-12	618+0.0	626+1.0	NB	29.088409	-98.594748	Traprock		X	0-6746
80	Seal Coat-SH 16-Atascosa-San Antonio-B	Grade 3	Jun-12	638	644		28.828613	-98.539960	Limestone + Trap Rock		X	0-6746
81	Seal Coat-SH 36-Austin-Yoakum	Grade 3	Aug-08	613	NA	SB	29.699914	-96.134508	Limestone	X		New
82	Seal Coat-US 59-Angelina-Lufkin	Grade 3	Jun-10	400+0.0	402+1.2	SB	31.182188	-94.782272	Traprock		X	0-6746
83	Seal Coat-US 69-Angelina-Lufkin	Grade 4	Jun-12	424+1.442	426+1.442	SB	31.288922	-94.636185	Lightweight	X	X	0-6746
84	Seal Coat-US 287-Trinity-Lufkin	Grade 4	Jun-13	650+1.76	660+1.2		31.158165	-95.218990	Lightweight	X	X	0-6746
85	Seal Coat-FM 2213-San Augustine-Lufkin	Grade 5	Jun-12	344+0.53	348+0.1	SB	31.286063	-94.614971	Lightweight	X	X	0-6746
86	Seal Coat-US 59-Shelby-Lufkin	Grade 4	Jun-12	338+1.1	344+0.18	SB	31.899911	-94.411839	Sandstone	X	X	0-6746
87	Seal Coat-LP 338-Ector-Odessa	Grade 4	Jun-12	252+.02	256+0.0	NB	31.780129	-102.378416	Rhyollite		X	0-6746
88	Seal Coat-US 385-Crane-Odessa	Grade 4	Jun-09	370+0.0	380+0.0	NB	31.619377	-102.327865	Limestone		X	0-6746
89	Seal Coat-US 385-Ector-Odessa	Grade 3	Jun-10	346	348	NB	31.973937	-102.414058	Limestone		X	0-6746
90	Seal Coat-SH 82-Jefferson-Beaumont	Grade 4	Sep-10	460+0.0	468+0.0	NB	29.773557	-93.932522	Lightweight		X	0-6746
91	Seal Coat-FM 365-	Grade 4	Jul-13	752+ 1.244	766+1.592	WB	29.913316	-94.095998	Lightweight		X	0-6746

	Jefferson-Beaumont											
92	Seal Coat-FM 105-Orange-Beaumont	Grade 4	Jul-13	436+1.128	438+1.598	SBOL	30.181897	-94.023913	Lightweight		X	0-6746
93	Seal Coat-US 80-Harrison-Atlanta	Grade 4	Jun-12	824 +0.0	826+0.5	EB and WB	32.478939	-94.080411	Lightweight	X	X	0-6746
94	Seal Coat-SH 7-Houston-Lufkin	NA	Aug-17	NA	NA	EB			Lightweight	X		0-6932
95	Seal Coat-US 59-Cass-Atlanta	Grade 3, Precoated	Jun-13	238	236	NB and SB	33.113397	-94.182777	Gravel		X	0-6746
96	Seal Coat-SH 77-Cass-Atlanta-A	Grade 4, Precoated	Jun-12	746	744	EB and WB	33.101678	-94.155448	Sandstone		X	0-6746
97	Seal Coat-SH 77-Cass-Atlanta-B	Grade 4, Precoated	Jun-13	720+0.986	728+0.974	EB	33.194653	-94.455649	Gravel		X	0-6746
98	Seal Coat-US 59-Panola-Atlanta	Grade 3	Jun-09	NA	NA	NB			Sandstone	X	X	0-6746
99	HFST-SH 22-Navarro-Dallas		01-Apr-16	610	NA	WB and EB	32.088270	-96.728973	Calcined Bauxite	X		New
100	HFST-US 287-Navarro-Dallas-A		Unknown	549.8	NA	NB and SB			Calcined Bauxite	X		New
101	HFST-IH 20-Nolan-Abilene		01-Apr-16	0.037 MI W of CR 104	1.1 MI E of CR 104		32.442048	-100.510797	Calcined Bauxite	X		New
102	HFST-FM 89-Taylor-Abilene		01-Apr-16	0.127 mi S of CR 277	1.855 MI S of CR 277		32.228419	-99.925726	Calcined Bauxite	X		New
103	HFST-FM 2035-Nolan-Abilene		01-Apr-16	0.170 MI N of CR 253	0.420 MI S of CR 253		32.378732	-100.290270	Calcined Bauxite	X		New
104	HFST-SH 47-Brazos-Bryan		01-Feb-17	Curve W of FM 60		Both			Calcined Bauxite	X		New

105	HFST-Kimbro-Travis-Austin		01-May-15	OLD HWY 20	KIMBRO RD		30.334883	-97.510813	Calcined Bauxite	X		New
106	HFST-Lp 1604-Bexar-San Antonio	Unitex	Oct-2010	NE I-35	at 1604 E-N connector		29.569161	-98.335096	Calcined Bauxite	X		0-6714
107	Eau Gallie Blvd, Indian River-Brevard	E-Bond 526	4/27/2013	5.836	6.385		28.134253	-80.613341	Flint			FDOT
108	EB Royal Palm to NB I-75-Broward	Tyregrip	May-2006	300' befr Gore	Gore		26.086311	-80.360892	Calcined Bauxite			FDOT
109	I-595 to Ft L Airport-Broward	MARK-154	12/18/2011	0.337	0.955		26.068618	-80.133462	Calcined Bauxite			FDOT
110	I-95 (6th Ave S and Lake Worth Blvd)-Palm Beach	E-Bond 526	6/6/2014	20.476	20.911		26.614620	-80.068789	Calcined Bauxite			FDOT
111	NB I-75 to WB Royal Palm-Broward	Tyregrip	8/20/2008	0.270	0.498		26.086407	-80.360527	Calcined Bauxite			FDOT
112	NB I-75, SR 869 over SR 84 and I-595-Broward	MARK-154	6/20/2010	0.440	0.638		26.119187	-80.345279	Flint			FDOT
113	NB I-95 to WB SR 810-Broward	Bauxite	8/20/2014	0.000	0.225		26.319893	-80.114686	Calcined Bauxite			FDOT
114	SB I-275 to WB SR 60-Hillsborough	MARK-154	1/19/2012	0.000	0.291		27.948455	-82.530799	Calcined Bauxite			FDOT
115	SB I-75 to Big Bend Rd-Hillsborough	TrafficGrip	4/8/2013	0.030	0.198		27.789969	-82.358708	Calcined Bauxite			FDOT
116	SB I-95 Off-Ramp to Congress Ave.-Palm Beach	Safe-T-Grip	10/28/2010	800' N of Gore	Gore		26.420986	-80.090439	Calcined Bauxite			FDOT
117	SB I-95 to Belvedere Rd-Palm Beach	Safe-T-Grip	10/28/2010	0.030	0.198		26.689155	-80.067885	Calcined Bauxite			FDOT

118	SB I-95, EB SR 84-Broward	MARK-154	4/7/2013	0.187	0.303		26.088631	-80.167655	Flint			FDOT
119	SB SR 869, SB I-75 over WB SR 84-Broward	MARK-154	6/20/2010	0.542	0.616		26.122541	-80.345185	Flint			FDOT
120	Sheridan St-Broward	TyreGrip	7/1/2008	2.525	2.639		26.033359	-80.166614	Calcined Bauxite			FDOT
121	SR 736, I-95 and CSX RR-Broward	MARK-154	4/7/2013	1.970	2.155		26.106786	-80.168545	Flint			FDOT
122	SR 84 WB over I-95 NB Ramps-Broward	MARK-154	4/7/2013	0.208	0.264		26.088932	-80.167472	Flint			FDOT
123	SR A1A and 27 St- Miami-Dade	Safe-T-Grip	8/1/2011	1.034	0.232		25.802630	-80.126720	Calcined Bauxite			FDOT
124	US 301 over US 41-Manatee	Unitex	10/14/2013	7.464	7.689		27.481529	-82.562192	Calcined Bauxite			FDOT
125	US 41 and SR 684 Intersection-Manatee	Unitex	6/30/2014	5.117	5.451		27.462386	-82.575367	Calcined Bauxite			FDOT
126	WB Memorial Blvd to I-4 Ramps-Polk	HFST	11/2/2011	0.264	0.035		28.051493	-82.014055	Calcined Bauxite			FDOT
127	WB Polk Co. Pkwy to WB I-4-Polk	Tyregrip	1/26/2008	0.000	0.652		28.039022	-82.041489	Calcined Bauxite			FDOT
128	WB SR 60 to NB I-75-Hillsborough	MARK-154	12/12/2011	0.000	0.182		27.941138	-82.327455	Calcined Bauxite			FDOT
129	WB SR 810 to NB I-95-Broward	HFST	8/20/2014	0.000	0.268		26.316219	-80.114654	Calcined Bauxite			FDOT
130	WB US 192 to SB US 27-Polk	Crafco HFS	7/30/2010	0.128	0.323		28.346323	-81.675314	Calcined Bauxite			FDOT

145	HMA-US 90-Uvalde-San Antonio	CAM	Jun-10	474+1.84	480+1.65	WB			Traprock			0-6746
146	PFC-US 59-Nacogdoches-Lufkin		1-Jun	372	380	NB			Quartzite			0-6746
148	HMA-IH 35-Williamson-Austin	TOM	Jul-11	265	276	NB			Sandstone + Limestone			0-6746
149	Seal Coat-SH 16-McMullen-San Antonio	Grade 3	Jun-09	669	656	NB			Limes Rock Asphalt			0-6746

Table 53. Treatment Texture and Friction Data.

Section ID	Mix/Section Label	Project	Field or Lab	Mix Type	Agg Type	Test Month	Cycles	CTM (MPD)	Avg DFT (µ)	Sp	F60
	Hoban-PFC	6615	Lab	Fine PFC	Rhyolite		0	1.44		143.4	
	Hoban-PFC	6615	Lab	Fine PFC	Rhyolite		5000	1.34	0.56	134.4	0.39
	Hoban-PFC	6615	Lab	Fine PFC	Rhyolite		10000	1.33	0.56	133.5	0.38
	Hoban-PFC	6615	Lab	Fine PFC	Rhyolite		20000	1.30	0.48	130.8	0.34
	Hoban-PFC	6615	Lab	Fine PFC	Rhyolite		50000	1.33	0.42	133.5	0.31
	Hoban-PFC	6615	Lab	Fine PFC	Rhyolite		100000	1.39	0.49	138.9	0.35
	Eastland-PFC	6615	Lab	Fine PFC	Limestone		0	1.31		131.7	
	Eastland-PFC	6615	Lab	Fine PFC	Limestone		5000	1.21	0.29	122.7	0.23
	Eastland-PFC	6615	Lab	Fine PFC	Limestone		10000	1.22	0.30	123.6	0.24
	Eastland-PFC	6615	Lab	Fine PFC	Limestone		20000	1.22	0.27	123.6	0.22
	Eastland-PFC	6615	Lab	Fine PFC	Limestone		50000	1.31	0.23	131.7	0.21
	Eastland-PFC	6615	Lab	Fine PFC	Limestone		100000	1.32	0.26	132.6	0.22
	Delta-PFC	6615	Lab	Fine PFC	Sandstone		0	1.62		159.5	
	Delta-PFC	6615	Lab	Fine PFC	Sandstone		5000	1.56	0.57	154.1	0.40
	Delta-PFC	6615	Lab	Fine PFC	Sandstone		10000	1.57	0.52	155.0	0.38
	Delta-PFC	6615	Lab	Fine PFC	Sandstone		20000	1.48	0.47	147.0	0.34
	Delta-PFC	6615	Lab	Fine PFC	Sandstone		50000	1.56	0.46	154.1	0.34
	Delta-PFC	6615	Lab	Fine PFC	Sandstone		100000	1.57	0.43	155.0	0.32
	Jones Mill-PFC	6615	Lab	Fine PFC	Quartzite		0	1.32		133.0	
	Jones Mill-PFC	6615	Lab	Fine PFC	Quartzite		5000	1.11	0.60	113.6	0.39
	Jones Mill-PFC	6615	Lab	Fine PFC	Quartzite		10000	1.11	0.58	113.9	0.38
	Jones Mill-PFC	6615	Lab	Fine PFC	Quartzite		20000	1.14	0.49	116.8	0.34
	Jones Mill-PFC	6615	Lab	Fine PFC	Quartzite		50000	1.19	0.46	121.0	0.32
	Jones Mill-PFC	6615	Lab	Fine PFC	Quartzite		100000	1.20	0.40	121.8	0.29
	TCS-PFC	6615	Lab	Fine PFC	Limestone		0	1.03		106.9	
	TCS-PFC	6615	Lab	Fine PFC	Limestone		5000	0.99	0.47	103.3	0.31
	TCS-PFC	6615	Lab	Fine PFC	Limestone		10000	1.12	0.45	114.9	0.31
	TCS-PFC	6615	Lab	Fine PFC	Limestone		20000	1.17	0.37	119.1	0.27
	TCS-PFC	6615	Lab	Fine PFC	Limestone		50000	1.19	0.33	121.2	0.25
	TCS-PFC	6615	Lab	Fine PFC	Limestone		100000	1.25	0.28	126.6	0.23
	Hoban-SMA	6615	Lab	Fine SMA	Rhyolite		0	0.85		90.4	
	Hoban-SMA	6615	Lab	Fine SMA	Rhyolite		5000	0.79	0.6	85.1	0.36
	Hoban-SMA	6615	Lab	Fine SMA	Rhyolite		10000	0.75	0.51	81.5	0.31
	Hoban-SMA	6615	Lab	Fine SMA	Rhyolite		20000	0.76	0.44	82.4	0.28
	Hoban-SMA	6615	Lab	Fine SMA	Rhyolite		50000	0.83	0.37	88.7	0.25
	Hoban-SMA	6615	Lab	Fine SMA	Rhyolite		100000	0.8	0.36	86.0	0.25
	Eastland-SMA	6615	Lab	Fine SMA	Limestone		0	0.78		84.2	
	Eastland-SMA	6615	Lab	Fine SMA	Limestone		5000	0.52	0.43	60.8	0.24
	Eastland-SMA	6615	Lab	Fine SMA	Limestone		10000	0.52	0.32	60.8	0.20
	Eastland-SMA	6615	Lab	Fine SMA	Limestone		20000	0.53	0.31	61.7	0.20

	Eastland-SMA	6615	Lab	Fine SMA	Limestone		50000	0.5	0.26	59.1	0.18
	Eastland-SMA	6615	Lab	Fine SMA	Limestone		100000	0.51	0.24	59.9	0.17
	Delta-Turner-SMA	6615	Lab	Fine SMA	Sandstone		0	0.71		77.6	
	Delta-Turner-SMA	6615	Lab	Fine SMA	Sandstone		5000	0.53	0.62	61.7	0.32
	Delta-Turner-SMA	6615	Lab	Fine SMA	Sandstone		10000	0.6	0.58	68.0	0.32
	Delta-Turner-SMA	6615	Lab	Fine SMA	Sandstone		20000	0.63	0.51	70.7	0.29
	Delta-Turner-SMA	6615	Lab	Fine SMA	Sandstone		50000	0.63	0.48	70.7	0.28
	Delta-Turner-SMA	6615	Lab	Fine SMA	Sandstone		100000	0.62	0.42	69.8	0.25
	Delta-Servtex-SMA	6615	Lab	Fine SMA	Sandstone		0	0.63		70.9	
	Delta-Servtex-SMA	6615	Lab	Fine SMA	Sandstone		5000	0.54	0.53	62.6	0.29
	Delta-Servtex-SMA	6615	Lab	Fine SMA	Sandstone		10000	0.55	0.50	63.5	0.28
	Delta-Servtex-SMA	6615	Lab	Fine SMA	Sandstone		20000	0.59	0.45	67.1	0.26
	Delta-Servtex-SMA	6615	Lab	Fine SMA	Sandstone		50000	0.59	0.43	67.1	0.25
	Delta-Servtex-SMA	6615	Lab	Fine SMA	Sandstone		100000	0.59	0.37	67.1	0.23
	Delta-Delta-SMA	6615	Lab	Fine SMA	Sandstone		0	0.87		92.6	
	Delta-Delta-SMA	6615	Lab	Fine SMA	Sandstone		5000	0.70	0.61	77.0	0.35
	Delta-Delta-SMA	6615	Lab	Fine SMA	Sandstone		10000	0.79	0.58	85.1	0.35
	Delta-Delta-SMA	6615	Lab	Fine SMA	Sandstone		20000	0.78	0.53	84.2	0.32
	Delta-Delta-SMA	6615	Lab	Fine SMA	Sandstone		50000	0.76	0.49	82.4	0.30
	Delta-Delta-SMA	6615	Lab	Fine SMA	Sandstone		100000	0.87	0.46	92.2	0.30
	Jones Mill #2-SMA	6615	Lab	Fine SMA	Quartzite		0	0.82		87.3	
	Jones Mill #2-SMA	6615	Lab	Fine SMA	Quartzite		5000	0.67	0.68	73.9	0.37
	Jones Mill #2-SMA	6615	Lab	Fine SMA	Quartzite		10000	0.67	0.63	74.7	0.35
	Jones Mill #2-SMA	6615	Lab	Fine SMA	Quartzite		20000	0.72	0.59	78.5	0.34
	Jones Mill #2-SMA	6615	Lab	Fine SMA	Quartzite		50000	0.73	0.57	79.9	0.33
	Jones Mill #2-SMA	6615	Lab	Fine SMA	Quartzite		100000	0.74	0.50	80.7	0.30
	TCS-SMA	6615	Lab	Fine SMA	Limestone		0	0.78		84.1	
	TCS-SMA	6615	Lab	Fine SMA	Limestone		5000	0.60	0.57	67.6	0.31
	TCS-SMA	6615	Lab	Fine SMA	Limestone		10000	0.59	0.51	67.1	0.29
	TCS-SMA	6615	Lab	Fine SMA	Limestone		20000	0.62	0.48	69.6	0.28
	TCS-SMA	6615	Lab	Fine SMA	Limestone		50000	0.60	0.37	67.7	0.23
	TCS-SMA	6615	Lab	Fine SMA	Limestone		100000	0.60	0.30	68.0	0.20
	Hoban-DGM	6615	Lab	Fine DGM	Rhyolite		0	0.67		74.3	
	Hoban-DGM	6615	Lab	Fine DGM	Rhyolite		5000	0.61	0.58	68.9	0.32
	Hoban-DGM	6615	Lab	Fine DGM	Rhyolite		10000	0.60	0.45	68.0	0.26
	Hoban-DGM	6615	Lab	Fine DGM	Rhyolite		20000	0.57	0.43	65.3	0.25
	Hoban-DGM	6615	Lab	Fine DGM	Rhyolite		50000	0.56	0.38	64.4	0.23
	Hoban-DGM	6615	Lab	Fine DGM	Rhyolite		100000	0.53	0.35	61.7	0.22
	Eastland-DGM	6615	Lab	Fine DGM	Limestone		0	0.56		64.4	
	Eastland-DGM	6615	Lab	Fine DGM	Limestone		5000	0.40	0.42	50.1	0.22
	Eastland-DGM	6615	Lab	Fine DGM	Limestone		10000	0.40	0.38	50.1	0.21
	Eastland-DGM	6615	Lab	Fine DGM	Limestone		20000	0.38	0.34	48.3	0.19
	Eastland-DGM	6615	Lab	Fine DGM	Limestone		50000	0.37	0.26	47.4	0.16

	Eastland-DGM	6615	Lab	Fine DGM	Limestone		100000	0.39	0.26	49.2	0.17
	Delta-DGM	6615	Lab	Fine DGM	Sandstone		0	0.55		63.8	
	Delta-DGM	6615	Lab	Fine DGM	Sandstone		5000	0.54	0.60	62.7	0.31
	Delta-DGM	6615	Lab	Fine DGM	Sandstone		10000	0.67	0.58	73.9	0.33
	Delta-DGM	6615	Lab	Fine DGM	Sandstone		20000	0.71	0.53	77.9	0.31
	Delta-DGM	6615	Lab	Fine DGM	Sandstone		50000	0.76	0.42	82.8	0.27
	Delta-DGM	6615	Lab	Fine DGM	Sandstone		100000	0.77	0.34	83.6	0.24
	Jones Mill-DGM	6615	Lab	Fine DGM	Quartzite		0	0.72		78.9	
	Jones Mill-DGM	6615	Lab	Fine DGM	Quartzite		5000	0.64	0.73	71.4	0.39
	Jones Mill-DGM	6615	Lab	Fine DGM	Quartzite		10000	0.63	0.63	70.7	0.34
	Jones Mill-DGM	6615	Lab	Fine DGM	Quartzite		20000	0.68	0.63	75.0	0.35
	Jones Mill-DGM	6615	Lab	Fine DGM	Quartzite		50000	0.68	0.59	75.2	0.33
	Jones Mill-DGM	6615	Lab	Fine DGM	Quartzite		100000	0.71	0.48	77.6	0.29
	TCS-DGM	6615	Lab	Fine DGM	Limestone		0	0.51		60.3	
	TCS-DGM	6615	Lab	Fine DGM	Limestone		5000	0.53	0.59	62.1	0.31
	TCS-DGM	6615	Lab	Fine DGM	Limestone		10000	0.59	0.53	67.1	0.29
	TCS-DGM	6615	Lab	Fine DGM	Limestone		20000	0.62	0.48	70.1	0.28
	TCS-DGM	6615	Lab	Fine DGM	Limestone		50000	0.65	0.36	72.7	0.23
	TCS-DGM	6615	Lab	Fine DGM	Limestone		100000	0.63	0.33	70.7	0.22
	5-2-1	FDOT-HFST	Lab	HFST	Calcined Bauxite		0	1.82	1.01	177.5	0.66
	5-2-1	FDOT-HFST	Lab	HFST	Calcined Bauxite		30000	1.67	0.91	164.0	0.60
	5-2-1	FDOT-HFST	Lab	HFST	Calcined Bauxite		100000	1.52	0.86	150.2	0.57
	5-2-2	FDOT-HFST	Lab	HFST	Calcined Bauxite		0	1.86	0.97	181.0	0.64
	5-2-2	FDOT-HFST	Lab	HFST	Calcined Bauxite		30000	1.47	0.92	146.4	0.60
	5-2-2	FDOT-HFST	Lab	HFST	Calcined Bauxite		100000	1.57	0.88	154.7	0.57
	Fine-A 100	6742	Lab	Fine DGM	Trap Rock		0	0.67	0.51	74.3	
	Fine-A 100	6742	Lab	Fine DGM	Trap Rock		2000	na	0.52		0.31
	Fine-A 100	6742	Lab	Fine DGM	Trap Rock		30000	na	0.48		0.30
	Fine-A 100	6742	Lab	Fine DGM	Trap Rock		100000	0.77	0.41	83.3	0.26
	Fine-B1-25	6742	Lab	Fine DGM	Trap Rock-Dolomite		0	0.63	0.42	71.1	
	Fine-B1-25	6742	Lab	Fine DGM	Trap Rock-Dolomite		2000	na	0.53		0.30
	Fine-B1-25	6742	Lab	Fine DGM	Trap Rock-Dolomite		30000	na	0.50		0.29
	Fine-B1-25	6742	Lab	Fine DGM	Trap Rock-Dolomite		100000	0.61	0.39	68.9	0.24
	Fine-B1-50	6742	Lab	Fine DGM	Trap Rock-Dolomite		0	0.63	0.49	70.9	
	Fine-B1-50	6742	Lab	Fine DGM	Trap Rock-Dolomite		2000	na	0.55		0.31
	Fine-B1-50	6742	Lab	Fine DGM	Trap Rock-Dolomite		30000	na	0.45		0.27
	Fine-B1-50	6742	Lab	Fine DGM	Trap Rock-Dolomite		100000	0.65	0.37	72.5	0.24
	Fine-B1-75	6742	Lab	Fine DGM	Dolomite-Trap Rock		0	0.71	0.45	78.1	
	Fine-B1-75	6742	Lab	Fine DGM	Dolomite-Trap Rock		2000	na	0.51		0.30
	Fine-B1-75	6742	Lab	Fine DGM	Dolomite-Trap Rock		30000	na	0.43		0.28
	Fine-B1-75	6742	Lab	Fine DGM	Dolomite-Trap Rock		100000	0.76	0.35	82.4	0.24
	Fine-B1-100	6742	Lab	Fine DGM	Dolomite		0	0.64	0.42	72.0	
	Fine-B1-100	6742	Lab	Fine DGM	Dolomite		2000	na	0.49		0.28

	Fine-B1-100	6742	Lab	Fine DGM	Dolomite		30000	na	0.41		0.25
	Fine-B1-100	6742	Lab	Fine DGM	Dolomite		100000	0.64	0.35	71.6	0.23
	Fine-B2-25	6742	Lab	Fine DGM	Trap Rock-Dolomite		0	0.82	0.37	87.8	
	Fine-B2-25	6742	Lab	Fine DGM	Trap Rock-Dolomite		2000	na	0.56		0.34
	Fine-B2-25	6742	Lab	Fine DGM	Trap Rock-Dolomite		30000	na	0.45		0.29
	Fine-B2-25	6742	Lab	Fine DGM	Trap Rock-Dolomite		100000	0.86	0.36	91.3	0.25
	Fine-B2-50	6742	Lab	Fine DGM	Trap Rock-Dolomite		0	0.45	0.34	54.6	
	Fine-B2-50	6742	Lab	Fine DGM	Trap Rock-Dolomite		2000	na	0.52		0.26
	Fine-B2-50	6742	Lab	Fine DGM	Trap Rock-Dolomite		30000	na	0.39		0.21
	Fine-B2-50	6742	Lab	Fine DGM	Trap Rock-Dolomite		100000	0.44	0.40	54.0	0.22
	Fine-B2-75	6742	Lab	Fine DGM	Dolomite-Trap Rock		0	0.51	0.36	59.8	
	Fine-B2-75	6742	Lab	Fine DGM	Dolomite-Trap Rock		2000	na	0.51		0.27
	Fine-B2-75	6742	Lab	Fine DGM	Dolomite-Trap Rock		30000	na	0.36		0.22
	Fine-B2-75	6742	Lab	Fine DGM	Dolomite-Trap Rock		100000	0.60	0.37	67.7	0.23
	Fine-B2-100	6742	Lab	Fine DGM	Dolomite		0	0.61	0.44	69.1	
	Fine-B2-100	6742	Lab	Fine DGM	Dolomite		2000	na	0.49		0.28
	Fine-B2-100	6742	Lab	Fine DGM	Dolomite		30000	na	0.33		0.21
	Fine-B2-100	6742	Lab	Fine DGM	Dolomite		100000	0.60	0.28	68.0	0.19
	Fine-B3-25	6742	Lab	Fine DGM	Trap Rock-Limestone		0	0.61	0.39	68.9	
	Fine-B3-25	6742	Lab	Fine DGM	Trap Rock-Limestone		2000	na	0.53		0.30
	Fine-B3-25	6742	Lab	Fine DGM	Trap Rock-Limestone		30000	na	0.48		0.29
	Fine-B3-25	6742	Lab	Fine DGM	Trap Rock-Limestone		100000	0.68	0.41	74.9	0.26
	Fine-B3-50	6742	Lab	Fine DGM	Trap Rock-Limestone		0	0.55	0.51	63.5	
	Fine-B3-50	6742	Lab	Fine DGM	Trap Rock-Limestone		2000	na	0.53		0.29
	Fine-B3-50	6742	Lab	Fine DGM	Trap Rock-Limestone		30000	na	0.42		0.25
	Fine-B3-50	6742	Lab	Fine DGM	Trap Rock-Limestone		100000	0.58	0.34	66.0	0.21
	Fine-B3-75	6742	Lab	Fine DGM	Limestone-Trap Rock		0	0.70	0.43	77.0	
	Fine-B3-75	6742	Lab	Fine DGM	Limestone-Trap Rock		2000	na	0.45		0.28
	Fine-B3-75	6742	Lab	Fine DGM	Limestone-Trap Rock		30000	na	0.43		0.26
	Fine-B3-75	6742	Lab	Fine DGM	Limestone-Trap Rock		100000	0.60	0.38	68.0	0.23
	Fine-B3-100	6742	Lab	Fine DGM	Limestone		0	0.40	0.33	49.7	
	Fine-B3-100	6742	Lab	Fine DGM	Limestone		2000	na	0.48		0.24
	Fine-B3-100	6742	Lab	Fine DGM	Limestone		30000	na	0.39		0.24
	Fine-B3-100	6742	Lab	Fine DGM	Limestone		100000	0.62	0.31	70.1	0.21
	Coarse-A-100	6742	Lab	Fine SMA	Trap Rock		0	1.36	0.27	136.0	
	Coarse-A-100	6742	Lab	Fine SMA	Trap Rock		2000	na	0.52		0.37
	Coarse-A-100	6742	Lab	Fine SMA	Trap Rock		30000	na	0.47		0.32
	Coarse-A-100	6742	Lab	Fine SMA	Trap Rock		100000	1.19	0.36	120.6	0.26
	Coarse-B3-25	6742	Lab	Fine SMA	Trap Rock-Limestone		0	1.26	0.37	127.2	
	Coarse-B3-25	6742	Lab	Fine SMA	Trap Rock-Limestone		2000	na	0.49		0.35
	Coarse-B3-25	6742	Lab	Fine SMA	Trap Rock-Limestone		30000	na	0.41		0.29
	Coarse-B3-25	6742	Lab	Fine SMA	Trap Rock-Limestone		100000	1.17	0.34	119.1	0.25
	Coarse-B3-50	6742	Lab	Fine SMA	Trap Rock-Limestone		0	1.12	0.42	115.0	

	Coarse-B3-50	6742	Lab	Fine SMA	Trap Rock-Limestone		2000	na	0.49		0.34
	Coarse-B3-50	6742	Lab	Fine SMA	Trap Rock-Limestone		30000	na	0.36		0.26
	Coarse-B3-50	6742	Lab	Fine SMA	Trap Rock-Limestone		100000	1.00	0.32	104.2	0.24
	Coarse-B3-75	6742	Lab	Fine SMA	Limestone-Trap Rock		0	1.15	0.45	117.4	
	Coarse-B3-75	6742	Lab	Fine SMA	Limestone-Trap Rock		2000	na	0.46		0.32
	Coarse-B3-75	6742	Lab	Fine SMA	Limestone-Trap Rock		30000	na	0.32		0.23
	Coarse-B3-75	6742	Lab	Fine SMA	Limestone-Trap Rock		100000	0.94	0.26	98.5	0.21
	Coarse-B3-100	6742	Lab	Fine SMA	Limestone		0	0.95	0.42	99.2	
	Coarse-B3-100	6742	Lab	Fine SMA	Limestone		2000	na	0.42		0.30
	Coarse-B3-100	6742	Lab	Fine SMA	Limestone		30000	na	0.27		0.21
	Coarse-B3-100	6742	Lab	Fine SMA	Limestone		100000	0.82	0.28	87.8	0.21
	Coarse-B1-25	6742	Lab	Fine SMA	Trap Rock-Dolomite		0	1.03	0.41	106.9	
	Coarse-B1-25	6742	Lab	Fine SMA	Trap Rock-Dolomite		2000	na	0.48		0.33
	Coarse-B1-25	6742	Lab	Fine SMA	Trap Rock-Dolomite		30000	na	0.42		0.29
	Coarse-B1-25	6742	Lab	Fine SMA	Trap Rock-Dolomite		100000	1.00	0.34	103.9	0.25
	Coarse-B1-50	6742	Lab	Fine SMA	Trap Rock-Dolomite		0	0.89	0.46	94.2	
	Coarse-B1-50	6742	Lab	Fine SMA	Trap Rock-Dolomite		2000	na	0.46		0.31
	Coarse-B1-50	6742	Lab	Fine SMA	Trap Rock-Dolomite		30000	na	0.38		0.26
	Coarse-B1-50	6742	Lab	Fine SMA	Trap Rock-Dolomite		100000	0.88	0.33	92.8	0.24
	Coarse-B1-75	6742	Lab	Fine SMA	Dolomite-Trap Rock		0	1.20	0.41	122.0	
	Coarse-B1-75	6742	Lab	Fine SMA	Dolomite-Trap Rock		2000	na	0.45		0.32
	Coarse-B1-75	6742	Lab	Fine SMA	Dolomite-Trap Rock		30000	na	0.35		0.26
	Coarse-B1-75	6742	Lab	Fine SMA	Dolomite-Trap Rock		100000	1.15	0.34	117.7	0.25
	Coarse-B1-100	6742	Lab	Fine SMA	Dolomite		0	1.04	0.39	107.7	
	Coarse-B1-100	6742	Lab	Fine SMA	Dolomite		2000	na	0.43		0.30
	Coarse-B1-100	6742	Lab	Fine SMA	Dolomite		30000	na	0.34		0.24
	Coarse-B1-100	6742	Lab	Fine SMA	Dolomite		100000	0.94	0.29	98.2	0.22
	Coarse-B2-25	6742	Lab	Fine SMA	Trap Rock-Dolomite		0	1.18	0.39	120.4	
	Coarse-B2-25	6742	Lab	Fine SMA	Trap Rock-Dolomite		2000	na	0.48		0.33
	Coarse-B2-25	6742	Lab	Fine SMA	Trap Rock-Dolomite		30000	na	0.43		0.28
	Coarse-B2-25	6742	Lab	Fine SMA	Trap Rock-Dolomite		100000	0.96	0.31	100.0	0.23
	Coarse-B2-50	6742	Lab	Fine SMA	Trap Rock-Dolomite		0	1.08	0.39	111.3	
	Coarse-B2-50	6742	Lab	Fine SMA	Trap Rock-Dolomite		2000	na	0.48		0.33
	Coarse-B2-50	6742	Lab	Fine SMA	Trap Rock-Dolomite		30000	na	0.38		0.25
	Coarse-B2-50	6742	Lab	Fine SMA	Trap Rock-Dolomite		100000	0.86	0.28	91.0	0.21
	Coarse-B2-75	6742	Lab	Fine SMA	Dolomite-Trap Rock		0	1.10	0.36	112.9	
	Coarse-B2-75	6742	Lab	Fine SMA	Dolomite-Trap Rock		2000	na	0.47		0.32
	Coarse-B2-75	6742	Lab	Fine SMA	Dolomite-Trap Rock		30000	na	0.34		0.25
	Coarse-B2-75	6742	Lab	Fine SMA	Dolomite-Trap Rock		100000	1.02	0.28	106.0	0.22
	Coarse-B2-100	6742	Lab	Fine SMA	Dolomite		0	0.85	0.36	90.1	
	Coarse-B2-100	6742	Lab	Fine SMA	Dolomite		2000	na	0.43		0.30
	Coarse-B2-100	6742	Lab	Fine SMA	Dolomite		30000	na	0.38		0.25
	Coarse-B2-100	6742	Lab	Fine SMA	Dolomite		100000	0.82	0.26	87.8	0.20

	Coarse-B4-25	6742	Lab	Fine SMA	Trap Rock-Limestone		0	1.10	0.40	113.0	
	Coarse-B4-25	6742	Lab	Fine SMA	Trap Rock-Limestone		2000	na	0.47		0.33
	Coarse-B4-25	6742	Lab	Fine SMA	Trap Rock-Limestone		30000	na	0.39		0.28
	Coarse-B4-25	6742	Lab	Fine SMA	Trap Rock-Limestone		100000	1.06	0.37	109.0	0.27
	Coarse-B4-50	6742	Lab	Fine SMA	Trap Rock-Limestone		0	0.92	0.49	96.7	
	Coarse-B4-50	6742	Lab	Fine SMA	Trap Rock-Limestone		2000	na	0.48		0.32
	Coarse-B4-50	6742	Lab	Fine SMA	Trap Rock-Limestone		30000	na	0.39		0.27
	Coarse-B4-50	6742	Lab	Fine SMA	Trap Rock-Limestone		100000	0.85	0.34	90.7	0.24
	Coarse-B4-75	6742	Lab	Fine SMA	Limestone-Trap Rock		0	0.96	0.40	100.7	
	Coarse-B4-75	6742	Lab	Fine SMA	Limestone-Trap Rock		2000	na	0.46		0.31
	Coarse-B4-75	6742	Lab	Fine SMA	Limestone-Trap Rock		30000	na	0.33	#VALUE!	0.24
	Coarse-B4-75	6742	Lab	Fine SMA	Limestone-Trap Rock		100000	1.00	0.32	104.2	0.24
	Coarse-B4-100	6742	Lab	Fine SMA	Limestone		0	1.07	0.42	110.5	
	Coarse-B4-100	6742	Lab	Fine SMA	Limestone		2000	na	0.42		0.30
	Coarse-B4-100	6742	Lab	Fine SMA	Limestone		30000	na	0.32		0.23
	Coarse-B4-100	6742	Lab	Fine SMA	Limestone		100000	1.00	0.30	104.2	0.23
	PadreCanyon	Firestone	Lab	Type D	Granite		2000	0.98	0.62	102.1	0.39
	PadreCanyon	Firestone	Lab	Type D	Granite		2000	1.00	0.61	103.9	0.38
	PadreCanyon	Firestone	Lab	Type D	Granite		2000	1.07	0.60	110.2	0.39
	PadreCanyon	Firestone	Lab	Type D	Granite		30000	0.98	0.51	102.1	0.33
	PadreCanyon	Firestone	Lab	Type D	Granite		30000	1.06	0.52	109.3	0.34
	PadreCanyon	Firestone	Lab	Type D	Granite		30000	1.04	0.51	107.5	0.34
	PadreCanyon	Firestone	Lab	Type D	Granite		80000	0.96	0.52	100.6	0.34
	PadreCanyon	Firestone	Lab	Type D	Granite		80000	1.04	0.52	107.1	0.34
	PadreCanyon	Firestone	Lab	Type D	Granite		80000		0.52	14.2	0.10
	Vado	Firestone	Lab	Type D	Rhyolite		2000	0.84	0.65	89.5	0.38
	Vado	Firestone	Lab	Type D	Rhyolite		2000	0.85	0.62	90.4	0.37
	Vado	Firestone	Lab	Type D	Rhyolite		2000	0.84	0.63	89.5	0.37
	Vado	Firestone	Lab	Type D	Rhyolite		30000	0.88	0.57	93.1	0.35
	Vado	Firestone	Lab	Type D	Rhyolite		30000	0.88	0.55	93.1	0.34
	Vado	Firestone	Lab	Type D	Rhyolite		30000	0.83	0.55	88.7	0.34
	Vado	Firestone	Lab	Type D	Rhyolite		80000	0.83	0.56	88.6	0.34
	Vado	Firestone	Lab	Type D	Rhyolite		80000	0.83	0.55	88.6	0.34
	Vado	Firestone	Lab	Type D	Rhyolite		80000	0.89	0.54	93.7	0.34
	Sawyer	Firestone	Lab	Type D	Sandstone		2000	0.69	0.63	76.1	0.36
	Sawyer	Firestone	Lab	Type D	Sandstone		2000	0.72	0.65	78.8	0.37
	Sawyer	Firestone	Lab	Type D	Sandstone		2000	0.70	0.63	77.0	0.36
	Sawyer	Firestone	Lab	Type D	Sandstone		30000	0.65	0.61	72.5	0.34
	Sawyer	Firestone	Lab	Type D	Sandstone		30000	0.73	0.60	79.7	0.35
	Sawyer	Firestone	Lab	Type D	Sandstone		30000	0.62	0.60	69.8	0.33
	Sawyer	Firestone	Lab	Type D	Sandstone		80000	0.65	0.52	72.7	0.30
	Sawyer	Firestone	Lab	Type D	Sandstone		80000	0.66	0.52	73.3	0.30
	Sawyer	Firestone	Lab	Type D	Sandstone		80000	0.63	0.52	70.4	0.30

	Knippa	Firestone	Lab	Type D	Trap Rock		2000	0.72	0.68	78.8	0.38
	Knippa	Firestone	Lab	Type D	Trap Rock		2000	0.75	0.67	81.5	0.38
	Knippa	Firestone	Lab	Type D	Trap Rock		2000	0.75	0.66	81.5	0.38
	Knippa	Firestone	Lab	Type D	Trap Rock		30000	0.82	0.59	87.8	0.35
	Knippa	Firestone	Lab	Type D	Trap Rock		30000	0.77	0.58	83.3	0.35
	Knippa	Firestone	Lab	Type D	Trap Rock		30000	0.77	0.59	83.3	0.35
	Knippa	Firestone	Lab	Type D	Trap Rock		80000	0.87	0.57	92.0	0.35
	Knippa	Firestone	Lab	Type D	Trap Rock		80000	0.94	0.57	98.1	0.36
	Knippa	Firestone	Lab	Type D	Trap Rock		80000	0.89	0.55	94.1	0.34
	Jones Mill	Firestone	Lab	Type D	Quartzite		2000	0.61	0.59	68.9	0.32
	Jones Mill	Firestone	Lab	Type D	Quartzite		2000	0.58	0.57	66.2	0.31
	Jones Mill	Firestone	Lab	Type D	Quartzite		2000	0.58	0.57	66.2	0.31
	Jones Mill	Firestone	Lab	Type D	Quartzite		30000	0.58	0.51	66.2	0.29
	Jones Mill	Firestone	Lab	Type D	Quartzite		30000	0.55	0.49	63.5	0.27
	Jones Mill	Firestone	Lab	Type D	Quartzite		30000	0.51	0.51	59.9	0.27
	Jones Mill	Firestone	Lab	Type D	Quartzite		80000	0.61	0.49	69.3	0.28
	Jones Mill	Firestone	Lab	Type D	Quartzite		80000	0.60	0.49	68.2	0.28
	Jones Mill	Firestone	Lab	Type D	Quartzite		80000	0.57	0.49	65.3	0.28
	BSJ	Firestone	Lab	Type D	Igneous		2000	0.52	0.60	60.8	0.31
	BSJ	Firestone	Lab	Type D	Igneous		2000	0.56	0.57	64.4	0.31
	BSJ	Firestone	Lab	Type D	Igneous		2000	0.55	0.59	63.5	0.31
	BSJ	Firestone	Lab	Type D	Igneous		30000	0.55	0.58	63.5	0.31
	BSJ	Firestone	Lab	Type D	Igneous		30000	0.55	0.55	65.3	0.30
	BSJ	Firestone	Lab	Type D	Igneous		30000	0.57	0.55	65.3	0.30
	BSJ	Firestone	Lab	Type D	Igneous		30000	0.53	0.57	61.7	0.30
	BSJ	Firestone	Lab	Type D	Igneous		80000	0.56	0.51	64.0	0.28
	BSJ	Firestone	Lab	Type D	Igneous		80000	0.58	0.52	66.5	0.29
	BSJ	Firestone	Lab	Type D	Igneous		80000	0.57	0.52	65.7	0.29
81	Seal Coat-SH 36-Austin-Yoakum	Arif	Field		Limestone	402		0.74	0.39	80.6	0.25
81	Seal Coat-SH 36-Austin-Yoakum	Arif	Field		Limestone	402		0.77	0.40	83.3	0.26
81	Seal Coat-SH 36-Austin-Yoakum	Arif	Field		Limestone	402		0.7	0.37	77.0	0.24
81	Seal Coat-SH 36-Austin-Yoakum	Arif	Field		Limestone	402		0.65	0.49	72.5	0.29
81	Seal Coat-SH 36-Austin-Yoakum	Arif	Field		Limestone	402		0.65	0.50	72.5	0.29
18	HMA-IH 10-Jefferson-Beaumont	Arif	Field		Granite + ?	1552		0.77	0.42	83.3	0.27
21	HMA-Loop 207-Chambers-Beaumont	Arif	Field		Sandstone + Limestone	154		0.67	0.50	74.3	0.29
20	HMA-SH 82-Jefferson-Beaumont	Arif	Field		Granite + ?	182		0.5	0.52	59.1	0.27
64	PFC-US 69-Jefferson-Beaumont	Arif	Field		Granite + Limestone	760		1.63	0.61	160.4	0.43
19	HMA-US 90-Jefferson-Beaumont	Arif	Field		Sandstone + Limestone	152		1.02	0.53	105.7	0.35
18	HMA-IH 10-Jefferson-Beaumont	Arif	Field		Granite + ?	1552		0.97	0.40	101.2	0.28
21	HMA-Loop 207-Chambers-Beaumont	Arif	Field		Sandstone + Limestone	154		0.69	0.54	76.1	0.31
20	HMA-SH 82-Jefferson-Beaumont	Arif	Field		Granite + ?	182		0.59	0.52	67.1	0.29
64	PFC-US 69-Jefferson-Beaumont	Arif	Field		Granite + Limestone	760		1.7	0.40	166.7	0.31
19	HMA-US 90-Jefferson-Beaumont	Arif	Field		Sandstone + Limestone	152		0.98	0.54	102.1	0.35
25	HMA-IH 30-Bowie-Atlanta	Arif	Field		Sandstone + Gravel	1268		0.61	0.73	68.9	0.38

25	HMA-IH 30-Bowie-Atlanta	Arif	Field		Sandstone + Gravel	1268		0.68	0.73	75.2	0.39
25	HMA-IH 30-Bowie-Atlanta	Arif	Field		Sandstone + Gravel	1268		0.71	0.73	77.9	0.40
25	HMA-IH 30-Bowie-Atlanta	Arif	Field		Sandstone + Gravel	1268		0.71	0.73	77.9	0.40
25	HMA-IH 30-Bowie-Atlanta	Arif	Field		Sandstone + Gravel	1268		0.66	0.78	73.4	0.41
25	HMA-IH 30-Bowie-Atlanta	Arif	Field		Sandstone + Gravel	1268		0.79	0.78	85.1	0.44
1	HMA-US 77-Kennedy-Pharr	Arif	Field		Gravel	384		0.73	0.47	79.7	0.29
1	HMA-US 77-Kennedy-Pharr	Arif	Field		Gravel	384		0.69	0.46	76.1	0.28
1	HMA-US 77-Kennedy-Pharr	Arif	Field		Gravel	384		0.73	0.45	79.7	0.28
1	HMA-US 77-Kennedy-Pharr	Arif	Field		Gravel	384		0.33	0.62	43.8	0.26
1	HMA-US 77-Kennedy-Pharr	Arif	Field		Gravel	384		0.34	0.61	44.7	0.26
2	HMA-US 281-Hidalgo-Pharr	Arif	Field		Gravel	934		0.7	0.44	77.0	0.27
2	HMA-US 281-Hidalgo-Pharr	Arif	Field		Gravel	934		0.69	0.43	76.1	0.27
2	HMA-US 281-Hidalgo-Pharr	Arif	Field		Gravel	934		0.73	0.43	79.7	0.27
2	HMA-US 281-Hidalgo-Pharr	Arif	Field		Gravel	934		0.33	0.57	43.8	0.25
2	HMA-US 281-Hidalgo-Pharr	Arif	Field		Gravel	934		0.34	0.54	44.7	0.24
27	HMA-US 271-Camp-Atlanta	Arif	Field		Siliceous Gravel	2028		0.81	0.71	86.9	0.41
27	HMA-US 271-Camp-Atlanta	Arif	Field		Siliceous Gravel	2028		0.73	0.71	79.7	0.40
27	HMA-US 271-Camp-Atlanta	Arif	Field		Siliceous Gravel	2028		0.77	0.73	83.3	0.41
27	HMA-US 271-Camp-Atlanta	Arif	Field		Siliceous Gravel	2028		0.71	0.76	77.9	0.41
27	HMA-US 271-Camp-Atlanta	Arif	Field		Siliceous Gravel	2028		0.7	0.73	77.0	0.40
27	HMA-US 271-Camp-Atlanta	Arif	Field		Siliceous Gravel	2028		0.66	0.77	73.4	0.41
27	HMA-US 271-Camp-Atlanta	Arif	Field		Siliceous Gravel	2028		0.52	0.85	60.8	0.40
11	HMA-IH 35-Webb-Laredo	Arif	Field		Traprock + Gravel	1879		1.2	0.43	121.8	0.31
11	HMA-IH 35-Webb-Laredo	Arif	Field		Traprock + Gravel	1879		1.1	0.44	112.9	0.31
11	HMA-IH 35-Webb-Laredo	Arif	Field		Traprock + Gravel	1879		1.25	0.40	126.3	0.29
11	HMA-IH 35-Webb-Laredo	Arif	Field		Traprock + Gravel	1879		0.83	0.62	88.7	0.37
11	HMA-IH 35-Webb-Laredo	Arif	Field		Traprock + Gravel	1879		0.98	0.63	102.1	0.39
10	HMA-SH 7-Houston-Lufkin	Arif	Field		Granite + Limestone	107		0.62	0.63	69.8	0.34
10	HMA-SH 7-Houston-Lufkin	Arif	Field		Granite + Limestone	107		0.6	0.00	68.0	0.08
10	HMA-SH 7-Houston-Lufkin	Arif	Field		Granite + Limestone	107		0.61	0.61	68.9	0.33
10	HMA-SH 7-Houston-Lufkin	Arif	Field		Granite + Limestone	107		0.55	0.59	63.5	0.31
10	HMA-SH 7-Houston-Lufkin	Arif	Field		Granite + Limestone	107		0.66	0.74	73.4	0.40
10	HMA-SH 7-Houston-Lufkin	Arif	Field		Granite + Limestone	107		0.8	0.76	86.0	0.43
8	HMA-IH 10-Austin-Yoakum	Arif	Field		Dolomite-Limestone	692		0.45	0.40	54.6	0.22
8	HMA-IH 10-Austin-Yoakum	Arif	Field		Dolomite-Limestone	692		0.45	0.41	54.6	0.23
8	HMA-IH 10-Austin-Yoakum	Arif	Field		Dolomite-Limestone	692		0.36	0.40	46.5	0.20
8	HMA-IH 10-Austin-Yoakum	Arif	Field		Dolomite-Limestone	692		0.39	0.41	49.2	0.21
8	HMA-IH 10-Austin-Yoakum	Arif	Field		Dolomite-Limestone	692		0.71	0.59	77.9	0.34
8	HMA-IH 10-Austin-Yoakum	Arif	Field		Dolomite-Limestone	692		0.64	0.64	71.6	0.35
9	HMA-SH 36-Austin-Yoakum	Arif	Field		Limestone	2518		0.63	0.29	70.7	0.20
9	HMA-SH 36-Austin-Yoakum	Arif	Field		Limestone	2518		0.69	0.33	76.1	0.22
9	HMA-SH 36-Austin-Yoakum	Arif	Field		Limestone	2518		0.59	0.30	67.1	0.20
9	HMA-SH 36-Austin-Yoakum	Arif	Field		Limestone	2518		0.56	0.29	64.4	0.20

9	HMA-SH 36-Austin-Yoakum	Arif	Field		Limestone	2518		0.56	0.61	64.4	0.32
9	HMA-SH 36-Austin-Yoakum	Arif	Field		Limestone	2518		0.54	0.63	62.6	0.32
7	HMA-IH 45-Leon-Bryan	Arif	Field		Sandstone + Silliceous River Gravel + Limestone	2229		1	0.34	103.9	0.25
7	HMA-IH 45-Leon-Bryan	Arif	Field		Sandstone + Silliceous River Gravel + Limestone	2229		0.91	0.34	95.8	0.24
7	HMA-IH 45-Leon-Bryan	Arif	Field		Sandstone + Silliceous River Gravel + Limestone	2229		0.97	0.37	101.2	0.26
7	HMA-IH 45-Leon-Bryan	Arif	Field		Sandstone + Silliceous River Gravel + Limestone	2229		0.86	0.33	91.3	0.24
61	PFC-I 45-NA-Bryan	Arif	Field		Limestone	1872		1.3	0.35	130.8	0.27
61	PFC-I 45-NA-Bryan	Arif	Field		Limestone	1872		1.21	0.33	122.7	0.26
61	PFC-I 45-NA-Bryan	Arif	Field		Limestone	1872		1.59	0.41	156.8	0.31
61	PFC-I 45-NA-Bryan	Arif	Field		Limestone	1872		1.59	0.39	156.8	0.30
62	PFC-SH 6-New-Bryan	Arif	Field		Sandstone/Limestone	1100		1.8	0.31	175.7	0.26
62	PFC-SH 6-New-Bryan	Arif	Field		Sandstone/Limestone	1100		1.53	0.29	151.4	0.24
62	PFC-SH 6-New-Bryan	Arif	Field		Sandstone/Limestone	1100		2.14	0.37	206.2	0.30
62	PFC-SH 6-New-Bryan	Arif	Field		Sandstone/Limestone	1100		1.85	0.33	180.1	0.27
63	PFC-SH 6-Old-Bryan	Arif	Field		Sandstone/Limestone	2660		1.54	0.36	152.3	0.28
63	PFC-SH 6-Old-Bryan	Arif	Field		Sandstone/Limestone	2660		1.71	0.35	167.6	0.28
63	PFC-SH 6-Old-Bryan	Arif	Field		Sandstone/Limestone	2660		1.89	0.45	183.7	0.35
63	PFC-SH 6-Old-Bryan	Arif	Field		Sandstone/Limestone	2660		1.87	0.44	181.9	0.34
92	Seal Coat-FM 105-Orange-Beaumont	Arif	Field		Lightweight	93		2.38	0.93	227.7	0.65
92	Seal Coat-FM 105-Orange-Beaumont	Arif	Field		Lightweight	93		2.42	0.84	231.3	0.60
92	Seal Coat-FM 105-Orange-Beaumont	Arif	Field		Lightweight	93		2.46	0.91	234.9	0.64
92	Seal Coat-FM 105-Orange-Beaumont	Arif	Field		Lightweight	93		2.42	0.84	231.3	0.60
90	Seal Coat-SH 82-Jefferson-Beaumont	Arif	Field		Lightweight	1126		1.18	0.98	120.0	0.60
90	Seal Coat-SH 82-Jefferson-Beaumont	Arif	Field		Lightweight	1126		1.2	0.98	121.8	0.60
90	Seal Coat-SH 82-Jefferson-Beaumont	Arif	Field		Lightweight	1126		2.28	0.90	218.7	0.63
90	Seal Coat-SH 82-Jefferson-Beaumont	Arif	Field		Lightweight	1126		2.1	0.93	202.6	0.64
91	Seal Coat-FM 365-Jefferson-Beaumont	Arif	Field		Lightweight	92		2.62	0.88	249.2	0.63
91	Seal Coat-FM 365-Jefferson-Beaumont	Arif	Field		Lightweight	92		2.54	0.00	242.0	0.08
91	Seal Coat-FM 365-Jefferson-Beaumont	Arif	Field		Lightweight	92		2.61	0.83	248.3	0.60
91	Seal Coat-FM 365-Jefferson-Beaumont	Arif	Field		Lightweight	92		2.42	0.87	231.3	0.62
91	Seal Coat-FM 365-Jefferson-Beaumont	Arif	Field		Lightweight	92		3.12	0.42	294.1	0.35
91	Seal Coat-FM 365-Jefferson-Beaumont	Arif	Field		Lightweight	92		3	0.80	283.3	0.59
87	Seal Coat-LP 338-Ector-Odessa	Arif	Field		Rhyollite	493		0.81	0.44	86.9	0.28
87	Seal Coat-LP 338-Ector-Odessa	Arif	Field		Rhyollite	493		0.94	0.50	98.5	0.32
87	Seal Coat-LP 338-Ector-Odessa	Arif	Field		Rhyollite	493		0.96	0.50	100.3	0.33
87	Seal Coat-LP 338-Ector-Odessa	Arif	Field		Rhyollite	493		1.72	0.55	168.5	0.40
87	Seal Coat-LP 338-Ector-Odessa	Arif	Field		Rhyollite	493		1.96	0.56	190.0	0.41
88	Seal Coat-US 385-Crane-Odessa	Arif	Field		Limestone	1589		1.55	0.35	153.2	0.28
88	Seal Coat-US 385-Crane-Odessa	Arif	Field		Limestone	1589		1.53	0.35	151.4	0.28
88	Seal Coat-US 385-Crane-Odessa	Arif	Field		Limestone	1589		2.14	0.45	206.2	0.35
88	Seal Coat-US 385-Crane-Odessa	Arif	Field		Limestone	1589		2.26	0.43	216.9	0.34
88	Seal Coat-US 385-Crane-Odessa	Arif	Field		Limestone	1589		2.97	0.64	280.6	0.49
89	Seal Coat-US 385-Ector-Odessa	Arif	Field		Limestone	1224		0.72	0.20	78.8	0.17

89	Seal Coat-US 385-Ector-Odessa	Arif	Field		Limestone	1224		0.96	0.26	100.3	0.21
89	Seal Coat-US 385-Ector-Odessa	Arif	Field		Limestone	1224		0.83	0.25	88.7	0.20
89	Seal Coat-US 385-Ector-Odessa	Arif	Field		Limestone	1224		1.51	0.35	149.6	0.28
89	Seal Coat-US 385-Ector-Odessa	Arif	Field		Limestone	1224		1.56	0.34	154.1	0.27
93	Seal Coat-US 80-Harrison-Atlanta	Arif	Field		Lightweight	566		2.03	0.98	196.3	0.67
93	Seal Coat-US 80-Harrison-Atlanta	Arif	Field		Lightweight	566		1.9	0.97	184.6	0.65
93	Seal Coat-US 80-Harrison-Atlanta	Arif	Field		Lightweight	566		1.9	0.99	184.6	0.66
93	Seal Coat-US 80-Harrison-Atlanta	Arif	Field		Lightweight	566		2.49	0.97	237.6	0.68
93	Seal Coat-US 80-Harrison-Atlanta	Arif	Field		Lightweight	566		2.61	0.98	248.3	0.69
95	Seal Coat-US 59-Cass-Atlanta	Arif	Field		Gravel	201		1.8	0.56	175.7	0.41
95	Seal Coat-US 59-Cass-Atlanta	Arif	Field		Gravel	201		2.03	0.60	196.3	0.44
95	Seal Coat-US 59-Cass-Atlanta	Arif	Field		Gravel	201		1.9	0.57	184.6	0.42
95	Seal Coat-US 59-Cass-Atlanta	Arif	Field		Gravel	201		3.13	0.79	295.0	0.59
95	Seal Coat-US 59-Cass-Atlanta	Arif	Field		Gravel	201		3.38	0.73	317.4	0.55
66	Seal Coat-US 77-Cameron-Pharr	Arif	Field		Limestone	295		1.9	0.31	184.6	0.26
66	Seal Coat-US 77-Cameron-Pharr	Arif	Field		Limestone	295		2.27	0.28	217.8	0.25
66	Seal Coat-US 77-Cameron-Pharr	Arif	Field		Limestone	295		2	0.29	193.6	0.25
66	Seal Coat-US 77-Cameron-Pharr	Arif	Field		Limestone	295		1.79	0.30	174.8	0.26
66	Seal Coat-US 77-Cameron-Pharr	Arif	Field		Limestone	295		2.42	0.31	231.3	0.27
66	Seal Coat-US 77-Cameron-Pharr	Arif	Field		Limestone	295		2.27	0.36	217.8	0.30
67	Seal Coat-US 281-Hidalgo-Pharr	Arif	Field		Limestone	1027		0.62	0.28	69.8	0.20
67	Seal Coat-US 281-Hidalgo-Pharr	Arif	Field		Limestone	1027		1.57	0.30	155.0	0.25
67	Seal Coat-US 281-Hidalgo-Pharr	Arif	Field		Limestone	1027		0.7	0.33	77.0	0.22
67	Seal Coat-US 281-Hidalgo-Pharr	Arif	Field		Limestone	1027		2.33	0.58	223.2	0.44
67	Seal Coat-US 281-Hidalgo-Pharr	Arif	Field		Limestone	1027		2.37	0.58	226.8	0.44
77	Seal Coat-US 90/IH 10-Bexar-San Antonio	Arif	Field		Limestone	283		2.48	0.39	236.7	0.32
77	Seal Coat-US 90/IH 10-Bexar-San Antonio	Arif	Field		Limestone	283		2.25	0.34	216.0	0.29
77	Seal Coat-US 90/IH 10-Bexar-San Antonio	Arif	Field		Limestone	283		3	0.41	283.3	0.34
77	Seal Coat-US 90/IH 10-Bexar-San Antonio	Arif	Field		Limestone	283		2.37	0.43	226.8	0.34
78	Seal Coat-FM 1518-Bexar-San Antonio	Arif	Field		Sandstone	283		2.31	0.69	221.4	0.50
78	Seal Coat-FM 1518-Bexar-San Antonio	Arif	Field		Sandstone	283		2.04	0.66	197.2	0.48
78	Seal Coat-FM 1518-Bexar-San Antonio	Arif	Field		Sandstone	283		2.81	0.75	266.3	0.55
79	Seal Coat-SH 16-Atascosa-San Antonio-A	Arif	Field		Traprock	649		1.29	0.53	129.9	0.37
79	Seal Coat-SH 16-Atascosa-San Antonio-A	Arif	Field		Traprock	649		1.73	0.53	169.4	0.39
79	Seal Coat-SH 16-Atascosa-San Antonio-A	Arif	Field		Traprock	649		2.72	0.65	258.2	0.49
79	Seal Coat-SH 16-Atascosa-San Antonio-A	Arif	Field		Traprock	649		2.82	0.61	267.2	0.47
80	Seal Coat-SH 16-Atascosa-San Antonio-B	Arif	Field		Limestone? Trap Rock?	649		1.05	0.56	108.4	0.36
80	Seal Coat-SH 16-Atascosa-San Antonio-B	Arif	Field		Limestone? Trap Rock?	649		1.22	0.57	123.6	0.38
80	Seal Coat-SH 16-Atascosa-San Antonio-B	Arif	Field		Limestone? Trap Rock?	649		2.49	0.69	237.6	0.51
80	Seal Coat-SH 16-Atascosa-San Antonio-B	Arif	Field		Limestone? Trap Rock?	649		2.14	0.71	206.2	0.51
81	Seal Coat-SH 36-Austin-Yoakum	Arif	Field		Limestone	1756		1.37	0.44	137.1	0.32
81	Seal Coat-SH 36-Austin-Yoakum	Arif	Field		Limestone	1756		1.24	0.41	125.4	0.30
81	Seal Coat-SH 36-Austin-Yoakum	Arif	Field		Limestone	1756		3.48	0.74	326.4	0.56

73	Seal Coat-US 67-Coleman-Brownwood	Arif	Field		Limestone	1561		0.82	0.23	87.8	0.19
73	Seal Coat-US 67-Coleman-Brownwood	Arif	Field		Limestone	1561		0.71	0.19	77.9	0.16
73	Seal Coat-US 67-Coleman-Brownwood	Arif	Field		Limestone	1561		2.05	0.31	198.1	0.27
74	Seal Coat-US 67-Brown-Brownwood	Arif	Field		Limestone	1196		1.15	0.19	117.4	0.18
74	Seal Coat-US 67-Brown-Brownwood	Arif	Field		Limestone	1196		1.01	0.18	104.8	0.17
74	Seal Coat-US 67-Brown-Brownwood	Arif	Field		Limestone	1196		1.96	0.24	190.0	0.22
74	Seal Coat-US 67-Brown-Brownwood	Arif	Field		Limestone	1196		1.9	0.00	184.6	0.08
74	Seal Coat-US 67-Brown-Brownwood	Arif	Field		Limestone	1196		2.38	0.41	227.7	0.33
75	Seal Coat-US 183-Eastland-Brownwood	Arif	Field		Limestone	830		1.45	0.32	144.3	0.26
75	Seal Coat-US 183-Eastland-Brownwood	Arif	Field		Limestone	830		1.48	0.22	147.0	0.20
75	Seal Coat-US 183-Eastland-Brownwood	Arif	Field		Limestone	830		1.71	0.31	167.6	0.26
75	Seal Coat-US 183-Eastland-Brownwood	Arif	Field		Limestone	830		1.68	0.32	164.9	0.26
76	Seal Coat-US 377-Brown-Brownwood	Arif	Field		Limestone	830		1.89	0.22	183.7	0.21
76	Seal Coat-US 377-Brown-Brownwood	Arif	Field		Limestone	830		1.96	0.26	190.0	0.24
76	Seal Coat-US 377-Brown-Brownwood	Arif	Field		Limestone	830		2.68	0.00	254.6	0.08
70	Seal Coat-US 377-Hood-Dallas-FW	Arif	Field		Limestone	1601		2.49	0.24	237.6	0.23
70	Seal Coat-US 377-Hood-Dallas-FW	Arif	Field		Limestone	1601		2.9	0.59	274.3	0.45
70	Seal Coat-US 377-Hood-Dallas-FW	Arif	Field		Limestone	1601		3	0.00	283.3	0.08
71	Seal Coat-SH 199-Parker-Dallas-FW	Arif	Field		Limestone	1601		2.65	0.27	251.9	0.25
71	Seal Coat-SH 199-Parker-Dallas-FW	Arif	Field		Limestone	1601		2.14	0.25	206.2	0.23
71	Seal Coat-SH 199-Parker-Dallas-FW	Arif	Field		Limestone	1601		2.92	0.39	276.1	0.33
71	Seal Coat-SH 199-Parker-Dallas-FW	Arif	Field		Limestone	1601		2.69	0.30	255.5	0.27
72	Seal Coat-US 377-Tarrant-Dallas-FW	Arif	Field		Limestone	1236		2.23	0.22	214.2	0.21
72	Seal Coat-US 377-Tarrant-Dallas-FW	Arif	Field		Limestone	1236		0.48	0.16	57.3	0.14
72	Seal Coat-US 377-Tarrant-Dallas-FW	Arif	Field		Limestone	1236		2.38	0.24	227.7	0.23
72	Seal Coat-US 377-Tarrant-Dallas-FW	Arif	Field		Limestone	1236		3.21	0.00	302.1	0.08
72	Seal Coat-US 377-Tarrant-Dallas-FW	Arif	Field		Limestone	1236		3.41	0.51	320.1	0.41
82	Seal Coat-US 59-Angelina-Lufkin	Arif	Field		Traprock	1161		1.97	0.00	190.9	0.08
82	Seal Coat-US 59-Angelina-Lufkin	Arif	Field		Traprock	1161		2	0.31	193.6	0.27
82	Seal Coat-US 59-Angelina-Lufkin	Arif	Field		Traprock	1161		1.96	0.31	190.0	0.26
82	Seal Coat-US 59-Angelina-Lufkin	Arif	Field		Traprock	1161		1.93	0.31	187.3	0.26
82	Seal Coat-US 59-Angelina-Lufkin	Arif	Field		Traprock	1161		2.83	0.45	268.1	0.36
82	Seal Coat-US 59-Angelina-Lufkin	Arif	Field		Traprock	1161		2.53	0.56	241.1	0.43
83	Seal Coat-US 69-Angelina-Lufkin	Arif	Field		Lightweight	430		1.15	0.86	117.4	0.53
83	Seal Coat-US 69-Angelina-Lufkin	Arif	Field		Lightweight	430		1.12	0.87	114.7	0.53
83	Seal Coat-US 69-Angelina-Lufkin	Arif	Field		Lightweight	430		1.64	0.88	161.3	0.58
83	Seal Coat-US 69-Angelina-Lufkin	Arif	Field		Lightweight	430		1.74	0.89	170.3	0.60
83	Seal Coat-US 69-Angelina-Lufkin	Arif	Field		Lightweight	430		2.88	0.83	272.5	0.61
83	Seal Coat-US 69-Angelina-Lufkin	Arif	Field		Lightweight	430		3.33	0.83	312.9	0.62
84	Seal Coat-US 287-Trinity-Lufkin	Arif	Field		Lightweight	76		2.78	0.72	263.6	0.53
84	Seal Coat-US 287-Trinity-Lufkin	Arif	Field		Lightweight	76		2.82	0.00	267.2	0.08
84	Seal Coat-US 287-Trinity-Lufkin	Arif	Field		Lightweight	76		2.86	0.41	270.7	0.34
84	Seal Coat-US 287-Trinity-Lufkin	Arif	Field		Lightweight	76		3.09	0.71	291.4	0.53

84	Seal Coat-US 287-Trinity-Lufkin	Arif	Field		Lightweight	76		3.26	0.79	306.6	0.59
85	Seal Coat-FM 2213-San Augustine-Lufkin	Arif	Field		Lightweight	816		1.53	0.00	151.4	0.08
85	Seal Coat-FM 2213-San Augustine-Lufkin	Arif	Field		Lightweight	816		1.65	0.86	162.2	0.57
85	Seal Coat-FM 2213-San Augustine-Lufkin	Arif	Field		Lightweight	816		1.93	0.00	187.3	0.08
85	Seal Coat-FM 2213-San Augustine-Lufkin	Arif	Field		Lightweight	816		2.02	0.81	195.4	0.56
86	Seal Coat-US 59-Shelby-Lufkin	Arif	Field		Sandstone	816		1.62	0.59	159.5	0.42
86	Seal Coat-US 59-Shelby-Lufkin	Arif	Field		Sandstone	816		1.42	0.58	141.6	0.40
86	Seal Coat-US 59-Shelby-Lufkin	Arif	Field		Sandstone	816		1.43	0.55	142.5	0.39
86	Seal Coat-US 59-Shelby-Lufkin	Arif	Field		Sandstone	816		2.24	0.65	215.1	0.48
86	Seal Coat-US 59-Shelby-Lufkin	Arif	Field		Sandstone	816		2.2	0.66	211.5	0.48
15	HMA-IH 20-Midland-Odessa-A	Arif	Field		Rhyollite and LS (dolomite)	494		0.7	0.53	77.0	0.31
15	HMA-IH 20-Midland-Odessa-A	Arif	Field		Rhyollite and LS (dolomite)	494		0.73	0.52	79.7	0.31
15	HMA-IH 20-Midland-Odessa-A	Arif	Field		Rhyollite and LS (dolomite)	494		0.71	0.53	77.9	0.31
15	HMA-IH 20-Midland-Odessa-A	Arif	Field		Rhyollite and LS (dolomite)	494		0.8	0.73	86.0	0.42
15	HMA-IH 20-Midland-Odessa-A	Arif	Field		Rhyollite and LS (dolomite)	494		0.65	0.75	72.5	0.40
16	HMA-IH 20-Martin-Odessa	Arif	Field		Rhyollite and LS (dolomite)	402		0.74	0.39	80.6	0.25
16	HMA-IH 20-Martin-Odessa	Arif	Field		Rhyollite and LS (dolomite)	402		0.77	0.40	83.3	0.26
16	HMA-IH 20-Martin-Odessa	Arif	Field		Rhyollite and LS (dolomite)	402		0.7	0.37	77.0	0.24
16	HMA-IH 20-Martin-Odessa	Arif	Field		Rhyollite and LS (dolomite)	402		0.65	0.49	72.5	0.29
16	HMA-IH 20-Martin-Odessa	Arif	Field		Rhyollite and LS (dolomite)	402		0.65	0.50	72.5	0.29
17	HMA-IH 20-Midland-Odessa-B	Arif	Field		Rhyollite and LS (dolomite)	129		0.76	0.49	82.4	0.30
17	HMA-IH 20-Midland-Odessa-B	Arif	Field		Rhyollite and LS (dolomite)	129		0.66	0.48	73.4	0.28
17	HMA-IH 20-Midland-Odessa-B	Arif	Field		Rhyollite and LS (dolomite)	129		0.65	0.48	72.5	0.28
17	HMA-IH 20-Midland-Odessa-B	Arif	Field		Rhyollite and LS (dolomite)	129		0.82	0.61	87.8	0.36
17	HMA-IH 20-Midland-Odessa-B	Arif	Field		Rhyollite and LS (dolomite)	129		0.73	0.60	79.7	0.35
65	PFC-I 20-Martin-Odessa	Arif	Field		Rhyolite Gravel	3416		1.61	0.55	158.6	0.39
65	PFC-I 20-Martin-Odessa	Arif	Field		Rhyolite Gravel	3416		1.61	0.57	158.6	0.41
65	PFC-I 20-Martin-Odessa	Arif	Field		Rhyolite Gravel	3416		1.61	0.68	158.6	0.47
65	PFC-I 20-Martin-Odessa	Arif	Field		Rhyolite Gravel	3416		1.57	0.72	155.0	0.49
22	HMA-US 59-Panola-AtlantaS Carthage	Arif	Field		Quartzite	992		0.38	0.57	48.3	0.26
22	HMA-US 59-Panola-AtlantaS Carthage	Arif	Field		Quartzite	992		0.35	0.60	45.6	0.26
22	HMA-US 59-Panola-AtlantaS Carthage	Arif	Field		Quartzite	992		0.34	0.56	44.7	0.25
22	HMA-US 59-Panola-AtlantaS Carthage	Arif	Field		Quartzite	992		0.31	0.57	42.0	0.24
22	HMA-US 59-Panola-AtlantaS Carthage	Arif	Field		Quartzite	992		0.69	0.79	76.1	0.42
22	HMA-US 59-Panola-AtlantaS Carthage	Arif	Field		Quartzite	992		0.56	0.79	64.4	0.39
23	HMA-US 59-Panola-AtlantaN Carthage	Arif	Field		Quartzite	931		0.52	0.54	60.8	0.28
23	HMA-US 59-Panola-AtlantaN Carthage	Arif	Field		Quartzite	931		0.53	0.54	61.7	0.29
23	HMA-US 59-Panola-AtlantaN Carthage	Arif	Field		Quartzite	931		0.6	0.55	68.0	0.30
23	HMA-US 59-Panola-AtlantaN Carthage	Arif	Field		Quartzite	931		0.59	0.53	67.1	0.29
23	HMA-US 59-Panola-AtlantaN Carthage	Arif	Field		Quartzite	931		0.5	0.72	59.1	0.35
23	HMA-US 59-Panola-AtlantaN Carthage	Arif	Field		Quartzite	931		0.44	0.74	53.7	0.34
24	HMA-US 59-Panola-Atlanta	Arif	Field		Quartzite	3061		0.68	0.49	75.2	0.29
24	HMA-US 59-Panola-Atlanta	Arif	Field		Quartzite	3061		0.6	0.51	68.0	0.29

24	HMA-US 59-Panola-Atlanta	Arif	Field		Quartzite	3061		0.7	0.53	77.0	0.31
24	HMA-US 59-Panola-Atlanta	Arif	Field		Quartzite	3061		0.64	0.54	71.6	0.31
24	HMA-US 59-Panola-Atlanta	Arif	Field		Quartzite	3061		0.67	0.66	74.3	0.36
24	HMA-US 59-Panola-Atlanta	Arif	Field		Quartzite	3061		0.62	0.71	69.8	0.37
13	HMA-IH 35-La Salle-Laredo-B	Arif	Field		Traprock + Limestone	3340		0.48	0.37	57.3	0.22
13	HMA-IH 35-La Salle-Laredo-B	Arif	Field		Traprock + Limestone	3340		0.47	0.37	56.4	0.21
13	HMA-IH 35-La Salle-Laredo-B	Arif	Field		Traprock + Limestone	3340		0.47	0.36	56.4	0.21
13	HMA-IH 35-La Salle-Laredo-B	Arif	Field		Traprock + Limestone	3340		0	0.36	14.2	0.10
13	HMA-IH 35-La Salle-Laredo-B	Arif	Field		Traprock + Limestone	3340		0.94	0.57	98.5	0.36
13	HMA-IH 35-La Salle-Laredo-B	Arif	Field		Traprock + Limestone	3340		0.96	0.54	100.3	0.35
5	HMA-SH 71-Travis-Austin-A	Arif	Field		Sandstone + Limestone	422		0.8	0.49	86.0	0.31
5	HMA-SH 71-Travis-Austin-A	Arif	Field		Sandstone + Limestone	422		0.74	0.50	80.6	0.30
5	HMA-SH 71-Travis-Austin-A	Arif	Field		Sandstone + Limestone	422		0.83	0.51	88.7	0.32
5	HMA-SH 71-Travis-Austin-A	Arif	Field		Sandstone + Limestone	422		0.97	0.62	101.2	0.39
5	HMA-SH 71-Travis-Austin-A	Arif	Field		Sandstone + Limestone	422		0.75	0.63	81.5	0.36
6	HMA-FM 3238-Travis-Austin	Arif	Field		Sandstone + Limestone	934		0.58	0.64	66.2	0.34
6	HMA-FM 3238-Travis-Austin	Arif	Field		Sandstone + Limestone	934		0.51	0.65	59.9	0.33
6	HMA-FM 3238-Travis-Austin	Arif	Field		Sandstone + Limestone	934		0.47	0.65	56.4	0.31
6	HMA-FM 3238-Travis-Austin	Arif	Field		Sandstone + Limestone	934		0.45	0.84	54.6	0.38
6	HMA-FM 3238-Travis-Austin	Arif	Field		Sandstone + Limestone	934		0.43	0.86	52.8	0.38
45	PFC-SH 6-Waller-Houston	Arif	Field		Igneous Rock	2911		1.55	0.41	153.2	0.31
45	PFC-SH 6-Waller-Houston	Arif	Field		Igneous Rock	2911		1.6	0.44	157.7	0.33
45	PFC-SH 6-Waller-Houston	Arif	Field		Igneous Rock	2911		1.42	0.41	141.6	0.31
45	PFC-SH 6-Waller-Houston	Arif	Field		Igneous Rock	2911		1.74	0.40	170.3	0.31
45	PFC-SH 6-Waller-Houston	Arif	Field		Igneous Rock	2911		1.96	0.40	190.0	0.32
45	PFC-SH 6-Waller-Houston	Arif	Field		Igneous Rock	2911		2.13	0.45	205.3	0.35
14	HMA-US 385-Ector-Odessa	Arif	Field		Rhyollite and LS Scrn (?)	2928		0.89	0.54	94.0	0.34
14	HMA-US 385-Ector-Odessa	Arif	Field		Rhyollite and LS Scrn (?)	2928		0.78	0.54	84.2	0.33
14	HMA-US 385-Ector-Odessa	Arif	Field		Rhyollite and LS Scrn (?)	2928		0.74	0.54	80.6	0.32
14	HMA-US 385-Ector-Odessa	Arif	Field		Rhyollite and LS Scrn (?)	2928		0.77	0.69	83.3	0.39
14	HMA-US 385-Ector-Odessa	Arif	Field		Rhyollite and LS Scrn (?)	2928		0.85	0.69	90.4	0.41
96	Seal Coat-SH 77-Cass-Atlanta-A	Arif	Field		Sandstone	566		1.31	0.72	131.7	0.47
96	Seal Coat-SH 77-Cass-Atlanta-A	Arif	Field		Sandstone	566		1.33	0.71	133.5	0.47
96	Seal Coat-SH 77-Cass-Atlanta-A	Arif	Field		Sandstone	566		1.53	0.00	151.4	0.08
96	Seal Coat-SH 77-Cass-Atlanta-A	Arif	Field		Sandstone	566		1.26	0.78	127.2	0.50
96	Seal Coat-SH 77-Cass-Atlanta-A	Arif	Field		Sandstone	566		3.26	0.96	306.6	0.70
96	Seal Coat-SH 77-Cass-Atlanta-A	Arif	Field		Sandstone	566		2.39	0.84	228.6	0.60
97	Seal Coat-SH 77-Cass-Atlanta-B	Arif	Field		Gravel	201		2.57	0.63	244.7	0.47
97	Seal Coat-SH 77-Cass-Atlanta-B	Arif	Field		Gravel	201		2.44	0.61	233.1	0.46
97	Seal Coat-SH 77-Cass-Atlanta-B	Arif	Field		Gravel	201		2.79	0.69	264.5	0.52
97	Seal Coat-SH 77-Cass-Atlanta-B	Arif	Field		Gravel	201		2.81	0.64	266.3	0.48
68	Seal Coat-US 281-Brooks-Pharr-A	Arif	Field		Limestone	1027		0.81	0.24	86.9	0.19
68	Seal Coat-US 281-Brooks-Pharr-A	Arif	Field		Limestone	1027		0.8	0.27	86.0	0.21

68	Seal Coat-US 281-Brooks-Pharr-A	Arif	Field		Limestone	1027		0.8	0.25	86.0	0.20
68	Seal Coat-US 281-Brooks-Pharr-A	Arif	Field		Limestone	1027		1.84	0.27	179.2	0.24
68	Seal Coat-US 281-Brooks-Pharr-A	Arif	Field		Limestone	1027		1.61	0.26	158.6	0.23
69	Seal Coat-US 281-Brooks-Pharr-B	Arif	Field		Limestone	904		0.45	0.25	54.6	0.17
69	Seal Coat-US 281-Brooks-Pharr-B	Arif	Field		Limestone	904		0.51	0.28	59.9	0.19
69	Seal Coat-US 281-Brooks-Pharr-B	Arif	Field		Limestone	904		0.48	0.26	57.3	0.18
69	Seal Coat-US 281-Brooks-Pharr-B	Arif	Field		Limestone	904		0	0.55	14.2	0.11
69	Seal Coat-US 281-Brooks-Pharr-B	Arif	Field		Limestone	904		1.27	0.51	128.1	0.35
149	Seal Coat-SH 16-McMullen-San Antonio	Arif	Field		Limestone Rock Asphalt	1745		1.42	0.47	141.6	0.34
149	Seal Coat-SH 16-McMullen-San Antonio	Arif	Field		Limestone Rock Asphalt	1745		1.35	0.49	135.3	0.35
149	Seal Coat-SH 16-McMullen-San Antonio	Arif	Field		Limestone Rock Asphalt	1745		2.93	0.67	277.0	0.51
149	Seal Coat-SH 16-McMullen-San Antonio	Arif	Field		Limestone Rock Asphalt	1745		2.98	0.63	281.5	0.48
145	HMA-US 90-Uvalde-San Antonio	Arif	Field		Traprock	1379		0.39	0.00	49.2	0.08
145	HMA-US 90-Uvalde-San Antonio	Arif	Field		Traprock	1379		0.35	0.58	45.6	0.26
145	HMA-US 90-Uvalde-San Antonio	Arif	Field		Traprock	1379		0.33	0.58	43.8	0.25
145	HMA-US 90-Uvalde-San Antonio	Arif	Field		Traprock	1379		0.36	0.73	46.5	0.31
145	HMA-US 90-Uvalde-San Antonio	Arif	Field		Traprock	1379		0.4	0.75	50.1	0.33
146	PFC-US 59-Nacogdoches-Lufkin	Arif	Field		Quartzite	76		1.76	0.45	172.1	0.34
146	PFC-US 59-Nacogdoches-Lufkin	Arif	Field		Quartzite	76		1.71	0.40	167.6	0.31
146	PFC-US 59-Nacogdoches-Lufkin	Arif	Field		Quartzite	76		1.79	0.43	174.8	0.33
146	PFC-US 59-Nacogdoches-Lufkin	Arif	Field		Quartzite	76		1.86	0.53	181.0	0.39
146	PFC-US 59-Nacogdoches-Lufkin	Arif	Field		Quartzite	76		1.81	0.46	176.6	0.35
148	HMA-IH 35-Williamson-Austin	Arif	Field		Sandstone + Limestone	1154		0.82	0.49	87.8	0.31
148	HMA-IH 35-Williamson-Austin	Arif	Field		Sandstone + Limestone	1154		0.77	0.44	83.3	0.28
148	HMA-IH 35-Williamson-Austin	Arif	Field		Sandstone + Limestone	1154		0.78	0.49	84.2	0.30
148	HMA-IH 35-Williamson-Austin	Arif	Field		Sandstone + Limestone	1154		0.84	0.56	89.5	0.34
148	HMA-IH 35-Williamson-Austin	Arif	Field		Sandstone + Limestone	1154		0.8	0.57	86.0	0.34
	HFST-CB1_Yash	6932	Lab	HFST	Calcined Bauxite		0	2.07	0.90	199.6	0.62
	HFST-CB1_Yash	6932	Lab	HFST	Calcined Bauxite		1000	1.88	0.80	183.0	0.55
	HFST-CB1_Yash	6932	Lab	HFST	Calcined Bauxite		5000	1.74	0.71	170.4	0.49
	HFST-CB1_Yash	6932	Lab	HFST	Calcined Bauxite		30000	1.72			
	HFST-CB1_Yash	6932	Lab	HFST	Calcined Bauxite		80000	1.71	0.68	167.4	0.48
	HFST-CB2_Yash	6932	Lab	HFST	Calcined Bauxite		0	2.11	0.96	203.8	0.66
	HFST-CB2_Yash	6932	Lab	HFST	Calcined Bauxite		1000	1.84	0.88	179.2	0.60
	HFST-CB2_Yash	6932	Lab	HFST	Calcined Bauxite		5000	1.88	0.89	183.1	0.60
	HFST-CB2_Yash	6932	Lab	HFST	Calcined Bauxite		30000	1.70	0.85	166.7	0.57
	HFST-CB2_Yash	6932	Lab	HFST	Calcined Bauxite		80000	1.73	0.82	169.7	0.56
	HFST-Flint	6932	Lab	HFST	Flint		0	2.235	0.77	214.7	0.55
	HFST-Flint	6932	Lab	HFST	Flint		1000	1.91	0.71	185.2	0.50
	HFST-Flint	6932	Lab	HFST	Flint		5000	1.87	0.66	181.6	0.47
	HFST-Flint	6932	Lab	HFST	Flint		30000	1.93	0.63	187.6	0.45
	HFST-Flint	6932	Lab	HFST	Flint		80000	1.87	0.58	181.6	0.42
	Pharr-Epoxy	6932	Lab	HFST-Gr4	Gravel		0	5.08	0.71	469.6	0.56

	Pharr-Epoxy	6932	Lab	HFST-Gr4	Gravel		1000	3.37	0.60	316.2	0.47
	Pharr-Epoxy	6932	Lab	HFST-Gr4	Gravel		5000	3.49	0.56	327.0	0.44
	Pharr-Epoxy	6932	Lab	HFST-Gr4	Gravel		30000	3.56			
	Pharr-Epoxy	6932	Lab	HFST-Gr4	Gravel		80000	3.47	0.56	325.5	0.44
	Riverlite-Epoxy	6932	Lab	HFST-Gr4	Lightweight		0	4.61	0.88	427.4	0.66
	Riverlite-Epoxy	6932	Lab	HFST-Gr4	Lightweight		1000	3.54	0.82	332.0	0.61
	Riverlite-Epoxy	6932	Lab	HFST-Gr4	Lightweight		5000	3.50			
	Riverlite-Epoxy	6932	Lab	HFST-Gr4	Lightweight		30000	3.41	0.72	320.1	0.55
	Riverlite-Epoxy	6932	Lab	HFST-Gr4	Lightweight		80000	3.47	0.74	325.8	0.56
	Streetman-Epoxy	6932	Lab	HFST-Gr4	Lightweight		0	4.54	0.89	421.4	0.68
	Streetman-Epoxy	6932	Lab	HFST-Gr4	Lightweight		1000	3.94	0.83	367.9	0.63
	Streetman-Epoxy	6932	Lab	HFST-Gr4	Lightweight		5000	3.62	0.95	338.9	0.70
	Streetman-Epoxy	6932	Lab	HFST-Gr4	Lightweight		30000	3.60	0.87	337.4	0.65
	Streetman-Epoxy	6932	Lab	HFST-Gr4	Lightweight		80000	3.68	0.84	344.6	0.63
	TCS-Epoxy	6932	Lab	HFST-Gr4	Limestone		0	5.00			
	TCS-Epoxy	6932	Lab	HFST-Gr4	Limestone		1000	4.02	0.69	375.1	0.54
	TCS-Epoxy	6932	Lab	HFST-Gr4	Limestone		5000	3.74	0.60	349.4	0.47
	TCS-Epoxy	6932	Lab	HFST-Gr4	Limestone		30000	3.91	0.59	364.9	0.47
	TCS-Epoxy	6932	Lab	HFST-Gr4	Limestone		80000	3.65	0.55	341.6	0.44

APPENDIX C: DETAILED PRECIPITATION RATE TRENDS

Table 54. Annual Average Precipitation (in.) by County.

County	Annual Avg. Precipitation (in.) 1971–2000 NOAA Normal	Annual Avg. Precipitation (in.) 1981–2010 NOAA Normal
Anderson	46.38	45.14
Andrews	15.15	14.74
Angelina	46.62	49.25
Aransas	35.96	41.01
Archer	29.78	30.72
Armstrong	22.39	22.25
Atascosa	29.00	26.57
Austin	40.68	41.75
Bailey	17.37	18.38
Bandera	35.78	37.37
Bastrop	38.04	36.53
Baylor	27.79	25.64
Bee	33.48	31.97
Bell	35.81	33.08
Bexar	32.92	34.86
Blanco	34.75	34.87
Borden	19.68	19.06
Bosque	35.07	33.51
Bowie	51.24	54.11
Brazoria	57.24	53.50
Brazos	39.67	40.06
Brewster	17.19	17.00
Briscoe	19.17	22.41
Brooks	22.34	26.47
Brown	25.42	30.43
Burleson	28.32	39.50
Burnet	38.50	33.09
Caldwell	32.43	35.19
Calhoun	36.86	42.39
Callahan	34.78	27.42
Cameron	27.55	27.49
Camp	45.10	45.10*
Carson	22.21	21.78
Cass	48.20	48.84
Castro	19.71	21.22
Chambers	54.08	57.11
Cherokee	48.50	47.01
Childress	22.65	26.43
Clay	31.66	32.39
Cochran	18.34	18.93
Coke	23.00	23.20

**Data from this county are not available for the full period from 1981 to 2010. The provided data are from 1971–2000.*

Table 54. Annual Average Precipitation (in.) by County (cont'd.).

County	Annual Avg. Precipitation (in.) 1971–2000 NOAA Normal	Annual Avg. Precipitation (in.) 1981–2010 NOAA Normal
Coleman	28.70	29.82
Collin	41.01	42.07
Collingsworth	22.80	22.26
Colorado	44.72	43.93
Comal	35.74	34.42
Comanche	31.12	31.28
Concho	25.50	26.99
Cooke	36.90	42.70
Coryell	33.43	33.66
Cottle	24.11	22.63
Crane	15.38	15.60
Crockett	18.95	22.70
Crosby	22.95	23.34
Culberson	11.98	21.24
Dallam	18.57	16.73
Dallas	37.05	38.67
Dawson	19.07	19.14
Deaf Smith	18.65	20.05
Delta	45.00	45.00*
Denton	37.79	38.09
DeWitt	36.08	36.08*
Dickens	18.68	22.71
Dimmit	20.21	22.37
Donley	23.89	24.02
Duval	25.40	25.99
Eastland	27.53	29.02
Ector	13.29	16.61
Edwards	24.76	25.21
El Paso	9.43	10.54
Ellis	38.81	38.74
Erath	29.71	34.53
Falls	37.99	38.46
Fannin	44.56	46.13
Fayette	40.31	37.68
Fisher	24.22	24.76
Floyd	20.95	21.60
Foard	26.40	26.40*
Fort Bend	49.34	50.13
Franklin	47.65	47.42
Freestone	42.31	43.12
Frio	25.73	24.88
Gaines	18.20	17.52
Galveston	43.84	56.81
Garza	21.29	20.89

Table 54. Annual Average Precipitation (in.) by County (cont'd.).

County	Annual Avg. Precipitation (in.) 1971–2000 NOAA Normal	Annual Avg. Precipitation (in.) 1981–2010 NOAA Normal
Gillespie	31.65	31.69
Glasscock	17.32	17.57
Goliad	38.58	36.54
Gonzales	36.02	33.09
Gray	22.74	21.63
Grayson	42.04	41.27
Gregg	49.06	48.09
Grimes	44.70	43.51
Guadalupe	34.50	33.54
Hale	19.90	20.79
Hall	22.51	22.59
Hamilton	28.59	31.47
Hansford	20.30	20.34
Hardeman	26.76	27.34
Hardin	56.50	61.70
Harris	53.96	46.84
Harrison	51.22	51.34
Hartley	17.20	21.02
Haskell	24.93	26.40
Hays	37.19	35.74
Hemphill	21.68	22.79
Henderson	42.03	42.94
Hidalgo	22.61	24.07
Hill	37.15	36.06
Hockley	19.58	19.84
Hood	33.10	35.08
Hopkins	47.69	44.80
Houston	45.48	45.18
Howard	20.12	20.70
Hudspeth	11.93	11.11
Hunt	43.70	44.46
Hutchinson	21.98	22.85
Irion	19.90	20.15
Jack	31.44	32.11
Jackson	42.10	43.25
Jasper	60.57	54.75
Jeff Davis	15.86	17.47
Jefferson	59.89	60.42
Jim Hogg	23.75	23.79
Jim Wells	27.52	28.79
Johnson	36.25	37.28
Jones	26.00	26.06
Karnes	28.40	30.14
Kaufman	38.90	40.15

Table 54. Annual Average Precipitation (in.) by County (cont'd.).

County	Annual Avg. Precipitation (in.) 1971–2000 NOAA Normal	Annual Avg. Precipitation (in.) 1981–2010 NOAA Normal
Kendall	37.36	38.10
Kenedy	27.90	28.40
Kent	22.94	23.51
Kerr	32.60	33.63
Kimble	23.24	24.53
King	25.00	24.82
Kinney	22.79	23.56
Kleberg	29.03	31.94
Knox	26.36	26.43
La Salle	22.56	24.70
Lamar	47.82	47.07
Lamb	18.69	18.87
Lampasas	31.08	32.23
Lavaca	42.23	41.06
Lee	36.02	37.99
Leon	43.08	42.29
Liberty	60.52	59.92
Limestone	41.40	40.34
Lipscomb	22.57	21.39
Live Oak	22.00	26.36
Llano	27.33	27.70
Loving	9.10	9.10*
Lubbock	18.69	21.09
Lynn	20.48	21.21
Madison	44.00	45.12
Marion	49.26	48.96
Martin	18.20	17.56
Mason	27.95	29.19
Matagorda	48.03	48.89
Maverick	21.48	20.41
McCulloch	27.63	27.63*
McLennan	33.34	33.34*
McMullen	23.87	23.87*
Medina	26.30	30.32
Menard	24.90	25.09
Midland	14.80	14.80
Milam	35.52	36.97
Mills	28.78	30.49
Mitchell	19.43	20.42
Montague	33.72	37.56
Montgomery	49.32	48.77
Moore	17.75	18.37

Table 54. Annual Average Precipitation (in.) by County (cont'd.).

County	Annual Avg. Precipitation (in.) 1971–2000 NOAA Normal	Annual Avg. Precipitation (in.) 1981–2010 NOAA Normal
Morris	48.76	46.79
Motley	22.90	23.85
Nacogdoches	48.40	55.52
Navarro	39.48	39.78
Newton	54.90	57.45
Nolan	23.54	22.42
Nueces	32.26	32.93
Ochiltree	20.88	21.09
Oldham	18.18	19.45
Orange	59.00	59.13
Palo Pinto	31.79	32.19
Panola	51.51	51.43
Parker	34.70	36.01
Parmer	18.38	20.14
Pecos	14.06	15.25
Polk	51.85	57.98
Potter	19.71	21.14
Presidio	15.79	13.72
Rains	43.50	44.47
Randall	19.19	20.15
Reagan	18.79	19.29
Real	27.99	27.38
Red River	47.83	52.61
Reeves	11.61	13.54
Refugio	40.10	34.43
Roberts	23.30	24.08
Robertson	39.03	39.70
Rockwall	39.40	38.58
Runnels	23.76	24.04
Rusk	48.22	49.36
Sabine	54.40	54.60
San Augustine	51.10	51.89
San Jacinto	51.77	50.68
San Patricio	35.54	34.28
San Saba	27.72	27.33
Schleicher	19.00	23.21
Scurry	22.51	21.59
Shackelford	28.45	28.36
Shelby	53.01	54.20
Sherman	17.89	17.77
Smith	45.40	46.63
Somervell	34.82	36.87
Starr	21.61	20.60
Stephens	27.04	29.98
Sterling	19.40	20.46

Table 54. Annual Average Precipitation (in.) by County (cont'd.).

County	Annual Avg. Precipitation (in.) 1971–2000 NOAA Normal	Annual Avg. Precipitation (in.) 1981–2010 NOAA Normal
Stonewall	23.24	23.77
Sutton	22.40	23.03
Swisher	20.71	21.57
Tarrant	34.01	39.60
Taylor	23.78	27.15
Terrell	14.94	14.72
Terry	18.89	19.58
Throckmorton	26.60	27.67
Titus	48.57	47.70
Tom Green	20.91	24.34
Travis	33.65	34.89
Trinity	48.10	49.31
Tyler	54.79	56.18
Upshur	47.08	46.84
Upton	14.45	15.14
Uvalde	23.30	25.63
Val Verde	18.80	18.81
Van Zandt	43.68	45.80
Victoria	40.10	41.08
Walker	48.51	49.08
Waller	38.20	38.20*
Ward	13.23	14.40
Washington	44.15	45.14
Webb	21.53	22.68
Wharton	45.92	46.38
Wheeler	24.32	26.49
Wichita	28.83	31.39
Wilbarger	28.55	27.94
Willacy	27.97	25.91
Williamson	35.11	33.58
Wilson	27.60	27.35
Winkler	12.92	14.61
Wise	34.02	36.83
Wood	45.88	48.20
Yoakum	18.41	19.20
Young	31.35	31.51
Zapata	19.53	22.52
Zavala	20.70	23.09
All Counties	31.39	32.13

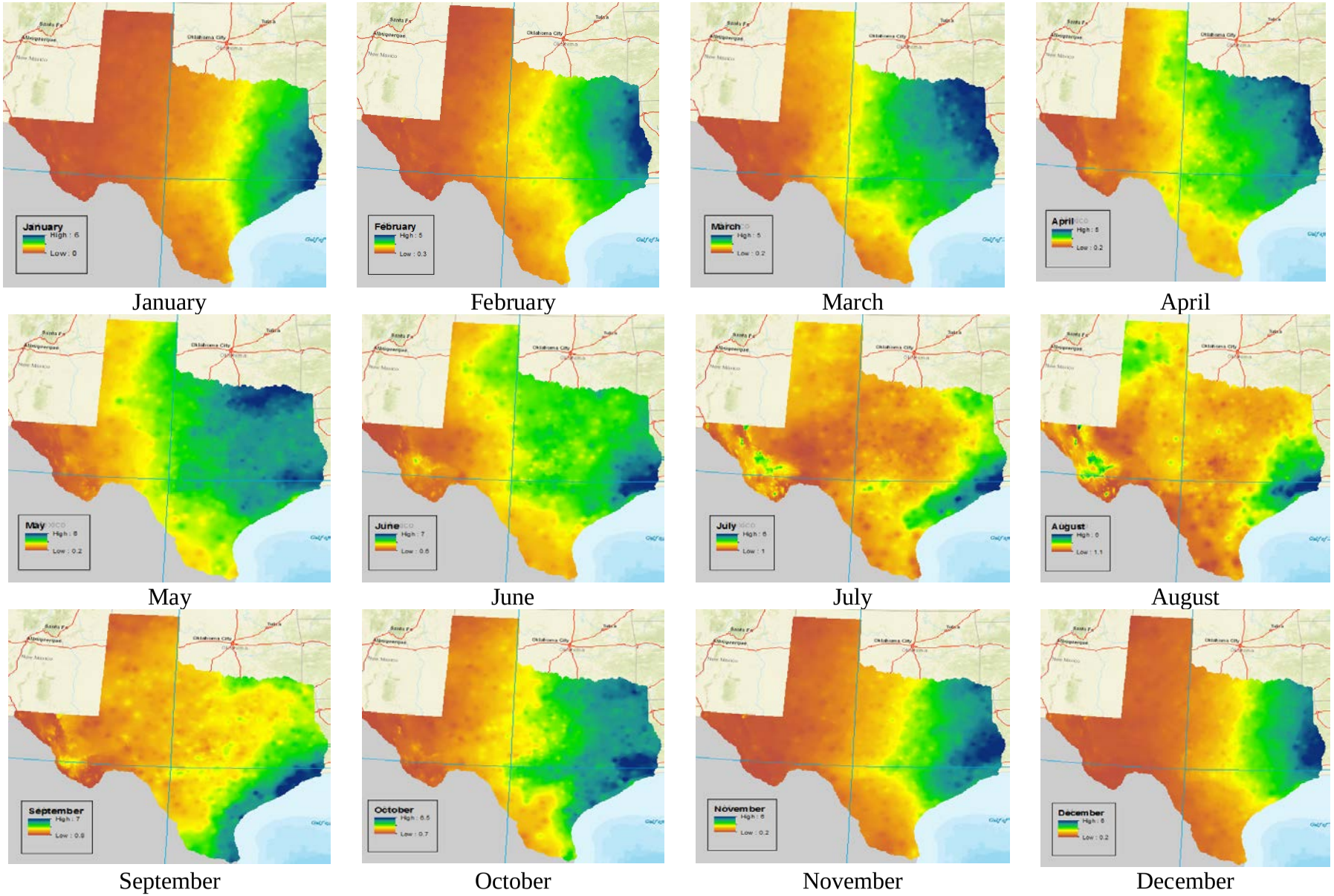

Figure 61. Average Monthly Precipitation (in.) (1981–2010 NOAA Normal Data Set).

REFERENCES

1 Lord, D., M. Brewer, K. Fitzpatrick, S. Geedipally, and Y. Peng. *Analysis of Roadway Departure Crashes on Two-Lane Rural Roads in Texas*. Report FHWA/TX-11/0-6031-1, Texas Transportation Institute, College Station, Texas, 2011.

2 Pratt, Michael P., Srinivas R. Geedipally, Adam M. Pike, Paul J. Carlson, Amelia M. Celoza, and Dominique Lord. *Evaluating the Need for Surface Treatments to Reduce Crash Frequency on Horizontal Curves.* Report FHWA/TX-14/0-6714-1, Texas A&M Transportation Institute, College Station, Texas, 2014.

3 Glennon, J., and G. Weaver. *The Relationship of Vehicle Paths to Highway Curve Design.* Research Report 134-5. Texas Transportation Institute, College Station, Texas, 1971.

4 Pavement Design Guide. Texas Department of Transportation, Austin, Texas, 2011.

5 Highway Safety Manual. American Association of State Highway and Transportation Officials, Washington, D.C., 2010.

6 A Policy on Geometric Design of Highways and Streets. American Association of State Highway and Transportation Officials, Washington, D.C., 2011.

7 Zegeer, C. V., J. R. Stewart, F. M. Council, and D. W. Reinfurt. *Safety Effects of Geometric Improvements on Horizontal Curves*. Report No. UNC-HSRC-91. University of North Carolina, Chapel Hill, North Carolina, 1991.

8 Schneider, W. H., K. Zimmerman, D. Van Boxel, and S. Vavilikolanu. "Bayesian Analysis of the Effect of Horizontal Curvature on Truck Crashes Using Training and Validation Data Sets." In *Transportation Research Record: Journal of the Transportation Research Board, No. 2096,* TRB, National Research Council, Washington, D.C., 2009, pp. 41-46.

9 Harwood, D., F. M. Council, E. Hauer, W. E. Hughes, and A. Vogt. *Prediction of the Expected Safety Performance of Rural Two-Lane Highways*. Midwest Research Institute, McLean, Virginia, 2000.

10 Wu, L., D. Lord, and S. R. Geedipally. "Developing Crash Modification Factors for Horizontal Curves on Rural Two Lane Undivided Highways using a Cross-Sectional Study." Presented at the 96th Annual Meeting of Transportation Research Board (TRB), Washington D.C., 2017.

11 Glennon, J., and G. Weaver. "Highway Curve Design for Safe Vehicle Operations." In *Highway Research Record, No. 390,* Highway Research Board, National Research Council, Washington, D.C., 1972, pp. 15-26.

12 Bonneson, J., and M. Pratt. "Procedure for Developing Accident Modification Factors from Cross-Sectional Data." In *Transportation Research Record: Journal of the Transportation Research Board, No. 2083,* TRB, National Research Council, Washington, D.C., 2008, pp. 40-48.

13 Bonneson, J., and M. Pratt. *Roadway Safety Design Workbook*. Report FHWA/TX-09-0-4703-P2, Texas Transportation Institute, College Station, Texas, 2009.

14 Gooch, J. P., V. V. Gayah, and E. T. Donnell. "Quantifying the safety effects of horizontal curves on two-way, two-lane rural roads." In *Accident Analysis & Prevention*, Vol. 92, pp. 71-81, 2016.

15 Fitzpatrick, K., D. Lord, and B.J. Park. "Horizontal Curve Accident Modification Factor with Consideration of Driveway Density on Rural Four-Lane Highways in Texas." In *Journal of Transportation Engineering*, Vol. 136, No. 9, pp. 827-835, 2010.

16 Banihashemi, M. "Is Horizontal Curvature a Significant Factor of Safety in Rural Multilane Highways?" In *Transportation Research Record: Journal of the Transportation Research Board, No. 2515*, TRB, National Research Council, Washington, D.C., 2015, pp. 50-56.

17 Banihashemi, M. "Effect of horizontal curves on urban arterial crashes." In *Accident Analysis & Prevention*, Vol. 95, pp. 20-26, 2016.

18 Lalani, N. 1991. "Comprehensive Safety Program Produces Dramatic Results." In *ITE Journal*, Vol. 61, No. 10, Institute of Transportation Engineers, 1991, pp. 31-34.

19 Srinivasan, R., J. Baek, D. Carter, B. Persaud, C. Lyon, K. A. Eccles, F. Gross, and N. X. Lefler. *Safety Evaluation of Improved Curve Delineation*. Report FHWA-HRT-09-045, Vanasse Hangen Brustlin, Vienna, Virginia, 2009.

20 Choi, Y.-Y., S.-Y. Kho, C. Lee, D.-K. Kim, and B. "Development of Crash Modification Factors of Alignment Elements and Safety Countermeasures for Korean Freeways." Paper No. 15-0503. Presented at the 94th Annual Meeting of the Transportation Research Board, Washington, D.C., 2015.

21 Montella, A. "Safety Evaluation of Curve Delineation Improvements Empirical Bayes Observational Before-and-After Study." In *Transportation Research Record: Journal of the Transportation Research Board, No. 2103*, TRB, National Research Council, Washington, D.C., 2009, pp. 69-79.

22 Tsyganov, A. R., R. B. Machemehl, and N. Warrenchuk. "Driver Performance and Safety Effects of Edge Lines on Rural Two-Lane Highways." Paper No. 09-0751. Presented at the 88th Annual Meeting of the Transportation Research Board, Washington, D.C., 2009.

23 Elvik, R., and T. Vaa. *The Handbook of Road Safety Measures*. Oxford, United Kingdom: Elsevier, 2004.

24 Neuman, T.R., R. Pfefer, K.L. Slack, K.K. Hardy, F. Council, H. McGee, L. Prothe, and K. Eccles. *Guidance for Implementation of the AASHTO Strategic Highway Safety Plan. Volume 6: A Guide for Addressing Run-Off-Road Collisions.* NCHRP Report 500, Transportation Research Board, Washington, DC., 2003.

25 Lamm, R., Choueiri, E.M., Mailaender, T. “Comparison of Operating Speeds on Dry and Wet Pavements of Two-Lane Rural Highways.” In *Transportation Research Record: Journal of the Transportation Research Board, No. 1280*, TRB, National Research Council, Washington, D.C., 1990, pp. 199-207.

26 Andrey, J. and Yagar, S. “A Temporal Analysis of Rain-Related Crash Risk.” In *Accident Analysis & Prevention*, Vol. 25, No. 4, pp. 465-472, 1993.

27 Satterthwaite, S. “An Assessment of Seasonal and Weather Effects on the Frequency of Road Accidents in California.” In *Accident Analysis & Prevention*, Vol. 8, No. 2, pp. 87-96, 1976.

28 Jackson, T. L., and H. O. Sharif. “Rainfall Impacts on Traffic Safety: Rain-Related Fatal Crashes in Texas.” In *Geomatics, Natural Hazards & Risk,* Vol. 7, No. 2, pp. 843-860, 2016.

29 Merritt, D. K., C. A. Lyon, and B. N. Persaud. *Evaluation of Pavement Safety Performance.* Report No. FHWA-HRT-14-065, Federal Highway Administration, Washington, D.C., 2015.

30 Julian, F. and S. Moler. “Gaining Traction in Roadway Safety.” In *Public Roads,* Vol. 72, No. 1, pp. 38-44, 2008.

31 Gransberg, D. D. and D. M. B. James. *NCHRP Synthesis 342: Chip Seal Best Practices.* Project 20-05, Topic 35-02, Transportation Research Board, Washington, D.C., 2005.

32 Lawson, W. D. *Short Term Solutions to "Bleeding" Asphalt Pavements.* Report No. 0-5230-P1, TECHMRT Multidisciplinary Research in Transportation, Lubbock, Texas, 2006

33 McCullough, B., and Hankins, K. “Skid Resistance Guidelines for Surface Improvements on Texas Highways.” In *Highway Research Record, No. 131*, HRB, National Research Council, Washington, D.C., 1966, pp. 204-217.

34 Larson, R. *Consideration of Tire/Pavement Friction/Texture Effects on Pavement Structural Design and Materials Mix Design.* Office of Pavement Technology, HIPT. 1999.

35 Xiao, J., Kulakowski, B., and El-Gindy, M. “Prediction of Risk of Wet-Pavement Accidents: Fuzzy Logic Model.” In *Highway Research Record, No. 131*, HRB, National Research Council, Washington, D.C., 1966, pp. 28-36.

36 Tighe, S., Li, N., Falls, L., and Haas, R. “Incorporating Road Safety into Pavement Management.” In *Transportation Research Record: Journal of the Transportation Research Board, No. 1699*, TRB, National Research Council, Washington, D.C., 2000, pp. 1-10.

37 Mayora, J., and Pina, R. “An assessment of the skid resistance effect on traffic safety under wet-pavement conditions.” In *Accident Analysis & Prevention*, Vol. 41, No. 4, pp. 881-886, 2009.

38 Milton, J., Shankar, V., Mannering, F.L. “Highway accident severities and the mixed logit model: an exploratory empirical analysis.” In *Accident Analysis & Prevention*, Vol. 40, No. 1, pp. 260–266, 2008.

39 Shankar, V., Mannering, F., Barfield, W. “Statistical analysis of accident severity on rural freeways.” In *Accident Analysis & Prevention*, Vol. 28, No. 3, pp. 391–401, 1996.

40 Noyce, D., Bahia, H., Yambó, J., and Kim, G. *Incorporating Road Safety into Pavement Management: Maximizing Asphalt Pavement Surface friction for Road Safety Improvements.* Midwest Regional University Transportation Center, Wisconsin, 2005.

41 McCarthy, R., Flintsch, G., Katicha, S., McGhee, K., and Medina-Flintsch, A. “New Approach for Managing Pavement Friction and Reducing Road Crashes.” In *Transportation Research Record: Journal of the Transportation Research Board, No. 2591*, TRB, National Research Council, Washington, D.C., pp. 23–32, 2016.

42 Buddhavarapu, P., Banerjee, B., Prozzi, J.A. “Influence of pavement condition on horizontal curve safety.” In *Accident Analysis & Prevention*, Vol. 52, pp. 9-18, 2013.

43 Chan, C., Huang, B., Yan, X., and Richards, S. “Investigating effects of asphalt pavement conditions on traffic accidents in Tennessee based on the pavement management system (PMS).” In *Journal of Advanced Transportation*, Vol. 44, pp. 150–161, 2010.

44 Li, Y., Liu, C., and Ding, L. “Impact of pavement conditions on crash severity.” In *Accident Analysis & Prevention*, Vol. 59, pp. 399-406, 2013.

45 Li, Y., and Huang, J. “Safety Impact of Pavement Conditions.” In *Transportation Research Record: Journal of the Transportation Research Board, No. 2455*, TRB, National Research Council, Washington, D.C., pp. 77–88, 2014.

46 Zeng, H., Fontaine, M., and Smith, B. “Estimation of the Safety Effect of Pavement Condition on Rural, Two-Lane Highways.” In *Transportation Research Record: Journal of the Transportation Research Board, No. 2435*, TRB, National Research Council, Washington, D.C., pp. 45–52, 2014.

47 Najafi, S., Flintsch, G., and Medina, A. “Linking roadway crashes and tire-pavement friction: a case study.” In *International Journal of Pavement Engineering*, Vol. 18, No. 2, pp. 119-127, 2015.

48 Blackburn, R., D.W. Harwood, A.D. St John, and M.C. Sharp. *Effectiveness of Alternative Skid Reduction Measures*. Report FHWA-RD-79-22, Federal Highway Administration, Washington, D.C., 1978.

49 Wu, H. Z. Zhang, K. Long, and M. Murphy. “Considering Safety Impacts of Skid Resistance in Decision-Making Processes for Pavement Management.” In *Transportation Research Record: Journal of the Transportation Research Board, No. 2455*, TRB, National Research Council, Washington, D.C., pp. 19–27, 2014.

50 De Leon Izeppi, E., S. Katicha, G. Flintsch, and K. McGhee. “Pioneering Use of Continuous Pavement Friction Measurements to Develop Safety Performance Functions, Improve Crash Count Prediction, and Evaluate Treatments for Virginia Roads.” In *Transportation Research Record: Journal of the Transportation Research Board, No. 2583*, TRB, National Research Council, Washington, D.C., pp. 81–90, 2016.

51 EDC-2: High Friction Surface Treatments (HFST). https://www.fhwa.dot.gov/innovation/everydaycounts/edc-2/hfst.cfm. Accessed January 31, 2017.

52 Roadway Design Manual. Texas Department of Transportation, Austin, Texas, 2014.

53 Brewer, M., D. Murillo, and A. Pate. *Handbook for Designing Roadways for the Aging Population*. Report No. FHWA-SA-14-015. Federal Highway Administration, Washington, DC., 2014.

54 Schaffer, R., D. Heuer, F. Bents, J. Foglietta, D. Wieder, M. Jordan, and P. Tiwari. *Leading Practices for Motorcyclist Safety*. Scan Team Report, NCHRP Project 20-68A, Scan 09-04. Transportation Research Board, Washington, DC. 2011.

55 Arambula, E., C. Estakhri, A. Epps-Martin, M. Trevino, A. d. F. Smit, and J. Prozzi. *Performance and Cost Effectiveness of Permeable Friction Course (PFC) Pavements.* Report 0-5836-2, Texas A&M Transportation Institute, College Station, Texas, February 2013.

56 Chowdhury, A., E. Kassem, S. Aldagari, and E. Masad. *Validation of Asphalt Mixture Pavement Skid Prediction Model and Development of Skid Prediction Model for Surface Treatments.* Report 0-6746-01-1, Texas A&M Transportation Institute, Texas A&M University System, College Station, Texas, April 2017.

57 Wilson, B. T., T. Scullion, and C. Estakhri. *Design and Construction Recommendations for Thin Overlays in Texas.* Report 0-6615-1, Texas A&M Transportation Institute, College Station, Texas, September 2013.

58 Wilson, B. T., T. Scullion, and A. Faruk. *Evaluation of Design and Construction Issues of Thin HMA Overlays.* Report 0-6742-1, Texas A&M Transportation Institute, College Station, Texas, April 2015.

59 Wilson, B. T. and A. K. Mukhopadhyay. *Alternative Aggregates and Materials for High Friction Surface Treatments.* Final Report BDR74-977-05, Texas A&M Transportation Institute, College Station, Texas, May 2016.

60 Wambold, J. C., C. E. Antle, J. J. Henry, and Z. Rado. *International PIARC Experiment to Compare and Harmonize Texture and Skid Resistance Measurements.* PIARC: World Road Association, 1995.

61 Hall, J. W., K. L. Smith, L. Titus-Glover, J. C. Wambold, T. J. Yager, and Z. Rado. *Guide for Pavement Friction*. NCHRP Web-Only Document, No. 108, Washington D.C. February

2009. http://onlinepubs.trb.org/onlinepubs/nchrp/nchrp_w108.pdf. Accessed August 6, 2018.

62 Roque, R., A. Ravanshad, and G. Lopp. *Use of Aggregate Image Measurement System (AIM) to Evaluate Aggregate Polishing in Friction Surfaces*. Final Report BDK75-977-44, University of Florida, Department of Civil and Coastal Engineering, Gainesville, FL, August 2013.

63 Masad, E., A. Rezaei, A. Chowdhury, and T. J. Freeman. *Field Evaluation of Asphalt Mixture Skid Resistance and Its Relationship to Aggregate Characteristics*. Report No. 0-5627-3. Texas A&M Transportation Institute. Texas A&M University System, College Station, Texas, 2010.

64 Kassem, E., E. Masad, A. Awed, and D. Little. *Laboratory Evaluation of Friction Loss and Compactability of Asphalt Mixtures*. Report No. 476660-00025-1, Texas A&M Transportation Institute, Texas A&M University System, College Station, Texas, 2012.

65 Kassem, E., E. Masad, A. Awed, and D. Little. "Development of Predictive Model for Skid Loss of Asphalt Pavements." In the *Transportation Research Record: Journal of the Transportation Research Board, No. 2372*. Transportation Research Board of the National Academies, Washington D.C., 2013.

66 Roque, R., A. Ravanshad, and G. Lopp. *Use of Aggregate Imaging System (AIMS) to Evaluate Aggregate Polishing in Friction Surfaces*. Report No. BDK75 977-44, University of Florida, Gainsville, Florida, 2013.

67 Arambula, E., E. Fernando, R. Walker, W. Kuo, and B. Crockford. "Evaluation of a Laser-Based System for Measuring Texture of Coarse Aggregates." Paper No. 18-03359. Presented at the 97th Annual Meeting of the Transportation Research Board, Washington, D.C., 2018.

68 Das, S., Brimley, B., Lindheimer, T., and Zupancich, M. *Association of reduced visibility with crash outcomes.* IATSS Research, 2017. https://doi.org/10.1016/j.iatssr.2017.10.003.

69 Theofilatos, A., and Yannis, G. "A review of the effect of traffic and weather characteristic on road safety." *Accident Analysis and Prevention*, pp. 244–256, 2014.

70 Arguez, A., I. Durre, S. Applequist, R. S. Vose, M. F. Squires, X. Yin, R. R. Heim, Jr., and T. W. Owen. "NOAA's 1981-2010 U.S. Climate Normals: An Overview." *Bulletin of the American Meteorological Society*, 93, pp. 1687-1697, 2012.

71 Wet Surface Crash Reduction Program Guidelines. Texas Department of Transportation, Austin, Texas, 2011.

72 Miaou, S.P., and D. Lord. "Modeling Traffic Crash-Flow Relationships for Intersections: Dispersion Parameter, Functional Form, and Bayes Versus Empirical Bayes Methods." *Transportation Research Record*, No. 1840, Transportation Research Board, Washington, D.C., pp. 31–40. 2003.

73 Hauer, E. “Overdispersion in Modeling Accidents on Road Sections and in Empirical Bayes Estimation.” *Accident Analysis & Prevention*, Vol. 33, No. 6, pp. 799–808. 2001.

74 Heydecker, B.G., and J. Wu. “Identification of Sites for Road Accident Remedial Work by Bayesian Statistical Methods: An Example of Uncertain Inference.” *Advances in Engineering Software*, Vol. 32, University College London, Oxford, England, pp. 859–869. 2001.

75 Geedipally, S.R., D. Lord, and B.-J. Park. “Analyzing Different Parameterizations of the Varying Dispersion Parameter as a Function of Segment Length.” In *Transportation Research Record*, No. 2103, Transportation Research Board, Washington, D.C., pp. 108–118. 2009.

76 SAS/STAT User's Guide, Version 9.2. Second edition, SAS Institute, Inc., Cary, North Carolina, 2009.

77 Washington, S.P., Karlaftis, M.G., Mannering, F.L., 2010. *Statistical and Econometric Methods for Transportation Data Analysis*, second ed. Chapman Hall/ CRC, Boca Raton, FL.

78 Lord, D. and B. Persaud. Accident Prediction Models With and Without Trend: Application of the Generalized Estimating Equations (GEE) Procedure. In *Transportation Research Record*, No. 1717, Transportation Research Board, Washington, D.C., pp. 102–108. 2000.

79 Hauer, E., J. C. N. Ng, and P. Papaioannou. “Prediction in Road Safety Studies - an Empirical Inquiry.” *Accident Analysis and Prevention*, Vol. 23, No. 6, 1991, pp. 595-607.

80 Gross, F., B. Persaud, and C. Lyon. *A Guide to Developing Quality Crash Modification Factors.* Publication FHWA-SA-10-032. FHWA, U.S. Department of Transportation, 2010.

81 Wu, L., S. R. Geedipally, and A. M. Pike. *Safety Evaluation of Alternative Audible Lane Departure Warning Treatments in Reducing Traffic Crashes: An Empirical Bayes Observational Before-After Study*. In the 97th TRB Annual Meeting, Washington, D.C., 2018.

82 Hauer, E. Observational Before-After Studies in Road Safety. Pergamon Publications, London, 1997.

83 Automated Surface Observing System: ASOS User’s Guide. National Oceanic and Atmospheric Administration, Department of Defense, Federal Aviation Administration, and United States Navy, 1998.

84 Long, K., H. Wu, Z. Zhang, and M. Murphy. *Quantitative Relationship between Crash Risks and Pavement Skid Resistance*. Report FHWA/TX-13/0-6713-1, Center for Transportation Research, Austin, Texas, 2014.

85 Bonneson J., and K. Zimmerman. *Procedure for Using Accident Modification Factors in the Highway Design Process*. Report FHWA/TX-07/0-4703-P5, Texas Transportation Institute, College Station, Texas, 2007.

86 Economic Values Used in Analyses. US Department of Transportation, 2015. https://www.transportation.gov/regulations/economic-values-used-in-analysis. Accessed October 20, 2016.

87 Council, F., E. Zaloshnja, T. Miller, and B. Persaud. *Crash Cost Estimates by Maximum Police-Reported Injury Severity Within Selected Crash Geometries*. Report FHWA-HRT-05-0-051, Pacific Institute for Research and Evaluation, Calverton, Maryland, 2005.

88 Bonneson, J., M. Pratt, J. Miles, and P. Carlson. *Development of Guidelines for Establishing Effective Curve Advisory Speeds*. Report FHWA/TX-07/0-5439-1, Texas Transportation Institute, College Station, Texas, 2007.

89 Harkey, D. L., R. Srinivasan, J. Baek, F. M. Council, K. Eccles, N. Lefler, F. Gross, B. Persaud, C. Lyon, E. Hauer, and J. A. Bonneson. *Accident Modification Factors for Traffic Engineering and ITS Improvements.* NCHRP Report 617, National Cooperative Highway Research Program, Washington, D.C., 2008.

90 Brimley, B. and P. Carlson. *Using High Friction Surface Treatments to Improve Safety at Horizontal Curves*. Texas Transportation Institute, July 2012.

91 Bischoff, D. L. *Investigative Study of Italgrip System.* Report WI-04-08, Wisconsin Department of Transportation, Madison, Wisconsin, 2008.

92 Moravec, M. *High Friction Surface Treatments at High-Crash Horizontal Curves*. Arizona Pavements/Materials Conference, Tempe, AZ, November 13, 2013. https://pavement.engineering.asu.edu/wp-content/uploads/2013/12/High-Friction-Surface-Treatments-Mike-Moravec.pdf. Accessed January 27, 2017.

93 Seneviratne, P. N. and J. M. Bergener. *Effect of Aggregate Seal Coats on Skid Index Numbers and Low Volume Roads in Utah*. Utah Transportation Center, Utah State University, Logan, Utah, 1994.

94 King, W. Jr., M. S. Kabir, S. B. Cooper, Jr., C. Abadie. *Evaluation of Open Graded Friction Course (OGFC) Mixtures*. Report FWHA/LA.13/513. Louisiana Transportation Research Center, Baton Rouge, Louisiana, 2013.

95 Wong, S. Y. "Effectiveness of Pavement Grooving in Accident Frequency. *Institute of Transportation Engineers Journal*, Volume 60, No. 7. July 1990.

96 Smith, R.N. and L.E. Elliott. *Evaluation of Minor Improvements (Part 8), Grooved Pavement Supplement Report.* CADOTTR2152-11-75-01. California Department of Transportation. September 1975.

97 Adam, J. F. and E. Gansen. *Performance of Poly-Carb, Inc. Flexogrid Bridge Overlay System.* Report MLR-86-4, Iowa Department of Transportation, Ames, IA, December 2001.

98 Meggers, D. "Evaluation of High Friction Surface Locations in Kansas." Proceedings of *94th Annual Meeting, Transportation Research Board*, Washington, D.C., December 2015.

99 Romero, P. and D. Anderson. *Life Cycle of Pavement Preservation Seal Coats*. Report 03-9053. University of Utah, Salt Lake City, Utah, 2004.

100 Tate, T. R. and T. M. Clark. *Report on Evaluation of Thin Hot Mix Asphalt Overlays and SR164 Case Study*. Virginia Department of Transportation, Materials Division, Pavement Design and Evaluation Section, Richmond, Virignia, 2004.

101 Solaimanian, M, S. Stoffels, S. Milander, and D. Morian. *Evaluation of Thin Hot Mix Asphalt Overlay*. Report FHWA-PA-2016-005-110807. Pennsylvania Transportation Institute, PSU, University Park, Pennsylvania, 2016.

102 Anderson, K. W., J. S. Uhlmeyer, T. Sexton, M. Russell, and J. Weston. *Evaluation of Long-Term Pavement Performance and Noise Characteristics of Open-Graded Friction Courses*. Report WA-05-06. Washington State Department of Transportation, Olympia, WA. June 2012.

103 Santha, L. *A Comparison of Modified Open-Graded Friction Courses to Standard Open-Graded Friction Course.* FHWA-GA-97-9110. Georgia Department of Transportation. Forest Park, Georgia, 1997.

104 Cheung, J., F. Julian, and M. Moravec. *Frequently Asked Questions about High Friction Surface Treatments*. Federal Highway Administration. https://www.fhwa.dot.gov/everydaycounts/edctwo/2012/pdfs/fhwa-cai-14-019_faqs_hfst_mar2014_508.pdf. Accessed April 24, 2014.

105 Waters, J. *High Friction Surfacing Failure Mechanisms.* 3rd International Surface Friction Conference, Gold Coast, Australia. ARRB Group, 2011.

106 Krugler, P. E., T. J. Freeman, J. E. Wirth, J. P. Wikander, C. K. Estakhri, and A. J. Wimsatt. *Performance Comparison of Various Seal Coat Grades Used in Texas*. Report No. FHWA/TX-12/0-6496-1. Texas Transportation Institute, College Station, Texas, January 2012.

107 National Highway Institute (NHI). *Pavement Preservation: Preventative Maintenance Treatment, Timing, and Selection*. NHI Course No. 131115. Federal Highway Administration, Washington D.C. 2013.

108 Pierce, L. M. and N. Kebede. *Chip Seal Performance Measures – Best Practices*. Report WA-RD 841.1. Applied Pavement Technology, Inc., Urbana, IL. March 2015.

109 Ball, G. F. A., J. Patrick, and P. Herrington. *Solutions for Improving Chipseal Life*, Opus International Consultants Limited, 2004.

110 Hicks, R.G., F. Fee, J.S. Moulthrop. "Experiences with Thin and Ultra Thin HMA Pavements in the United States. In Proceedings of *World of Asphalt Pavements, 1st International Conference*, Sydney, New South Wales, Australia. 2000.

111 Walubita, L. F. and T. Scullion. *Thin HMA Overlays in Texas: Mix Design and Laboratory Material Property Characterization.* Report No. FHWA/TX-08/0-5598-1. Texas Transportation Institute, College Station, Texas, 2008.

112 Newcomb, David. *Thin Asphalt Overlays for Pavement Preservation*. Information Series 135. National Asphalt Pavement Association, 2009.

113 Gilbert, T. M., Olivier, P. A., and Gale, N. E. "Ultra Thin Friction Course: Five Years on in South Africa." In Proceedings of *Conference on Asphalt Pavements for Southern Africa*, South Africa, 2004.

114 Peshkin, D. G., T. E. Hoerner, and K. A. Zimmerman. *Optimal Timing of Pavement Preventive Maintenance Treatment Applications*. NCHRP Report 523, Transportation Research Board, Washington, D.C., 2004.

115 Stubstad, R., M. Darter, C. Rao, T. Pyle, and W. Tabet. *The Effectiveness of Diamond Grinding Concrete Pavements in California*. Applied Research Associates, ERES Consultants Division, Ventura, California, 2005.

116 Gransberg, D., Z. Musharraf, C. Riemer, D. Pittenger, and B. Aktas. *Quantifying the Costs and Benefits of Pavement Retexturing as a Pavement Preservation Tool*. Report OTCREOS7.1-16-F. Oklahoma Transportation Center, Midwest City, Oklahoma, 2010.

117 Gao, L., A. D. F. Smit, J. A. Prozzi, P. Buddhavarapu, M. Murphy, and L. Song. *Milled Pavement Texturing to Optimize Skid Improvements.* The University of Texas, Austin, Texas, 2015.

118 Gransberg, D. D. *Evaluate TxDOT Chip Seal Binder Performance Using Pavement Management Information System and Field Measurement Data San Antonio District. Interim Report #3*. Construction Science Division, University of Oklahoma, Norman, Oklahoma, 2008.

119 Morian, D. A. *Cost Benefit Analysis of Including Microsurfacing in Pavement Treatment Strategies & Cycle Maintenance*. Report No. FHWA-PA-2011-001-080503, Quality Engineering Solutions, Harrisburg, Pennsylvania, 2011.

120 Uzarowski, L., M. Maher, and G. Farrington. "Thin Surfacing – Effective Way of Improving Road Safety within Scarce Road Maintenance Budget". Presented at the 2005 Annual Conference of the Transportation Association of Canada, Calgary, Alberta, Canada, 2005.

121 Kandhal, P. S., and L. A. Cooley, Jr. *The Restricted Zone in the Superpave Aggregate Gradation Specification*. NCHRP Report: 464. 2014.

122 Wu, Z., J. L. Groeger, A. L. Simpon, and R. G. Hicks. *Performance Evaluation of Various Rehabilitation and Preservation Treatments*. Report No. FHWA-HIF-10-020, 2010.

123 Cooper, S. B., C. Abadie, and L. N. Mohammad, *Evaluation of Open-Graded Friction Course Mixture*. Report No. 04-1TA, Louisiana Transportation Research Center, Baton Rouge, 2004.